BNL 51539

Dr. 980

I-6403

METAL HYDRIDE/CHEMICAL HEAT-PUMP DEVELOPMENT PROJECT

PHASE I
FINAL REPORT

MASTER

Southern California Gas Company
810 South Flower Street
Los Angeles, California 90017

February 1982

Work supported by the
OFFICE OF ENERGY SYSTEMS RESEARCH
DIVISION OF PHYSICAL AND CHEMICAL ENERGY STORAGE SYSTEMS
UNITED STATES DEPARTMENT OF ENERGY

DEPARTMENT OF ENERGY AND ENVIRONMENT

BROOKHAVEN NATIONAL LABORATORY
UPTON, LONG ISLAND, NEW YORK 11973

bnl

DISCLAIMER

BNL 51539
UC-94d
(Energy Storage—Chemical — TIC-4500)

BNL--51539

DE83 002463

METAL HYDRIDE/CHEMICAL HEAT-PUMP DEVELOPMENT PROJECT

PHASE I
FINAL REPORT

Prepared by
Southern California Gas Company
810 Flower Street
Los Angeles, California 90017

T.A. Argabright

February 1982

Prepared for the
MATERIALS CHEMISTRY AND ENERGY CONVERSION DIVISION
DEPARTMENT OF ENERGY AND ENVIRONMENT
UNDER SUBCONTRACT NO. 534098-S

BROOKHAVEN NATIONAL LABORATORY
ASSOCIATED UNIVERSITIES, INC.
UPTON, NEW YORK 11973

UNDER CONTRACT NO. DE-AC02-76CH00016 WITH THE
UNITED STATES DEPARTMENT OF ENERGY

DISCLAIMER

Printed in the United States of America
Available from
National Technical Information Service
U.S. Department of Commerce
5285 Port Royal Road
Springfield, VA 22161

NTIS price codes:
Printed Copy: A10; Microfiche Copy: A01

TABLE OF CONTENTS

Section

tion

Page

LIST OF FIGURES

LIST OF TABLES

GLOSSARY OF TERMS

BNL	Brookhaven National Laboratory
SoCal	Southern California Gas Company
Solar	Solar Turbines Incorporated
Booz Allen	Booz, Allen and Hamilton, Inc.
MHHP	Metal Hydride/Chemical Heat Pump
EDTU	Engineering Development Test Unit
EETU	Engineering Evaluation Test Unit
COP	Coefficient of Performance
MTBF	Mean Time Between Failures

NOMENCLATURE

Symbol	Description
T_H	high temperature
T_M	medium temperature
T_L	low temperature
H/M	hydrogen/metal atoms ratio
COP	coefficient of performance
P_1	warm side alloy pressure at T_M
P_2	warm side alloy pressure at T_H
P_3	cold side alloy pressure at T_M
P_4	cold side alloy pressure at T_L
Q	quantity of heat
ΔH_f	hydride heat of formation
TMR	thermal mass ratio
t	time
H	external heat transfer coefficient
SH	sensible heat
ΔP	pressure drop

ABSTRACT

Southern California Gas Company (SoCal) is leading a team comprised of Solar Turbines Incorporated (Solar) and Booz, Allen and Hamilton, Inc. (Booz Allen) in the development and demonstration of a metal hydride/chemical heat pump (MHHP). Phase I of the three phase program was initiated in February 1981 and was completed in January 1982.

The MHHP is a chemical heat pump containing two hydrides for the storage and/or recovery of thermal energy. It utilizes the heat of reaction of hydrogen with specific metal alloys. The MHHP design can be tailored to provide heating and/or cooling or temperature upgrading over a wide range of input and ambient temperatures. The system can thus be used with a variety of heat sources including waste heat, solar energy or a fossil fuel.

The conceptual design of the MHHP was developed in Phase I. After initial technical definition, Booz Allen conducted a national market survey including a study of applications and market sectors. Solar performed the technical tasks in Phase I, including conceptual development, thermal and mechanical design, laboratory verification of design and material performance, cost analysis and the detailed design of the Engineering Development Test Unit (EDTU). A test plan for the EDTU was also developed and was published under separate cover.

As a result of the market study, the temperature upgrade cycle of the MHHP was chosen for development. Operating temperature ranges for the upgrader were selected to be 70-110°C (160-230°F) for the source heat and 140-190°C (280-375°F) for the product heat. These ranges are applicable to many processes in industries such as food, textile, paper and pulp, and chemical. The hydride pair well suited for these temperatures is $LaNi_5/LaNi_{4.5}Al_{0.5}$.

The EDTU was designed for the upgrade cycle. It is a compact finned tube arrangement enclosed in a pressure vessel. This design incorporates high heat transfer and low thermal mass in a system which maximizes the coefficient of performance (COP). It will be constructed in Phase II.

The project team recommends continuation of this effort into Phase II according to the original plan and schedule. An alternate plan is also presented. The alternate Phase II plan emphasizes the verification of critical components of the EDTU.

1

EXECUTIVE SUMMARY

The metal hydride heat pump is an innovative "solid state" heat pump that is based on the heat of absorption of hydrogen into selected metals. The alternating absorption and desorption of hydrogen into two different metal alloys can be used to provide refrigeration, heat amplification (COP > 1) or temperature upgrading without consumption of metals or hydrogen gas.

The MHHP is an invention of the 1970's and as such has received little research and development attention when compared to other absorption heat pumps. In 1981, Brookhaven National Laboratories (BNL) requested proposals to advance the technology of the MHHP to the point of determining commercial viability. Southern California Gas Company along with its team members, Solar Turbines Inc. and Booz Allen & Hamilton prepared the winning proposal for the current effort based on experience gained in earlier and on-going private efforts in similar areas.

The work described in this report was accomplished in Phase I of a three phase program (Fig. 1). The goal of Phase I was the detailed design of the EDTU. The EDTU will be fabricated and tested in Phase II. An Engineering Evaluation Test Unit (EETU) will be designed in Phase II and built and tested in Phase III.

SoCal has a long working relationship with members of the team. Since 1978, SoCal has had an ongoing contractual arrangement with Solar to develop and demonstrate a metal hydride/chemical heat pump. Booz Allen has an ongoing agreement with SoCal to study the marketing and commercialization aspects of energy saving devices that use new technology. SoCal has entered into these agreements because of its strong interest in bringing new, energy conserving products to the marketplace. These products, when produced and used by the public, will reduce our dependence on foreign oil. The MHHP, currently under development by the team, has the potential of being one of these energy conserving products.

Because of the prior experience with MHHP technology the team was able to identify the critical research and development needs and the work required to develop a design acceptable to the marketplace. Those critical areas, addressed in the proposal, formed the basis of the research and development work performed in Phase I. Each of the critical technology areas is addressed in this report, not as a subject unto itself, but as a part of an effort directed toward the design of a functional laboratory model to be built and tested in Phase II of this effort. The market analyses which led to technical requirements and targets is presented first. The technical design tradeoffs along with supporting analysis and experimental data follow the market chapter. The final design of the EDTU is described in detail in the third major chapter. A project summary and recommendations for Phase II conclude

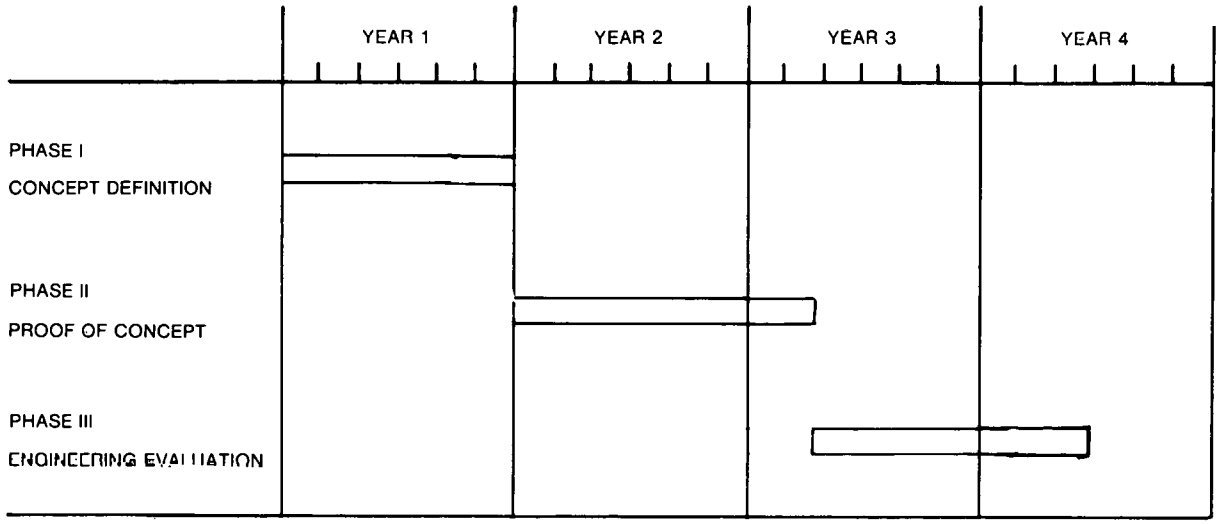

Figure 1. Overall Program Schedule

this report. The recommendations include an alternate program path that should resolve many technical uncertainties. The alternate would result in a technical position less complete than if the original plan is followed, but would optimize the available resources for the ultimate success of the MHHP.

Phase I goals included the completion of a preliminary market study and a defendable design for the EDTU. Both of the goals were met within the original funds of Phase I. (The results of the marketing effort by Booz Allen were furnished to the program without direct cost to BNL by SoCal. Both SoCal and Solar made significant reductions in program related fees.

The marketing study, performed by Booz Allen, investigated the potential applications for the MHHP in the residential, commercial, industrial and transportation market sectors. Then, the configurations were studied in each sector. The market needs (applications), cost structure, and energy source were examined for each configuration. Fourteen applications were selected from the study and subjected to a forced ranking. In the ranking process, the project team rated the market, technical and other characteristics for each application against the properties of the MHHP. The three highest rated applications, industrial heat amplification, industrial temperature upgrading and residential space heating, were examined in greater detail. Temperature upgrading was selected as the target application for the Phase II and Phase III efforts. This decision was based on the fact that this application had the least market risk. Target operating temperatures, capacities, performance and costs for this application were compiled and supplied to SoCal and Solar.

In the technical efforts numerous design parameters were studied using analytical models. Critical components and characteristics were also subjected to verification via laboratory tests. The major areas of study includ

h transfer enhancement, low thermal mass, mechanical configurations, hydride materials, cycle optimization, filters, and controls.

Heat transfer was considered the key technical study area. Since the MHHP is a cyclical device, rapid heat transfer allows more cycles per hour and thus a greater productive thermal capacity per pound of hydride material. High heat transfer leads to rapid cycling, high capacity, low hydride inventory per unit output and low system costs. While high heat transfer can be easily achieved with massive, large surface area heat exchangers, the goal was to provide the heat transfer with a low mass unit.

Since the heat exchanger must follow the cyclic temperatures of the MHHP, its mass is parasitic, lowering the coefficient of performance for the entire unit. Extensive design studies were conducted to maximize the heat transfer while minimizing the thermal mass of the heat exchanger. Two different concepts were considered for the best configuration. Laboratory test and additional calculations allowed the selection of the final configuration. It has hydride powder filling the voids between the external fins on a tube and heat transfer fluid flowing through the tube.

Hydride materials were selected for each side of the temperature upgrade. These materials, $LaNi_5$ and $LaNi_{4.5}Al_{0.5}$, meet the several requirements enumerated by the project metallurgists. The hydrided materials must exhibit reasonable hydrogen pressures (1-20 atm.) at the temperatures of interest for the temperature upgrader (70-190°C). Hysteresis of the metal hydrides must be low, the isotherms should have a broad plateau, and the metal alloy should be chemically stable. These are only a few of the properties considered in the selection of the hydride materials.

Control systems for Phase II and III were designed using microprocessor technology. Phase III controls are to be built from general purpose, commercially available components and thus offer a high degree of flexibility. Phase II controls are designed to be highly specialized, small and ultimately inexpensive.

Technical studies were also conducted on the flow rates of filter materials in different configurations to develop a filtering scheme with low pressure drops, and the ability to contain the particles. Design data is included in this report.

The final design embodies the best features of the market and design studies described above. The EDTU will consist of four tubular pressure vessels connected as two out-of-phase pairs. In each pair one vessel will contain $LaNi_5$ packed around 14 finned copper tubes while the second vessel will contain $LaNi_{4.5}Al_{0.5}$ in a similar configuration. Solid insulation will thermally isolate the tubes and hydride materials from the high mass pressure vessel. A single metallic filter in each vessel will prevent hydride migration from one vessel to the other. The hydrogen path between the vessels will be short and free of valves. Pressurized water will be used as the heat transfer fluid in the flow loops within the vessels and in the external heat exchangers.

A prime consideration in the design is the capability to open up the ve l for inspection or rebuild. Serious consideration was given to this feature to optimize data recovery while minimizing the possibility of hydrogen leaks during operation. The flange on the pressure vessel will satisfy both considerations. Alternate heat exchanger modules can be inserted into the pressure vessel during the mid-phase rebuild.

The capacity of the final design unit is about 40,000 Btu/hr of upgraded heat. It will produce 176°C (350°F) hot water using a source of 93°C (200°F) and a sink of 27°C (80°F). The calculated COP is 0.42.

It is recommended that Phase II continue according to the original plan and schedule. That plan called for the construction and operation of the Engineering Development Test Unit. The EDTU is to be operated for several weeks, rebuilt with new heat exchangers, filters or hydride materials as necessary and retested. From these tests, hardware modifications and concurrent laboratory tests, the engineers will gain sufficient knowledge of the temperature upgrader to minimize all known technical risk areas.

An alternate program plan for Phase II (Phase II - Alternate Plan) is also proposed which includes a reduction in reporting requirements, construction of a half-capacity (non-continuous) temperature upgrader, and a reduced testing schedule. In order to make the alternate plan technically valuable, the construction and testing of an alternate EDTU would be preceded by a laboratory phase in which several aspects of the final design would be individually tested before a large commitment of funds was made to build an operating unit and test facility. The alternate EDTU, when built in Phase II Alternate Plan, would pose fewer technical risks. It would be comprised of only two hydride vessels rather than four which would provide 20,000 Btu/hr rather than 40,000 Btu/hr. The alternate EDTU would operate in a noncontinuous fashion due to the required charge cycle (an accumulator could make the output virtually continuous). Data gained from these tests would verify the Phase I design of the hydride vessel in every respect. The major technical drawback in this alternate plan would be in the system operation including the development of the control system.

The original Phase II plan would move the MHHP technology ahead at the fastest pace. The Phase II alternate plan would verify the critical technologies in the hydride vessel and leave many of the system considerations for a future phase of this program.

At the conclusion of Phase I the team is enthusiastic about the market and technical prospects for the MHHP. SoCal views the metal hydride heat pump as a future energy saving appliance with great potential for the industrial and residential marketplace. Solar believes that the MHHP can be effectively used in industrial heat recovery installations once the technical risks have been minimized. In addition, Solar can envision the use of the MHHP as a potential energy recovery device for its line of gas turbine engines. Booz Allen sees great potential for this technology in the transportation sector for space conditioning. Since all major milestones of this effort have been met, the team endorses the continuation of the MHHP development program into Phase II.

ADDENDUM TO EXECUTIVE SUMMARY

The following comments are provided by the staff of the Chemical/Hydrogen Energy Systems Program, Brookhaven National Laboratory, who have technical oversight responsibility for the project:

- BNL agrees in essence with the findings and analyses presented in the report, but in our judgment it would be premature to start on the fabrication of an engineering development test unit (EDTU) as recommended by the contractor, in view of limitations in the current design.

- The key pacing problem with metal hydride chemical heat pump systems has been the limited capability for rapid cycling of the system. The approach to this problem is through an optimized heat/mass transfer component design which is planned for the second phase of this work rather than the EDTU development.

- An independent analysis of the design of metal hydride chemical heat pump systems in general, was performed by Argonne National Laboratory.* This analysis established the theoretical basis for the maximum coefficient of performance (COP) for a given hydride pair. The analysis also showed the critical areas where component design improvements could increase the heating COP from a baseline 1.12 to around 1.5 for the representative hydride pairs. Similar design studies will be conducted with the aim of improving the rapid cycling capabilities of the SOCAL/Solar CHP design.

- It is expected that the next phase of investigation will identify the technical and economic risks associated with metal hydride chemical heat pump systems with regard to commercial prospects. In accordance with current administration policies which emphasize longer-term research as opposed to near-term commercial projects, DOE support for the project would be discontinued at the end of the next phase, with further development of the concept turned over to the private sector.

*Abelson, H. I. and J. M. Clinch. Metal-Hydride Heat-Pump Performance Studies. Proc. of the Sixth Annual Thermal and Chemical Storage Contractors' Review Meeting, Washington, D.C., September 14-16, 1981.

2

INTRODUCTION

2.1 BACKGROUND

One of our nation's major goals is to reduce dependence on foreign oil. This goal will only be accomplished when energy efficient technologies are developed and utilized. The heat pump is an example of such a technology. However, most commercially available heat pumps are driven by electricity. There has long been a need for a high performance thermally-driven heat pump since it will utilize wasted energy sources and reduce the consumption of electricity or other premium fuels.

The metal hydride/chemical heat pump (MHHP) is a concept that could result in a highly efficient technology driven by oil, natural gas, waste heat or solar energy. Some of the competitive advantages of the metal hydride heat pump include:

- operation on low grade heat
- air or liquid heat exchange
- use of multiple energy sources in one unit
- environmentally acceptable
- compact
- shape and size can vary according to application
- quiet operation
- simplicity - no moving parts
- long life operation
- ability to tailor operation to available temperature source.

In the early 1970's, Solar Turbines Incorporated (Solar) performed internal research to investigate potential heat utilization technologies. Metal hydrides were identified as a potential foundation for a thermally driven heat pump. The concept was verified by experimental work and proved to be very promising. In 1978, Southern California Gas Company (SoCal) entered into an agreement with Solar to accelerate the development of this new technology. SoCal entered into this agreement because of the large potential energy savings in their service area and because of SoCal's strong interest

in investigating new energy conserving products. In 1980, Brookhaven National Laboratory (BNL) requested proposals for the development of similar technology for the benefit of the nation. SoCal, with Solar as a subcontractor, submitted the winning proposal and embarked on this current effort.

SoCal is leading a team which includes Solar, and Booz, Allen & Hamilton, Inc. (Booz Allen) in the development and demonstration of the MHHP (see Fig. 2). Booz Allen has an ongoing agreement with SoCal to determine the technical and market requirements of energy saving devices that use new technology. The MHHP is considered by the team members to have great potential as an energy conserving technology.

2.2 PROGRAM GOALS

The goal of this effort is research and development aimed at the design, development and demonstration of a metal hydride heat pump. This includes advancing the state-of-the-art of hydride heat pump technology to the point where performance and energy efficiency can be well established.

Development of this functional MHHP will proceed from conceptualization to preprototype fabrication and testing via a three-phase approach:

Phase I - Concept Definition
Phase II - Proof of Concept
Phase III - Engineering Evaluation

The scope of Phase I of this project includes development of a conceptual design, study of the applications and market sectors, analysis of the thermal and mechanical design, laboratory verification of design and material performance, and analysis of costs. The design, Engineering Evaluation Test Unit is also part of Phase I. The EDTU will be fabricated and tested in Phase II. An Engineering Evaluation Test Unit (EETU) will be designed in Phase II, and built and tested in Phase III. Figure 3 shows the relationship between the development and the marketing analysis programs.

2.3 FINAL REPORT ORGANIZATION

The final report is organized in the following manner:

- The Conceptual Design section outlines the basic hydride technology and how it is applied to the three hydride heat pump cycles. Also discussed are major technical design issues where further development was required and emphasized in this project.

- The Market Study chapter describes how Booz Allen focused the development program based on market needs. Included in this section are descriptions of the four market sectors, the MHHP applications in each market and the iterative process which resulted in the selection of the most promising MHHP configuration.

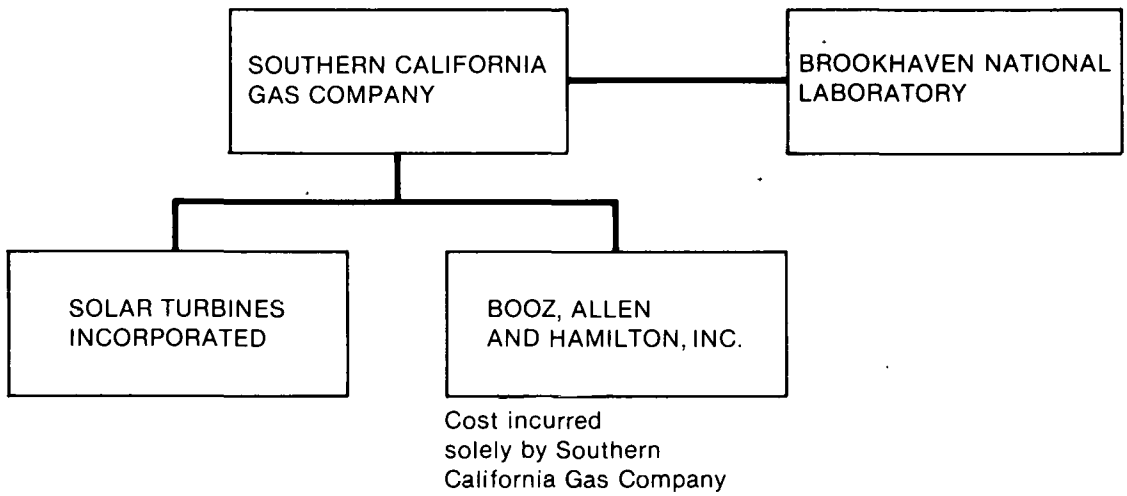

Figure 2. Project Organization

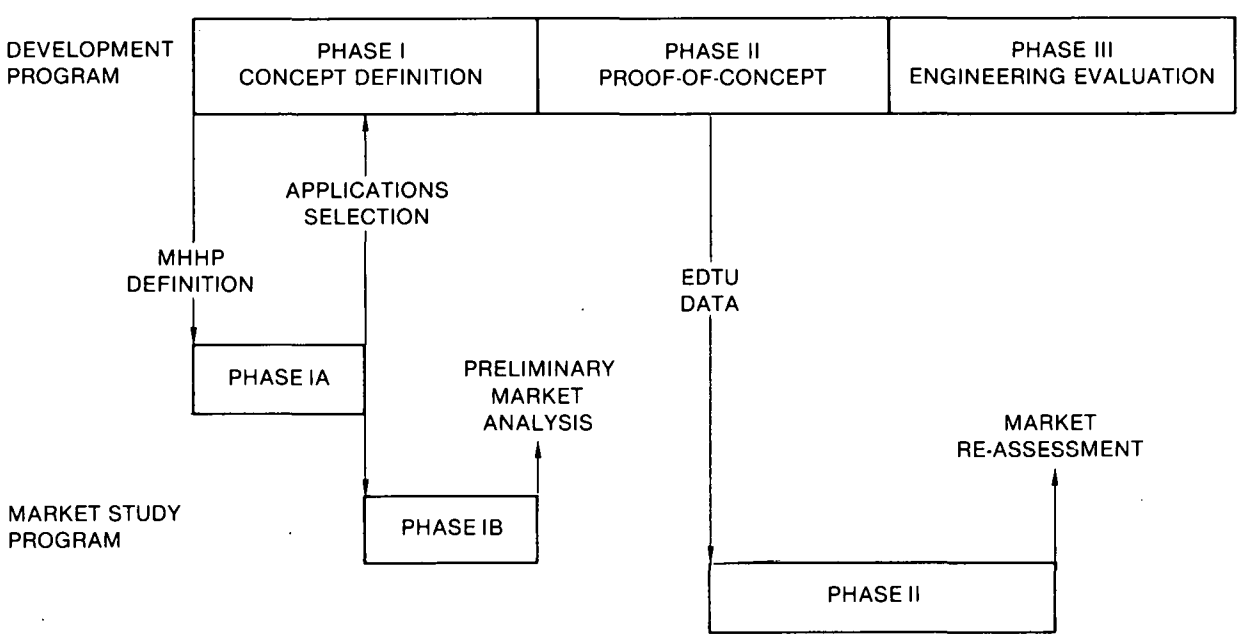

Figure 3. Relationship Between Development and Market Study Program

- The section on System Design Analysis describes each important c sideration in the design of the MHHP. Hydride materials, heat exchanger design, performance, filters, controls and economics are all discussed.

- The Final Design of the EETU is outlined in this next section. The design is supported by calculations and layout drawings.

- The chapter on Conclusions and Recommendations discusses the major results of Phase I and the plans and recommendations for Phase II.

3

CONCEPTUAL DESIGN

This section outlines the basic hydride technology and how it is applied to the three hydride heat pump cycles. Also discussed are major technical design issues where further development was required and emphasized in this project.

3.1 PHYSICAL DESCRIPTION OF METAL HYDRIDES

Many crystalline metals can absorb large amounts of hydrogen in their interstitial crystal lattice locations. When this absorption occurs, the resulting material is a metal hydride. Hydrogen can be readily dissociated from hydrides by the application of thermal energy. When this is done, the metal exhibits its original properties. In principle, hydrogen can be reintroduced into the metal and removed from it an indefinite number of times with little or no metallurgical change in the host metal.

Metal hydrides have several common features which make them candidates for heat pumps.

- Hydriding is a reversible reaction.
- Hydriding is an exothermic reaction.
- Dehydriding is an endothermic reaction.
- The diffusion rate of the hydrogen within the hydrides is rapid.
- Pressure-composition isotherms display a plateau over a large range of hydrogen compositions.

Reversibility is an important feature because it allows the hydrogen to act as the heat pump working fluid. Neither the metal alloy nor the hydrogen is consumed when it is operated in a heat pump mode.

The hydrogen is absorbed into the metal through a two-step process. First, the H_2 molecule is adsorbed and reduced to atomic hydrogen at the surface of the material. Then atomic hydrogen is absorbed into the material and diffuses rapidly into the metal lattice to occupy the interstitial locations. Once a threshold temperature or pressure has been attained, the formation of the hydride in this manner is almost always exothermic.

The heat-of-formation of the metal hydrides is vastly different for diffe : base metal systems. One alloy, $LaNi_5$, has a heat-of-formation of 7.3 kcal/mole H_2; Mg hydride shows a heat-of-formation of nearly 17.8 kcal/mole H_2; and Ce hydride has a heat-of-formation near 49.2 kcal/mole H_2. Due to the wide range in the thermal stability of different hydride alloys, one can optimize a hydride thermal property for the temperature of the heat source used. For use in heat pumps, the hydrides must be fairly unstable. In applications for which suitable materials are not yet available, there is reason to believe that existing alloys can be modified to exhibit the necessary properties.

3.2 BASIC HYDRIDE HEAT PUMP CYCLES

Hydride-forming metal alloys with different thermodynamic characteristics can be used as thermal working elements to provide heat pump operation. The heat pump cycle requires two different alloys chosen to operate together as a working pair. One can be designated as the warm side alloy and the other the cold side alloy. These hydride alloys must be chosen to operate as a pair based on their natural pressure-temperature response characteristics.

Characteristic hydride curves result when the hydrogen pressure is measured and plotted as a function of hydrogen content (H/M = hydrogen/metal atoms) for a given constant temperature (Fig. 4). Curve A shows a typical hydrogen desorption isotherm, and curve B is the hydrogen absorption isotherm for the same alloy at the same temperature. The vertical space between the two curves indicates the magnitude of pressure hysteresis characteristic of the particular alloy. It is desirable to select alloys with a flat plateau to achieve optimum heat pump performance. The plateaus for curves A and B are characteristic of $LaNi_5H_x$. Some alloys behave as shown in curves C and D where the sought-after flat plateau is either steeply sloped (curve C) or too narrow (curve D).

There are three heat pump cycles considered in this study: refrigeration, heat amplification and temperature upgrade. The refrigeration side of the heat pump cycle is illustrated in Figure 5 along with the pressure/temperature cycle diagram. The cycle functions as follows. The fully hydrided warm side alloy is exposed to T_H, which allows it to desorb hydrogen at a pressure P_2 while absorbing thermal energy from the heat source. Simultaneously, the hydrogen-depleted cold side alloy is exposed to a heat sink at T_M, which allows it to absorb hydrogen at pressure P_3 ($P_2 > P_3$). The hydrogen flows from the warm side alloy to the cold side alloy. Heat is rejected bythe cold side alloy at T_M. The flat character of the plateaus in the isotherms guarantees that the relative driving pressure differential between the two sides will remain fairly constant while the majority of the hydrogen passes from one side to the other. This action constitutes the charge half of the cycle.

The refrigeration half of the cycle occurs when the warm side alloy is exposed to the heat sink T_M, lowering its equilibrium pressure to P_1. The cold side alloy is exposed to the chilled fluid loop and estabishes equilibrium at T-

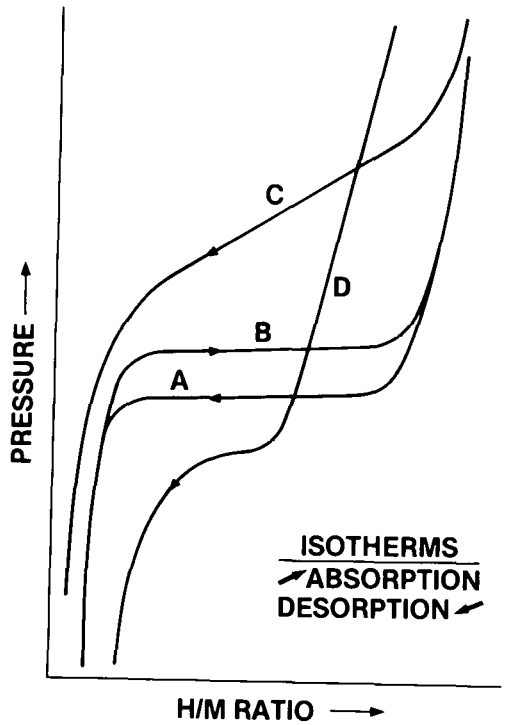

Figure 4. Typical Isotherms for Hydride Alloys

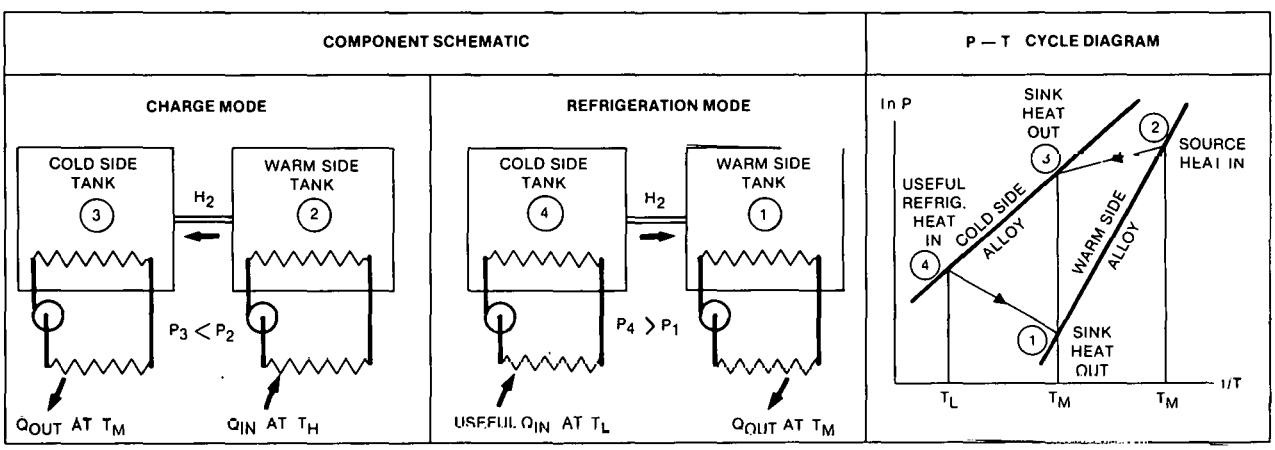

Figure 5. Cycle Name: Refrigeration

and P_4 ($P_4 > P_1$) as heat is absorbed from the chilled fluid and hydrogen desorbed. The hydrogen can then flow back to the warm side by virtue of the fact that P_4 is greater than P_1. Thus to produce refrigeration (T_L), high temperature heat (T_H) is used to fire the system, while heat is rejected to the atmosphere at the ambient temperature (T_M).

For heat amplification, the heat pump operation is identical to the refrigeration cycle; only the temperature use is altered (see Fig. 6). As in the refrigeration mode, the high temperature heat (T_H) is used to fire the system. The low temperature heat (T_L) that was previously used for refrigeration is obtained from a lower temperature, ambient condition source. The medium temperature heat (T_M), which was rejected to the atmosphere in the refrigeration cycle, is used for heating, such as space heating in a dwelling. The advantage of this mode of operation is that theoretically almost twice the energy used to fire the system can be used for heating.

Another application for the MHHP is the temperature upgrade cycle (see Fig. 7). In this cycle, the heat pump operation is reversed compared to the other two modes. Instead of requiring a high temperature heat source to drive the system, this cycle upgrades a medium grade waste heat stream (T_M) to a higher temperature (T_H) without the use of a fossil fuel input. Specifically, this cycle uses an intermediate temperature heat source (T_M) and low temperature ambient conditions (T_L) to produce the high temperature process stream (T_H).

As shown in Figures 5 through 7, the cycles would operate intermittently, requiring charge cycles between cycles of useful output. Continuous output would require dual heat pumps and appropriate controls to establish 180 degrees out of phase operation.

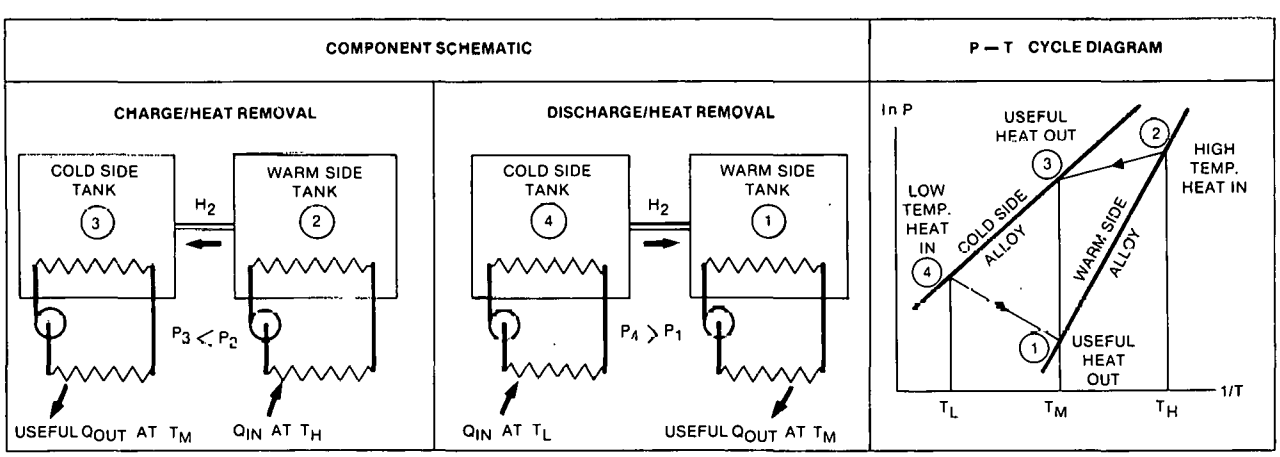

Figure 6. Cycle Name: Heat Amplification

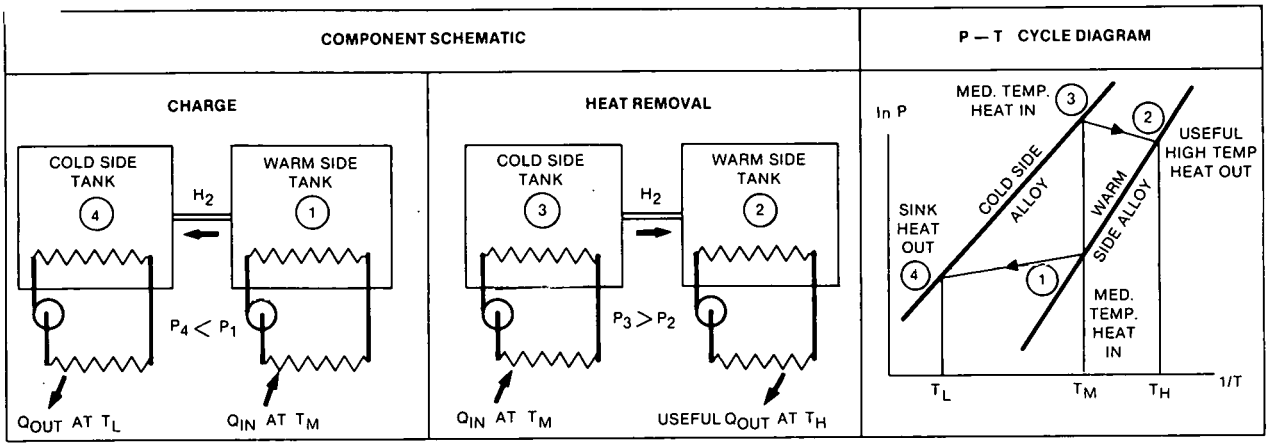

Figure 7. Cycle Name: Temperature Upgrade

3.3 PRELIMINARY HYDRIDE SELECTION FOR THE MHHP

The cost and availability of hydride alloys are important considerations for their selection in a heat pump design. From these considerations alone, it would appear that hydrides of the FeTi system would be ideally suited for this particular application; iron and titanium are both plentiful and relatively low in cost. However, the $LaNi_5$ type hydrides have some important technical advantages over the FeTi type.

$LaNi_5$ is the best known representative of a class of alloys known as AB_5. This class has a hexagonal crystal structure, where A is a rare-earth element such as lanthanum, or cerium, or a combination of these rare-earth metals, such as mischmetal. The B in the formula is a transition metal, usually nickel, cobalt, iron, or a combination thereof. The transition metal may also be partially substituted with aluminum, copper, or manganese to introduce a radical change in the alloy's plateau pressure. The AB_5 class of alloys exhibits rapid hydriding kinetics at or near room temperature. Table 1 summarizes the pertinent properties of candidate AB_5 hydrides.

The pressure-composition isotherms at 40°C (104°F) of hydrided FeTi and $LaNi_5$ are shown in Figure 8 (Ref. 1). Note the constant and relatively low plateau pressure of $LaNi_5$ over the entire hydrogen compositional range. The lower pressure simplifies and economizes the mechanical design of the heat pump, while the broad, flat plateau allows for a proportionally wider hydrogen excursion. In contrast, $FeTiH_x$ has a constant equilibrium pressure for only about half of its hydrogen content. The AB_5 class of hydrides, in general, has a wider range of pressures from which to select for heat pump applications, require lower pressures and temperatures for activation, are relatively insensitive to impurities in the hydrogen gas and, due to good hydriding kinetics, require a lesser quantity than FeTi alloys in a comparable system. Based on the current state of hydride knowledge, the technical advantages of the AB_5 alloys discussed above outweigh the cost advantage the FeTi alloys. Accordingly, the team selected a hydride pair from the AB_5 class to use in the MHHP Project.

Table 1

Properties of Selected Intermetallic Hydrides

Intermetallic Compound	Plateau Pressure, Atm (psi-abs)			ΔH, k cal/ mole H_2	H/AB_5 Ratio at end of Plateau	H, Btu Per lb of Alloy	Cost, Dollars[b]		Reference
	20°C	50°C	100°C				Per lb Alloy	Per Btu	
$LaNi_5$	1.8 (26.5)	5.8 (85.3)	22 (323)	-7.28	6	-90.2	15.00	0.166	(1,2)
$LaNi_4Cu$	~0.7 (10.3)	2.2 (32.3)	~10.5 (154)	-9.66	5	-99.4	14.50	0.146	(1)
$CaNi_5$	0.4 (5.9)	1.3 (19.1)	10.6 (155)	-7.5	5	-100.3	6.50	0.065	(3)
$LaNi_{4.6}Al_{0.4}$	0.18 (2.7)	0.6 (8.8)	4 (58.8)	-8.7	6	-114.9	~15.00	0.134	(5)
[c]$(La_{0.67}Nd_{0.25}Pr_{0.08})Ni_5$	3.3 (48.5)	10 (147)	42 (617)	-6.9	6	-85.8	13.00	0.152	(2)
$MMNi_5$[a]	17 (250)	42 (265)	150 (2205)	-5.46	5	-67.9	11.00	0.162	(2)
$LaNi_{4.6}Mn_{0.4}$	0.13 (1.9)	0.54 (7.9)	3.6 (52.8)	-9.1	5.4	-120.5	15.00	0.124	(1)
$MMNi_{4.7}Mn_{0.3}$	9.3 (137)	24.8 (365)	90.1 (1324)	-5.5	5.8	-68.3	11.00	0.167	(1)
$MMNi_{4.5}Al_{0.5}$	3.1 (45.6)	9.2 (135)	37.9 (557)	-6.7	5.2	-75.0	~11.00	0.147	(4)
$MMNi_4Fe$	6.4 (94.1)	17.2 (253)	62.9 (925)	-6.3	5.1	-67.1	~10.00	0.149	(4)
$MMNi_{4.15}Fe_{0.85}$	12 (176)	--	--	~-6.3	5.2	-63.3	~10.00	0.146	(4)
$MMNi_{3.5}Cu_{1.5}$	5.1 (75.0)	18.9 (278)	63 (1000)	-6.4	4.9	-64.0	~10.00	0.156	(4)
$Ca_{0.7}MM_{0.3}Ni_5$	3.2 (47.0)	80 (118)	40.0 (588)	-6.5	6	-96.5	~7.00	0.073	(5)
$(CFM)Ni_{4.8}Al_{0.2}$	1.6 (23.8)	5.6 (81.8)	28.1 (413)	-7.5	6	-94.7	~13.00	0.137	(5)

[a]MM - mischmetal
[b]Based upon 50 tons of AB_5 per year as of May 1980. Communications with J. G. Cannon, Molycorp.
[c]Cerium-free mischmetal (CFM)
(1) Communication with C. E. Lundin, University of Denver, Denver, CO, also "Modification of Hydriding Properties of AB_5 Type Hexagonal Alloys Through Manganese Substitution", C. E. Lundin, et al.
(2) Overview, No. 56, Molycorp, Inc., White Plains, New York.
(3) Argonne National Laboratory, ANL-79-8 (1979).
(4) "Development of Low Cost Nickel-Rare Earth Hydrides for Hydrogen Storage", G. D. Sandrock.
(5) M. H. Mendelsohn, et al, J. Less Common Met., Vol. 63 (1979).

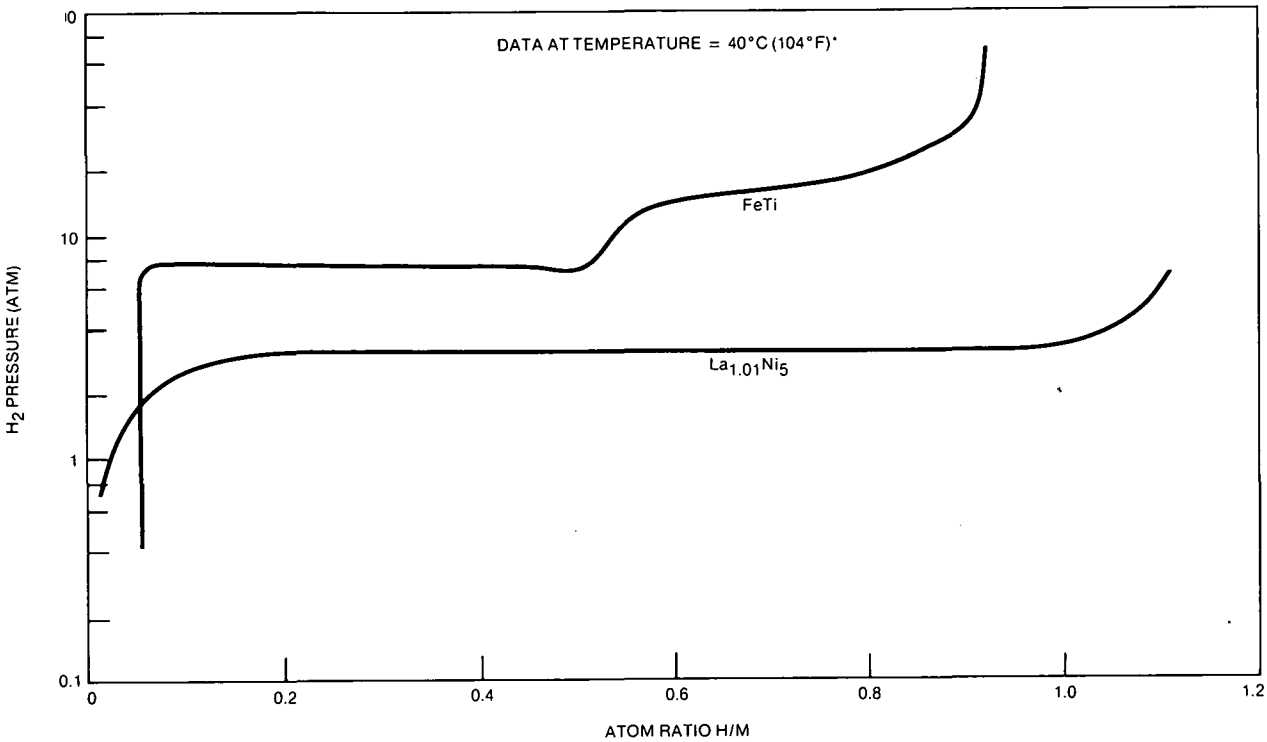

Figure 8. Plateau Pressures as a Function of Hydrogen Content

3.4 MAJOR TECHNICAL ISSUES

The specific technical issues below were areas where further development was required and emphasized in this program to provide a technically-sound design.

3.4.1 Heat Transfer

The primary cost item in the heat pump is the metal hydride powder. AB_5 compounds, the materials selected, cost $10/lb (1981$, large quantity estimates). Thus, it is imperative to minimize the quantity of metal hydride powder per useful output. This is accomplished by reducing the cycle time and minimizing the parasitic thermal losses to the structure of the heat pump. The reduction of cycle time is the most critical, since a factor of two reduction in cycle time provides almost a factor of two in reduction of hydride material. The cycle time is controlled by the heat transfer characteristics of the powdered metal hydride. Since particle-to-particle heat transfer is extremely slow, it is necessary to enhance the transfer with a low mass, extended surface, heat transfer device imbedded in the metal powder. The heat transfer device is designed as an integral part of a strong, lightweight structure that contains the powders and the hydrogen gas. This is due to the importance of minimizing the mass of the structure to

reduce the parasitic self-heating and cooling losses. Heat transfer f the heat transfer fluid to the structure is not considered to be as critical as the heat transfer from the structure to the individual metal hydride particles.

3.4.2 Performance

The performance of a hydride heat pump is expressed in terms of the coefficient of performance (COP) and the output capacity. The COP is a ratio of the net useful output energy to the required driving energy. COP values for the MHHP are maximized by minimizing parasitic losses -- the less energy required to heat and cool the heat exchanger structure, the more net useful output energy.

Similarly, the capacity of an MHHP is expressed in terms of the rate at which useful output energy is exchanged. It is calculated by dividing the energy output per cycle by the total cycle time. Thus, total cycle time is inversely proportional to capacity. A reduction in cycle time would increase the capacity.

3.4.3 Particle Containment

If filters are used to contain the metal hydrides separately in two beds, large hydrogen pressure drops occur unless the filters are properly designed and installed. The pressure drops slow the flow of hydrogen and increase the cycle time, thus increasing the amount of hydride material needed per useful output.

3.4.4 Particle Expansion

The process of hydrogen absorption and desorption causes the metal crystal lattice to expand and contract leading to the comminution of the original hydride alloy particles. After many such cycles, the process of comminution produces a progressively greater proportion of fine particles. The MHHP must be designed with the ability to absorb this hydride powder expansion or risk rupturing under internal pressure.

3.4.5 Design

To be commercially acceptable, a heat pump must be adaptable to a variety of site or application dependent conditions. Those requirements are determined largely by the climate of the site, the application of the system, installation procedures and the physical, electrical and thermal interfaces of the heat pump. In each application, high reliabilty and low maintenance must be

nasized. Among the specific interfaces of the heat pump are its heat source, heat output, heat rejection, thermostatic control, AC power and physical placement. The heat interfaces include the heat transfer media, flow rates and temperature ranges; while the physical placement includes size, weight, and shape.

An effective design also requires that the assembly of the hydride beds be accomplished with high reliability and repeatability. This includes the processes of filling the beds with hydride powder, activating the hydride, and charging the heat pump with the proper quantity of hydrogen gas.

The resulting heat pump should have a high mean time between failures (MTBF) and be relatively easy to service. To the greatest extent possible, the design should incorporate module component replacement rather than provisions for in-situ repair. Commonality of parts within a module and the potential to scale modules to achieve units of different capacity should be strong design criteria.

3.4.6 Controls

Since the MHHP can operate from low temperatures, small changes in the design temperatures can have a large effect on the unit's performance. Therefore, control strategies must be developed to maximize the output capacity of the MHHP at and off the design point.

Development is aimed at methods to use in sensing test conditions, how to interpret the data from the sensors and what control strategy to take. Temperature and rate of change of transfer fluid temperature is considered basic data.

4

MARKET STUDY

This chapter describes how Booz, Allen & Hamilton Inc. (Booz Allen) focused the development program based on market needs. Included in this section are descriptions of the potential market sectors, the MHHP applications in each market and the iterative process which resulted in the selection of the most promising MHHP configuration.

The market study undertaken by Booz Allen was an integral component of the overall MHHP development effort for the following reasons:

- The concept of the MHHP could be technically applied over a very wide range of markets and applications.

- Although the basic hydride technology is broadly applicable, the MHHP took on different characteristics in each application. Some of these specific application requirements include:

  - Product size and weight
  - First cost and operating economics
  - Dominant operating mode (heating vs. cooling) and temperature ranges
  - Type of low grade and driving energy sources.

- From the standpoint of development cost, it was not practical at this stage of the technology development program to attempt to configure and develop heat pumps to meet the demands for every possible MHHP application.

Thus, it was critical that decisions were made early in the MHHP program as to the most promising market sectors and applications for the MHHP technology.

The purpose of the market study task was twofold:

- To confirm in general that the identified market segments hold promise for the application of metal hydride technology. This potential appeared to exist for each of four markets: residential, commercial, industrial and transportation.

- To develop specific information on the market-related technical requirements likely to affect the competitiveness in each market of a specific MHHP configuration.

4.1 GENERAL DESCRIPTION OF MARKET SECTORS

From the market and technical data acquired, a general description of each of the four market sectors was developed. These descriptions served as the basis for judging the potential of alternative MHHP configurations.

Preliminary characterization of the residential sector suggested that it is a very interesting market for several reasons:

- The market is large (Fig. 9). The annual dollar volume of shipments of residential heating and cooling equipment is over $2 billion and rising at about 5 percent per year.

- The market is stable (Fig. 10). There are no significant fast growing segments within the residential HVAC equipment market. Heat pumps have made significant penetration of new house construction, but gas heating is envisioned as maintaining its traditional market share of about 44 percent of annual units shipped for new housing, equipment replacement and add-on/conversion market segments.

- Competing technologies will not be radically improved. Over the 1980's it is expected that MHHP devices could compete with conventional HVAC equipment and with advanced pulse combustion/recuperative furnaces and variable speed central air conditioners. This advanced equipment is expected to have efficiency improved by 50 percent over current conventional equipment. As now envisioned, the MHHP could compete effectively within this range of performance. Radical changes in the equipment market caused by introduction of highly efficient gas heat pumps or signficiant penetration of solar systems are not expected during the 1980's.

- The cost implications for the MHHP are favorable. Prelminary indications are favorable for MHHP technology. In order to be comparable to conventional residential space conditioning on first cost, the MHHP, assuming $200 for base furnace components, should aim for a factory cost of $400-600 for a 54,000 Btu/hr unit. This appears to be a reasonable development goal.

- No major physical impediments are forseen to MHHP product adoption (Table 2). Despite its possible larger size and weight, the fuel-fired MHHP product should be acceptable for most applications within the residential sector.

A preliminary characterization of the commercial HVAC market (Fig. 11) indicated that it may hold some opportunities for the MHHP, but that competition in this market segment is likely to be intense during the next 10 to 15 years.

- The commercial market has a larger need for cooling. Larger commercial buildings are cooling-load dominated and the currently available electrically-driven devices are very efficient.

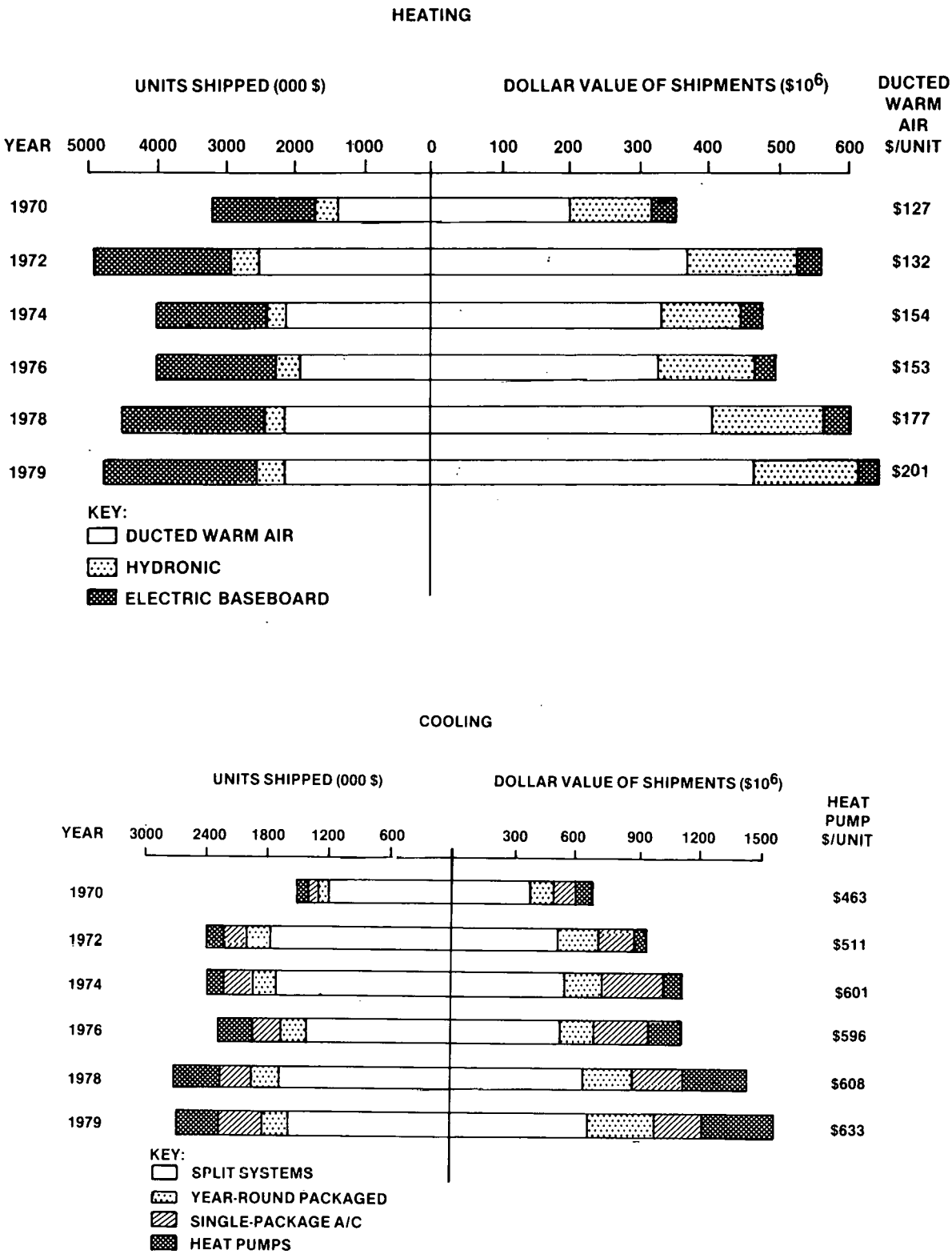

Figure 9. Annual Shipments of Residential Heating and Cooling Equipment

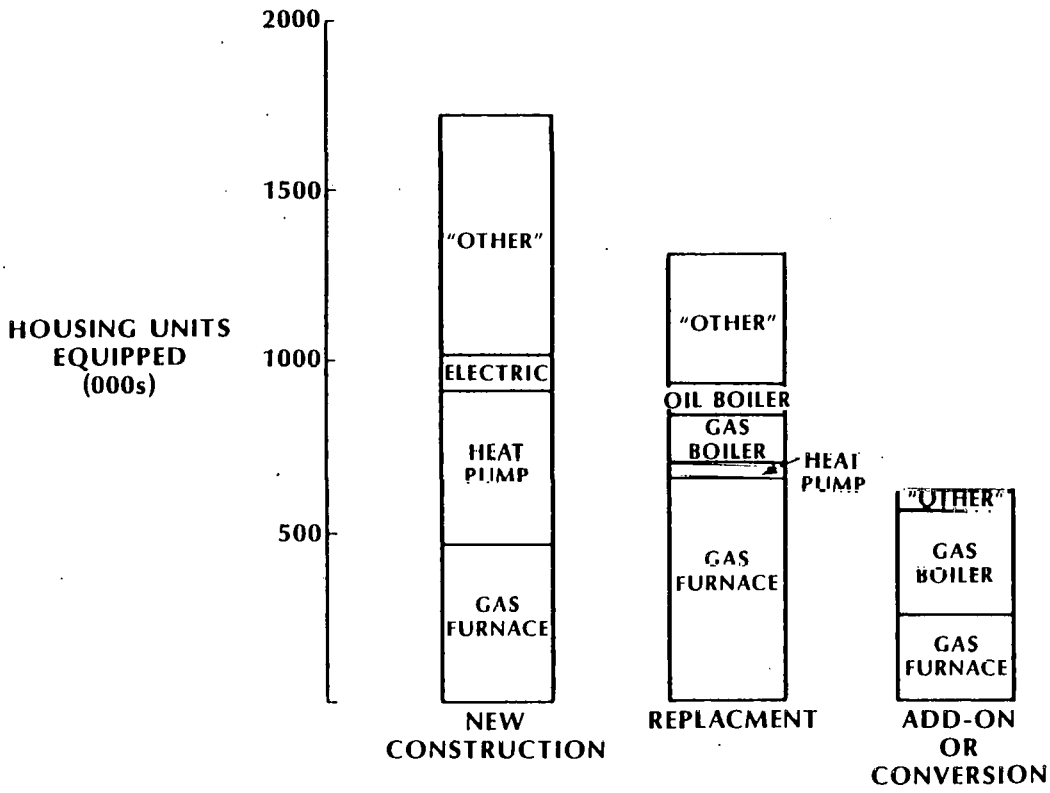

Figure 10. Residential Heating Equipment Use

Table 2

Physical Characteristics Comparison

Unit	Volume Comparison m^3	(ft^3)	Weight Comparison kg	(lb)
Residential Split System Electric Heat Pump	0.7-1.0	(25-35)	113-159	(250-350)
Residential Furnace Only	0.4-0.6	(15-20)	68-79	(150-175)
Furnace and A/C Combination	0.7-1.0	(25-35)	113-159	(250-350)
Fuel-Fired MHHP	1.0-1.3	(35-45)	204-250	(450-550)

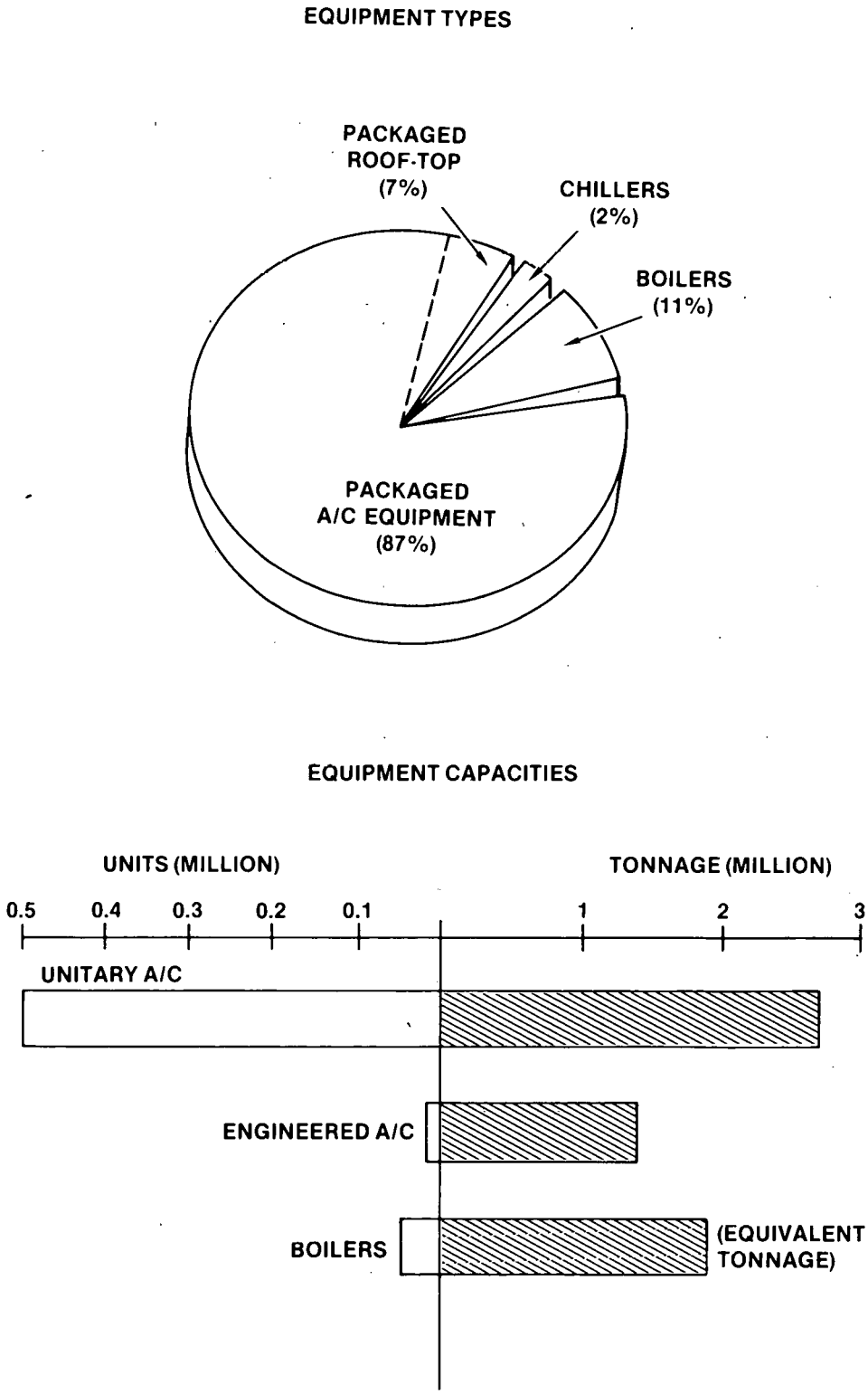

Figure 11. Commercial Building Space Conditioning Equipment Classifications

- Advanced, highly efficient technologies are expected to be introduced and agressively marketed during the 1980's. The commercial sector is the focus of much HVAC development activity. During the 1980's several significant developments are expected. These include introduction of advanced unitary space conditioning equipment with an electric COP of 4-5 and pulse combustion heating of 95 percent efficiency. In addition, engineered HVAC systems are likely to incorporate advanced electric heat pumps over this period. Finally, advanced gas fired heat pumps are expected to be introduced.

- Allowable unit costs for commercial equipment are projected to be 60 percent greater than residential equipment. Projected capital costs are greater for commercial MHHP units compared to residential units because of the greater restrictions in the commercial market on quality of construction and ease of maintenance and parts replacement.

The implications of this activity are that MHHP products would encounter more competition than in other sectors. Fuel-driven MHHP cooling in particular would be at a disadvantage because of low-projected cooling COP.

Preliminary characterization efforts for the industrial marketplace indicated a number of features which suggest promise for the MHHP.

- There are significant amounts of waste heat produced in many industries (Fig. 12). A great number of U.S. industrial processes generate significant amounts of waste heat in the form of reject

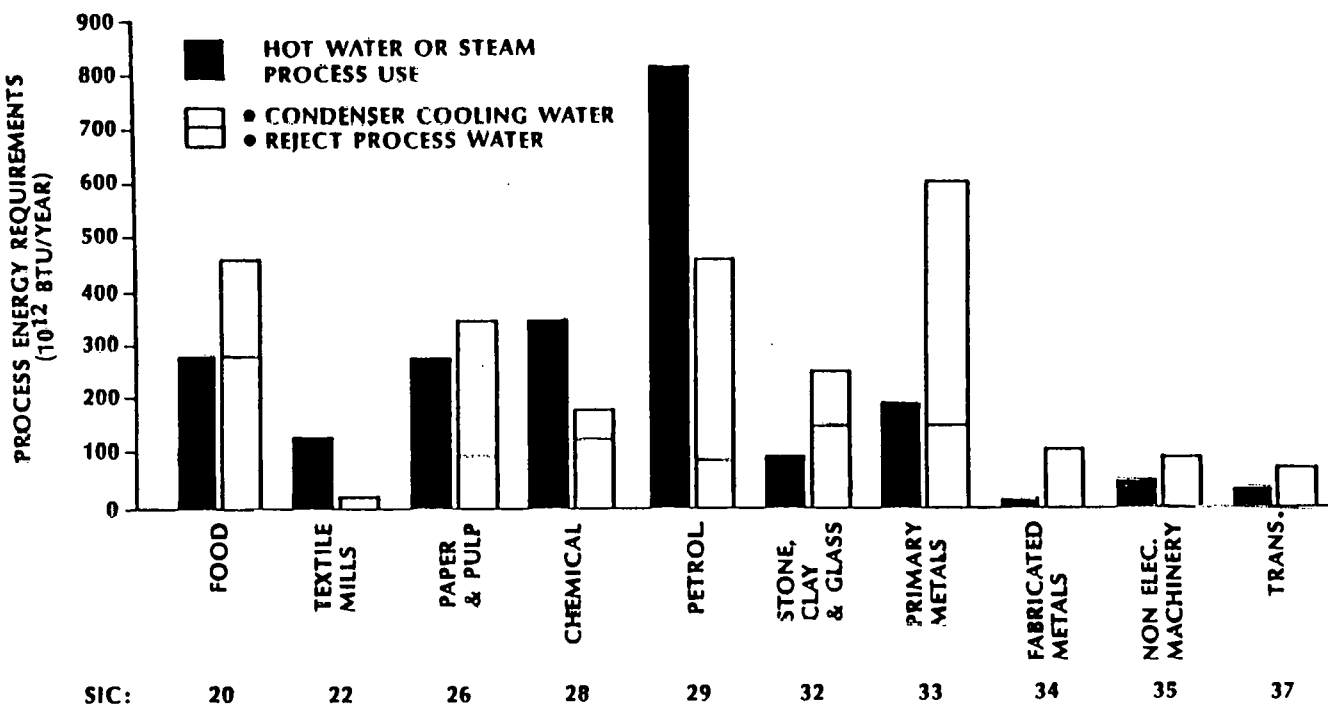

Figure 12. Industrial Waste Heat

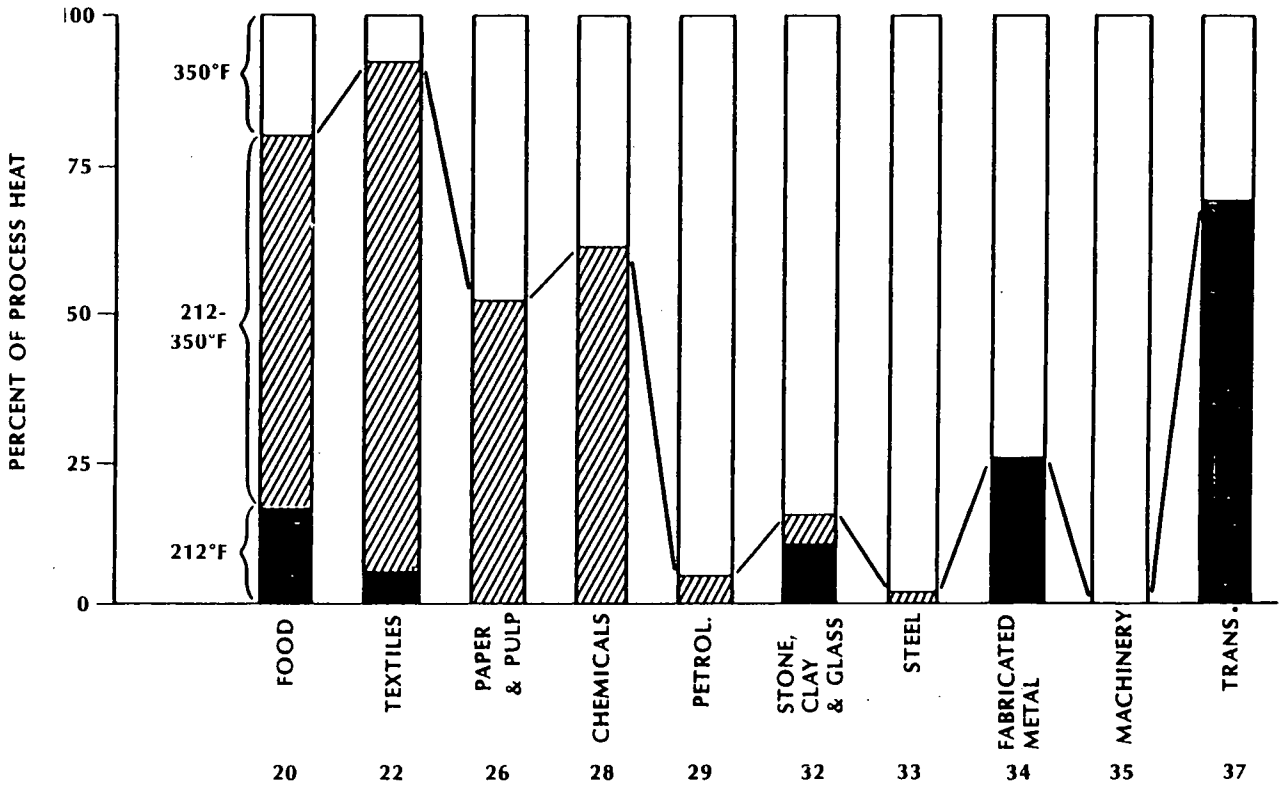

Figure 13. Industrial Process Heat Usage

process hot water or condenser cooling water. This is potentially available as a low grade or driving energy source for MHHP devices.

- There are a number of industries using process streams of low to intermediate temperatures (Fig. 13). The ten most energy-intensive industries use significant amounts of process energy with temperatures of 177°C (350°F) or less. Four industries in particular (food, textiles, paper and pulp and chemical) could be targets for the MHHP.

- Cost targets for the MHHP appear not to be prohibitive. The MHHP product configuration selected could compete in the industrial market with conventional and advanced process energy technologies such as traditional process heat recovery equipment, absorption heat pumps and boilers, the electric industrial heat pump and bottoming cycle equipment (e.g., organic rankine). These competing technologies are typically expensive.

- A MHHP refrigeration unit may have a unique competitive advantage. Because of its ability to operate at temperatures below 0°C (32°F), an envisioned MHHP refrigeration device may have an advantage, especially in the food industry, over conventional absorpton refrigeration equipment, which cannot operate below these temperatures because it uses water as a working medium.

Characterization of various metal hydride applications in the transportat market suggested that this may be an attractive early market for the MHHP.

- The transportation industry is concerned about energy efficiency. Energy costs are a significant component of total operating costs in this sector, and both transportation users and manufacturers have been actively looking for ways to improve vehicle efficiency as measured in miles per gallon of transportation fuel. MHHP waste heat-driven cooling, because it does not reduce the efficiency of vehicle engines, could be particularly attractive in this sector.

- There is no competition for waste heat-driven cooling. Most vehicular cooling equipment is less than three tons and uses a freon vapor compression cycle. This equipment is powered by belts from the vehicle engine for truck/tractor air conditioning, reducing vehicle engine efficiency. In other applications, vehicle/container cooling is driven by auxiliary diesel engines or indirectly off the vehicle engine through the vehicle's electrical system. No cooling product driven by engine-generated waste heat exists on the market.

4.2 MHHP MARKET APPLICATIONS

A process of identifying meaningful MHHP applications was a critical step in the market study because:

- the technology is inherently flexible and adaptable to a range of uses, and,

- at this stage of technology development, no application envisioned could be eliminated from consideration on a purely technical basis.

Classifying and ultimately reducing the variety of possible MHHP applications was required in order to proceed efficiently with engineering development.

The first step in the MHHP definition process was the development of a sixteen-cell matrix (Fig. 14) consisting of four MHHP uses and four possible market sectors. Within this framework, most possible MHHP functions and applications could be considered and evaluated on the basis of engineering judgement. This framework was developed from both a technical understanding of the nature of MHHP technology, as well as an understanding of the pertinent characteristics of the four major energy consuming sectors of the U.S. economy.

Booz Allen identified four functional uses for MHHP technology that were based on the previous research and development of SoCal and Solar and the projected performance of metal hydride devices under real world conditions. The functional capabilities of the technology are described below:

- Stationary space conditioning of buildings. MHHP technology could be useful in at least supplementing conventional HVAC equipment. The MHHP technology appears promising in residential and commerci

MHHP USES	POSSIBLE MARKET SECTORS			
	RESIDENTIAL	COMMERCIAL	INDUSTRIAL	TRANSPORTATION
• STATIONARY SPACE CONDITIONING	●	●	●	
• HEAT OR TEMPERATURE BOOST		●	●	
• REFRIGERATION			●	●
• MOBILE/TRANSPORATION AIR CONDITIONING				●

Figure 14. MHHP Uses

structures because of its ability to deliver both heating and cooling energy. Further, a MHHP device intended for these applications would likely have a minimum number of moving parts, which could provide:

- a long equipment lifetime, comparable to that of conventional HVAC equipment now on the market, and
- low maintenance requirements for a MHHP device, which could be a competitive advantage in the residential and commercial markets.

- Heat or temperature boost. The MHHP technology has the ability to use and interact with a variety of other low grade heat sources including air, water, waste heat from processes and devices, as well as solar energy. In addition, MHHP technology can provide almost 50 percent higher temperature lifting than the vapor compression heat pumps now on the market. This means that a MHHP could provide a high temperature stream for various processes and this feature widens the range of applications for the technology.

- Refrigeration. MHHP devices can deliver significant amounts of chilled air or water and might be used to at least supplement conventional fuel driven or electric cooling equipment. A distinct advantage of metal hydride technology in this use is its ability to function at subfreezing temperatures, which heat-driven absorption chillers using water as a working fluid cannot do. This may widen the range of application for MHHP refrigerating devices.

- Mobile Space Conditioning. The ability of MHHP technology to provide waste heat-driven cooling suggests the use of metal hydride devices in a range of mobile space conditioning applications such as truck or tractor cab air conditioning or truck trailer cooling.

A MHHP device in these applications may have distinct competit advantages over currently available equipment by not using the vehicle engine for mechanical driving power, which is likely to result in greater system reliability and efficiency. Further, a MHHP device could be located remote from the vehicle engine compartment, which could be a competitive advantage in the mobile space conditioning market.

These four functional uses of the metal hydride technology appeared promising as opportunities for near-term application. They served as one dimension of the analytical framework used to screen possible MHHP applications. The following section presents the second dimension of the framework - specific market sectors.

- Residential buildings - includes single family homes and multi-family buildings, which together constitute 21 percent of U.S. total energy use. In numbers of potential applications (85 million individual dwelling units), the residential sector represents the largest potential market for the MHHP technology. The dominant pattern of energy use in homes is for space heating (60%) with a smaller requirement (5%) for cooling energy.

- Commercial buildings - represents the second largest potential market for the MHHP, in terms of numbers of applications (four million separate commercial buildings) and represents 16 percent of U.S. energy use. Heating and cooling energy use is more balanced within this sector (43 and 22% of total energy consumption, respectively).

- Industry processes - use 37 percent of U.S. total energy needs, of which a small amount (less than 5 percent of industrial consumption) is required for space conditioning. There are about 156,000 establishments in the ten most energy-intense U.S. manufacturing industries, which constitutes the potential industrial market for MHHP devices[1].

- Transportation - Accounts for 26 percent of U.S. energy use. Excluding transport fuels, the predominant energy need is for cooling energy in a variety of vehicles and mobile containers.

Figure 14 presents the matrix of uses and market sectors which was employed to represent the universe of possible MHHP aplications. Each cell of the matrix was examined to judge whether it represented a significant potential market[2] for energy equipment. From this examination, eight of the sixteen

---

[1]Source: Oak Ridge National Laboratory: Industrial Energy Use Data Book, 1980

[2]The evaluation of a "signficiant potential market" included quantitative factors (e.g., market size in unit sales per year, market growth in compounded annual growth rates) and qualitative factors (e.g., history of market segment to embrace new technologies, such as the electric heat pump in the residential sector).

...sible market/use combinations were eliminated, as follows:

- Transportation air conditioning, which is definitionally meaningless in all but the transportation sector (3 segments eliminated).
- Stationary space conditioning and temperature boost in the transportation sector, which are insignificant in terms of energy use (2 segments).
- Temperature boost in the residential sector, for which no addressable market was judged to exist (1 segment).
- Refrigeration in residential and commercial buildings, which is a very small component of energy use relative to space conditioning (2 segments).

This process of matching metal hydride uses and markets enabled the MHHP development project to proceed with eight combinations that appeared to be practical applications of metal hydride technology. However, it was necessary to further refine and focus the development effort by defining and limiting the number of configurations that met both market needs and the capabilities of metal hydride technology.

4.3 SPECIFICATIONS FOR MHHP APPLICATIONS

Potential MHHP configurations were determined on the basis of four descriptive factors that characterize conventional energy devices serving various markets, as shown in Figure 15:

- Low grade heat sources are those by which basic energy transference is accomplished and by which the MHHP interacts with its environment. These sources include air, water, waste heat and solar energy.
- Driving sources are those that give motive force to the operation of an energy device. These sources include fossil fuels (oil, gas) and electricity, waste heat and solar energy.

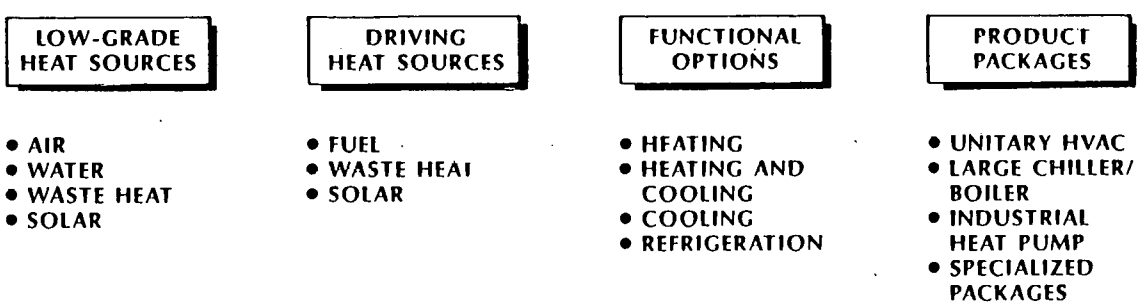

Figure 15. Potential Configurations

- Functional options include differing combinations of the form energy delivered by a device. Equipment can be designed to heat or cool exclusively, to perform both functions or to provide refrigeration.

- Packages relates to the scale and assembly of conventional equipment on the market serving different energy using segments. Packages include unitary equipment, boilers, industrial heat pumps and other specialized assemblies.

Taken together, these variables described the important features of energy equipment (example: an air source fuel-driven, heating and cooling unitary heat pump).

Based upon the variables above, fourteen different possible MHHP configurations were developed for the four market sectors. These configurations for residential, commercial and industrial sectors are shown in Figure 16 and are described as follows:

- In the residential sector, two heating-only devices were selected: one a fuel driven warm air furnace; and a similar product assisted by a low temperature solar energy system. Additionally, two heat pumps were selected: one driven by fuel; and one driven by a high temperature solar energy system.

- For the commercial buildings sector, four MHHP product configurations were selected. These products include three air source packaged heat pumps; one with conventional electrical vapor compression cooling technology; one driven by a medium temperature solar system; and one employing an air-cooled evaporator and condenser. In addition, a hydronic heating only product was included, comparable to a commercial boiler.

- For the industrial sector two heating only products were selected: one fossil fuel-driven; and one waste heat-driven. One waste heat-driven refrigeration unit was also selected.

For the transportation sector one basic MHHP product configuration was selected -- a waste heat-driven cooling device. However, the distinction between the applications of such a device in this sector is sharp:

- Truck or tractor cab air conditioning; a small cooling energy need which is required only during vehicle engine operation.

- Truck trailer or railway freight car refrigeration; a mid-sized cooling energy need requiring continuous operation independent of vehicle engine operation.

- Cargo ship hold refrigeration; requiring a larger, continuous cooling capability.

Because of the differences in scale, type, and duration of energy needs these applications, a waste heat driven MHHP refrigeration device would ta

Residential

TYPE OF UNIT	KEY FEATURES
• FURNACE	FUEL-DRIVEN HEATING ONLY MHHP; USES AIR AS LOW-GRADE HEAT SOURCE; MAY BE USED WITH OR WITHOUT CONVENTIONAL ELECTRIC A/C
• FUEL-FIRED HEAT PUMP	FUEL-DRIVEN HEATING AND COOLING MHHP UNIT; SINGLE PACKAGE OR SPLIT SYSTEM; USES AIR-COOLED EVAPORATOR AND CONDENSER
• SOLAR-ASSISTED HEAT PUMP	FUEL-DRIVEN HEATING ONLY MHHP; USES LOW-GRADE SOLAR TO BOOST H.P. COP; MAY BE USED WITH OR WITHOUT ELECTRIC A/C
• SOLAR-DRIVEN HEAT PUMP	REQUIRES MEDIUM TO HIGH TEMPERATURE SOLAR SYSTEM (150°F+) TO DRIVE AIR SOURCE HEAT PUMP AND COOLING CYCLE; MAY ALSO USE SOLAR AS LOW-GRADE HEAT SOURCE

Commercial

TYPE OF UNIT	KEY FEATURES
• PACKAGED FUEL-FIRED UNITARY HEATING/COOLING UNIT	FACTORY ASSEMBLED, CENTRAL SYSTEM HEAT PUMP. USES AIR COOLED EVAPORATOR AND CONDENSER. CAN BE EITHER SINGLE PACKAGE OR SPLIT SYSTEM.
• PACKAGED FUEL-FIRED HEATING/ ELECTRIC COOLING UNIT	FUEL-DRIVEN, HEATING-ONLY MHHP IN A SINGLE PACKAGE WITH COOLING. USES AIR AS HEAT SOURCE. USES ELECTRICALLY DRIVEN VAPOR COMPRESSION FOR COOLING.
• PACKAGED SOLAR-DRIVEN HEATING/COOLING UNIT	USES MEDIUM GRADE SOLAR ENERGY TO DRIVE AIR-SOURCE MHHP. CAN USE EITHER AIR OR SOLAR AS HEAT SOURCE.
• FUEL-FIRED HEATING ONLY BOILER SUBSTITUTE UNIT	USES LOW-GRADE WASTE HEAT WITH A FOSSIL FUEL HEAT SOURCE TO PROVIDE LOW PRESSURE STEAM.

Industrial

CONFIGURATION	APPLICATION REQUIREMENTS
HEAT AMPLIFIER	• LOW LEVEL HEAT SOURCE • PROCESS NEED FOR HOT WATER OR LOW PRESSURE STEAM
TEMPERATURE UPGRADER	• LOW TEMPERATURE HEAT SINK • INTERMEDIATE TEMPERATURE HEAT SOURCE • NEED FOR HIGH TEMPERATURE PROCESS <375°F
REFRIGERATION UNIT	• LOW TEMPERATURE HEAT SINK • INTERMEDIATE TEMPERATURE HEAT SOURCE • NEED FOR PROCESS COOLING

Figure 16. Definition of Residential, Commercial and Industrial MHHP Project Configuration

a very different form in each application. Thus, these applications represent three distinct configurations applicable to the transportation sector.

4.4 SCREENING CRITERIA

This step of the market analysis was essentially a competitive assessment of each of the fourteen selected MHHP configurations. Information was developed from secondary sources and industry interviews on both market and technical factors that could inhibit or encourage adoption of metal hydride technology. The aim of this effort was to reduce the number of MHHP configurations considered for development from fourteen to a few that appear to hold the greatest near term potential.

A set of fourteen screening criteria was developed, which could be used to qualitatively evaluate the fit between each MHHP configuration and its respective market segment. In effect, these criteria, shown in Figure 17, served as qualitative measures of market, technical or other risks.

Specifically, three groups of ranking criteria were identified:

- Market criteria - this category included two measures of the attractiveness of an individual market: its overall size in the 1985-90 time frame and the portion of the market to which the MHHP could be addressed. A criterion concerning market structure was included, to provide judgement of the ability of the MHHP to adapt to the technology distribution system (from factory to end user) within each market segment. Finally, two economic criteria were included, as measures of the ability of the MHHP to compete with conventional or advanced energy products on a first cost or life cycle cost basis.

TECHNICAL (40%)	MARKET (50%)	OTHER (10%)
• SIZE, WEIGHT	• POTENTIAL IN 1985-1990	• TAX CREDIT
• SAFETY		
• THERMAL CAPACITY	• ADDRESSABLE SIZE	• NOISE
• TEMPERATURE RANGE	• ADAPTABILITY TO TECHNOLOGY DISTRIBUTION SYSTEM	• COMPETITIVE TECHNOLOGY ADVANTAGES/DISADVANTAGES
• COMPETITIVE TECHNOLOGY STATUS	• MAXIMUM FACTORY COST	
• DEVELOPMENT RISK	• COMPETITIVE TECHNOLOGY ECONOMICS	

Figure 17. Screening Criteria

- Technical criteria - this category included qualitative measures of the ability of the MHHP to compete with conventional devices on performance measures such as thermal capacity, operating temperature range and safety and on physical features such as size and weight. In addition a criterion was included dealing with the introduction of advanced technologies in each market segment, increasing the competition the MHHP might face. Finally, a criterion of development risk was included that served as a qualitative measure of likelihood that the MHHP development program could design, engineer and construct a unit that met or approached the physical and operating parameters imposed by competing technologies.

- Other measures - this category was included to consider any unique competitive advantages or disadvantages of the MHHP based on the nature of other technologies or the nature of the markets themselves. Included was a measure such as the applicability of tax credits to the MHHP which might improve their economic competitiveness. Also included was a factor to account for the silent operation of metal hydride devices which could be a distinctly favorable feature in certain applications. Finally, a factor measuring other positive or negative features was included. An example of such a feature would be the ability of industrial MHHP refrigeration units to operate at temperatures below 0°C (32°F).

Taken together, these criteria enabled the MHHP development team to make judgements about the favorable or unfavorable chances for metal hydride adoption for each configuration and market combination. Before this judgemental ranking took place, however, the criteria were weighted.

4.5 WEIGHTING OF THE CRITERIA

The aim of the entire MHHP development program was to develop a heat pump that will find acceptance because it competed favorably with other technologies in providing energy. This involves two elements of risk:

- Market risk - the chance that the needs of the market for equipment first cost and operating costs would favor competing technologies over MHHP technology; also, the risk that the size of a market would be reduced or that its distribution, sales and service channels would not accommodate the MHHP easily.

- Technical risk - the chance that the MHHP would not be developed to perform as efficiently or more efficiently than competing conventional and advanced equipment; also the chance that some other features would negatively affect MHHP adoption.

It was the judgement of the MHHP development team that the technical category was rated at 40 percent, the market category at 50 percent and other factors at 10 percent (Fig. 17). However, within each category, individual criteria were felt to have differing effects on the adoption of the technology. Thus

they were individually weighted by consensus between SoCal, Booz Allen Solar.

As with the weighting of individual market and technical risk factors, the team members were involved in scoring the commercial potential of individual MHHP configurations as described below:

- A total of a thousand points were assigned to the criteria (500 to market factors, 400 to technical and 100 to other factors); these were allocated to individual criteria according to their weights shown in Figure 17.
- A forced-ranking procedure was employed to establish the scores for each application on a scale of 1 (most market or technical risk) to 14 (least market risk).
- Scores from each of the three team members were summed by category of criteria (market, technical and other).
- These scores were summed and averaged to produce a consensus weighted average total.

What emerged from this process was two fairly distinct tiers of MHHP applications, as shown in Figure 18.

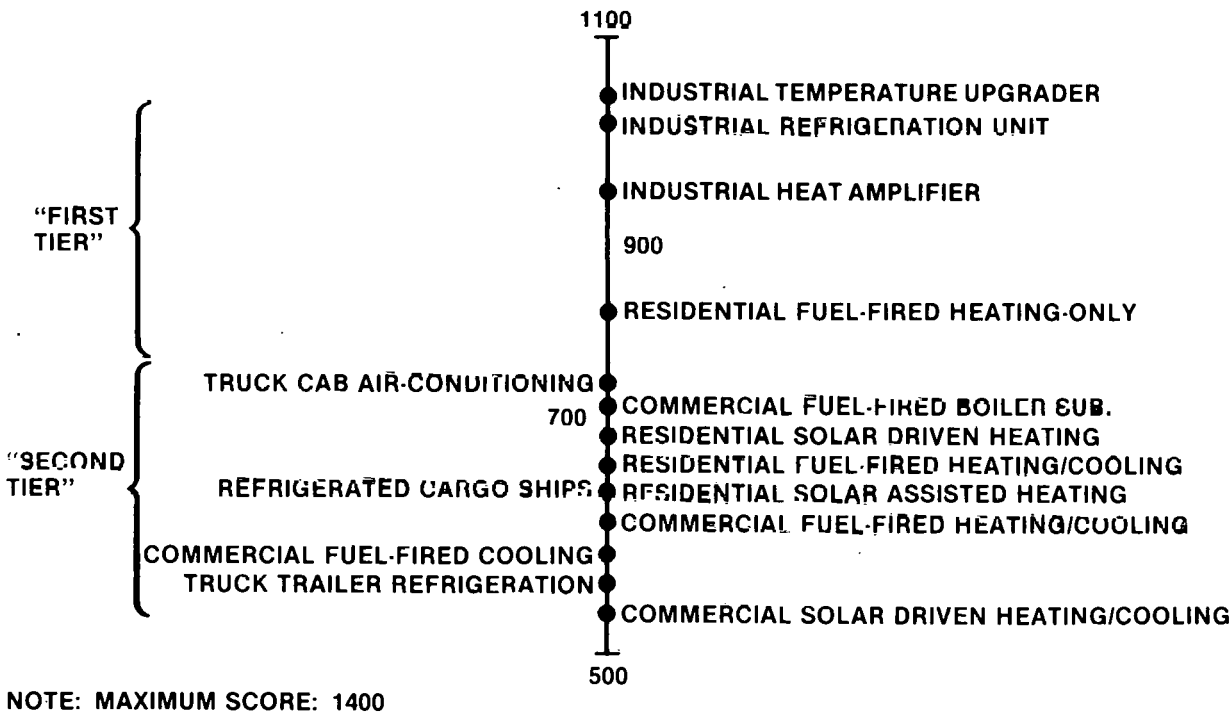

Figure 18. Ranking of MHHP Configuration

- A first tier of three industrial and one residential system judged to have high commercial potential.
- A second tier of ten MHHP products with lower and more closely grouped scores of commercial potential.

This first tier of MHHP applications thus represents a team consensus of those that offered the most commercial potential and should guide the design development work of SoCal/Solar.

4.6 SELECTION OF TOP MHHP APPLICATIONS

A shown in Figure 19, three of the four first tier MHHP configurations were judged to have relatively more technical than market risk. The industrial refrigeration configuration, however, was felt likely to confront a more uncertain market situation than to encounter difficulties in its technical development and competitive performance position. Because of this, the industrial refrigeration configuration was eliminated.

A result of the Booz Allen effort was the recommendation that future metal hydride research and development work should focus on the technical and market parameters associated with one of the following three applications, in order:

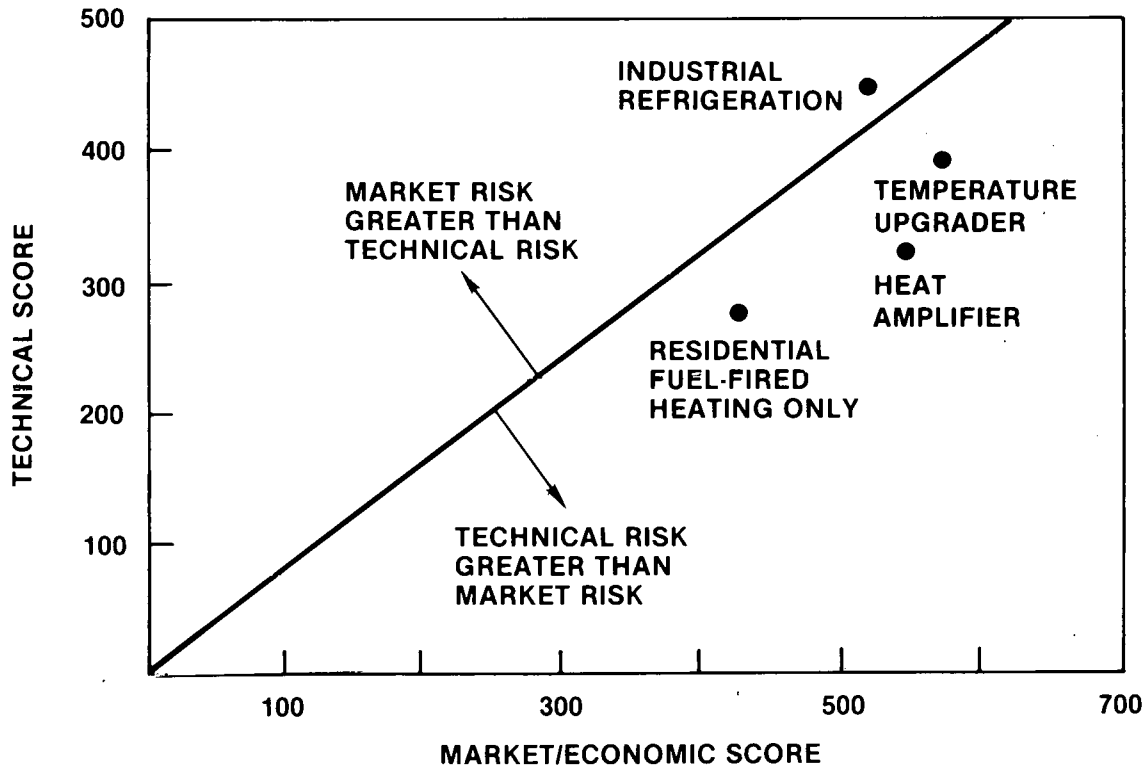

Figure 19. Comparison of Market at Technical Risks of Top Ranked MHHP Configurations

1. A waste heat driven industrial temperature upgrader.

2. A fuel-driven industrial heat amplifier.

3. A fuel-driven heating-only product for residential applications.

4.7 DESCRIPTION OF THE TOP MHHP APPLICATIONS

The three applications and their implications for MHHP design development are below:

1. <u>An Industrial Temperature Upgrading Product Using Metal Hydride Technology is Viewed as the Most Promising Design Configuration</u>

   As shown in Figure 20, the industrial MHHP would be designed to be driven by a waste heat stream to raise the temperature of a thermal process stream. As shown in the figure, this unit could be designed to operate in the following three-step cycle:

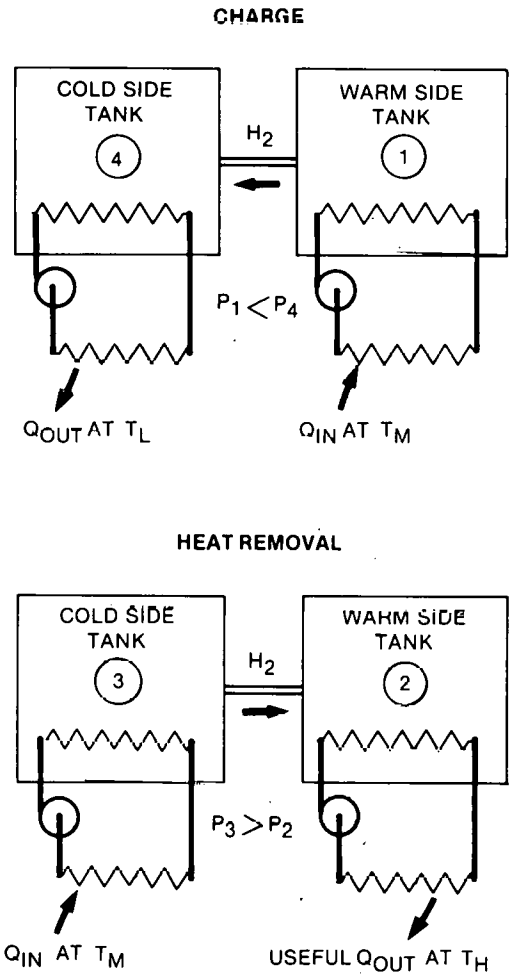

	LOW TEMPERATURE	HIGH TEMPERATURE
T_H	100-140°C (210-280°F)	140-190°C (280-375°F)
T_M	55-75°C (130-165°F)	70-110°C (160-230°F)
T_L	5-20°C (40-70°F)	– 1-45°C (30-110°F)

Figure 20. Temperature Upgrader Unit

- Use of intermediate temperature waste heat [from 71 to 110°C (160-230°F)] to charge the metal hydrides.

- Raising the same intermediate temperature energy stream, when charging, about 21-35°C (70-95°F), up to process temperatures of about 191°C (375°F).

- When discharging, the unit would reject heat to an available low temperature sink.

In this operating cycle, an industrial temperature upgrade MHHP device could be useful in about 5,000 industrial plants particularly in the food, textiles, pulp and paper and chemical industries. An example of such an application would be in a pulp mill where a 71-82°C (160-180°F) heat source is available from grinding machines. This would activate the charging cycle of the device, which would upgrade the same stream to about 149-177°C (300-350°F) process stream. In the discharging mode the device would employ 32-38°C (90-100°F) plant effluent as a heat sink.

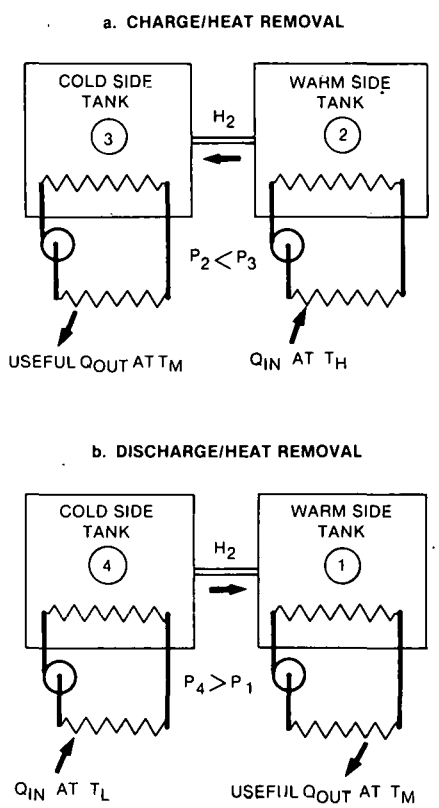

	LOW GRADE HEAT	HIGH GRADE HEAT (STEAM)
T_H	138°C (280°F)	191°C (375°F)
T_M	99-82°C (120-180°F)	121°C (250°F)
T_L	16-24°C (60-75°F)	38°C (100°F)

Figure 21. Heat Amplification Unit

2. A Fuel-Driven Heat Amplifier is also seen as a Promising MHHP Industrial Application

In this configuration the device would be functionally similar to the electrically driven industrial heat pump now on the market (Fig. 21):

- A fossil-fueled heat source would charge the device.
- The device would amplify a low level heat source to temperatures up to 138°C (280°F) for waste heat streams in the temperature range of 74°C (165°F), and up to 191°C (375°F) for waste heat at 121°C (250°F).

These capabilities make this device appear suitable for U.S. industrial plants in such industries as food, textiles, pulp and paper, and chemical. An example of its application might be in the meat packing industry, where 32°C (90°F) waste heat from refrigerator condensers could be upgraded by the device to provide 82°C (180°F) hot water for plant cleanup operations.

3. The Third Recommended Application is a Fuel-Fired Metal Hydride Device to Provide Residential Space Heating

This device (Fig. 22) would operate in a fashion similar to the fuel-fired industrial heat amplifier, but within lower temperature

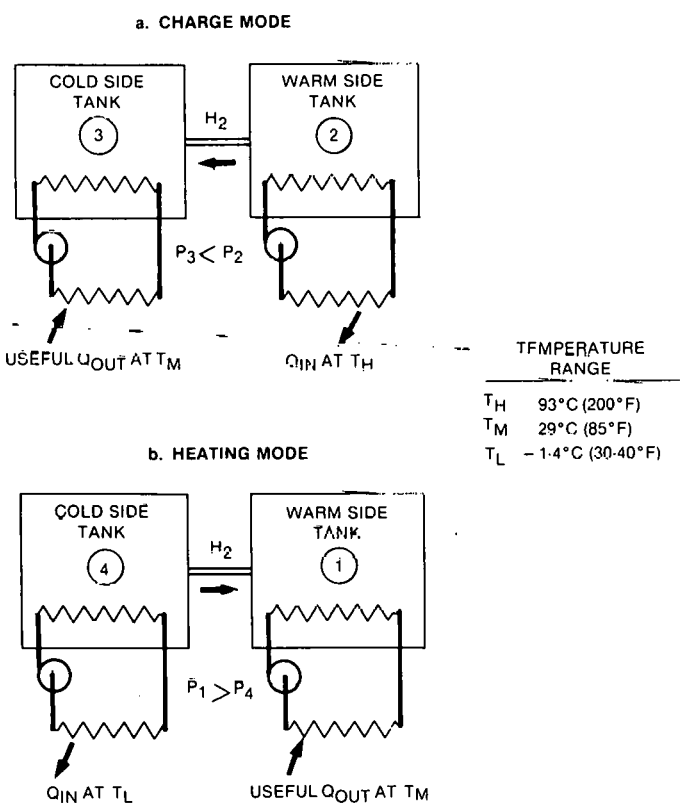

Figure 22. Space Heating Unit

ranges suitable for residential warm air space heating. Like warm air furnaces now on the market, this MHHP device would be fossil-fuel driven. It would use air as a low grade heat source and could be installed with or without conventional electric air conditioning. This furnace MHHP configuration would compete with other fossil-fired warm air furnaces, which represents the largest segment of the residential heating market (60% of 1980 shipment of residential central heating units).

4.8 FINAL MARKET RESULT

Table 3 is a summary of market-related technical requirements for the three MHHP applications. As a result of this extensive market survey and the collective opinion of the team members, the decision was made that the most promising MHHP configuration was the industrial waste heat driven temperature upgrade cycle. This configuration was felt to have the greatest market potential as well as the highest probability of technical success. Further engineering development efforts focused in this direction.

Table 3

Summary of Market-Related Technical Requirements

Target Market	Product Configuration	Typical Operating Temperatures	Factory Cost Target ($/ton)[1]	Typical Capacities (tons)
Industrial	Temperature Upgrade	Low Temperature T_H = 100-140°C (210-280°F) T_M = 55-75°C (130-165°F) T_L = 5-20°C (40-70°F) High Temperature T_H = 140-190°C (280-375°F) T_M = 70-110°C (160-230°F) T_L = -1-45°C (30-110°F)	800-1000	40-1500
Industrial	Heat Amplifier	Low Grade Heat T_H = ~138°C (280°F) T_M = 49-82°C (120-180°F) T_L = 16-24°C (60-75°F) High Grade Heat T_H = ~191°C (375°F) T_M = 121°C (250°F) T_L = 38°C (100°F)	550-750	40-1500
Residential	Space Heating	T_H = 93°C (200°F) T_M = 29°C (85°F) T_L = -1-4°C (30-40°F)	400-600[2]	3-10

[1] 1 ton = 12,000 Btu/hr

[2] based on a 4.5 ton unit

5

SYSTEM DESIGN ANALYSIS

This section describes each important consideration in the design of the MHHP. Hydride materials, heat exchanger design, performance, filters, controls and economics are all discussed. The design analysis approach is shown in Figure 23.

5.1 HYDRIDE MATERIALS

The hydride materials are the single most important component of the metal hydride heat pump. The properties of the AB_5 alloys available for use in the MHHP are the most critical data needed to predict the performance of the heat pump and to properly size the components. An extensive review of the AB_5 hydride literature lead to a detailed listing of alloys and the properties available for each alloy (see Appendix 1). Thirty-two papers which contained data on 122 different alloy compositions, all based on the AB_5 system, were reviewed. A total of twelve properties pertaining to hydride performance and utility were considered. Properties such as the van't Hoff relationship, plateau shape, hydrogen/metal ratio (H/M), heat of formation (ΔH_f) and hysteresis identify the possible operating and performance level of the alloys, whereas the specific heat and thermal conductivity are required for the thermal design of the intended application. The other properties, such as comminution, long term degradation, contamination, safety and chemical stability relate to the practicality of the alloy.

For each alloy and property listed in Appendix 1, the reference in which the appropriate data appears is entered. The number of alloys presented is quite great indicating the extent of the AB_5 type hydride research. However, very few alloys have a relatively complete set of data. In general, the most widely measured property is the pressure-composition isotherm, usually made at room temperature in desorption.

An extensive review of the AB_5 alloy data led to the identification of a number of alloy pairs that could be used in a temperature upgrade cycle. Table 4 lists the AB_5-type alloys with temperature-pressure properties acceptable for use in the temperature range specified by the Booz Allen market study. Both the low and high operating temperature ranges are identified in Table 5.

A clear distinction between the cold side alloys and the warm side alloys is apparent. The cold side alloys are typically less stable than $LaNi_5$ allowing the replacement of La with mischmetal. This is a highly desirable situation with regards to the cost of the alloy. However, the warm side alloys are typically more stable than $LaNi_5$. This is achieved by replacing a portion of the nickel with either Al, Mn or Cu.

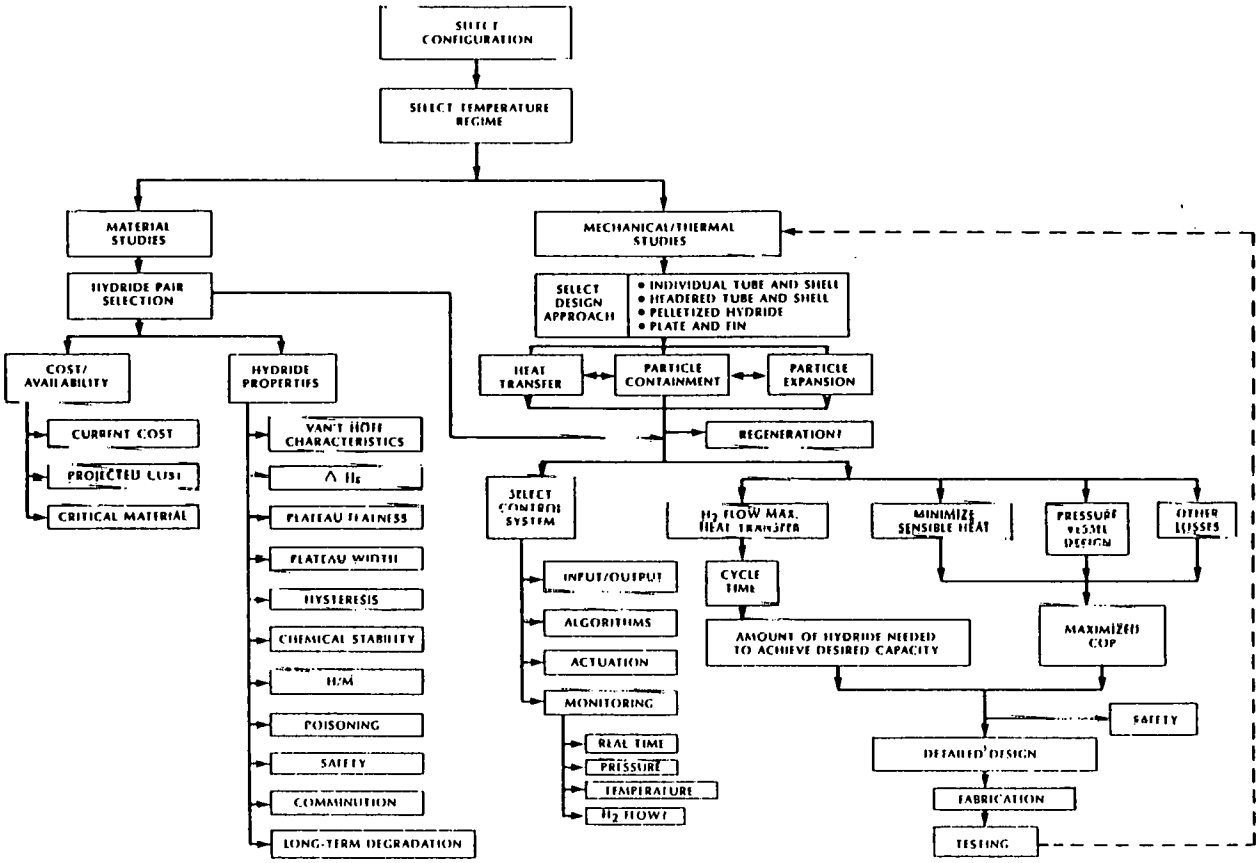

Figure 23. Design Procedure Flowchart

The rather lengthy list of candidate alloys would suggest a large number of possible alloys pairs and, indeed, this is the case. Table 6 gives for illustrative purposes twenty alloy pairs along with the typical P-T design conditions. The data is taken from the literature and the exact design condition must necessarily be confirmed experimentally.

The candidate alloy pairs were reduced to a few pairs that showed the greatest promise. All of the pertinent hydride parameters were considered in this evaluation.

The material requirements for a metal hydride heat pump are specified by the operating temperatures. A MHHP requires two different hydrides to work in tandem, one alloy operating on the cold side and the other operating on the hot side. The plateau pressures must be such that the hydrogen will be driven between the two alloys. Naturally, the hysteresis between the absorption and desorption plateau pressures is an important factor in selection of the MHHP temperature-pressure cycle. The hysteresis between the absorption-desorption plateau pressures tends to lower the maximum ΔT at which the MHHP can operate.

Table 4

AB_5-Type Alloys

Cold Side Alloys

$LaNi_5$, $La_{0.6}Ca_{0.4}Ni_5$, $MMCo_5$, $Mm_{0.3}Ca_{0.7}Ni_5$

$Mm_{0.25}Ca_{0.75}Ni_5$, $MmNi_{4.5}Al_{0.5}$, $MmNi_{4.5}Cr_{0.5}$

$MmNi_{4.15}Fe_{0.85}$, $MmNi_4Fe_1$, $MmNi_{2.5}Co_{2.5}$

$MmNi_2Co_3$, $MmNi_1Co_4$, $CFMmNi_{4.8}Al_{0.2}$

$Mm_{0.5}Ca_{0.5}Ni_{4.5}Al_{0.5}$, $Mm_{0.5}Ca_{0.5}Cr_{0.5}$

$Mm_{0.5}Ca_{0.5}Ni_{4.5}Mn_{0.5}$, and $MmNi_{4.5}Cr_{0.25}Mn_{0.25}$

Warm Side Alloys

$LaCu_5$, $LaCo_5$, $LaNi_{4.9}Al_{0.1}$, $LaNi_{4.8}Al_{0.2}$

$LaNi_{4.75}Al_{0.25}$, $LaNi_{4.7}Al_{0.3}$, $LaNi_{4.6}Al_{0.4}$

$LaNi_{4.5}Al_{0.5}$, $LaNi_{4.6}Mn_{0.4}$, $LaNi_{3.0}Co_{2.0}$

$LaNi_{4.0}Cu_{1.0}$ and $CaNi_5$

Table 5

MHHP Temperature Upgrade Operating Conditions

Low Temperature		
T_H	100-140°C	(210-280°F)
T_M	55-75°C	(130-165°F)
T_L	5-20°C	(40-70°F)
High Temperature		
T_H	140-190°C	(280-375°F)
T_M	70-110°C	(160-230°F)
T_L	-1-45°C	(30-110°F)

Table 6

List of Possible Hydride Alloy Pairs

	Cold Side Alloy	T_L P(abs)	T_M P(des)	P(des)	T_H P(abs)	Warm Side Alloy
1	$LaNi_5$	20°C 1.62 atm	96°C 18 2 atm	2.43 atm	162°C 17.3 atm	$LaNi_{4.5}Al_{0.5}$
2	$MmNi_{4.15}Fe_{0.85}$	34°C 17.6 atm	96°C 78.3 atm	18.6 atm	142°C 67.0 atm	$LaNi_5$
3	$LaNi_5$	24°C 1.91 atm	94°C 17.2 atm	3.17 atm	144°C 15.2 atm*	$LaNi_{4.6}Mn_{0.4}$
4	$Mm_{0.5}Ca_{0.5}Ni_{4.5}Al_{0.5}$	20°C 1.44 atm*	94°C 20.7 atm	3.17 atm	150°C 17.9 atm*	$LaNi_{4.6}Mn_{0.4}$
5	$Mm_{0.5}Ca_{0.5}Ni_{4.5}Al_{0.5}$	20°C 144 atm*	96°C 22.0 atm	2.43 atm	180°C 19.9 atm	$LaNi_{4.5}Al_{0.5}$
6	$MmNi_{4.5}Cr_{0.25}Mn_{0.25}$	20°C 5.0 atm*	96°C 62 atm	5.0 atm	180°C 54 atm	$LaNi_{4.6}Al_{0.4}$
7	$Mm_{0.5}Ca_{0.5}Ni_{4.5}Al_{0.5}$	20°C 1.44 atm*	96°C 22.0 atm	5.04 atm	140°C 20.8 atm	$LaNi_{4.6}Al_{0.4}$
8	$MmNi_{2.5}Co_{2.5}$	20°C 1.60 atm*	96°C 31.2 atm	3.43 atm	180°C 29.3 atm	$LaNi_{4.5}Al_{0.5}$
9	$MmNi_{2.5}Co_{2.5}$	20°C 1.60 atm*	96°C 31.2 atm	3.41 atm	168°C 28.4 atm*	$LaNi_{4.6}Mn_{0.4}$
10	$MmNi_{2.5}Co_{2.5}$	20°C 1.60 atm*	96°C 31.2 atm	2.43 atm	180°C 26.3 atm	$LaNi_{4.5}Al_{0.5}$
11	$MmNi_2Co_3$	36°C 2.1 atm*	96°C 22.8 atm	5.04 atm	140°C 20.8 atm	$LaNi_{4.6}Al_{0.4}$
12	$MmNi_2Co_3$	22°C 1.05 atm*	96°C 22.8 atm	2.43 atm	170°C 21.0 atm	$LaNi_{4.6}Al_{0.5}$
13	$MmNi_2Co_3$	22°C 1.05 atm*	96°C 22.8 atm	3.41 atm	156°C 20.9 atm	$LaNi_{4.6}Mn_{0.4}$
14	$MmNiCo_4$	28°C 1.02 atm*	96°C 19.09 atm	2.43 atm	162°C 17.3 atm	$LaNi_{4.5}Al_{0.5}$
15	$MmNiCo_4$	28°C 1.02 atm*	96°C 19.09 atm	3.41 atm	150°C 17.87 atm	$LaNi_{4.6}Mn_{0.4}$
16	$La_{0.6}Ca_{0.4}Ni_5$	20°C 1.68 atm*	96°C 20.8 atm	2.43 atm	164°C 18.1 atm	$LaNi_{4.5}Al_{0.5}$
17	$La_{0.6}Ca_{0.4}Ni_5$	20°C 1.68 atm*	96°C 20.8 atm	3.41 atm	152°C 18.8 atm	$LaNi_{4.6}Mn_{0.4}$
18	$Mm_{0.3}Ca_{0.7}Ni_5$	20°C 3.51 atm	96°C 29 87 atm	4 58 atm	146°C 22.6 atm*	$LaCu_5$
19	$Mm_{0.25}Ca_{0.75}Ni_5$	20°C 3.3 atm*	96°C 40.7 atm	4.58 atm	150°C 30.2 atm	$LaCu_5$
20	$MmNi_{2.5}Co_{2.5}$	20°C 1.60 atm*	96°C 31.2 atm	4.58 atm	148°C 28.3 atm*	$LaCu_5$

*Data based on absorption values only.

e heat of formation of a metal hydride is relatively independent of temperature; this allows the mid-plateau pressure/temperature relationships to be presented on a van't Hoff diagram (where the logarithm of the pressure is given versus the inverse of the temperature). Figure 24 is an illustration of a van't Hoff plot of several metal hydride alloys. The information can also be conveniently displayed in analytical form by giving the equation of the straight line. This equation can take the form

$$RT \ n\ell P = \Delta H + T\Delta S$$

or

$$P = A \exp[-B/T]$$

where ΔH is the enthalpy of formation, ΔS is the change in entropy and A and B are constants in pressure and degrees absolute respectively. This allows the calculation of the mid-plateau pressure at any reasonable temperature. In addition, only a few experimental points are necessary to extrapolate the data to other temperatures.

The fundamental representation of the absorption-desorption hysteresis is $\ell n(P_a/P_b)$ as suggested by Lundin and Lynch (Ref. 2). This ratio remains fairly constant over a wide range of temperatures. This provides a means of approximating the absorption pressure when only the desorption data is available if absorption data for one condition is known.

Three alloy pairs were selected as applicable to a temperature upgrade MHHP application. The operating temperature range chosen was the high temperature condition as shown in Table 5. The alloy pairs selected were:

	Cold Side	Warm Side
1.	$LaNi_5$	$LaNi_{4.6}Al_{0.4}$
2.	$LaNi_5$	$LaNi_{4.5}Al_{0.5}$
3.	$MmNi_{4.15}Fe_{0.85}$	$LaNi_5$

The second combination showed promise in a MHHP temperature upgrade application whereas the other two do not appear acceptable and are presented for illustrative purposes.

Using the above analytical representations of the plateau pressure and the hysteresis, pressure and temperature plots of the alloy pairs over the appropriate temperature range were generated for each alloy pair considered. Figure 25 shows the plot for the $LaNi_5/LaNi_{4.6}Al_{0.4}$ alloy pair. The van't Hoff parameters used were $LaNi_5$: $A = 4.25 \times 10^5$ atm. and $B = 3712$ K (taken from Ref. 3) and $LaNi_{4.6}Al_{0.4}$: $A = 8.74 \times 10^5$ atm. and $B = 4451$ K (taken from Ref. 4), the hysteresis parameter $\ell n(P_{abs.}/P_{des.})$ was 0.19 and 0.13 for for $LaNi_5$ and $LaNi_{4.6}Al_{0.4}$ taken from References 3 and 4 respectively. This alloy pair does not meet the requirements of $T_M < 110°C$ and $T_H > 140°C$, but is presented to illustrate the importance of considering the effects of hysteresis. The $LaNi_{4.6}Al_{0.4}$ absorption pressure is approximately 3 atm. igher than the desorption pressure. If only desorption data were considered,

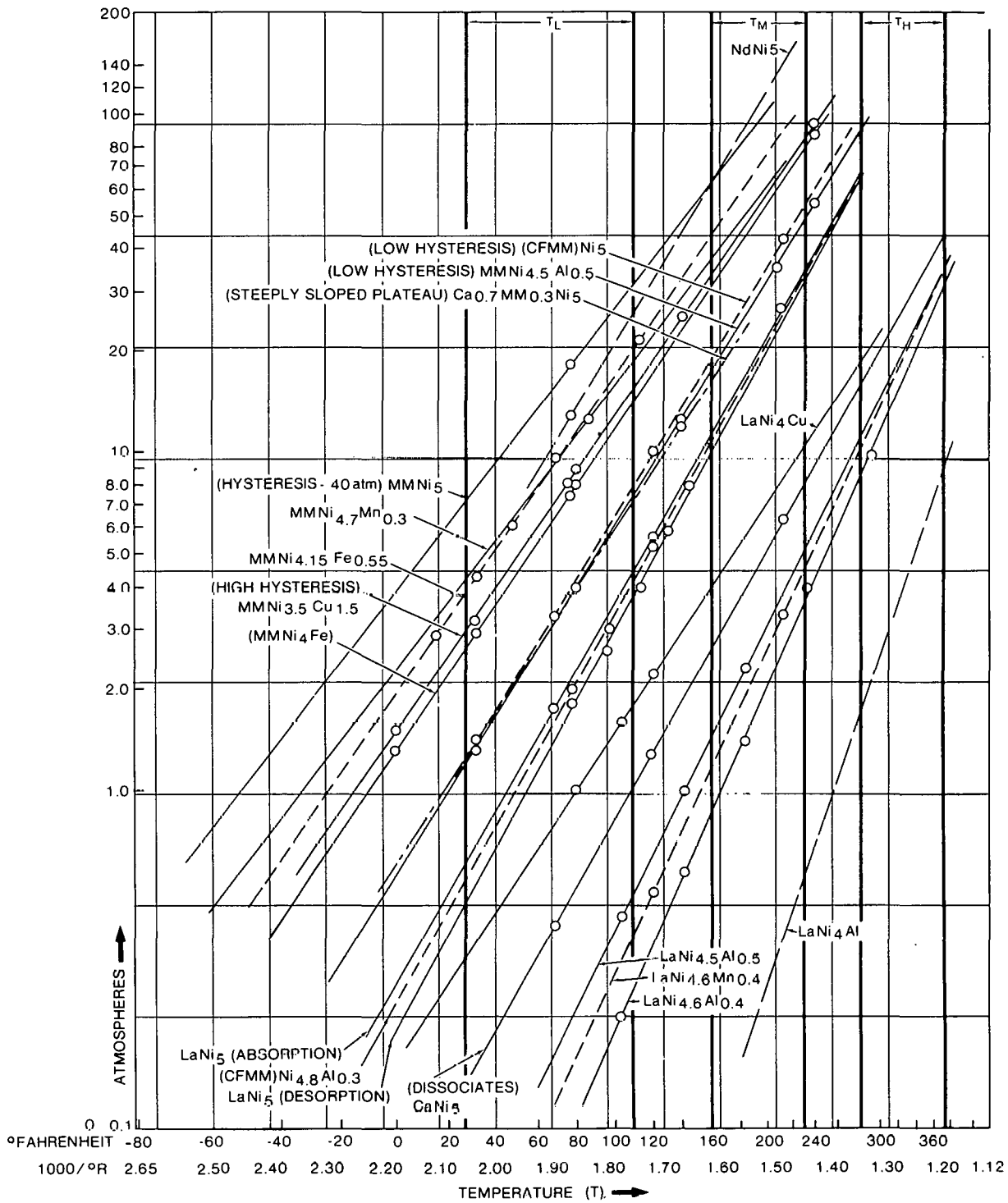

Figure 24. Pressure/Temperature Relationships at Mid-Plateau

cycle would work by relaxing the temperature requirement 4°C (i.e, T_M or T_H), whereas when the effects of hysteresis are considered a 12°C change in the temperature requirement is necessary. This represents a decrease in the temperature upgrade of nearly 25 percent.

The hydride alloy pair $LaNi_5/LaNi_{4.5}Al_{0.5}$ is an example of a combination that would operate in the specified temperature ranges. The van't Hoff parameters used were $LaNi_5$: A = 4.25 x 10^5 atm. and B = 3712 K (taken from Ref. 3) and $LaNi_{4.5}Al_{0.5}$: A = 5.97 x 10^5 atm. and B = 4580 K (taken from Ref. 4). The hysteresis parameter for $LaNi_5$ was 0.19 but due to a large difference in the reported values for $LaNi_{4.5}Al_{0.5}$, the calculations were performed twice using 0.08 (Ref. 4) and 0.52 (Ref. 5) with the results being shown in Figures 26 and 27 respectively. Even with the large variations in values for the hysteresis, the cycle will operate under either condition. As the hysteresis of the hot side alloy increases, the maximum upgrade temperature decreases. This is illustrated in the example P-T cycles, i.e., lowering T_H from 162°C to 144°C.

The third example of a possible alloy pair is $MMNi_{4.15}Fe_{0.85}/LaNi_5$ where the $LaNi_5$ is now the warm side alloy. The van't Hoff parameters used in the calculations were $MMNi_{4.15}Fe_{0.85}$: A = 2.97 x 10^5 atm and B = 3041 K (taken from Ref. 3) and $LaNi_5$: A = 4.25 x 10^5 atm and B = 3712 K (taken from Ref. 3). The hysteresis parameters used were 0.17 and 0.19 for $MMNi_{4.15}Fe_{0.85}$ and $LaNi_5$ respectively (taken from Ref. 3). As is shown in Figure 28 this alloy pair will sucessfully operate in a temperature upgrade cycle, however, the very high pressures required make it impractical.

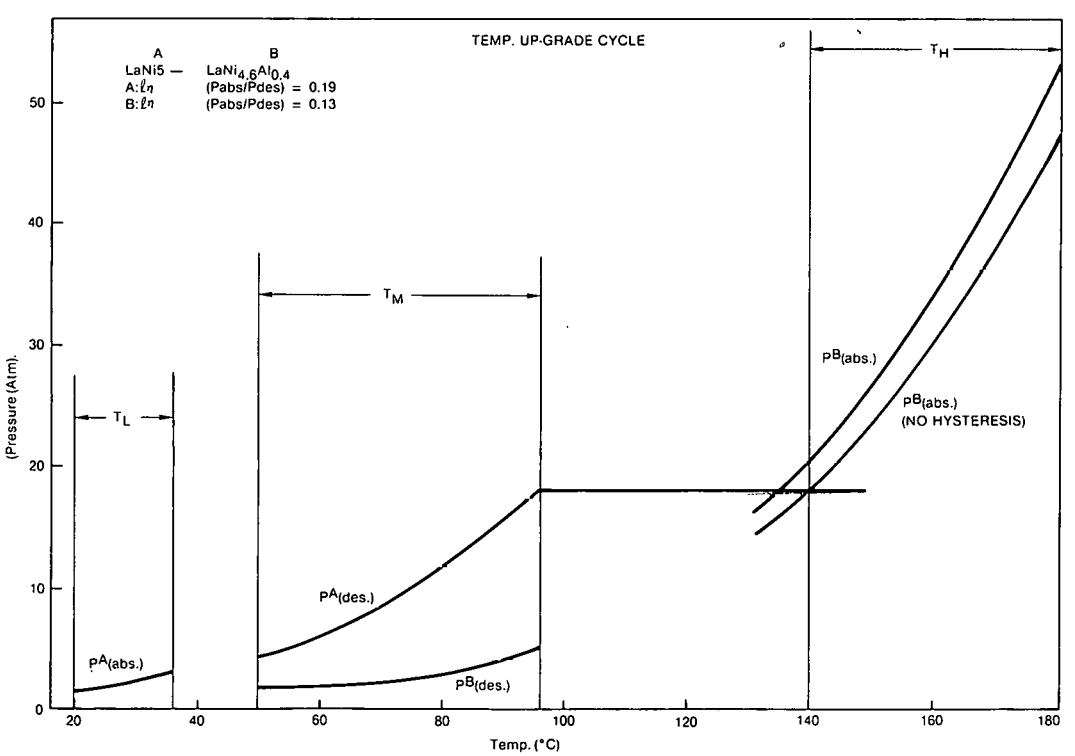

Figure 25. Pressure/Temperature Upgrade Cycle

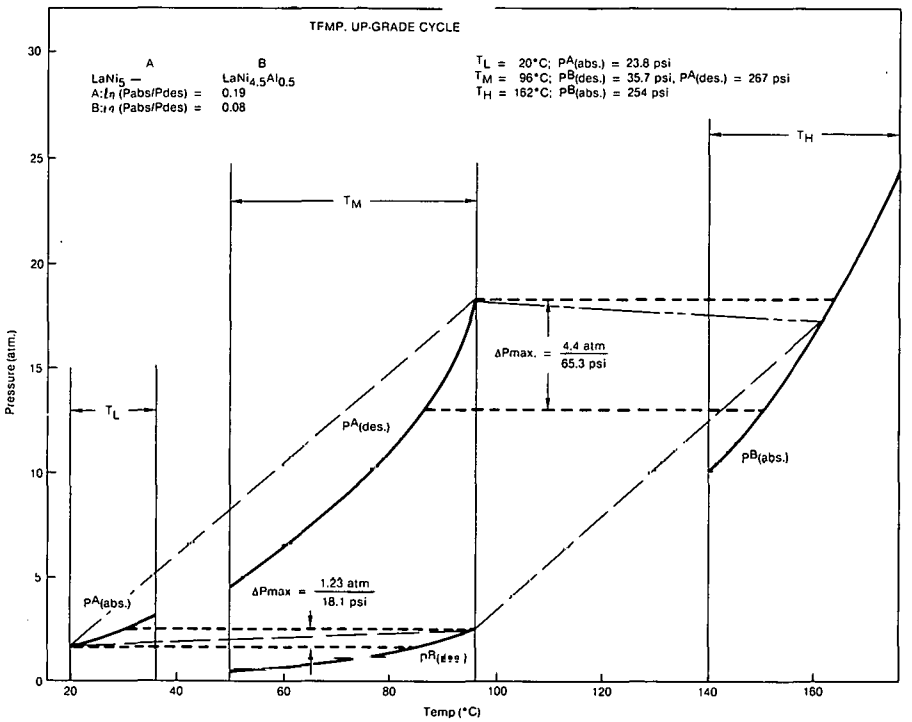

Figure 26. Pressure/Temperature Upgrade Cycle With Low Hysteresis

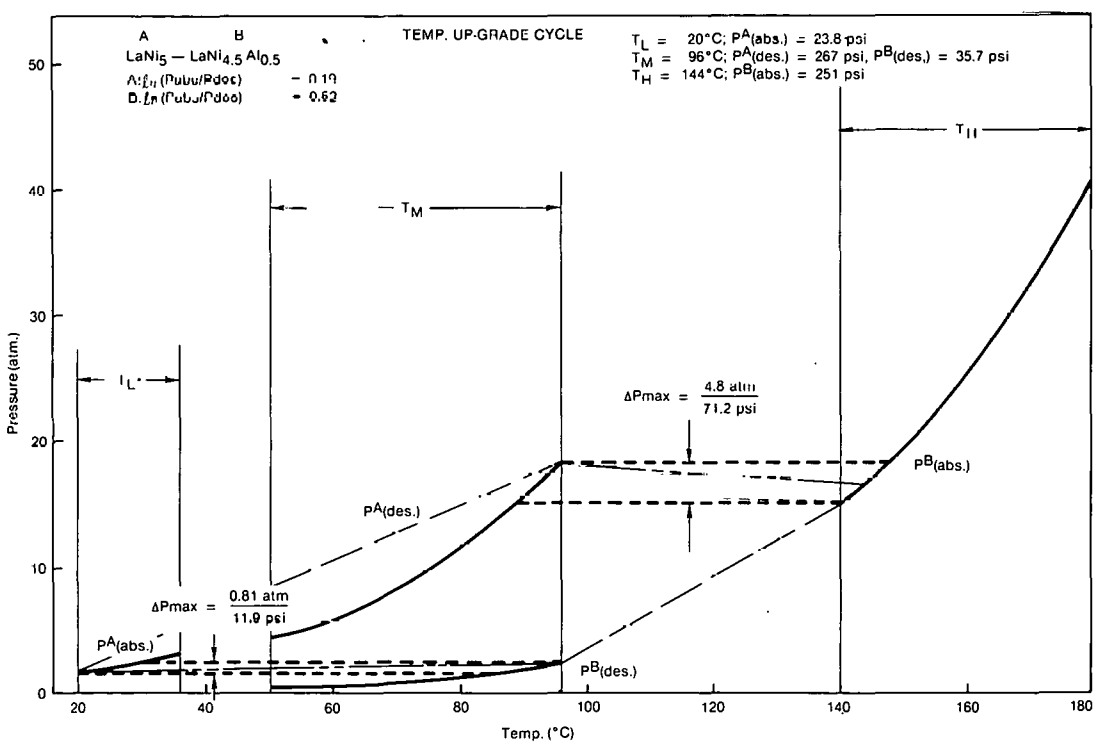

Figure 27. Pressure/Temperature Upgrade Cycle With High Hysteresis

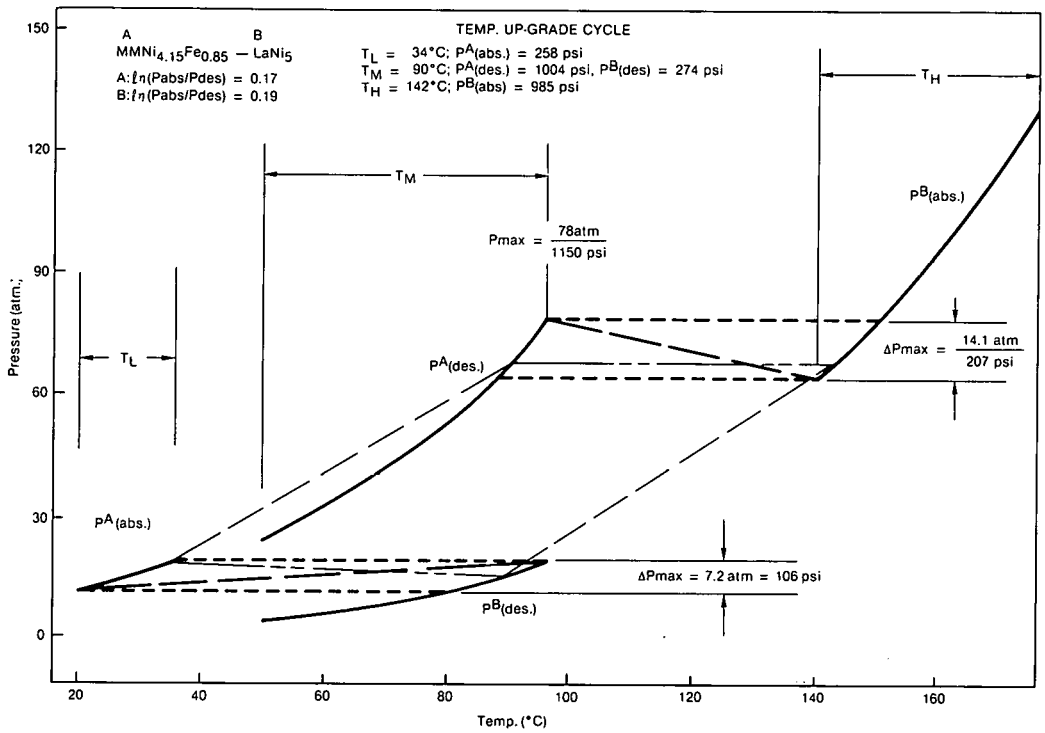

Figure 28. High Pressure/Temperature Upgrade Cycles

The alloy pair $LaNi_5/LaNi_{4.5}Al_{0.5}$ was selected for use in the MHHP operating in a temperature upgrade mode. The selection was based on the alloys favoring hydriding characteristics in the intended operating conditions. The van't Hoff plots of $LaNi_5$ and $LaNi_{4.5}Al_{0.5}$ are shown in Figure 29, also indicated are the high, middle and low temperature junctions. The alloys will operate in the specified temperature ranges of T_L = -1-45°C, T_M = 70-110°C and T_H = 140-190°C. The alloys have low hysteresis losses which allow flexibilty in the temperature and pressure operating conditions. Typically, the pressure drop between absorption-desorption of the alloys during the heat pump application can be in excess of 2 atm., giving enough pressure to move the hydrogen from one alloy to the other. Both $LaNi_5$ and $LaNi_{4.5}Al_{0.5}$ have a relatively high hydride heat of formation allowing for efficient use of the alloy. In general, based on all available data and information, the alloys will perform successfully and not suffer any long term degradation problem.

5.2 HYDRIDE HEAT EXCHANGER DESIGN

Major tradeoffs occur in the hydride heat exchanger design. In order to reduce the amount of hydride material necessary to produce useful output, the cycle times must be minimized by increasing the rate of heat transfer from the heat transfer media to the hydride particles. It is also important to reduce the parasitic thermal losses caused by the heating and cooling of the heat change structure (maximizing the coefficient of performance). Therefore, the thermal/mechanical design study of the metal hydride heat pump centered

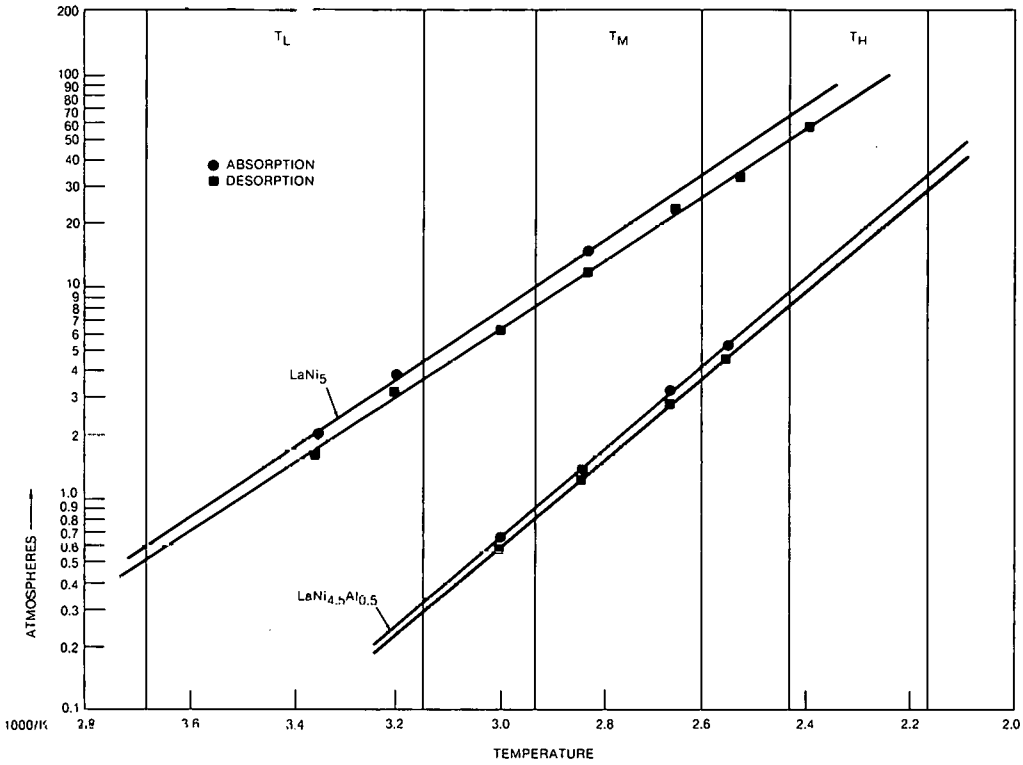

Figure 29. van't Hoff Plot of $LaNi_5$ and $LaNi_{4.5}Al_{0.5}$ With the MHHP Design Conditions

on the development of a high heat transfer, low thermal mass system which maximized the COP. The first step in this direction was to conduct a literature search on powder heat transfer enhancement techniques, hydride material property studies and thermal process modeling. A bibliographic listing of these references is located in Appendix 2.

As a result of the literature search and previous work performed by the team members, two design approaches for the hydride heat exchanger were investigated. Tubular hydride containers were the center of the first approach. The hydride powder and the heat transfer enhancement device are located inside the tube and the heat transfer media flows externally across the tube. The other geometric approach focused on an externally finned hydride heat exchanger. That model is a tube with external transverse fins in which the working fluid flows through the tube and the hydride powder is packed between the external fins.

5.2.1 Tubular Hydride Heat Exchanger Configurations

Computer Model Studies

A computer model was developed to simulate the thermal processes of t tubular configurations. The three approaches that were studied were:

1. Hydride/12% aluminum foam contained in a copper tube[3].

2. Copper tube with internal rectangular longitudinal copper fins.

3. Solid hydride/12% aluminum foam with a longitudinal filter in a copper tube.

The cross-sections of the physical model and the computer nodal analysis model are shown in Figure 30.

Development of the computer simulation was based on a single modular component rather than an entire system to reduce the complexity and increase the versatility of scaling the unit. The computer finite element heat transfer analysis program, P315A, was developed by Solar some years ago and was implemented on an IBM 370 computer. This program presents solutions in terms of temperature versus time information. The general theory of the program is explained in Appendix 3.

Prior to using P315A for each tubular size and configuration, the conductance and capacitance values of each node were calculated. A Hewlett-Packard 9830 mini-computer was used to calculate these values (Fig. 31). For example, Program CHY was for solid hydride/12% aluminum foam in a copper tube with no internal heat generation. This refers to a temperature rise based on sensible heat only, no hydrogen absorption or desorption. A listing of Program CHY and sample input and output is shown in Figure 32.

The output of Program CHY was then used as input to P315A. A listing of the actual data run is shown in Appendix 4. This case simulated the radial heat flow through the solid hydride/12% aluminum foam copper tube with a one inch OD and a temperature differential of 38°C (100°F). This model showed that, based on the sensible heat of the structure, i.e., no hydrogen exchange, it took 85 seconds for the temperature at the tube center to achieve 90 percent of the heat exchange fluid temperature.

Many cases were run which incorporated various external heat transfer coefficients, internal heat transfer enhancements, tube diameters and temperature differentials. All the computer models simulated radial heat flow through the tube to the tube center. In each of the three configurations, two different modes were applied, i.e., with and without heat generation.

Hydrides do not act as uniformly distributed heat sources because the hydrogen cannot be absorbed or desorbed unless the local conditions are such to permit that action. That is, as the hydrogen is absorbed into the metal, it generates heat that raises the temperature of the surrounding material if it

---

[3]Solid hydride/12% aluminum foam is a term used to describe a rigid, highly porous and permeable aluminum structure that has a controlled density of metal per unit volume (pores/inch). Density can be expresed on a percentage basis and, in this case, 12% density was used. Hydride powder is stored in he pores of aluminum structure forming a solid hydride and aluminum onfiguration.

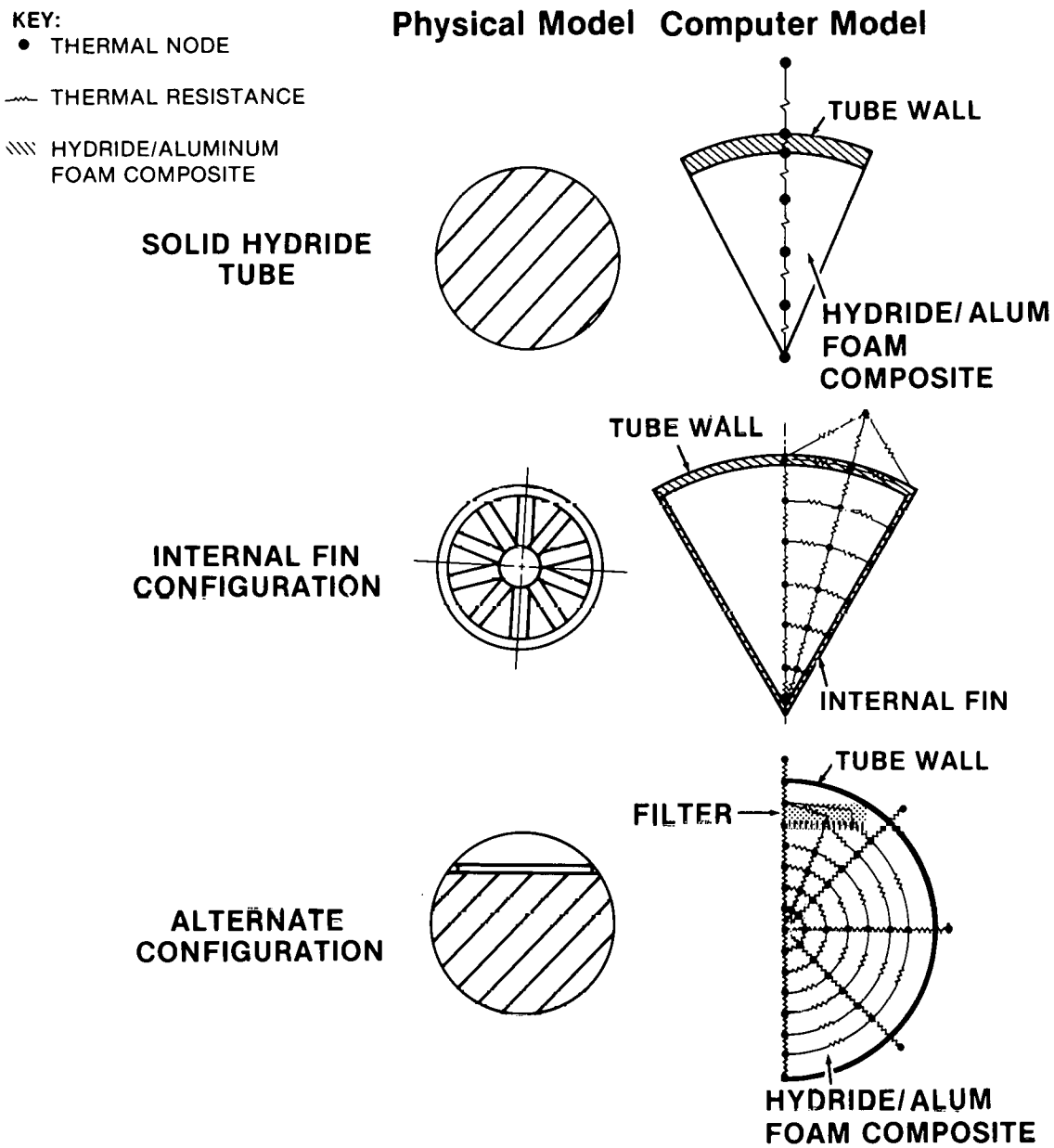

Figure 30. Tubular Hydride Heat Exchanger Configuration

is not rapidly removed. This rise in temperature will locally affect the ability of the surrounding hydride to absorb or desorb hydrogen based on the van't Hoff curve. Therefore, in modeling a multi node representation of the tubular configurations, the heat term ($\pm Q$) associated with each node was different from the others because of the temperature differences. In the real world, the heat is not uniformly distributed and since the computer model can only simulate constant heat generation based on a value for the hydride heat of formation, discrepancies exist between the computer model of heat generation and actual circumstances. Because of these differences, t

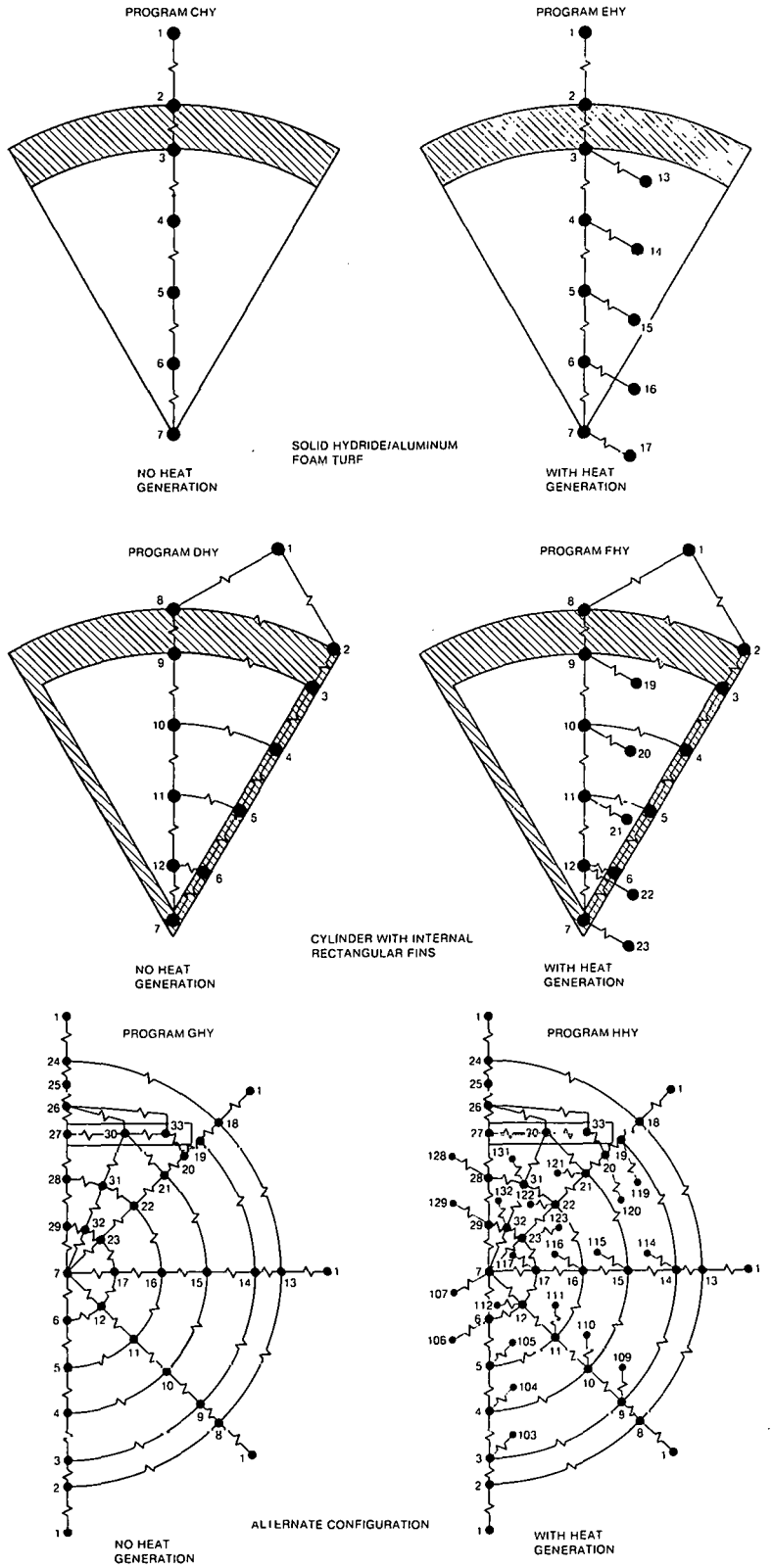

Figure 31. Conductance/Capacitance Calculation Program Models

```
10 REM VALUE CALCULATIONS FOR HYDRIDE SOLID CYLINDER
20 D1=550
30 E1=0.0915
40 D2=279.5
50 E2=0.1373
60 R1=0.47
70 R2=0.5
80 H=500
90 A1=200
100 A2=1.4653
110 K1=R2*H/12
120 K2=0.5*A1*((R2+R1)/(R2-R1))
130 K3=3.5*A2
140 K4=2.5*A2
150 K5=1.5*A2
160 K6=0.5*A2
170 C1=0
180 X1=D1*E1/288
190 X2=D2*E2/288
200 C2=X1*(R2↑2-R1↑2)
210 C3=X2*(R1↑2-(7*R1/8)↑2)
220 C4=X2*((7*R1/8)↑2-(5*R1/8)↑2)
230 C5=X2*((5*R1/8)↑2-(3*R1/8)↑2)
240 C6=X2*((3*R1/8)↑2-(R1/8)↑2)
250 C7=X2*(R1/8)↑2
260 PRINT "K1=";K1
270 PRINT "K2=";K2
280 PRINT "K3=";K3
290 PRINT "K4=";K4
300 PRINT "K5=";K5
310 PRINT "K6=";K6
320 PRINT
330 PRINT "C1=";C1
340 PRINT "C2=";C2
350 PRINT "C3=";C3
360 PRINT "C4=";C4
370 PRINT "C5=";C5
380 PRINT "C6=";C6
390 PRINT "C7=";C7
400 END
```

Sample Output of CHY
(input to P315A)

```
K1= 20.83333333
K2= 3233.333333
K3= 5.12855
K4= 3.66325
K5= 2.19795
K6= 0.73265

C1= 0
C2= 5.08492E-03
C3= 6.89869E-03
C4= 0.011037910
C5= 7.35861E-03
C6= 3.67930E-03
C7= 4.59913E-04
```

D1 = density of the copper tube wall, lb/ft^3
E1 = specific heat of copper tube wall, btu/lb °F
D2 = equivalent density of internal solid, lb/ft^3
E2 = equivalent specific heat of internal solid, btu/lb °F
R1 = inner radius of tube wall, inches
R2 = outer radius of tube wall, inches
H = external heat transfer coefficient, $btu/hr\ ft^2$ °F
A1 = thermal conductivity of the tube wall, btu/hr ft °F
A2 = equivalent thermal condutivity of the internal solid wall, btu/hr ft °F
K1-K6 = conductance values, btu/hr ft °F
C1-C7 = capacitance values, btu/°F

Figure 32. Computer Program CHY

dal analysis was checked and correlated with experimental results. These results will be described later in this report.

Figures 33 through 38 are plots of the tube center temperature versus time for the three configurations with and without heat generation. Tube diameters of 0.5 inch, 0.75 inch and 1.0 inch were used as parameters. Figure 39 is a summary plot which shows tube OD versus the time to achieve 90 percent of the heat exchange fluid temperature. A temperature differential of 38°C (100°F) was used in this computer model, therefore, 32°C (90°F) was the 90 percent timing point. Because the temperature approached the limits asyptotically the heat transfer time was defined as that time required to achieve 90 percent of the imposed differential. This is similar to the 90 percent risetime definition used in electronics. The internal rectangular fin configuration demonstrated promise in terms of achieving a low cycle time ($\approx$60 sec).

The thermal mass ratio is an important parameter as it describes the ratio of the sensible heat of the hydride powder to the sensible heat of the entire tubular structure including the hydride. The goal is to minimize the sensible heat of the structure and achieve maximum hydride usefulness. Therefore, the optimum value of the thermal mass ratio for a zero mass heat exchanger is one.

Table 7 lists the assumptions for sensible heat calculations. A sample calculation of sensible heat rate of energy output and thermal mass ratio for a one inch OD tube with eight internal rectangular copper fins is shown in Figure 40. Figures 41 through 43 are plots of thermal mass ratio versus time for the three configurations. These results show that the larger the tubular structure, the higher the thermal mass ratio and consequently, the higher the cycle time. Therefore, a trade-off must be made between the thermal mass ratio and the cycle time. Table 8 compares the three configurations in terms of cycle time and energy rate.

The internal rectangular copper fin tube structure was chosen over the tubes containing aluminum foam for further study due to low cycle times and a good thermal mass ratio. Computer studies were conducted on this tubular configuration to vary the number of internal fins, tube wall thickness, fin thickness and external heat transfer coefficient. Figures 44 through 46 are plots of thermal mass ratio versus time for various tube OD's and either varying numbers of fins, tube wall thicknesses or fin thicknesses. Figure 47 is a plot of the external heat transfer coefficient versus the time to achieve the 90 percent temperature for varying tube OD's.

The results of the computer study provided a guide for choosing the optimum tubular design. A nominal one inch OD copper tube with six internal fins, a wall thickness of 0.065 inch and a fin thickness of 0.035 inch was chosen based on cycle time and thermal mass ratio characteristics and manufacturing considerations. Figure 48 outlines this design approach. It is envisioned that a central cylindrical filter could be used within the tube structure or an end-cap (radial) filter could be utilized at one end of the tube.

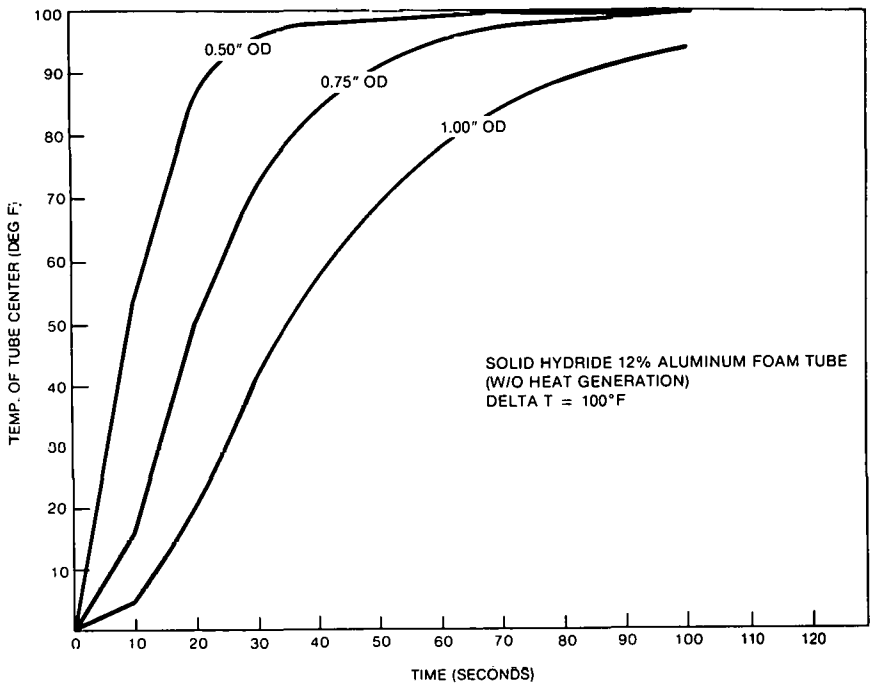

Figure 33. Temperature of Tube Center Vs. Time for Configuration #1 Without Heat Generation

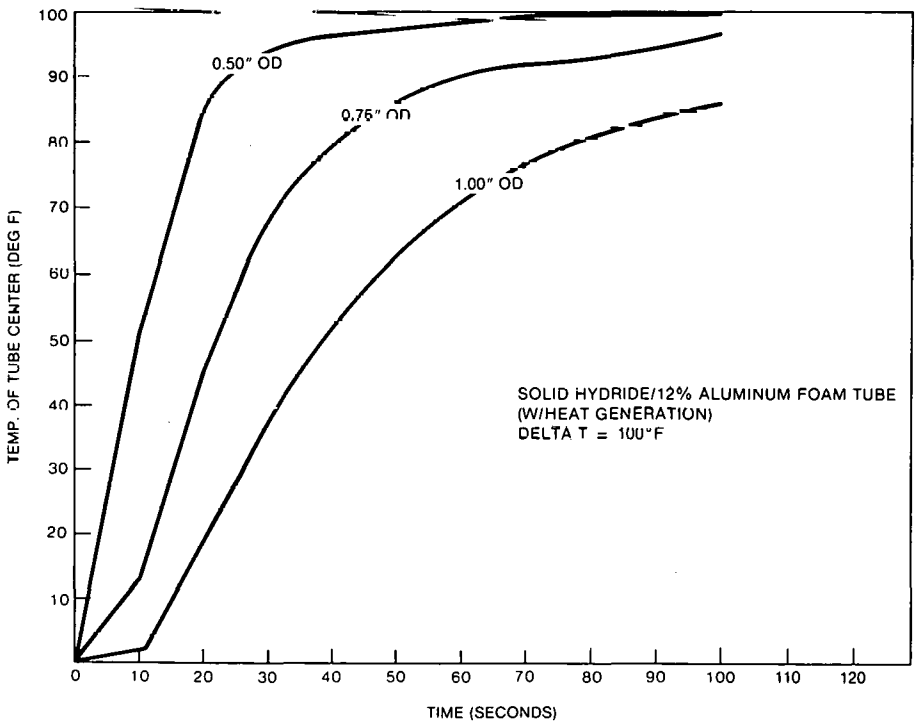

Figure 34. Temperature of Tube Center Vs. Time for Configuration #1 With Heat Generation

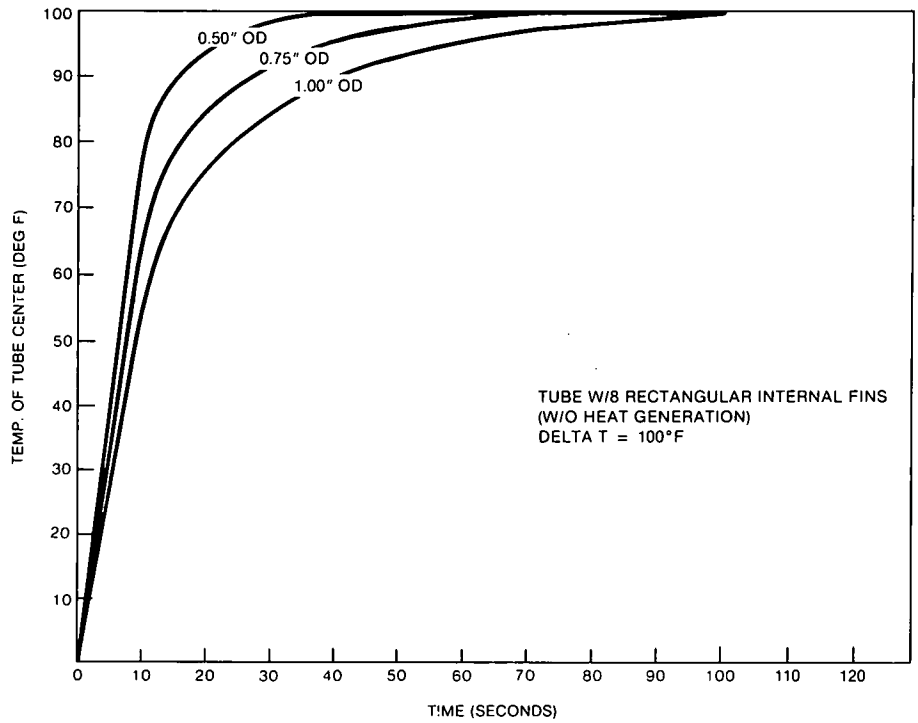

Figure 35. Temperature of Tube Center Vs. Time for Configuration #2 Without Heat Generation

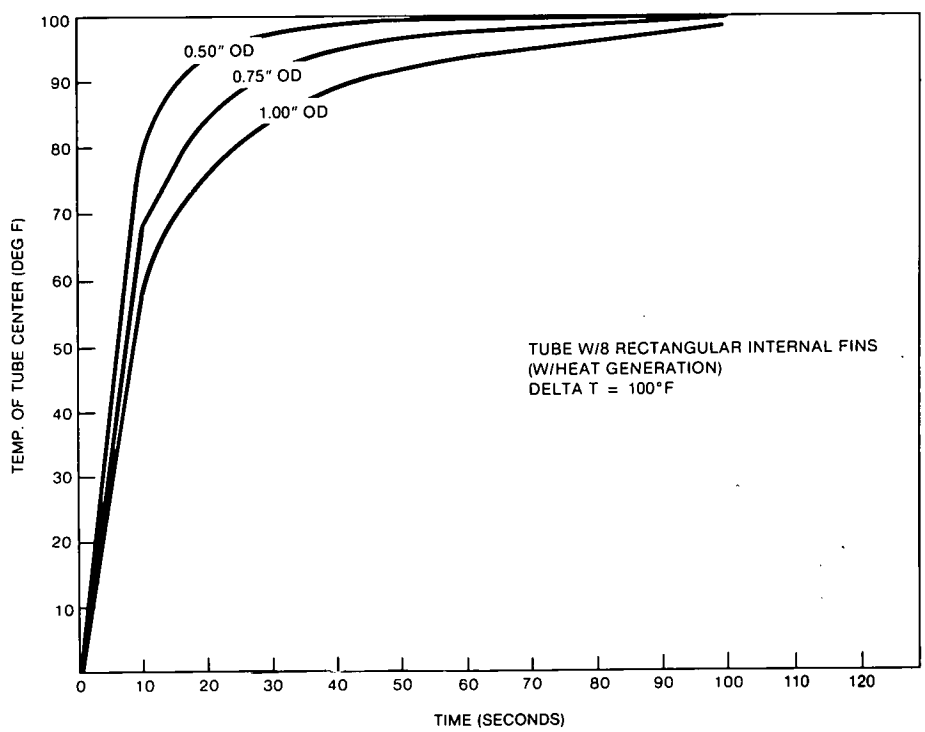

Figure 36. Temperature of Tube Center Vs. Time for Configuration #2 With Heat Generation

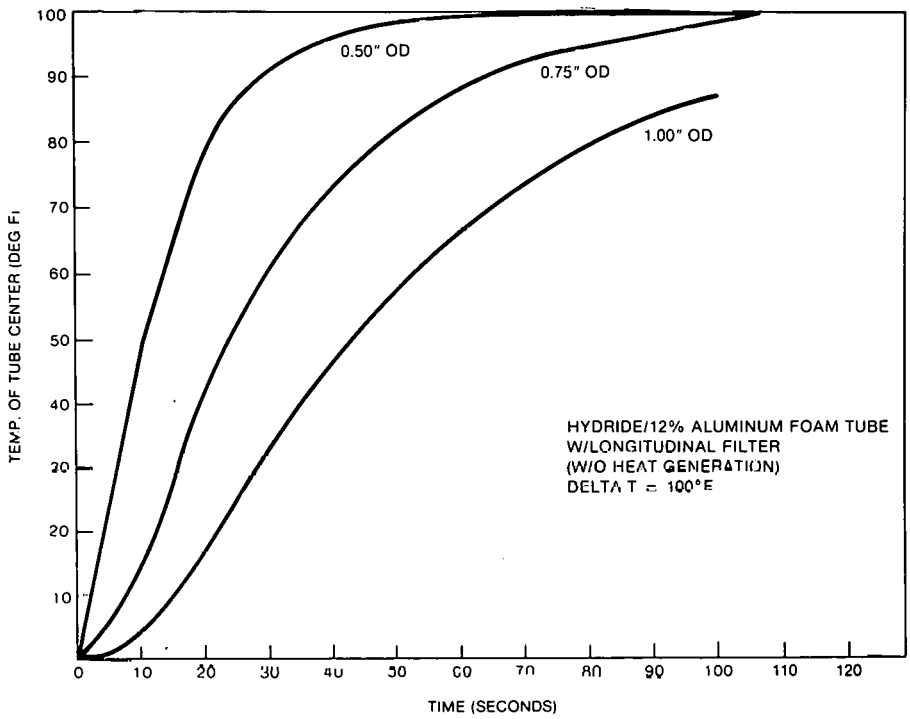

Figure 37. Temperature of Tube Center Vs. Time for Configuration #3 Without Heat Generation

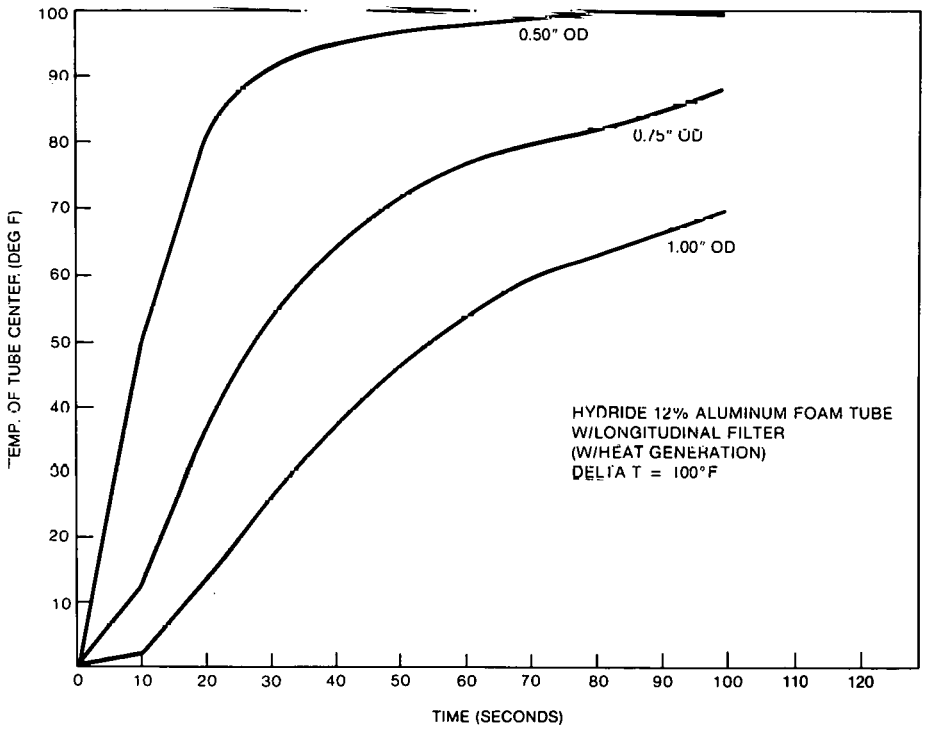

Figure 38. Temperature of Tube Center Vs. Time for Configuration #3 With Heat Generation

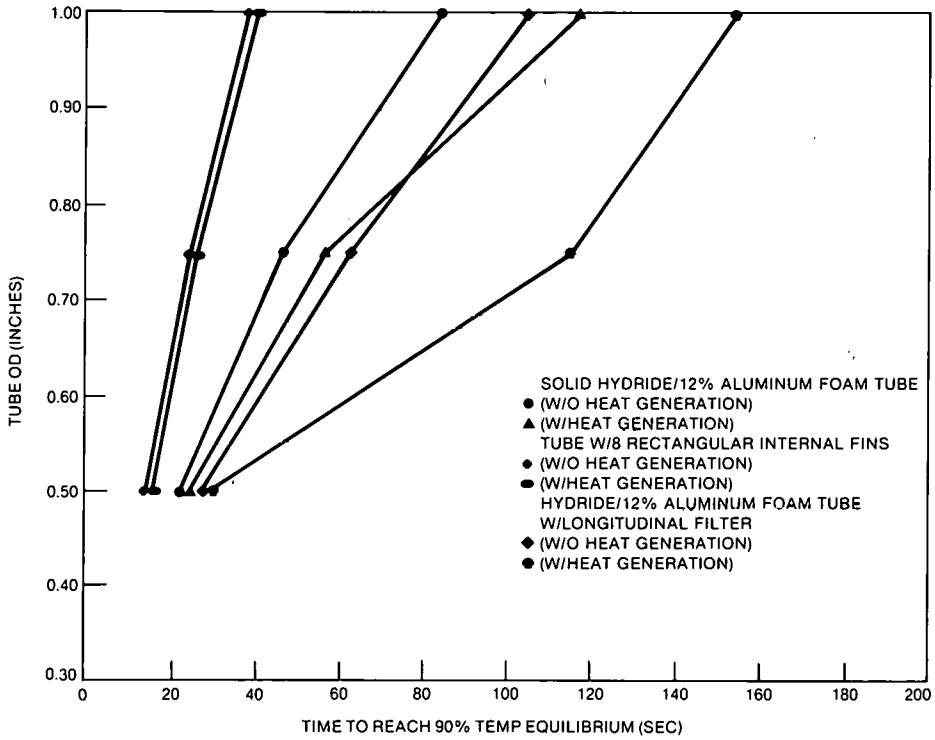

Figure 39. Summary of Plot of Tube OD Vs. Time to Reach 90% Temperature Equilibrium

Table 7

Assumptions in the Sensible Heat Calculations*

hydride powder = $LaNi_5$
ΔT = 32°C (90°F)
density of copper tube = 550.0 lbm/ft^3
density of $LaNi_5$ = 518.4 lbm/ft^3
density of aluminum foam = 169.34 lbm/ft^3
density of filter material = 339.0 lbm/ft^3
density of hydrogen gas = 0.0045 lbm/ft^3
specific heat of copper tube = 0.0915 Btu/lbm°F
specific heat of $LaNi_5$ = 0.107 Btu/lbm°F
specific heat of aluminum foam = 0.23 Btu/lbm°F
specific heat of filter material = 0.12 Btu/lbm°F
specific heat of hydrogen gas = 3.4 Btu/lbm°F
heat of formation of $LaNi_5$ = 60 Btu/lbm
hydride packing factor = 50%
tube wall thickness = 0.030 inch
tube length = 1.0 foot
external heat transfer coefficient = 500 Btu/hr ft^2°F

*English units are shown because the computer model was set-up in that fashion.

$V_{TUBE} = 6.35 \times 10^{-4}$ ft3
$V_{FINS} = 1.31 \times 10^{-3}$ ft3
$V_{LaNi5} = 2.41 \times 10^{-3}$ ft3
$V_{gas} = 1.09 \times 10^{-3}$ ft3

$V_{TOTAL} = 5.14 \times 10^{-3}$ ft3

$M_{TUBE} = 0.35$ lbm
$M_{FINS} = 0.72$ lbm
$M_{LaNi5} = 1.25$ lbm
$M_{gas} = 4.9 \times 10^{-6}$ lbm

$M_{TOTAL} = 2.32$ lbm

S.H. TUBE = 2.875 Btu
S.H. FINS = 5.872 Btu
S.H. LaNi5 = 12.029 Btu
S.H. gas = 1.5×10^{-3} Btu

S.H. TOTAL = 20.777 Btu
ASSUME ΔH_f for $LaNi_5$ = 60 $\frac{Btu}{lbm}$
ΔH_f = (1.25 lbm) (60 Btu/lbm) = 75.0 Btu
90% TEMP EQUILIBRIUM TIME = 41 SEC.

$$\text{NET ENERGY RATE} = \frac{(75.0 - 20.78)\ \text{Btu}}{(2)\ (41\ \text{sec})\ (\frac{1\ \text{hr}}{3600\ \text{sec}})} = 2380.5\ \frac{\text{Btu}}{\text{hr}}$$

Figure 40. Sample Calculations for Copper Tube With Eight Internal Rectangular Copper Fins (One-Inch OD)

Experimental Heat Transfer Analysis

A test rig was designed and built to study the heat transfer of the various tubular heat exchanger configurations. Figure 49 is a schematic of the rig; Figures 50 and 51 are actual views of the rig. The primary goal of testing actual tubular components was to verify the computer results. The rig operated as a calorimeter-type device by measuring the amount of heat released or absorbed by the tube under specified test conditions.

Three configurations were tested:

1. solid hydride/12% aluminum foam in a copper tube

2. copper tube with aluminum internal fin structure (an internally finned tube with copper fins was not readily available)

3. solid hydride/12% aluminum foam in a copper tube with longitudinal filter.

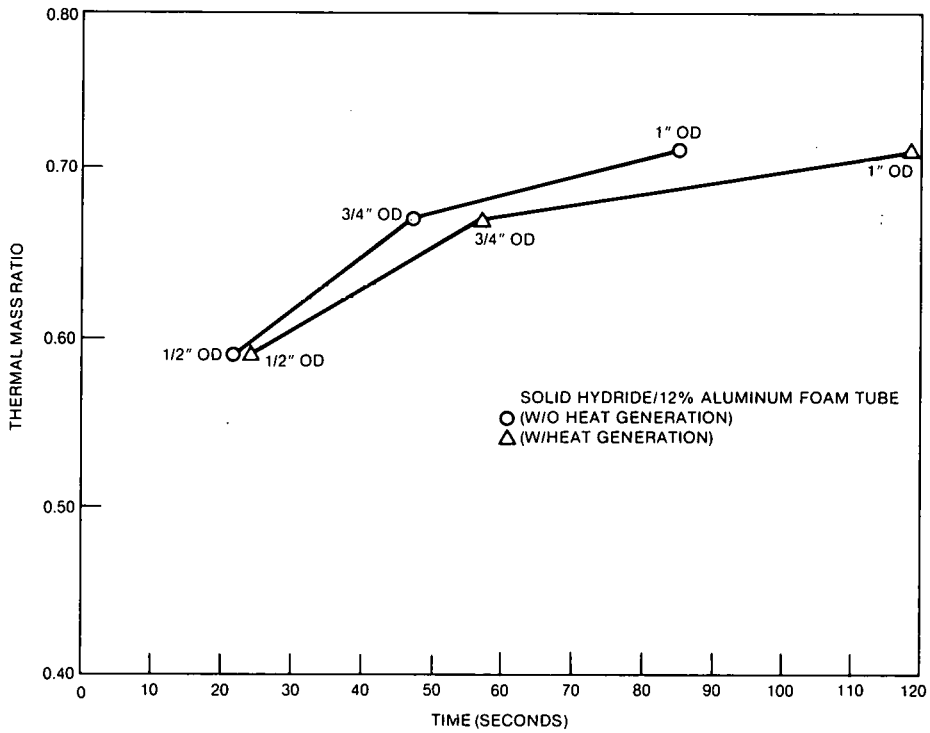

Figure 41. Thermal Mass Ratio Vs. Time for Configuration #1

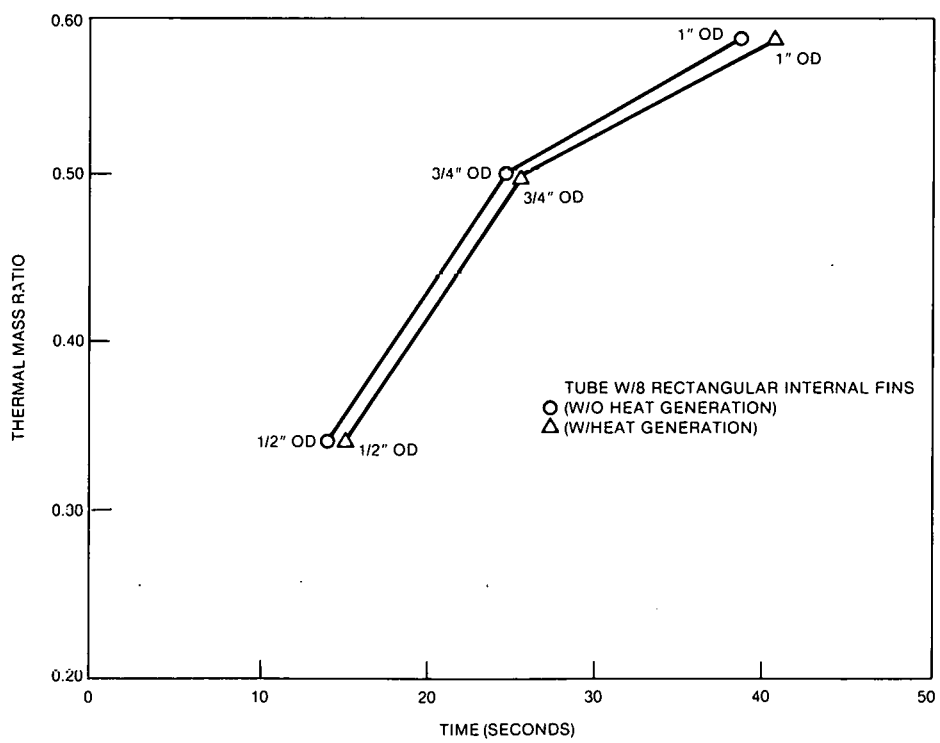

Figure 42. Thermal Mass Ratio Vs. Time for Configuration #2

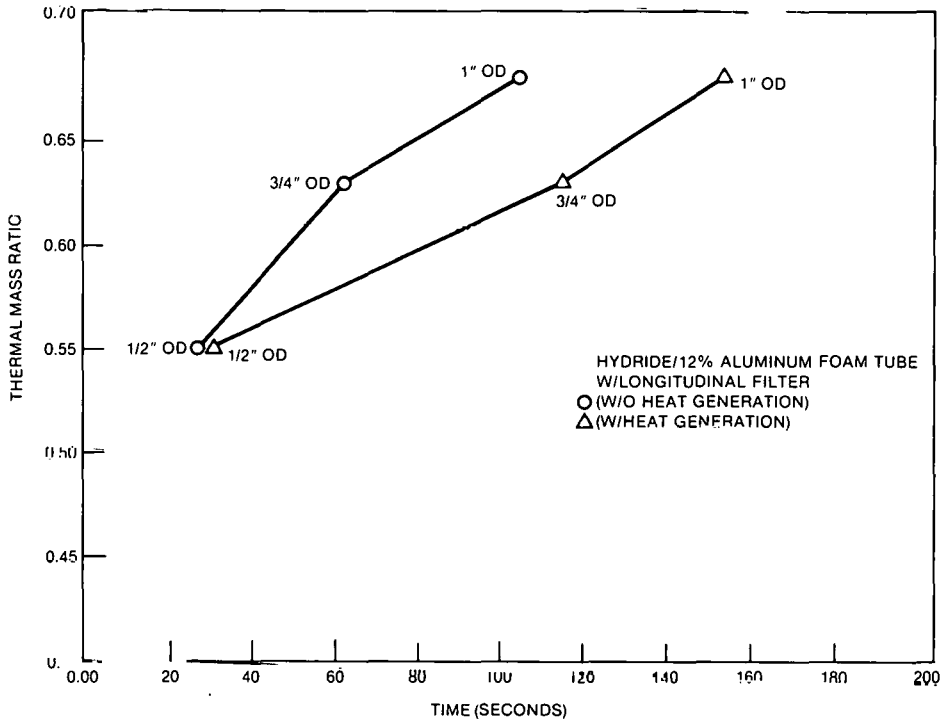

Figure 43. Thermal Mass Ratio Vs. Time for Configuration #3

Table 8

Comparison of the Three Hydride Tube Configurations

	Configuration #1: Solid Hydride/12% Al Foam Tube			Configuration #2: Tube With 8 Rectangular Internal Fins			Configuration #3: Hydride/12% Foam With Longitudinal Filter Tube		
	1.00 in. OD	0.75 in. OD	0.50 in. OD	1.00 in. OD	0.75 in. OD	0.50 in. OD	1.00 in. OD	0.75 in. OD	0.50 in. OD
Cycle Time (sec)	238	114	48	02	52	30	310	232	54
Net Energy Rate (Btu/hr)	878	903	880	2380	1887	835	666	464	758
Sensible Heat (Btu)	16.93	9.71	4.47	30.78	12.95	6.24	17.66	10.29	4.83
Thermal Mass Ratio	0.71	0.67	0.59	0.58	0.50	0.34	0.68	0.67	0.55

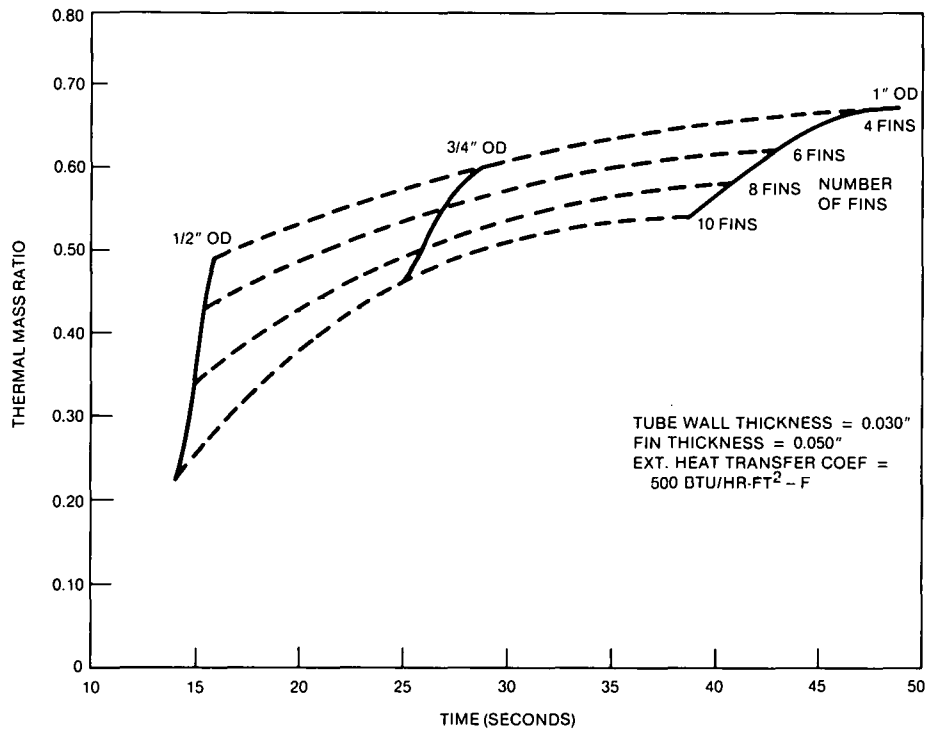

Figure 44. Thermal Mass Ratio Vs. Time for Varying Number of Fins

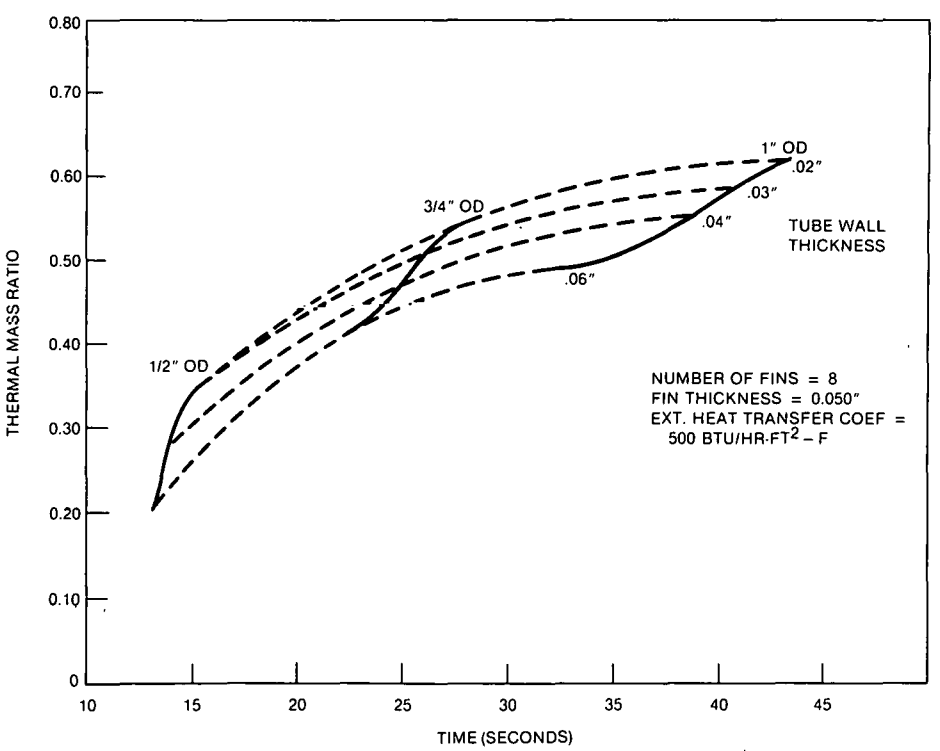

Figure 45. Thermal Mass Ratio Vs. Time for Varying Tube Wall Thickness

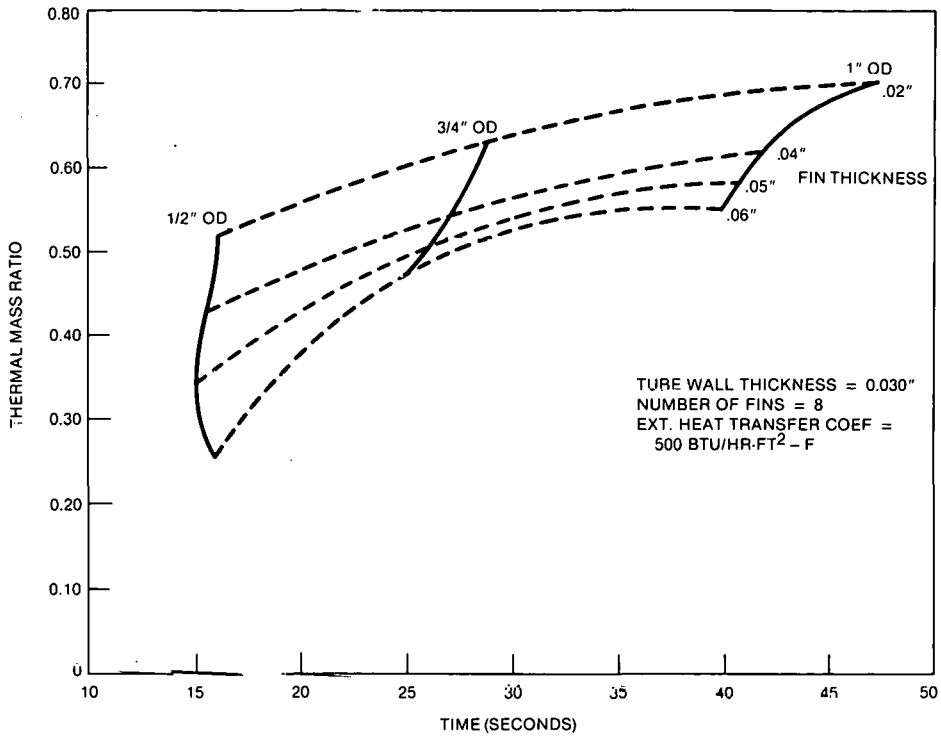

Figure 46. Thermal Mass Ratio Vs. Time for Varying Fin Thickness

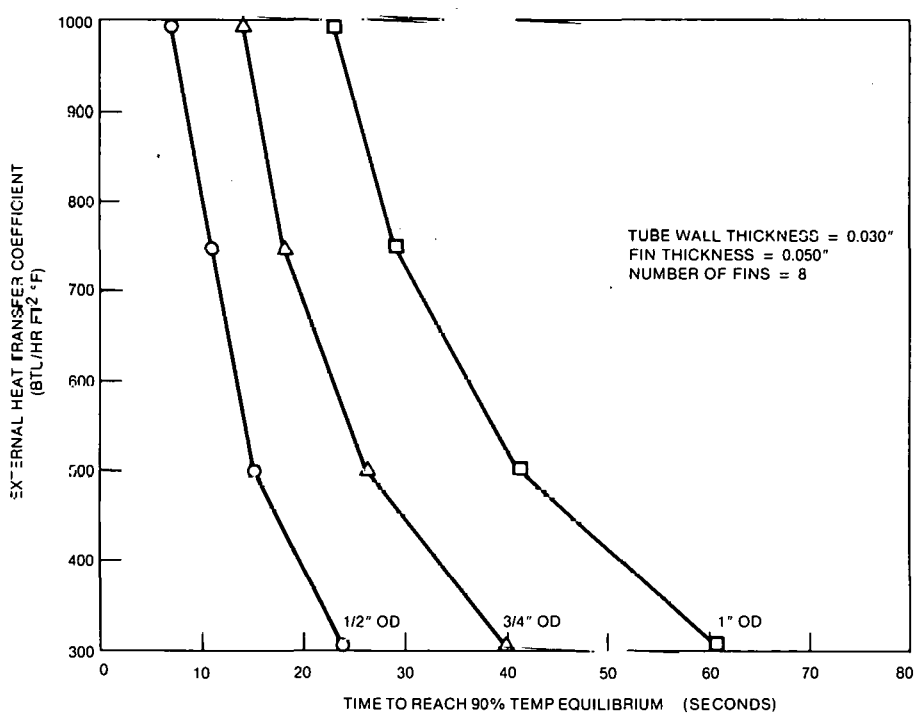

Figure 47. External Heat Transfer Coefficient Vs. 90% Temperature Equilibrium for Varying Tube OD's

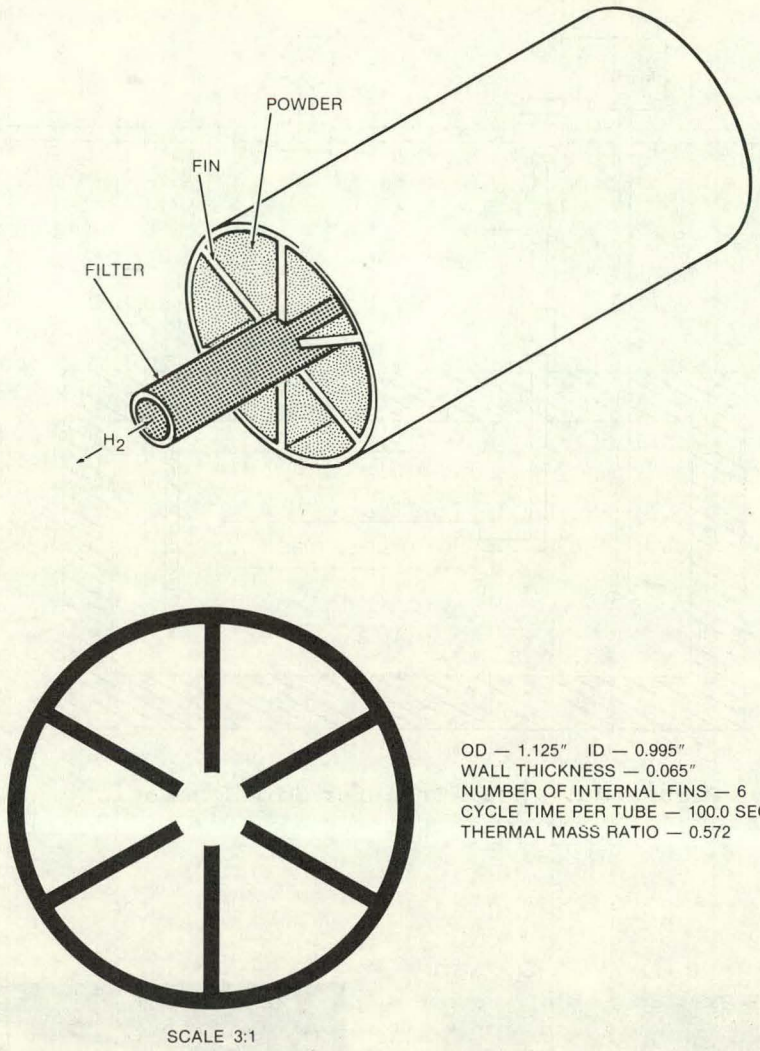

Figure 48. Optimum Tubular Design

Testing consisted of loading the tubular configuration with a known amount of activated $LaNi_5$ hydride. The tube was then connected to the test rig and a known amount of distilled water was placed in the calorimeter vessel. Heat energy was generated or absorbed by the hydride by absorbing or desorbing hydrogen gas. Temperature of the water versus time was measured to estimate the effect of the hydride-filled tube on the heat transfer media (water). The effectiveness of the three enhancement schemes on tubular design was then judged.

Temperature versus time information produced from each tubular structure test in the calorimeter rig was compared to computer tests previously run. The first tests were based on temperature rise for sensible heat only, i.e., no absorption or desorption of hydrogen occurred. Figures 52 and 53 are experimental versus computer data plots for configurations #1 and #2 as ntioned above. (This data was not available for configuration #3.) The mputer model matched the actual data very closely.

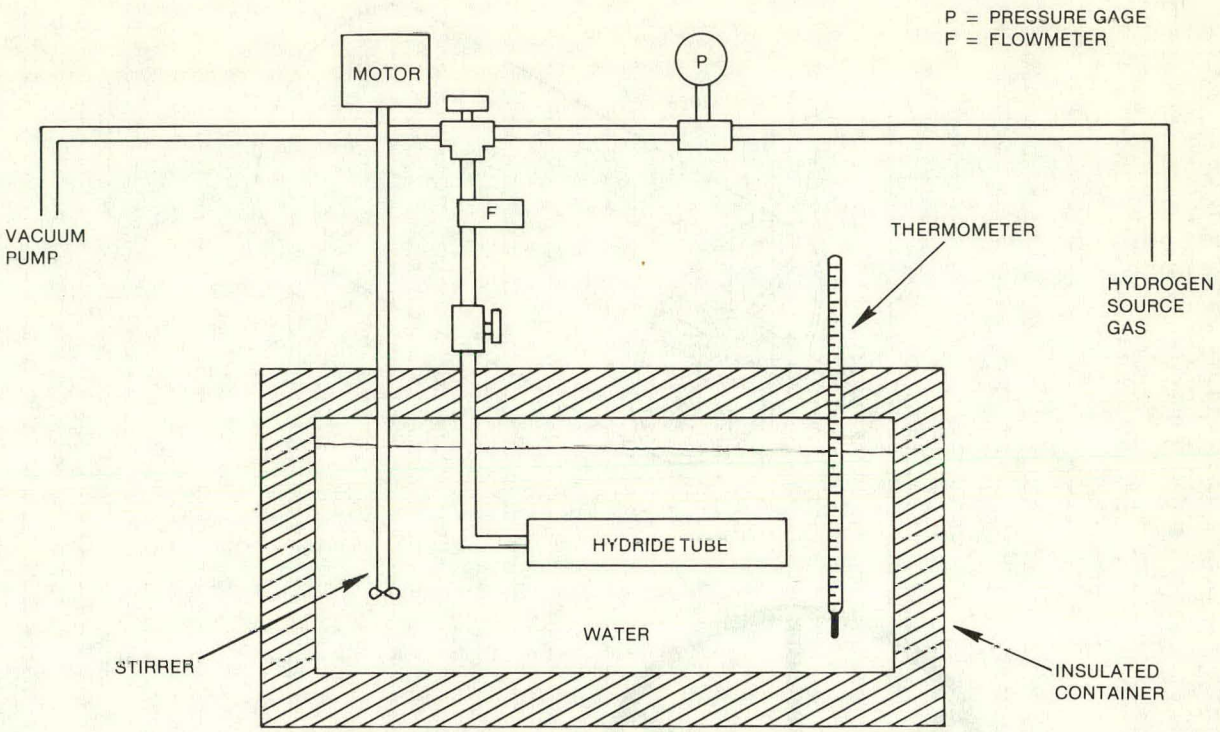

Figure 49. Heat Transfer Rig Schematic

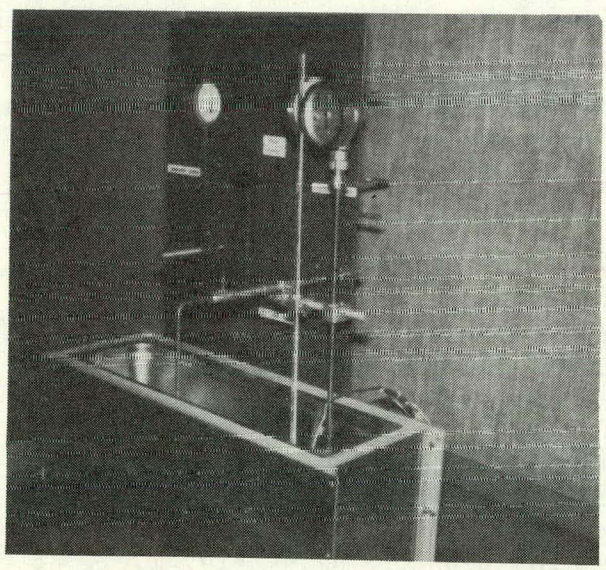

Figure 50.

Heat Transfer Test Rig - View 1

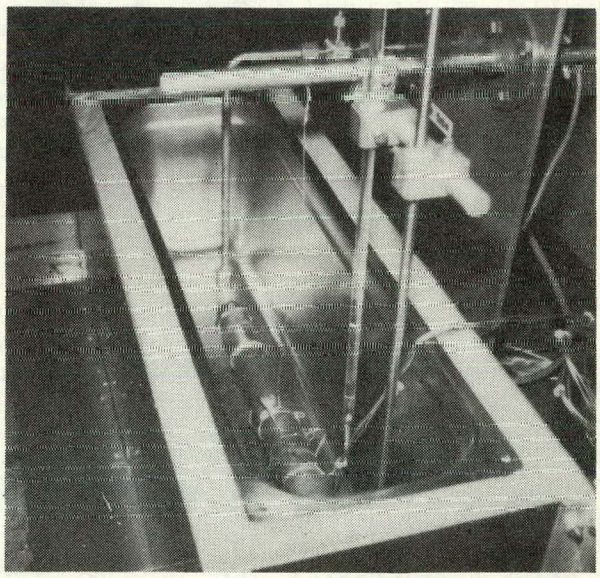

Figure 51.

Heat Transfer Test Rig - View 2

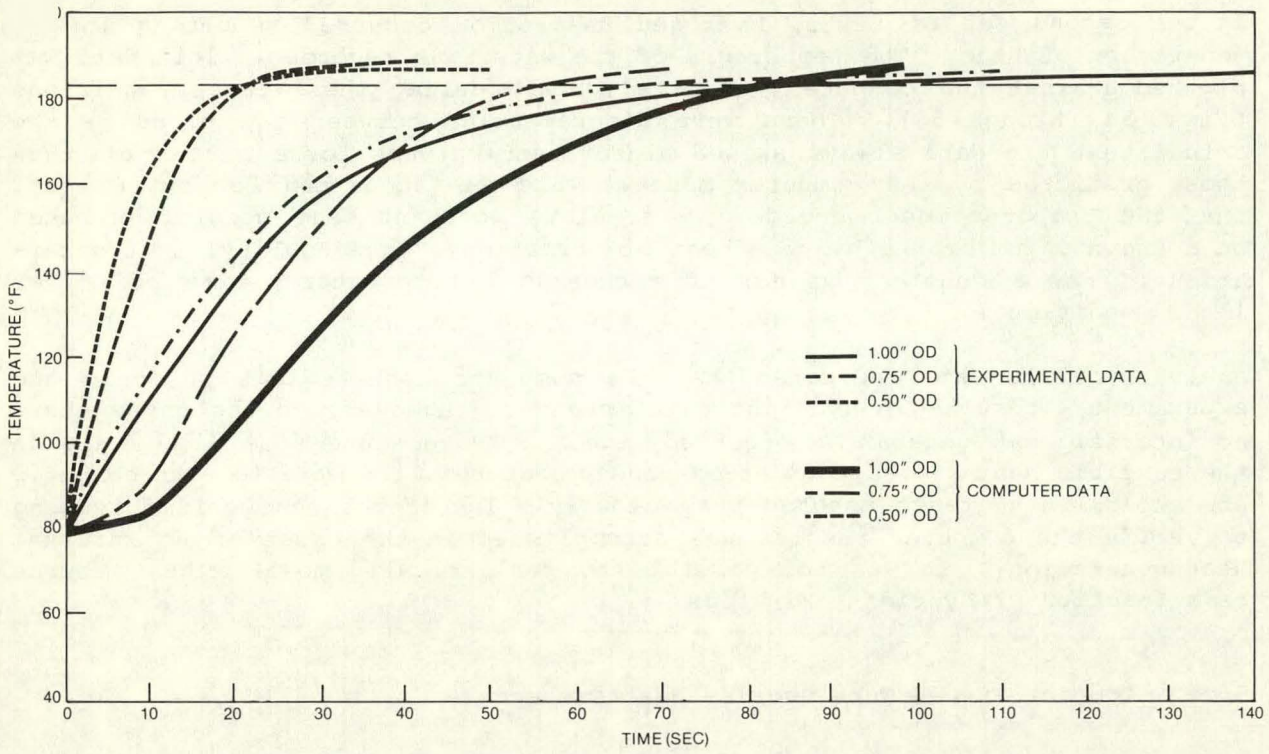

Figure 52. Experimental Vs. Computer Data Plot for Configuraiton #1

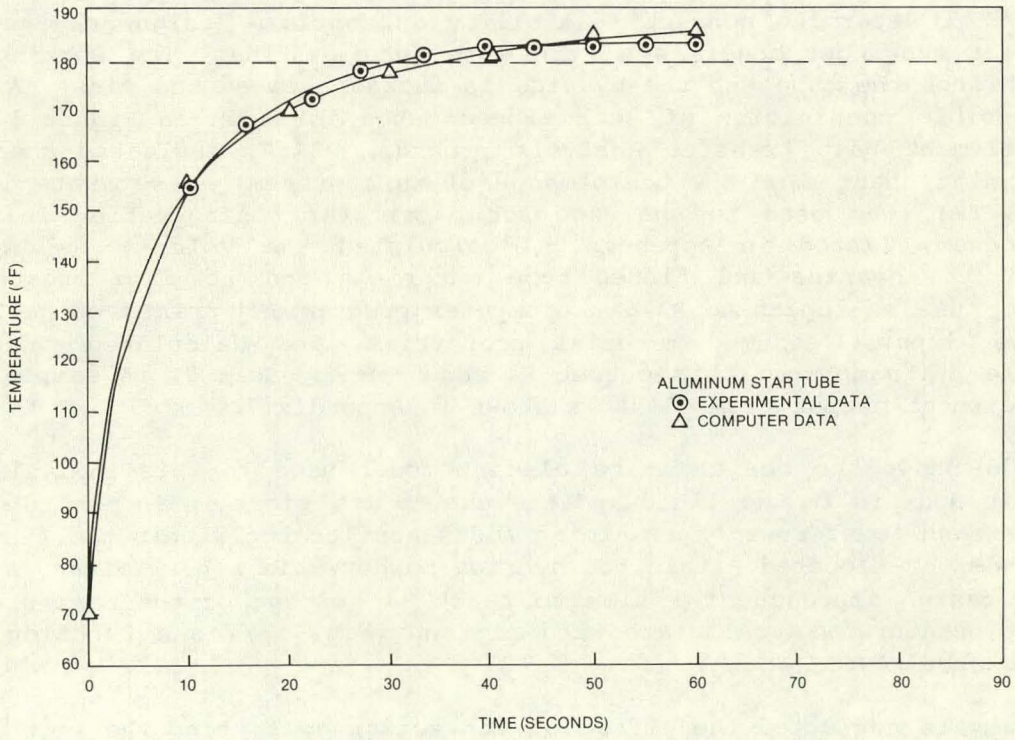

Figure 53. Experimental Vs. Computer Data Plot for Configuratin #2

In the second set of tests, hydrogen absorption occurred resulting in generation of heat. The temperaure of the water was recorded. This data was plotted against the computer simulated data modeling these tests conditions (Figs. 54 through 56). There were discrepancies between the plots -- the actual test rig data always showed higher temperatures for a given time than those predicted by the computer model. This was accounted for by the fact that the computer model could only simulate constant heat generation based on a known value of the hydride heat of formation. In actuality, heat generation is not a constant value; it varies with temperature, time and other local conditions.

Analysis of the data indicated that the computer results fell short of the experimental results in hydridng circumstances. However, in the cases where no internal heat generation occurred, i.e., a temperature rise based only on the sensible heat of the tubular component occurred, the data for the computer and experimental tests matched very closely. Therefore, the goal of testing to verify the computer results was accomplished in the cases of no internal heat generation. It was not possible to realistically model a heat source as a function of hydriding kinetics.

5.2.2 Compact Finned Tube Hydride Heat Exchanger

Computer Model Studies

A parametric study of an externally finned tube hydride heat exchanger was conducted to determine concept feasibility and optimum design geometry. The basic heat exchanger model is a tube with annular fins. The working fluid flows through the tube and the hydride is packed between the fins. A sketch of a possible combination of such finned tubes is shown in Figure 57. The finite element heat transfer analysis program, P315A, evaluated the effect of dimension changes on the performance of this system. A separate computer program, TF1, was used to analyze each particular configuration initially. This program, listed in Appendix 5, calculated the volumes and specific heats of the hydride and finned tube materials and it also created data files for use as inputs to P315A. Computer program TF1 prints out a list of the given inputs, assumed material properties, and calculated values for each case. A sample of this output is shown in Appendix 6. A sample of the finite element output from P315A is shown in Appendix 7.

Figure 58 shows the basic finite element model used in this analysis. The left most node is in the fluid and the one to its right is in the tube wall. The upper and lower rows of remaining nodes are located within the fins. All other nodes are located within the hydride powder. In a preliminary analysis of this design approach, the time to reach 90 percent of the heat exchanger fluid temperature was calculated and plotted (Fig. 59) as a function of the fin thickness.

This analysis neglected the effect of convection by setting the initial wall temperature equal to the fluid temperature. The information obtained fr this analysis was used to establish the range of fin and hydride thickne

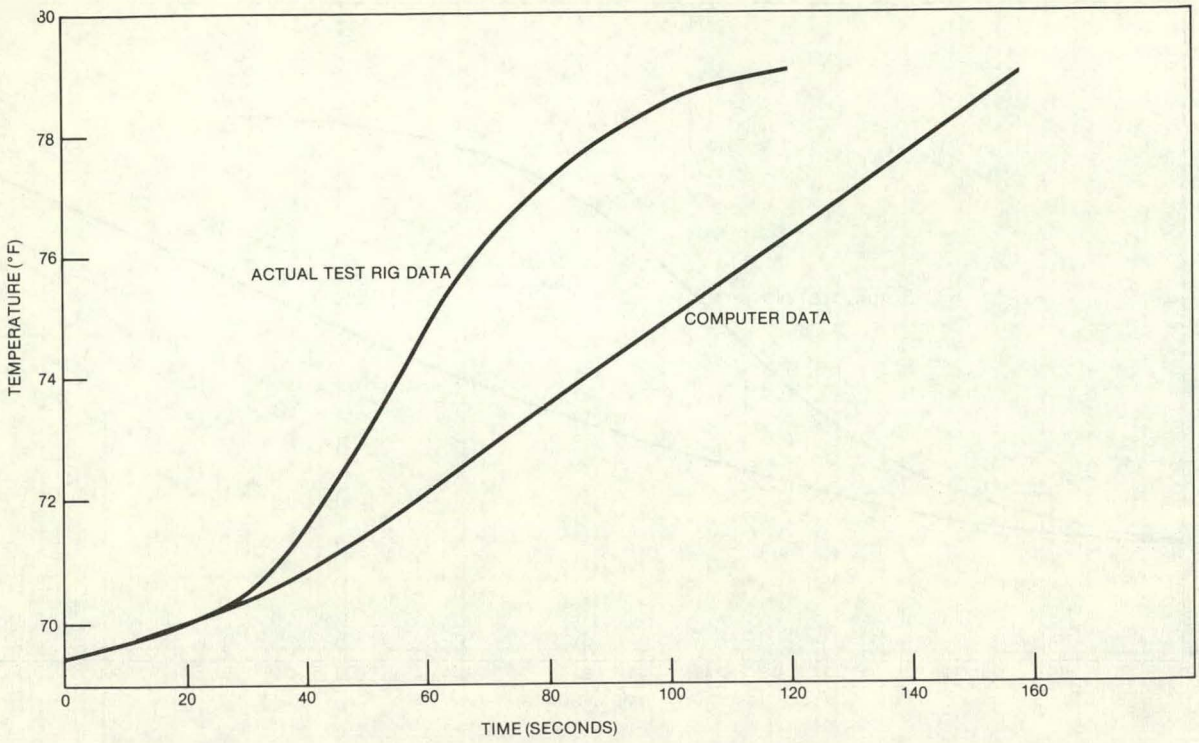

Figure 54. Solid Hydride/12% Aluminum Foam in a Copper Tube

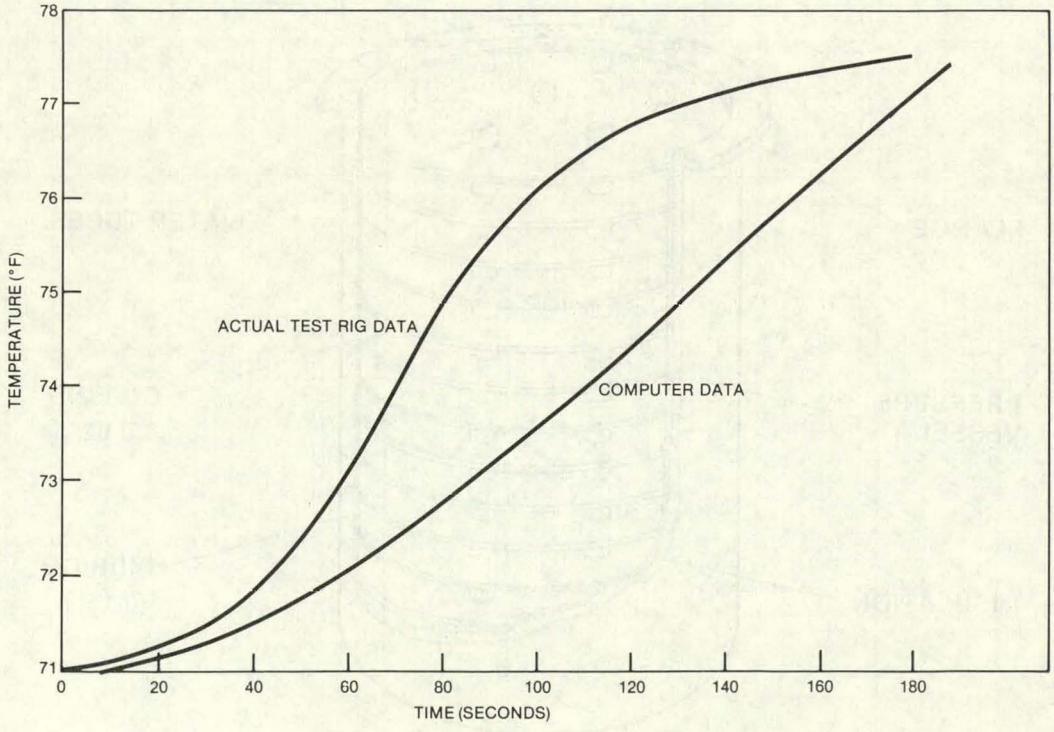

Figure 55. Copper Tube Within Aluminum Internally Finned Tube

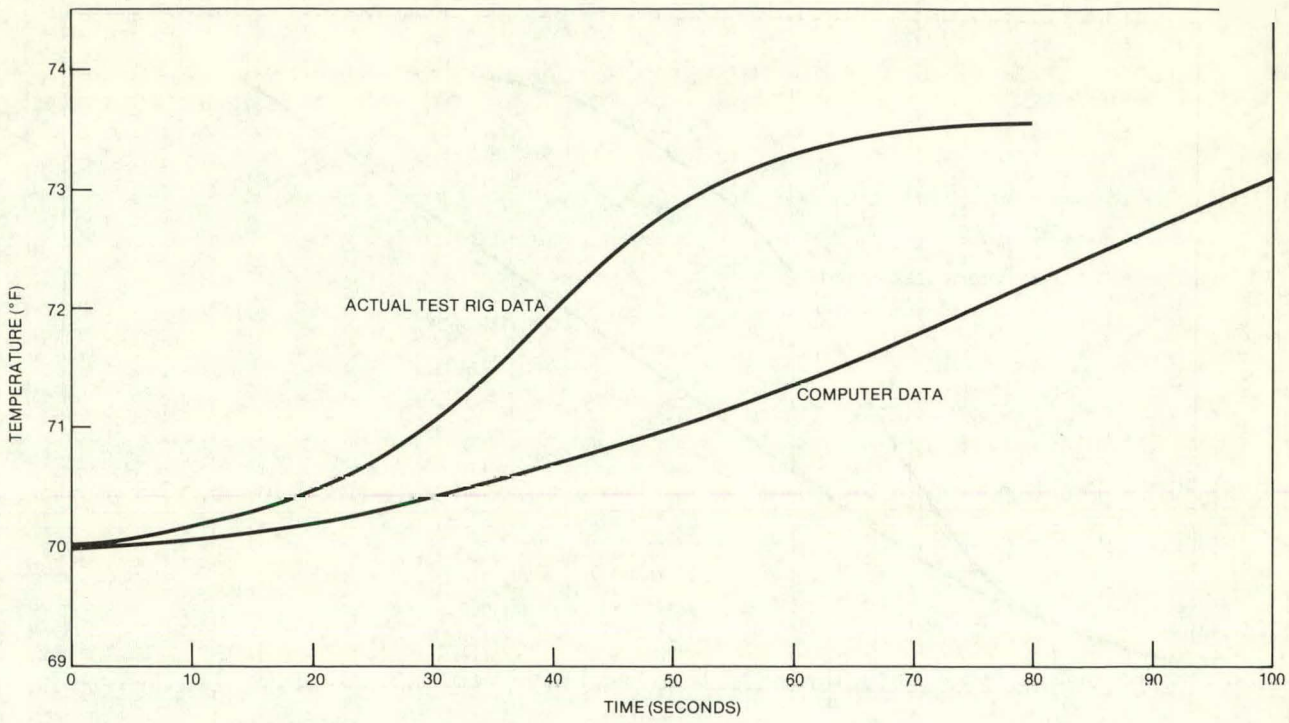

FIgure 56. Solid Hydride/12% Aluminum Foam in a Copper Tube With Longitudinal Filter

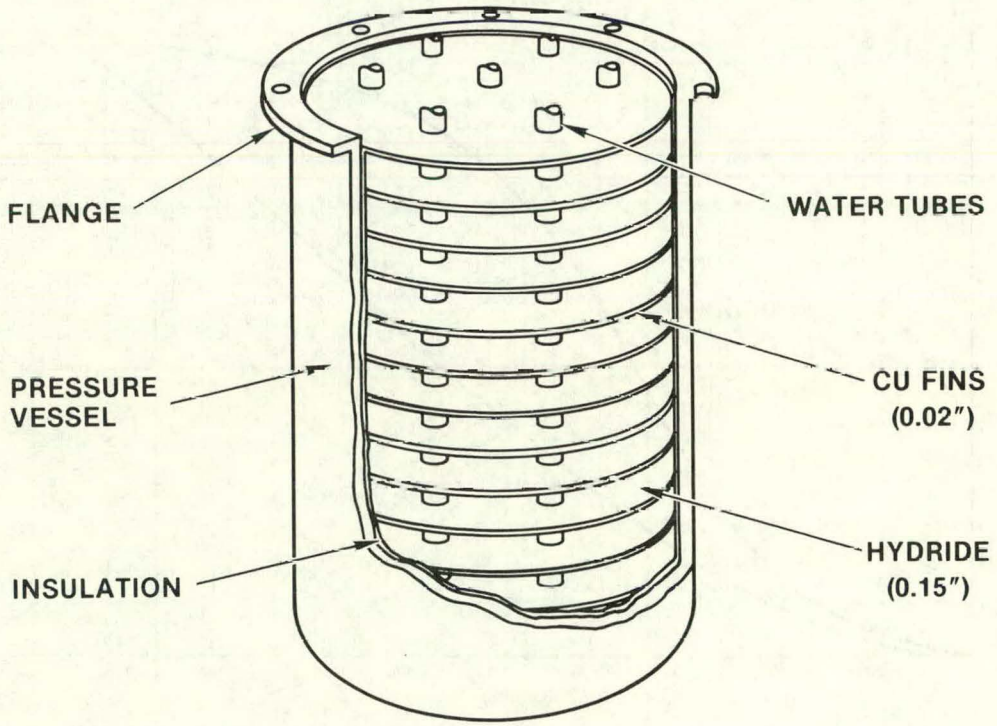

Figure 57. Finned Tube Hydride Heat Exchanger Package

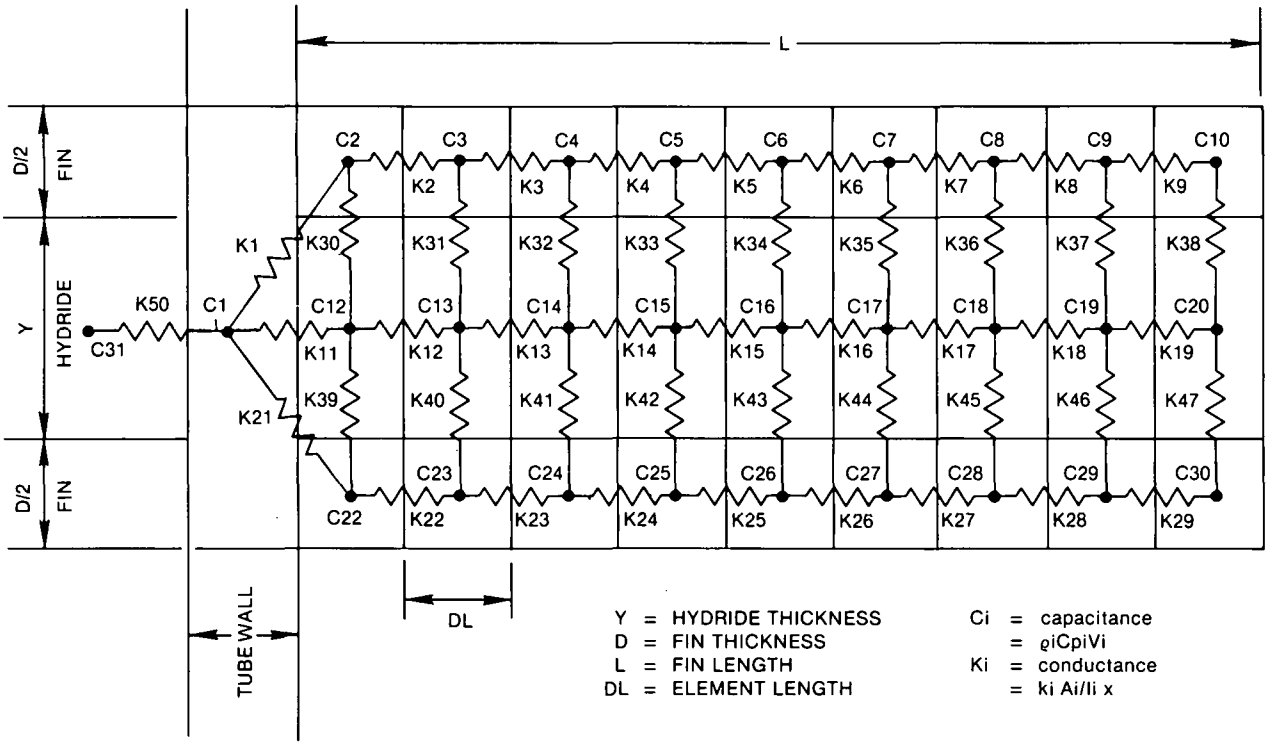

Figure 58. Finned Tube Hydride Heat Exchanger

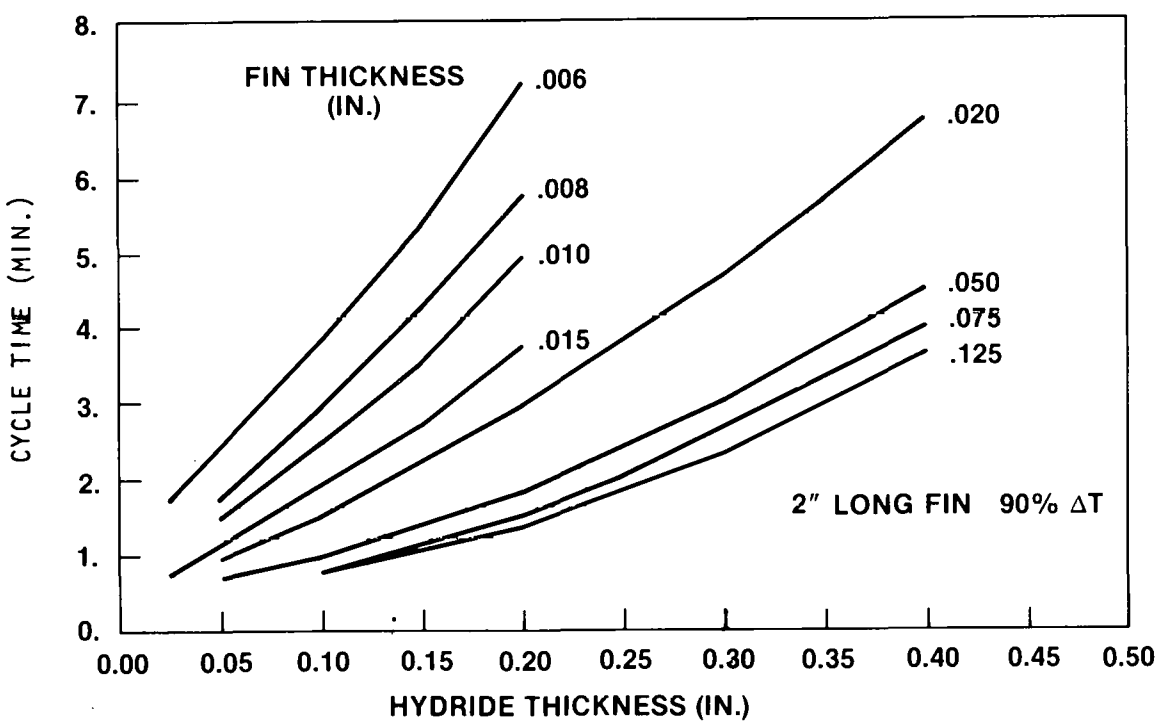

Figure 59. Time to Achieve Temperature for Eight Fin Thicknesses

combinations which minimized the cycle time. A similar analysis was perform varying the fin length for a specific fin thickness (Fig. 60).

This analysis was used to develop an initial system design. Two design parameters were considered of major importance during this development:

1. Thermal Mass Ratio, TMR: the ratio of hydride sensible heat to total system sensible heat.

2. Time, t: the time required to achieve 90 percent of the heat exchange fluid temperature.

To evaluate the optimum design configuration, plots of TMR versus time were constructed for various geometry combinations (Figs. 61 and 62). This information was used to choose geometry combinations that provided relatively low cycle times with relatively high thermal mass ratios. Two combinations of fin and hydride thickness were chosen for more detailed analysis:

1. fin thickness = 0.020, hydride thickness = 0.150

2. fin thickness = 0.010, hydride thickness = 0.05

Analysis of these chosen fin/hydride thickness combinations continued by incorporating the heat transfer coefficient (H) at the inner tube wall into the finite element analysis. The effect of the convective heat transfer coefficient on cycle time is shown in Figure 63 for the two geometry combinations described above and a fin length of 2 inches. The limits shown in

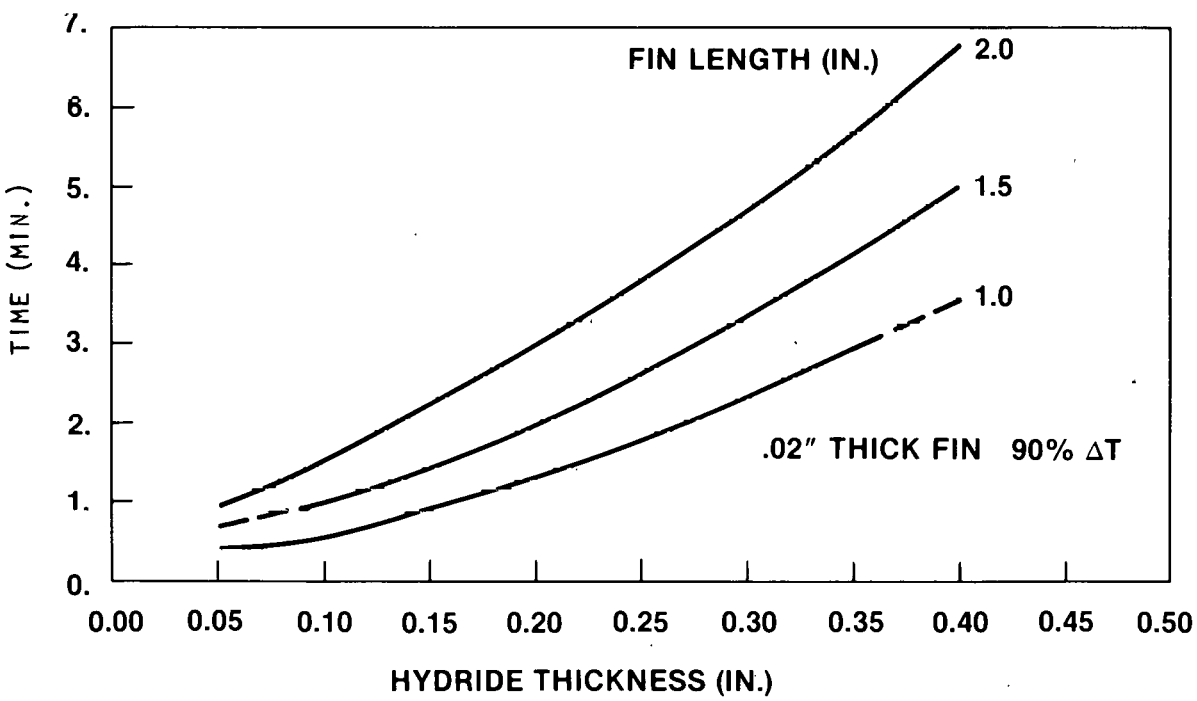

Figure 60. Time to Achieve Temperature for Three Fin Thicknesses

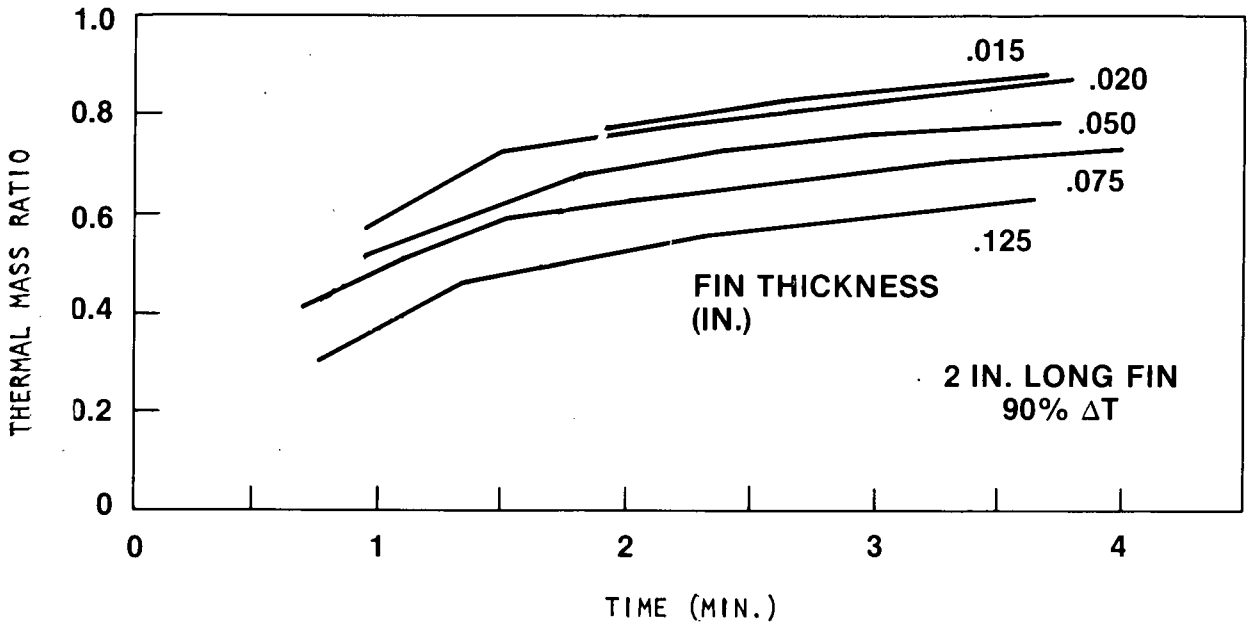

Figure 61. Ratio of Sensible Heat Versus Cycle Time

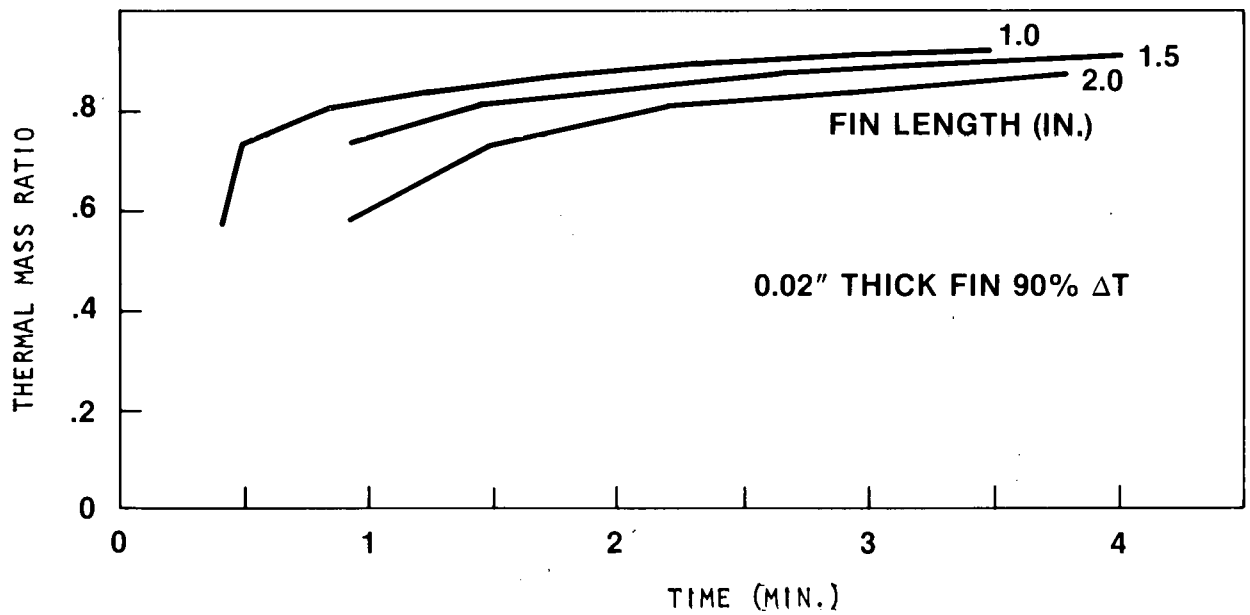

Figure 62. Ratio of Sensible Heat Versus Cycle Time

this figure represent the case of H = ∞. This data indicated that H should be greater than 500 Btu/hr $ft^2°F$, and preferably around 1000 Btu/hr $ft^2°F$. Using this latter value for H, the effect of tube diameter and fin length on cycle time were evaluated. A tube wall thickness of 0.03 inch was assumed for this analysis. This data is shown in Figures 64 and 65 for the two tin/hydride thickness combinations chosen previously. Using this information,

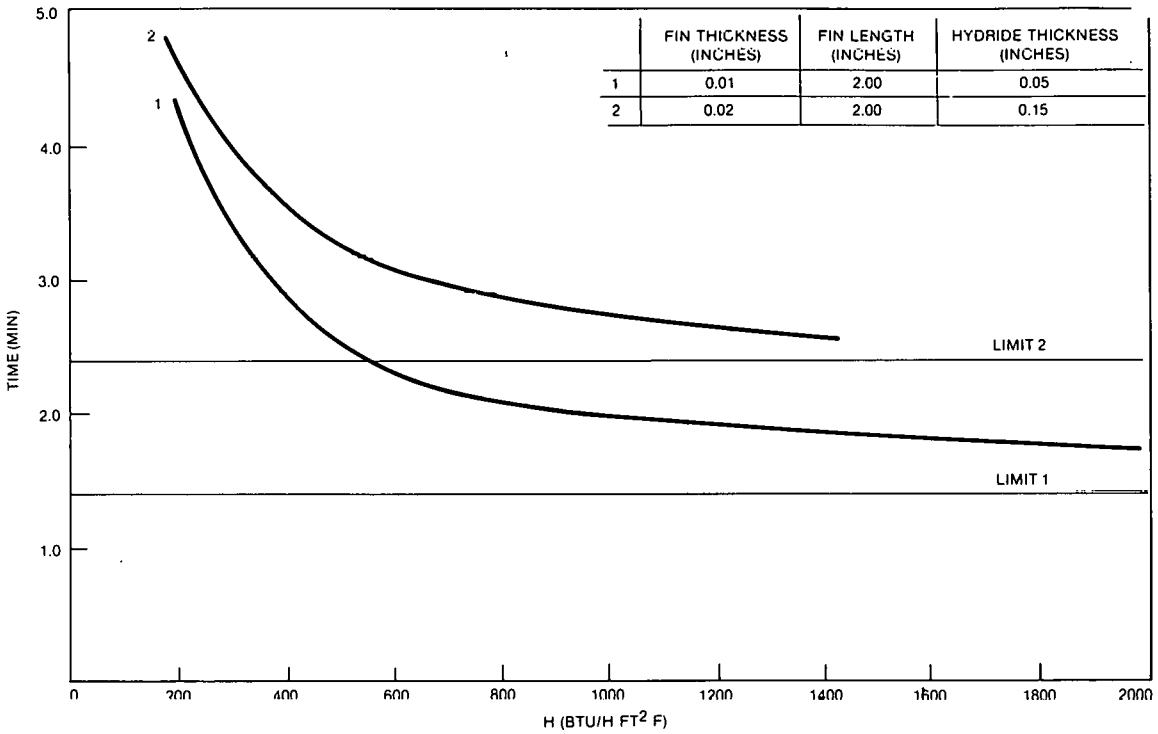

Figure 63. Effect of Convective Heat Transfer Coefficient (H) on Cycle Time

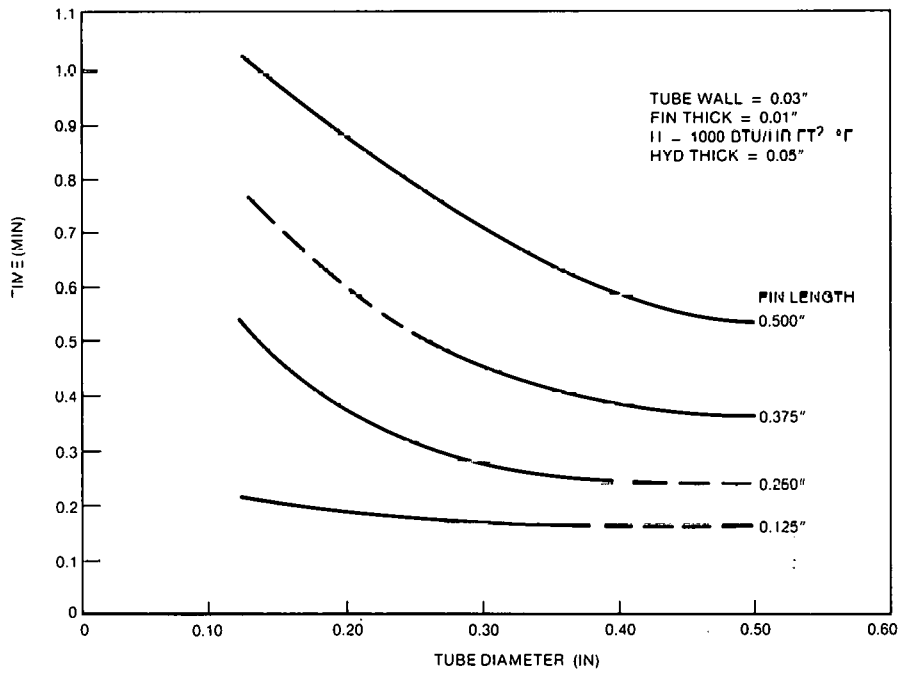

Figure 64. Effect of Tube Diameter on Cycle Time for Various Fin Lengths

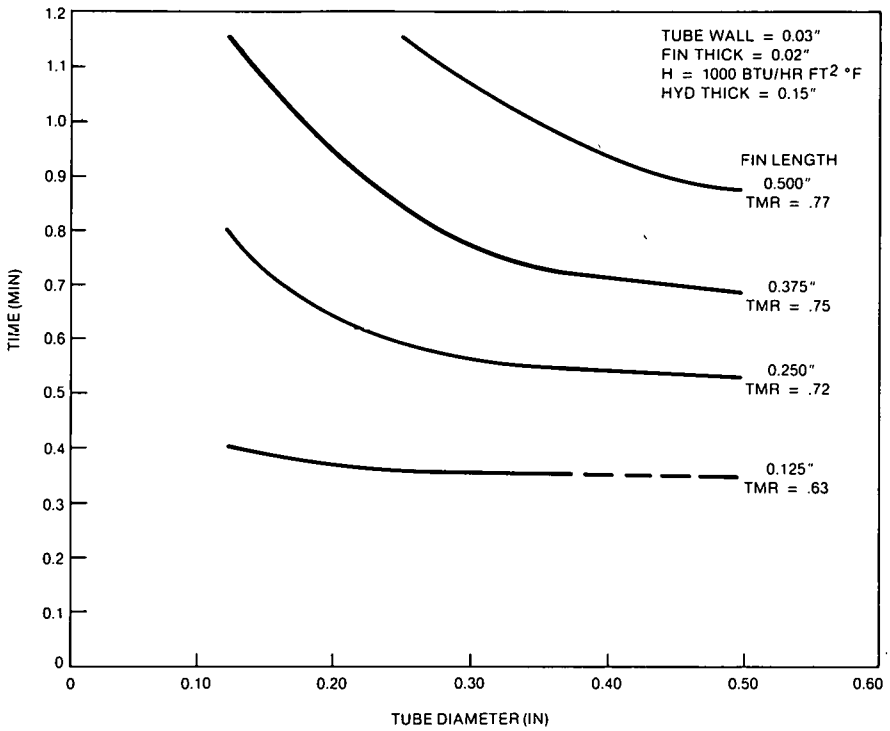

Figure 65. Effect of Tube Diameter on Cycle Time for Various Fin Lengths

an optimum design geometry was chosen based on practical manufacturing considerations. This optimum geometry is:

fin thickness	=	0.020 inch
hydride thickness	=	0.150 inch
fin length	=	0.250 inch
tube diameter	=	0.250 inch

The effect of an increase in tube wall thickness from 0.02 inch to 0.03 inch on cycle time was found to be of minor importance. A four percent increase in cycle time was calculated for this increase in the wall thickness. Thus, tube wall thickness will be dictated by strength and manufacturing considerations.

The effect of the convective heat transfer coefficient (H) was again evaluated, this time for the specific geometry chosen for the optimum design. This information is shown in Figure 66. As previously observed, a value of H greater than 500 Btu/hr ft^2°F is desirable.

Using the optimum design geometry and a value of H equal to 1000 Btu/hr ft^2°F, the net energy transfer rate for the finned tube heat exchanger was evaluated. Assumptions for these calculations are shown in Table 9 and the actual calculations are shown in Figure 67.

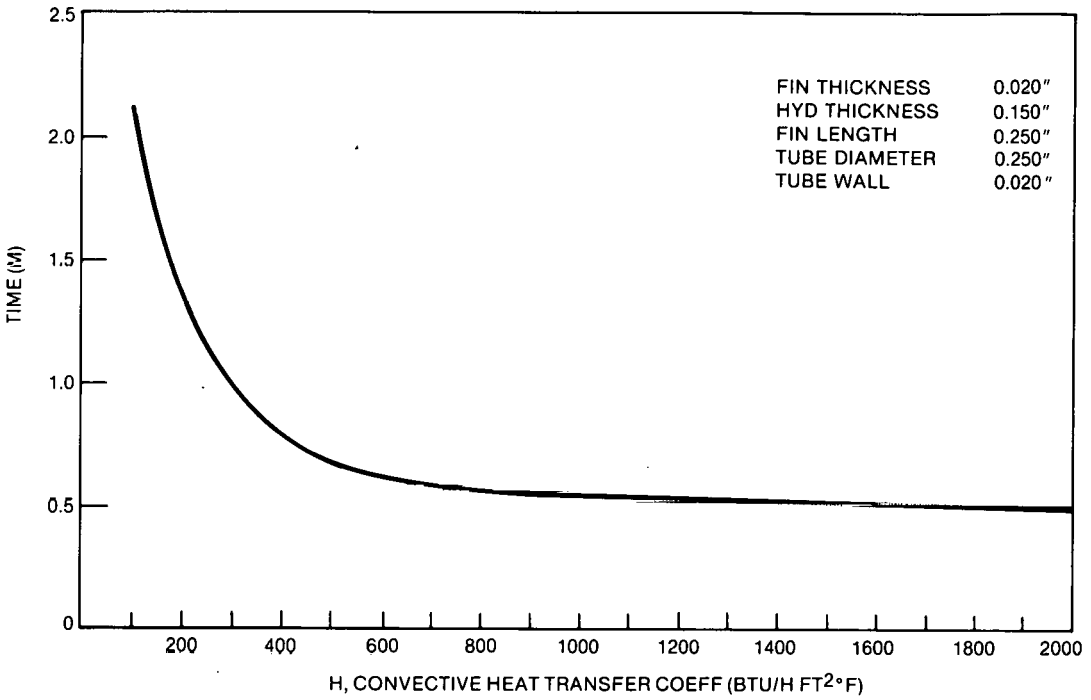

Figure 66. Effect of Convective Heat Transfer Coefficient on Cycle Time

Experimental Verification of Compact Finned Tube Heat Exchangers

A bench scale model of the finned tube hydride heat exchanger was constructed to experimentally evaluate the heat transfer characteristics of the finned tube design and compare them to the analytical predictions from finite element analysis.

A one foot length of helically wound finned tubing was obtained for this test. The fin material is 410 stainless steel, and the tube material is copper. The tube outer diameter is 0.50 inch and the wall thickness is 0.028 inch. The fin length is 0.25 inch and the fin thickness is 0.012 inch.

This finned tube was instrumented with thermocouples to measure tube wall and fin temperatures. The tube was then placed inside a one inch ID clear plastic tube and the voids between the fins were filled with inactive metal hydride powder ($LaNi_5$). The clear plastic tube was used so that complete filling of the fin spaces could be assured and viewed. Additional thermocouples were inserted through the clear plastic tube and into the metal hydride powder at different depths, and one thermocouple was attached to the outer surface of the clear plastic tube. Water temperature into and out of the model were measured. Figure 68 shows this test model and a picture of the finned tube.

The experimental model was plumbed into a hot water supply (Fig. 69). A bypass loop allowed water to be circulated outside of the test section until it reached the desired temperature, whereupon it was diverted to flow through

Table 9

Assumptions for Sensible Heat Calculations*

Material Properties:

density of copper (tubes and fins) = 550 lbm/ft^3
density of hydride = 518.4 lbm/ft^3
specific heat of copper (tubes and fins) = 0.092 Btu/lbm°F
specific heat of hydride = 0.107 Btu/lbm°F
conductivity of copper (tubes and fins) = 200 Btu/hr ft^2°F
conductivity of hydride = 0.30 Btu/hr ft^2°F
hydride heat of formation = 60 Btu/lbm
hydride packing factor = 50%

Physical Geometry:

Tube diameter = 0.25 inch
Fin length = 0.25 inch
Hydride thickness = 0.150 inch
Tube wall = 0.020 inch
Fin Thickness = 0.020 inch
Tube length = 12 inches

Assumed Operating Conditions:

ΔT = 38°C (100°F)
H = 1000 Btu/hr ft^2°F
Water temperature = 77°C (170°F)
Initial hydride temperature = 21°C (70°F)

*English units are shown because the computer model was set up in that fashion.

the test section. The test section was insulated to more accurately model the analytical design.

Data was accumulated using a MACSYM II data acquisition system (see Fig. 70). Data was recorded from 14 thermocouples every five seconds.

Results from the initial test of the finned tube model are shown in Figure 71. Due to limitations of the water pump, the water flowrate (and thus the inner tube wall heat transfer coefficient) was less than desired. The resulting heat transfer coefficient was 200 Btu/hr ft^2°F as opposed to the desired 1000 Btu/hr ft^2°F.

An attempt was made to increase the heat transfer coefficient inside the tube y placing a centerbody in the middle of the tube. Unfortunately, this estriction resulted in a lower water flowrate and actually decreased the heat

Calculated Parameters:

Volume: $V_{copper} = 0.00042\ ft^3$
$V_{hydride} = 0.00238\ ft^3$

Mass: $M_{copper} = 0.234$ lbm
$M_{hydride} = 0.616$ lbm

Sensible Heat: $SH_{copper} = 0.0216$ Btu/°F
$SH_{hydride} = 0.0659$ Btu/°F
$SH_{total} = 0.0875$ Btu/°F

Energy Release: $H_f = 60$ Btu/lbm hyd x $M_{hydride} = 37$ Btu
Energy Absorbed (from specific heat): $H_{SH} = SH_{tot}\ T = 8.75$ Btu

Cycle Time: $t = 1.13$ min.

Net Energy Release: $$E = \frac{H_f - H_{SH}}{t} = 25 \text{ Btu/min}$$

$$E = 1505 \text{ Btu/hr}$$

Figure 67. Sample Calculation for Finned Tube Hydride Heat Exchanger

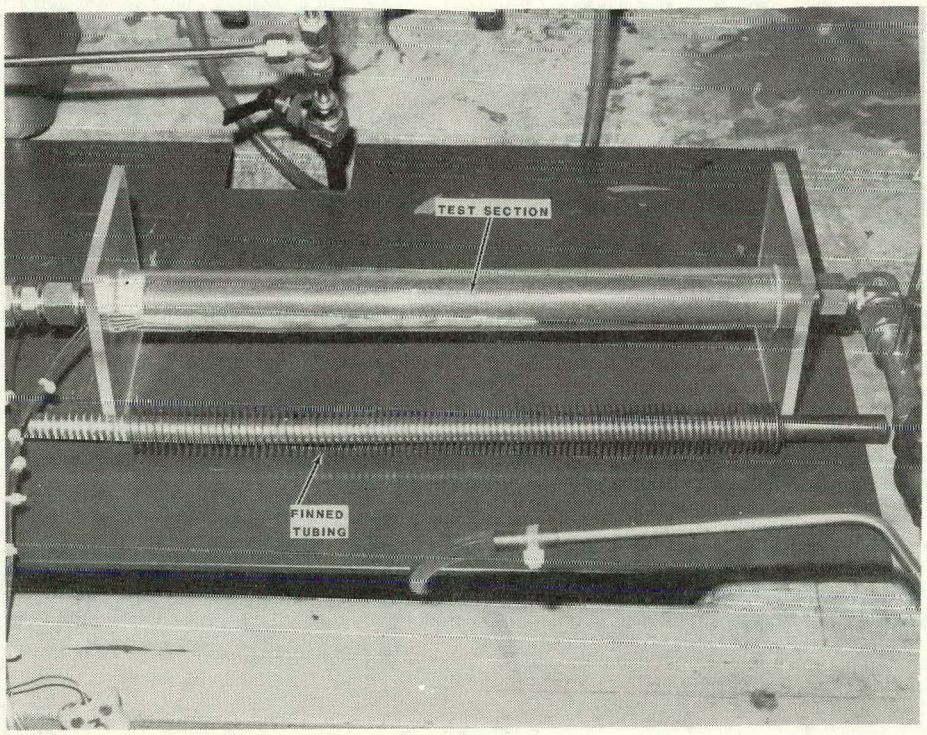

Figure 68. Finned Tube Test Section and Sample of Finned Tubing

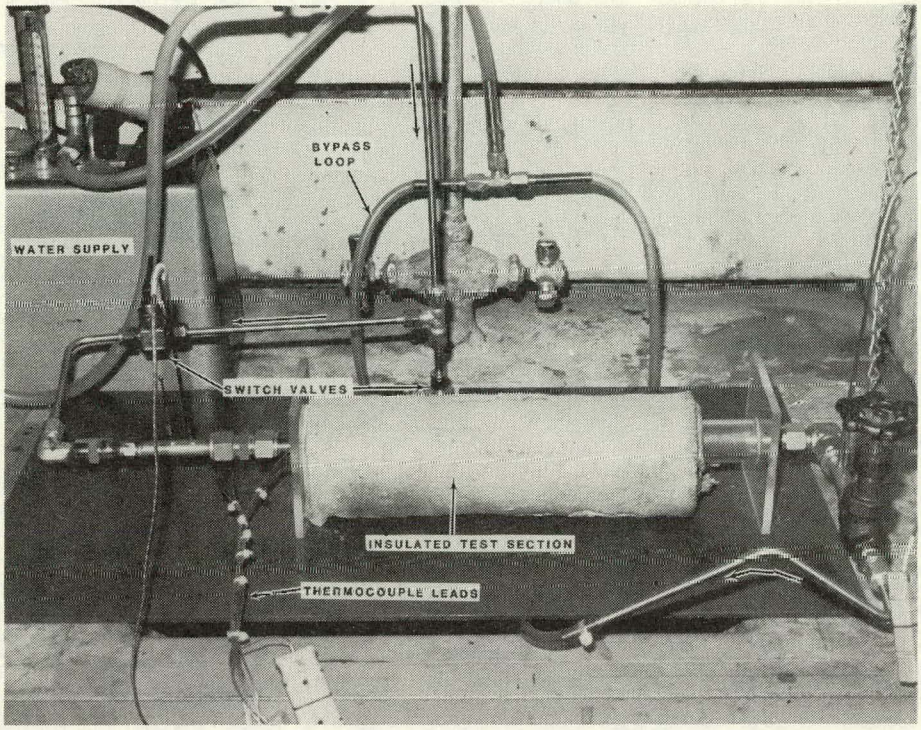

Figure 69. Finned Tube Test Section With Insulation and Water Supply

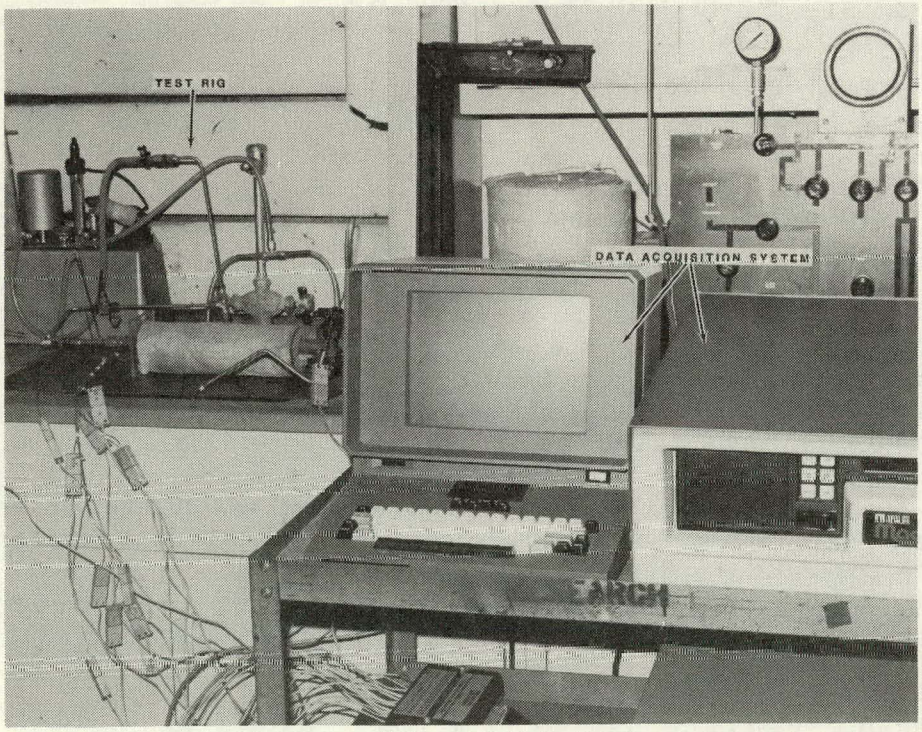

Figure 70. Data Acquisition System With Test Rig

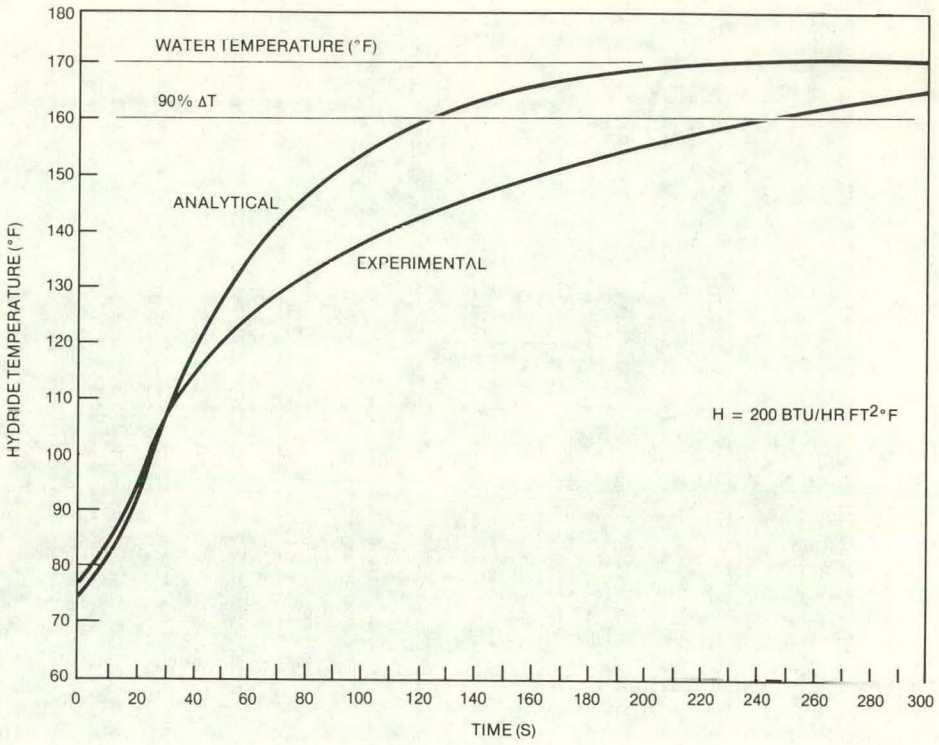

Figure 71. Comparison of Experimental Temperature Rise With That Predicted Analytically for Bench Scale Model of Finned Tube Hydride Heat Exchanger

transfer coefficient. Results from this test are shown in Figure 72. The heat transfer coefficient in this test was 150 Btu/hr $ft^{2}{}^{\circ}F$[4]. A second attempt to improve the heat transfer coefficient was made by using tap water from a laboratory sink. This provided an adequate flowrate to achieve a heat transer coefficient of 1000 Btu/hr $ft^{2}{}^{\circ}F$, but lowered the water temperature to 47°C (116°F). Data from this test is shown in Figure 73.

Initial inspection of this data indicated that the experimental results consistantly fell short of the analytical predictions (except perhaps for short time periods). The time required to achieve 90 percent of the temperature difference between the initial temperature and the water temperature are considerably longer than predicted (from 50 to 125%).

From a different aspect, the actual temperature rise achieved in the predicted cycle time varied from 74 to 79 percent of the maximum possible temperature rise, as opposed to the desired 90 percent. Thus, the actual temperature rise is from 82 to 88 percent of the desired temperature rise, for the predicted cycle time.

---

[4]These values are different from previous published numbers due to correction in the calculations.

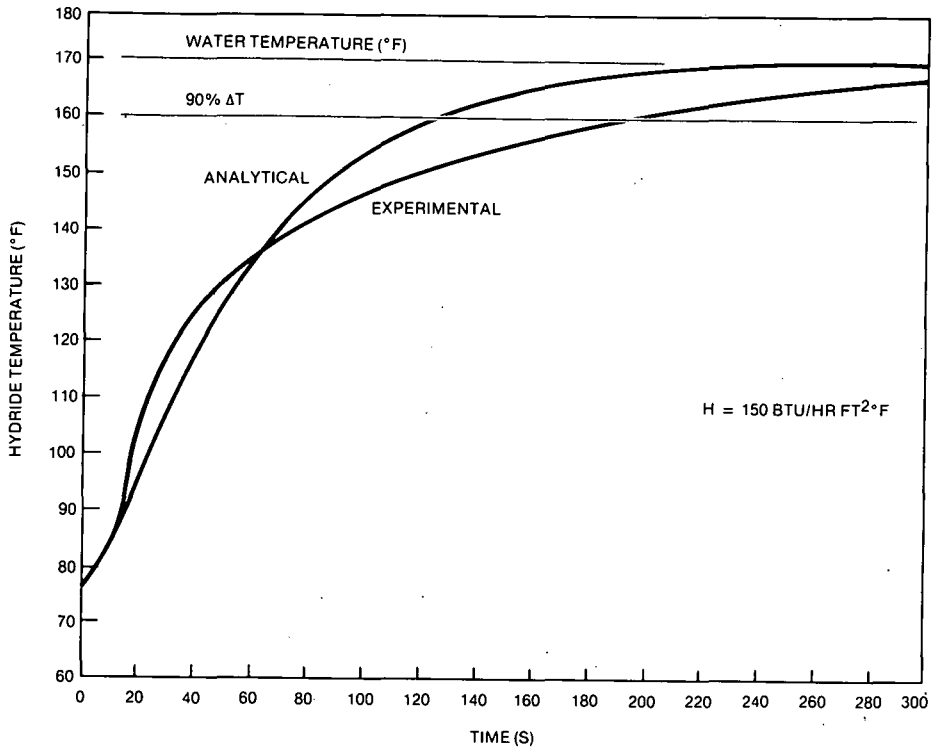

Figure 72. Comparison of Experimental Temperature Rise With That Predicted Analytically for Bench Scale Model Finned Tube Hydride Heat Exchanger

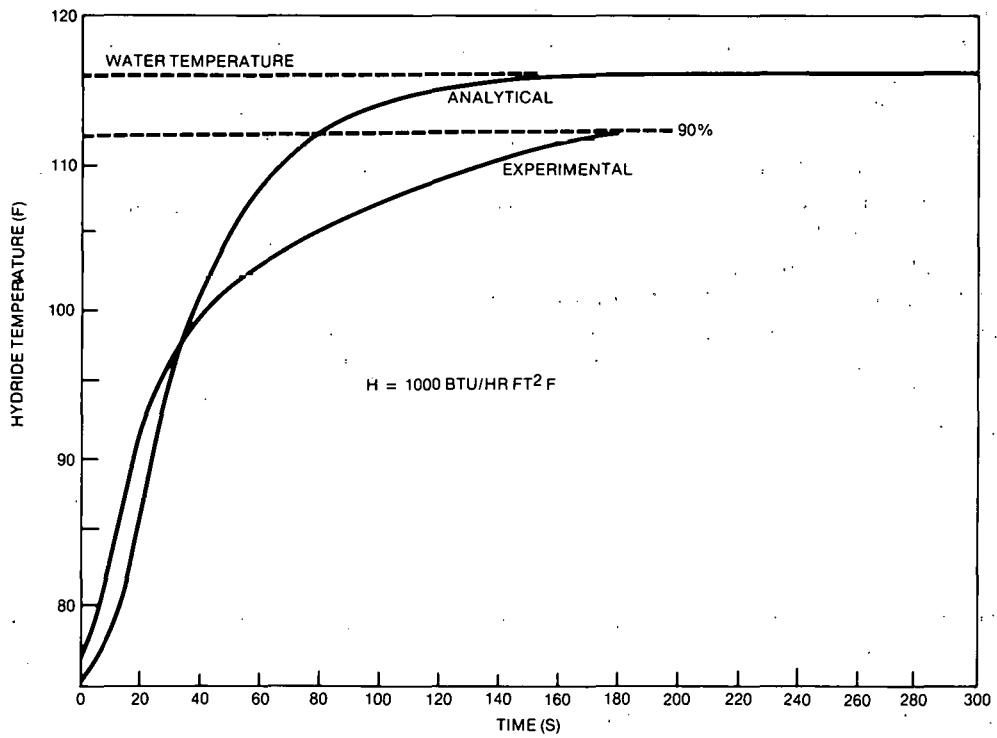

Figure 73. Finned Tube Heat Exchanger Data Using Low Temperature Tap Water for Bench Scale Model of Finned Tube Hydride Heat Exchanger

This experimental data was not used as conclusive evidence of the actu performance of the finned tube design since it was not possible to conduct tests with the desired combination of water flowrate and water temperature. The tests in which the desired water temperature was achieved had low flowrates and thus, low heat transfer coefficients (H). In this range, changes in H significantly affect the cycle time (see Fig. 66) and any error in the calculation of H is significant.

Another source of error may have resulted from the braze layer between the fins and tube, which was not accounted for in the analytical model. It is also believed that better insulation around the finned tube model would improve the performance.

5.3 COEFFICIENT OF PERFORMANCE ANALYSIS

The metal hydride heat pump can be utilized for heating, cooling and temperature upgrading. Depending on the mode of operation, heat is absorbed and desorbed by the MHHP at high (T_H), low (T_L), and intermediate (T_M) temperatures (Figs. 74 and 75). The coefficient of performance (COP) is useful in comparing the thermal efficiences of various MHHP heat transfer configurations.

The input and output heat of the MHHP is a function of the heat of absorption/desorption of the metal hydride powders and the sensible heat of the powder and heat exchangers in which the powder is located. The heat of absorption/desorption is determined from the hydriding reaction across the flat plateau region of the characteristic isotherms for each alloy. The published values for the heat of absorption/desorption for a given alloy assumes that all of the hydride is absorbing and desorbing hydrogen and the full plateau width is traversed. In actual MHHP operation, a small amount of the metal hydride will remain inactive (not absorbing hydrogen) and the full plateau width will not be utilized. Therefore, in computing the actual heat of absorption/desorption of the metal hydride powders, the theoretical value will be multiplied by a utilization factor derived from empirical results to adjust the heat of absorption/desorption to a more realistic value. In evaluating the sensible heat of the MHHP, the system boundaries are located at the outer surfaces of the heat exchanger containing the metal hydride. The method of applying heat to the unit can vary substantially (i.e., hot water, direct gas flame), so the sensible heat of the outer systems will not initially be included.

5.3.1 COP for Heating and Cooling

The heat pump operation is identical for heating or cooling cycles; only the temperature use is altered (Fig. 74). The refrigeration produced by hydride B at T_L is used for cooling, while the heat output by hydrides A and B at T_M is used for heating operations. The coefficient of performance of the MHHP for heating and cooling can be defined as:

a. STORAGE MODE

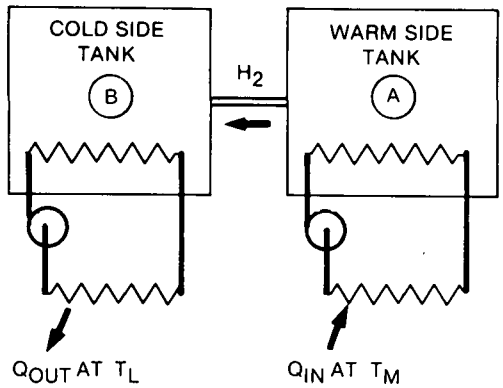

b. UPGRADING MODE

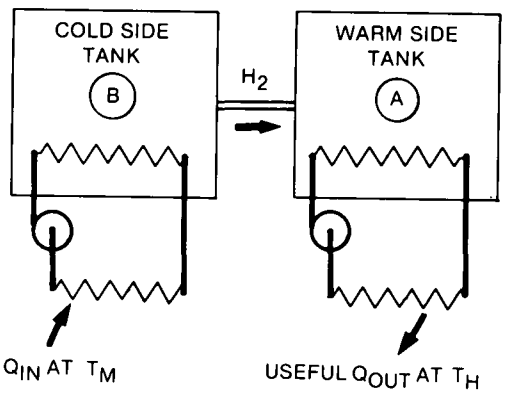

Figure 74. Temperature Upgrade Operation

$$COP_{cool} = \frac{\text{Net Heat Input at } T_L}{\text{Net Heat Input at } T_H}$$

$$COP_{heat} = \frac{\text{Net Heat Output at } T_M}{\text{Net Heat Output at } T_H}$$

In the storage mode (Fig. 74a), hydride A is heated from T_M to T_H and desorbs hydrogen. Hydride B absorbs hydrogen and heats up from T_L to T_M. The net heat transferred to hydride A and B is:[5]

$$Q_{net(A,\ T_H)} = Q_{des(A)} + SH_A\ (T_M - T_H)$$

$$Q_{net(B,\ T_M)} = Q_{abs(B)} + SH_B\ (T_L - T_M)$$

H = sensible heat

a. STORAGE MODE

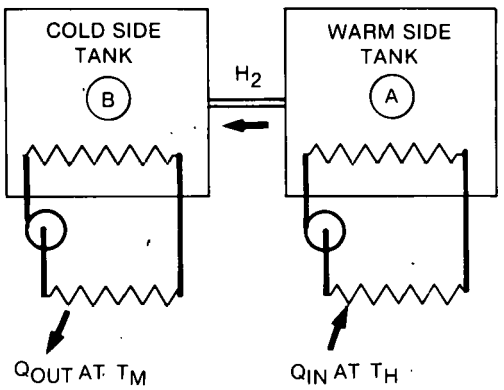

b. REFRIGERATION MODE

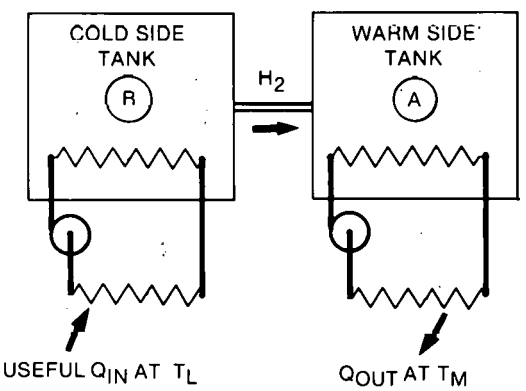

Figure 75. Heating and Cooling Operation

where $Q_{des(A)}$, the heat of desorption of hydride A, has a negative value and the heat of absorption has a positive value.

In the refrigeration mode (Fig. 74b), hydride A is cooled from T_H to T_M and absorbs hydrogen. Hydride B desorbs hydrogen and is cooled from T_M to T_L. The net heat transferred to hydride A and B is:

$$Q_{net(A,\ T_M)} = Q_{abs(A)} + SH_A\ (T_H - T_M)$$

$$Q_{net(B,\ T_L)} = Q_{des(b)} + SH_B\ (T_M - T_L)$$

The COP equations for heating and cooling are:

$$COP_{cool} = \frac{Q_{net(B,\ T_L)}}{Q_{net(A,\ T_H)}} = \frac{Q_{des(B)} + SH_B\ (T_M - T_L)}{Q_{des(A)} + SH_A\ (T_M - T_H)}$$

$$COP_{heat} = \frac{Q_{net(B,\ T_M)} + Q_{net\ (A,\ T_M)}}{Q_{net(A,\ T_H)}}$$

$$= \frac{Q_{abs(B)} + SH_B\ (T_L - T_M) + Q_{abs(A)} + SH_A\ (T_H - T_M)}{Q_{des(A)} + {}_{S}H_A\ (T_M - T_H)}$$

5.3.2 COP for Temperature Upgrade

The desired product when the MHHP is used as a temperature upgrader, is the heat produced by hydride A at T_H (Fig. 75). The coefficient of performance of the MHHP operating as a temperature upgrader is:

$$COP_{upgrade}\ (U) = \frac{\text{Net Heat Output at } T_H}{\text{Net Heat Input at } T_M}$$

In the storage mode (Fig. 75a), hydride A desorbs hydrogen and is cooled from T_H to T_M, while hydride B absorbs hydrogen and is heated from T_L to T_M.

$$Q_{net(A,\ T_M)U} = Q_{des(A)} + SH\ (T_H - T_M)$$

$$Q_{net(B,\ T_L)U} = Q_{abs(B)} + SH\ (T_M - T_L)$$

In the upgrade mode (Fig. 75b), hydride A absorbs hydrogen and is heated from T_M to T_H. Hydride B absorbs hydrogen and is heated from T_L to T_M.

$$Q_{net(A,\ T_H)U} = Q_{abs(A)} + SH\ (T_M - T_H)$$

$$Q_{net(B,\ T_M)U} = Q_{des(B)} + SH\ (T_L - T_M)$$

The COP equation for temperature upgrade is:

$$COP_{upgrade} = \frac{Q_{net(A,\ T_H)U}}{Q_{net(A,\ T_M)U} + Q_{net(B,\ T_M)U}}$$

$$= \frac{Q_{abs(A)} + SH\ (T_M - T_H)}{Q_{des(A)} + SH\ (T_H - T_M) + Q_{des(B)} + SH\ (T_L - T_M)}$$

The COP was calculated for the optimum MHHP design configurations (Table 10). Several assumptions were made as the basis for the calculations. It was assumed that the hydride powder was 70 percent active and had a 57 percent packing factor. Temperatures assumed were T_H = 177°C (350°F), T_M = 93°C (200°F) and T_L = 27°C (80°F) for temperature upgrade operation. The maximum theoretical $COP_{upgrade}$ is 0.55 (calculations in Appendix 8). This assumes no sensible heat gain or loss. The compact finned tube heat exchanger design resulted in a $COP_{upgrade}$ of 0.42 whereas the optimum tubular design -- one

Table 10

COP Values for Two MHHP Configurations

	COP Upgrade
Compact finned tube heat exchanger - 0.020 inch fin thickness, 0.150 inch hydride thickness, 0.250 inch fin length, 0.250 inch tube diameter	0.42
1 inch OD copper tube with six internal fins (optimum design as shown in Figure 48)	0.38

inch OD copper tube with six internal fins -- had a $COP_{upgrade}$ of 0.38. This was an important consideration in finalizing the MHHP design.

5.4 FILTER DESIGN STUDIES

It is essential that the fine particles of the two hydrides do not intermix by traveling with the hydrogen gas as it cycles from bed to bed. A particle separator/retainer (or filter) in the hydrogen flow path is required to isolate each hydride bed. Studies indicate that a critical parameter in the MHHP performance is cycle time and, if the ΔP across the filter is substantial, the result is a long cycle time. Therefore, a filter test rig was fabricated to determine the pressure drop across various hydride powder/filter configurations. Previous filter testing had indicated that the ΔP across a specific filter can vary substantially depending upon the orientation of the filter in relation to the metal hydride powder.

Filter tests performed by Solar in the past had concentrated upon particle containment, i.e., the impact of the filter upon removal of hydride particles from the hydrogen flow. Many filter materials were tested with the result that one of the most effective filters was a sintered stainless steel filter. This filter is 0.035 inch thick and is rated at 2 microns. Further work in the current program focused on the optimum filtering scheme with regards to orientation and configuration.

The filter test rig was constructed from a one inch diameter, six inch long copper tube with the sintered stainless steel filters at both ends (see Fig. 76). A U-tube manometer was used to determine the pressure drop across the powder/filter assembly. The assembly could be mounted in any position (i.e., horizontal, vertical) and any amount of hydride powder could be packed between the filters. The goal of this work was to develop a filtering scheme with the following parameters:

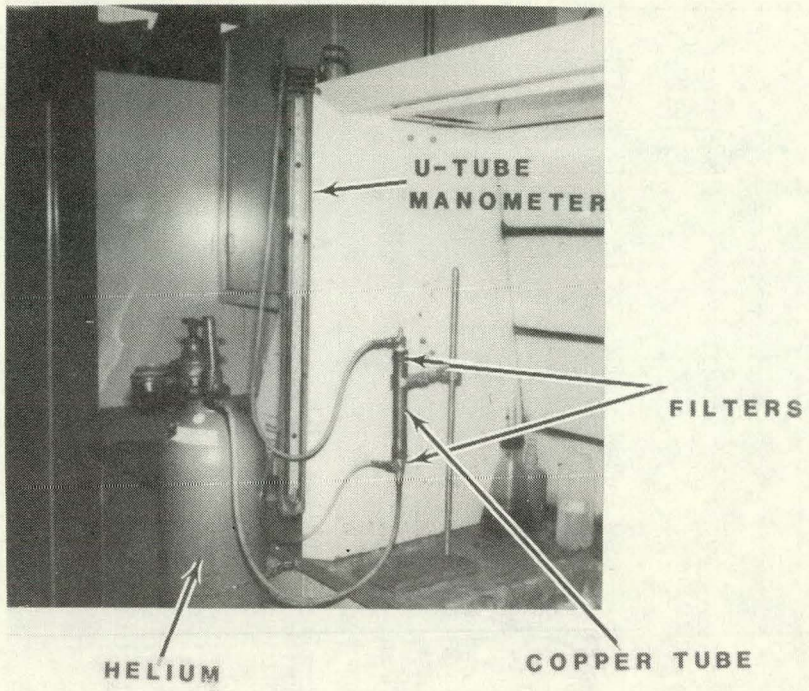

Figure 76. Filter Test Rig

1. Low pressure drop across the filter, less than 34.5 kPa (5 psi) (little restriction of hydrogen gas flow)

2. Containment of the hydride powder (no migration of one hydride bed to the other through the filter)

3. Long life (clog-free with time)

4. Economical

The six-inch copper tube with filters in place at both ends had pressure taps connected to a manometer to determine the pressure drop across the test assembly. Since the total ΔP was the sum of the pressure drops due to both filters, and since the pressure drop for each filter was different depending on direction of flow, certain simplifying assumptions were made to determine consistently the ΔP across the filter in a particular orientation. The first assumption was that only one filter was "working" at a time. It was assumed that when the flow tends to push the powder away from the filter surface, then that filter was not working as a filter and the ΔP was constant through this filter regardless of orientation. This means that the ΔP for the "working" filter was the total pressure drop minus the pressure drop due to the flow through the "non-working" filter.

The second assumption was that the presssure drop was inversely proportional to the surface area of the filter, i.e., doubling the area halved the pressure drop. In the data presented in Figures 77 through 79, the ΔP is plotted as function of flow density (ACFM/ft^2 - actual cubic feet per minute/square foot of filter surface area) and the height of hydride powder in the copper tube.

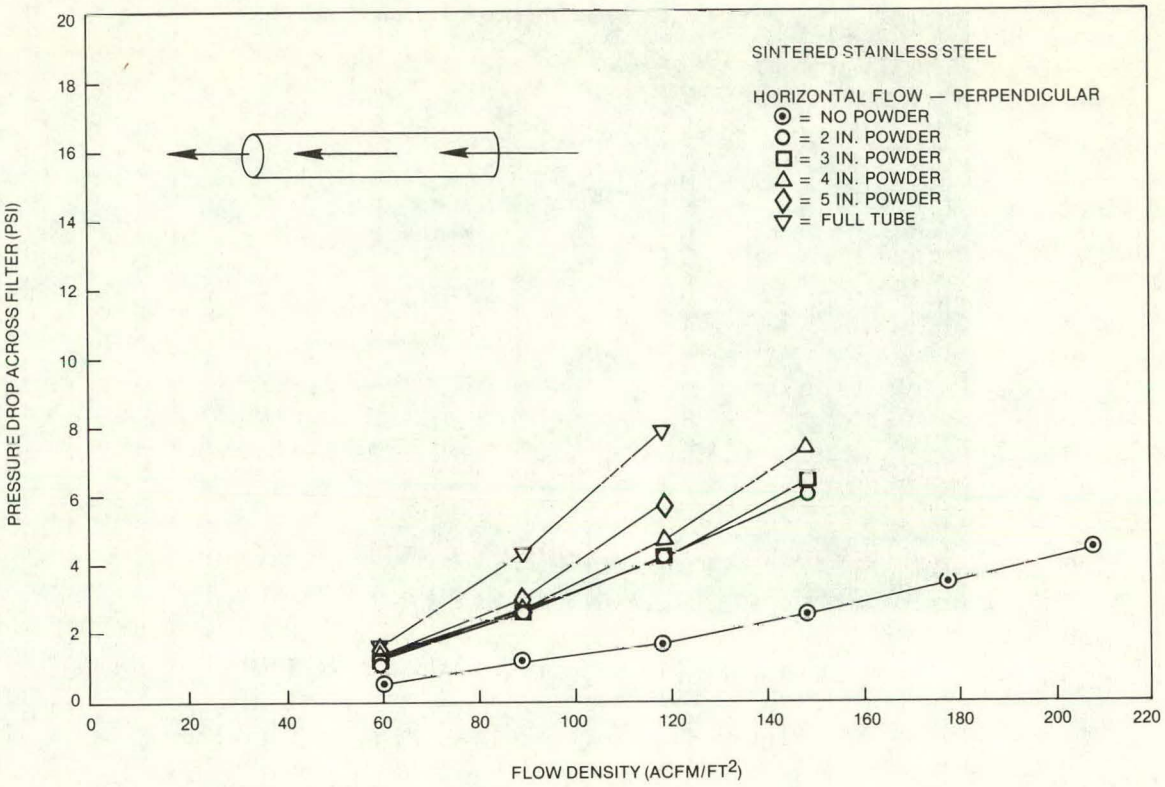

Figure 77. Pressure Drop Vs. Flow Density for Sintered Stainless Steel Filter - Horizontal Flow

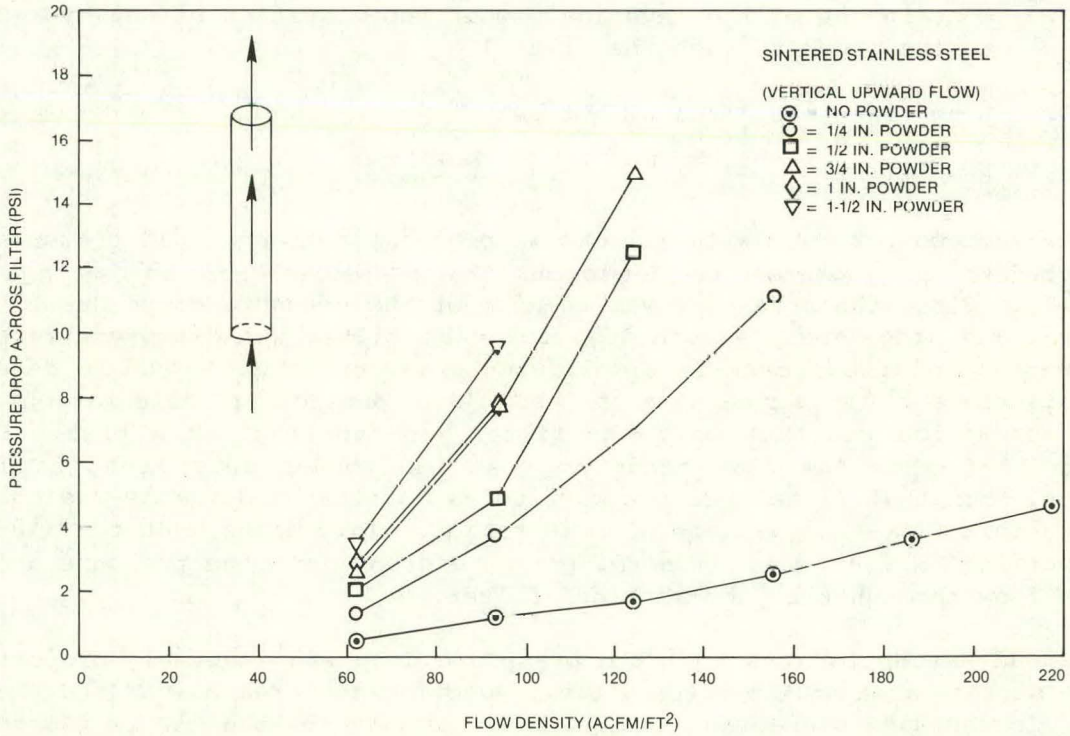

Figure 78. Pressure Drop Vs. Flow Density for Sintered Stainless Steel Filter - Vertical Upward Flow

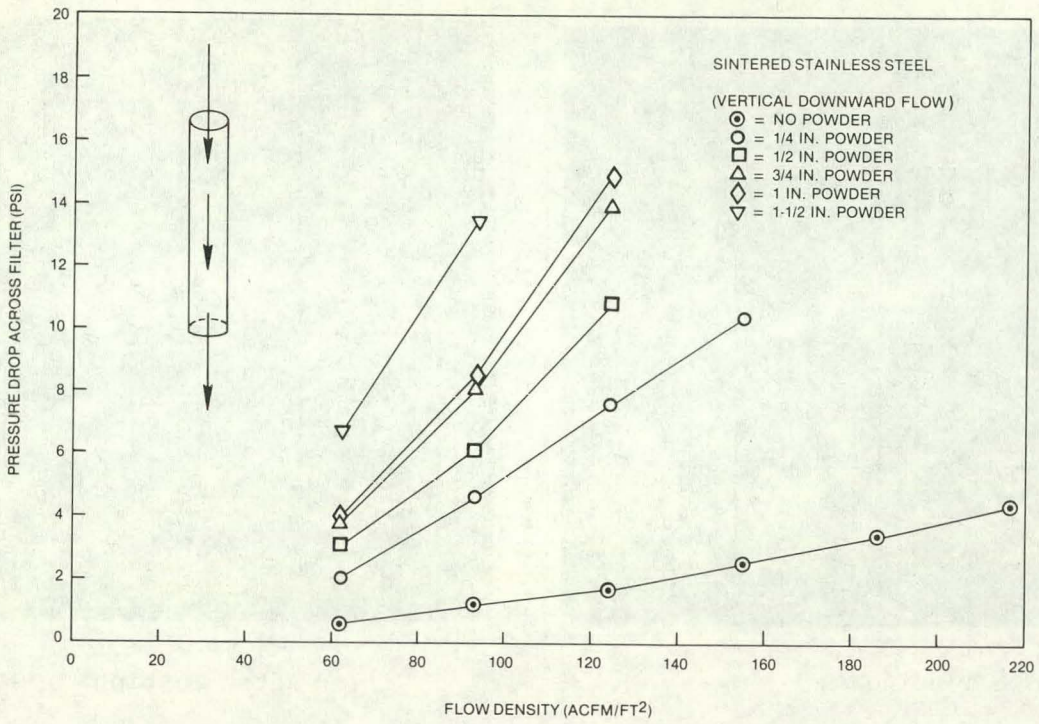

Figure 79. Pressure Drop Vs. Flow Density for Sintered Stainless Steel Filter - Vertical Downward Flow

A value for the required amount of filter surface area per pound of hydride powder could be determined from the graphs. This method is outlined in Appendix 9 with an example. The example illustrates that for a 12,000 Btu/hr (1 ton) capacity unit using 5 pounds of powder, the required filter surface area is 3.7 in^2 of 18.5 in^2 total.

The tests on the sintered stainless steel filter showed that the best powder orientation for the flat filter in terms of low pressure drop was with no powder in contact with the filter. A free-standing flat filter in any configuration whether with horizontal or vertical, upward or downward flow was decided to be the optimum configuration.

Another filter configuration was considered for the MHHP besides the sintered stainless steel filter. That filter is only available in sheet form and a tubular filter configuration was thought to be a possibility for the design. A tubular mesh filter was tested. The filter was 4.28 inches long and 5/16 inch OD and was rated at 40 microns. Figure 80 shows the filter before and after testing. The hydride powder had a tendency to cling to the filter and produce high pressure drops. Data is presented in Figures 81 through 83.

The optimum orientation for the tubular filter was also the free-standing mode. However, the hydride heat exchanger designs using this filtering scheme call for the filter to be in close contact with the powder. This produces gh pressure drops and clogging of the filter with time. This is unacceptable in the MHHP and was a consideration in the final design.

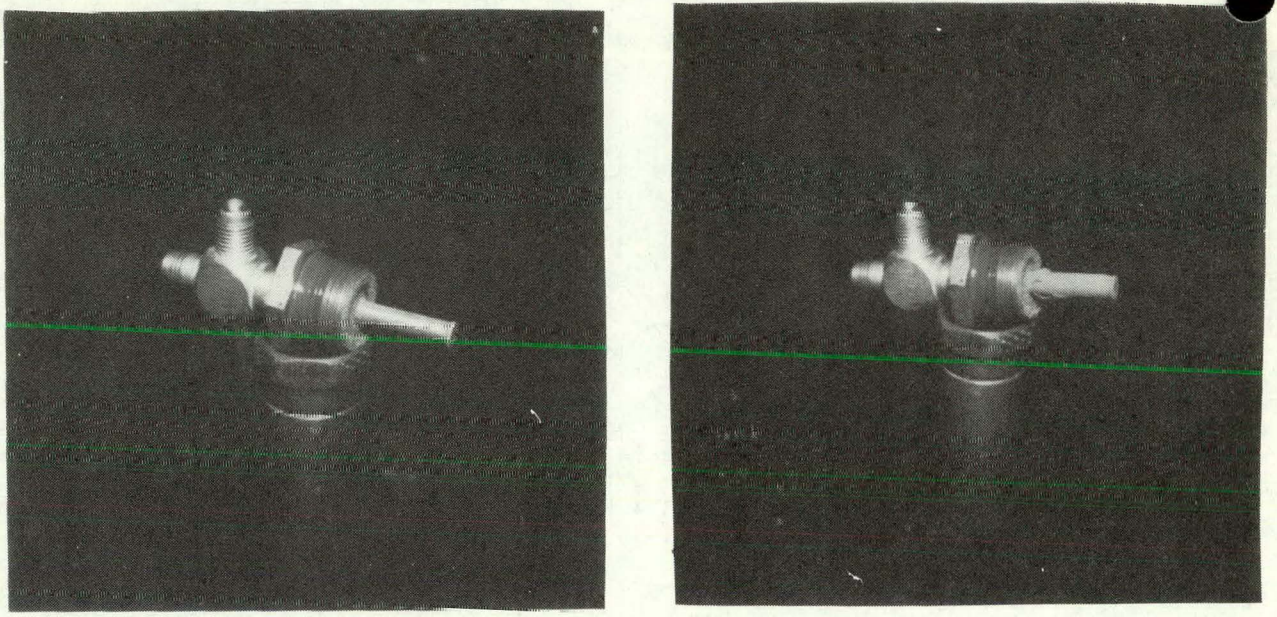

Before Testing

After Testing

Figure 80. Tubular Filter

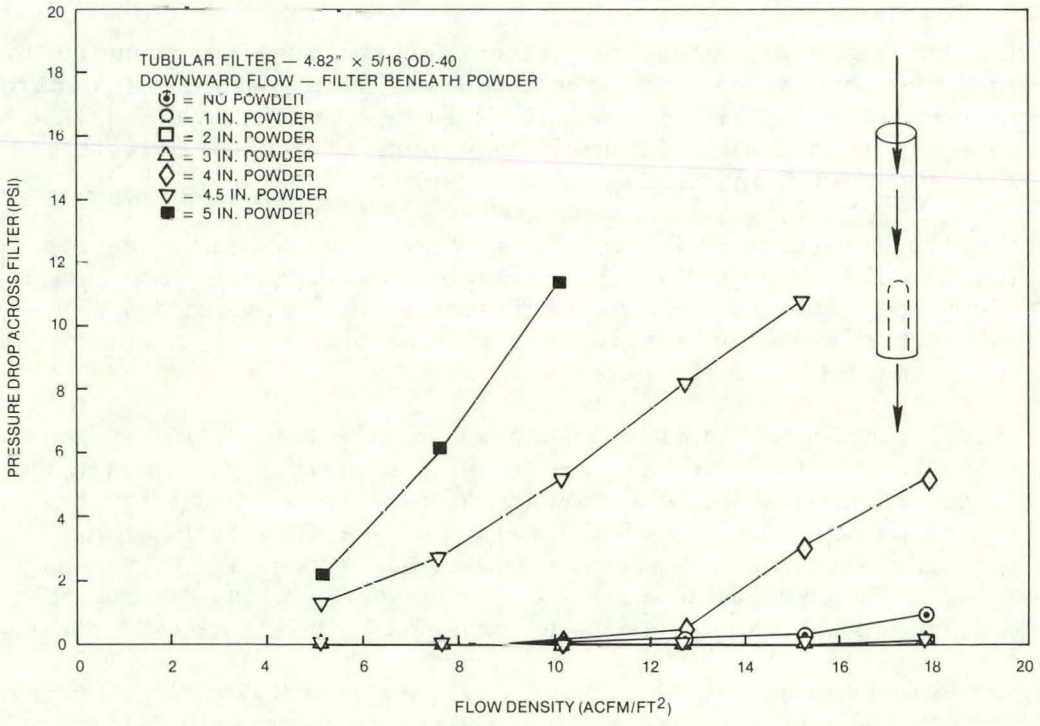

Figure 81. Pressure Drop Vs. Flow Density for Tubular Filter - Upward Flow, Filter Above Powder

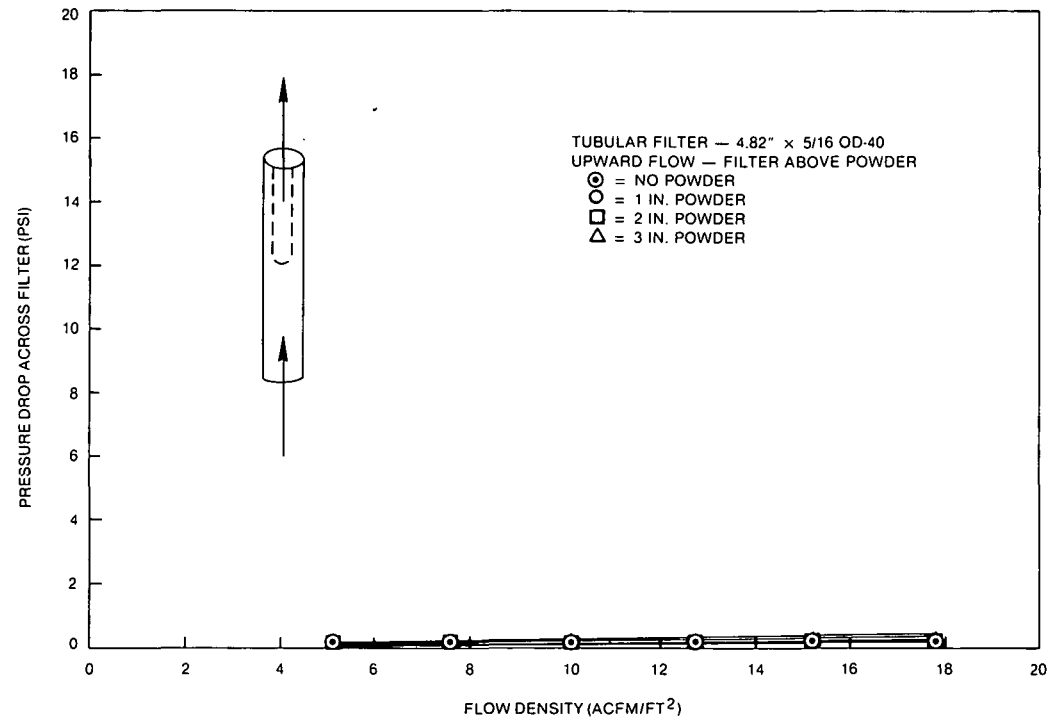

Figure 82. Pressure Drop Vs. Flow Density for Tubular Filter - Downward Flow, Filter Beneath Powder

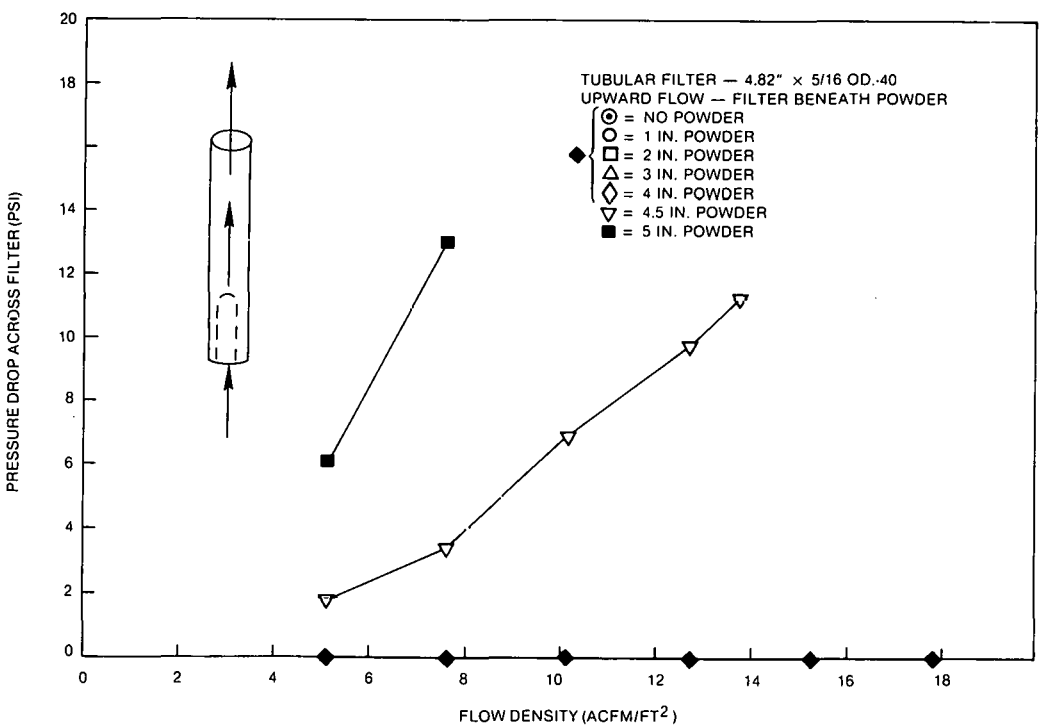

Figure 83. Pressure Drop Vs. Flow Density for Tubular Filter - Upward Flow, Filter Beneath Powder

5.5 CONTROL SYSTEMS STUDY

To do an effective job, the control unit for the MHHP must provide these capabilities:

1. Maintain a set point temperature for a given space.

2. Establish a flow circulation path for heating and cooling fluids.

3. Maintain rate of flow for heating and cooling flows.

4. Optimize heating and cooling cycles for maximum efficiency.

5. Display status and measured values on the system that indicates performance of the system (this will be limited on production system).

6. Maintain surveillance of key system parameters. Check for out-of-tolerance operation. If a condition exists which could produce harmful results take corrective action or effect a gradual shutdown.

These capabilities must be provided in both the EDTU phase and in the EETU phase. The distinction between the two phases is that more man-machine interface is required during EDTU development. A lower cost, concise configuration is required for the EETU phase. The EETU must include the following three additional capabilities:

1. Cost improvement

2. Size reduction

3. Enhanced reliability

The general functions of the MHHP controller is discussed in this section. Then the preliminary design for the Phase III EETU controller is presented. The design for the Phase II EDTU is included in Chapter 6 - Final Design.

5.5.1 Description of the MHHP Controller

The controller for the MHHP will have to handle a set of input and output tasks. The I/O section supplies information to and transfers commands from the basic intellegence of the control. The following two sections expand on the I/O requirements and describe the configuration of the control hardware.

Input/Output Requirements

(a) The control unit will sample temperatures of heating fluids, coo ing fluids, heat exchanger surface temperatures and the enviro

ment under control. This is to be accomplished with thermocouples and a reference junction for the thermocouples. The flow rates of heating and cooling fluids will be sampled for control purposes. The operator's input will be received via a keyboard.

(b) The control unit will control valve actuation sequences, fan activation, pump operation and transfer information to the operator via the display panel.

General Configuration of Control Hardware

The control hardware of the control unit can best be described by referring to the hardware block diagram (Fig. 84). The peripheral elements around the circuit card frame make up the interface and function as follows:

(a) Fan Control Circuit. This circuit translates the logic level signal from the computer circuits to levels which can activate the motor starter on the fan.

(b) Pump Control Circuit. This circuit translates the logic level signal from the computer circuits to levels which can activate the motor starter to the pumps.

(c) Valve Control Circuit. This circuit translates the logic level signal from the computer circuits to levels which will activate the solenoid valves in the system.

(d) Operator Control Panel (included with the Display Panel on the micro terminal). This is a keyboard device used by the operator to enter instructions to the computer circuits.

(e) Power Supply #1 (P.S.#1). This supply provides DC power to the computer circuits.

(f) Power Supply #2 (P.S.#2). This supply provides DC power to transducer signal conditioning circuits.

(g) Key Switch and Fuses. This circuitry provide the switched entry of 117 volt AC power to energize the control unit.

(h) Flow Measurement. This circuitry provides signal conditioning for flow measurement tranducers.

(i) Thermocouple Reference Junction. This circuitry provides signal conditioning for thermocouple temperature measurements (see Fig. 85).

(j) Display Panel (included in micro terminal). This is a combination of alpha numeric display elements auqmented with a set of (light emitting diode) discrete lamps to keep the operator aware of the functioning of the computer circuits.

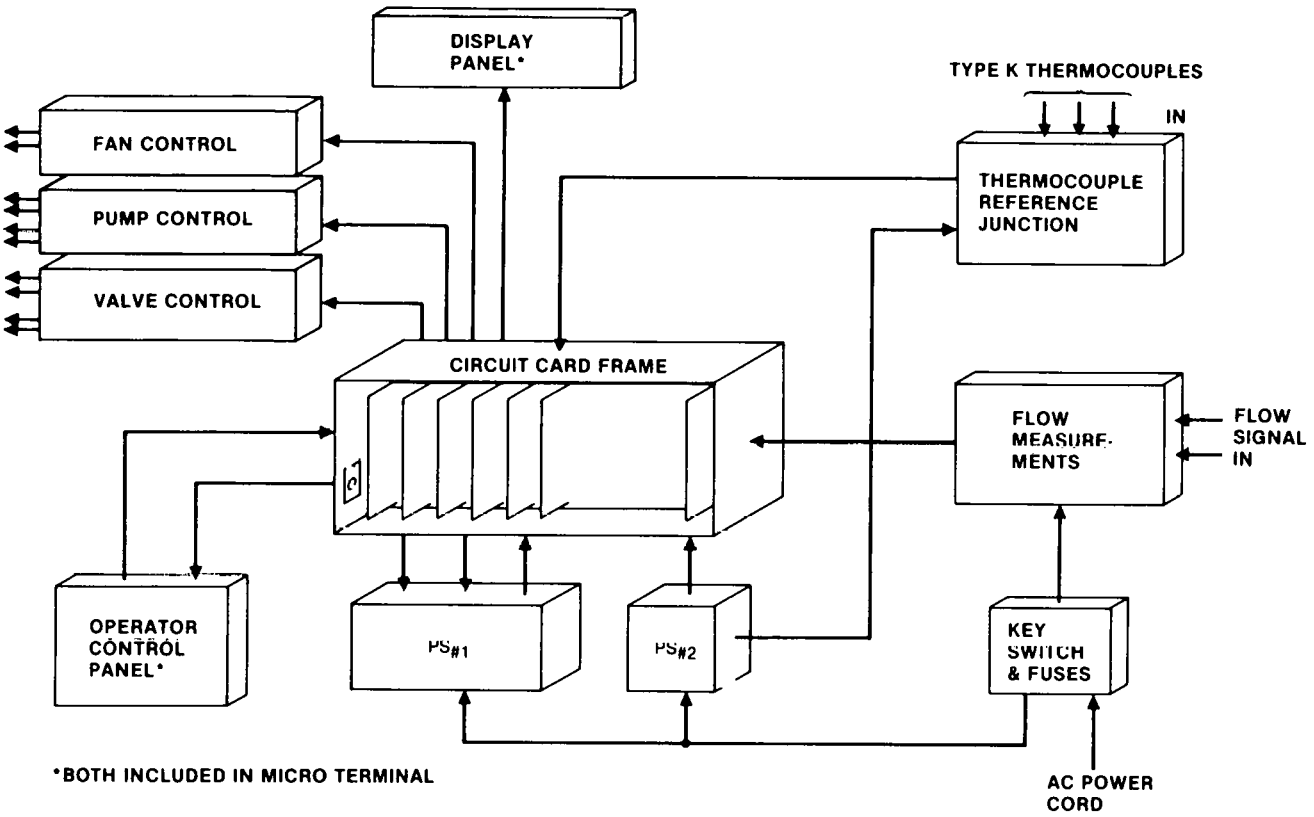

Figure 84. Hardware Block Diagram

5.5.2 Description of Controls for the EETU

The controller for the EETU in Phase III will be optimized for the specific objectives. Expensive general purpose instrumentation will be avoided. Thus, alternate transducers must be selected and validated. The hardware effort will include continued investigation to define specific transducer requirements. The task includes identifying cost effective devices in compliance with the specific requirements. If required, additional software will be created to make use of potential cost effective transducers.

The human/machine interface will become much more concise. There will no longer be a complex dialog inherent in an experimental system. The display will reduce in size and complexity. Simple dedicated switches will replace the general purpose keyboard approach. The control functions will be present but also tailored to a more specific set of tasks and more finite operating ranges.

5.5.3 Implementation of EETU Hardware

The EETU (Phase III) control unit can be implemented utilizing a single chi microcomputer (Fig. 86). The microcomputer under consideration, a Mode_

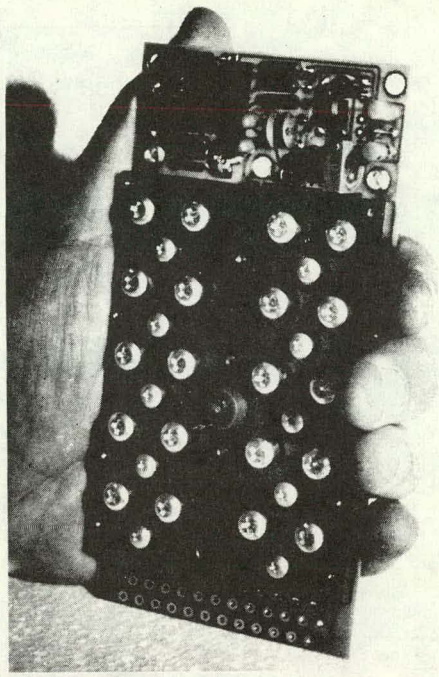

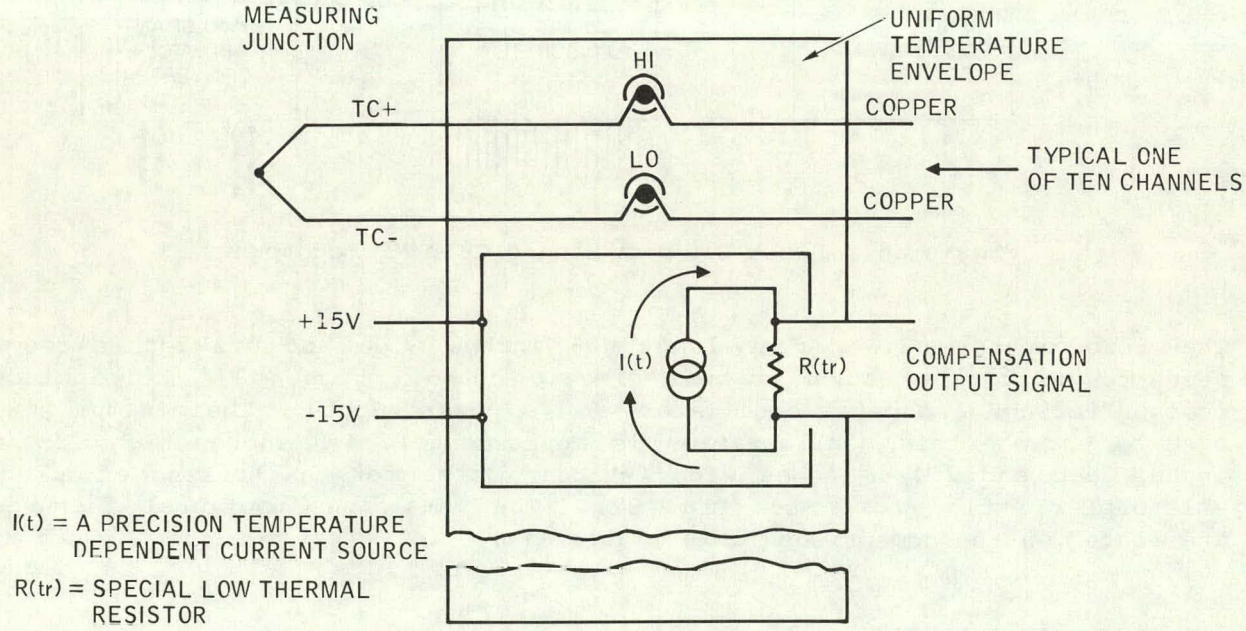

Figure 85. The SL1000 Ten-Channel Modular Reference Junction

8022 manufactured by Intel Corp, includes an on-chip analog to digital converter. It includes a 8 Bit CPU, a 8 Bit analog to digital converter, a 2048 byte read only memory, a 64 byte random access memory, 28 input-output lines, nd a 8 bit event timer. The single chip device is a 40 pin dual-in-line onolithic integrated circuit.

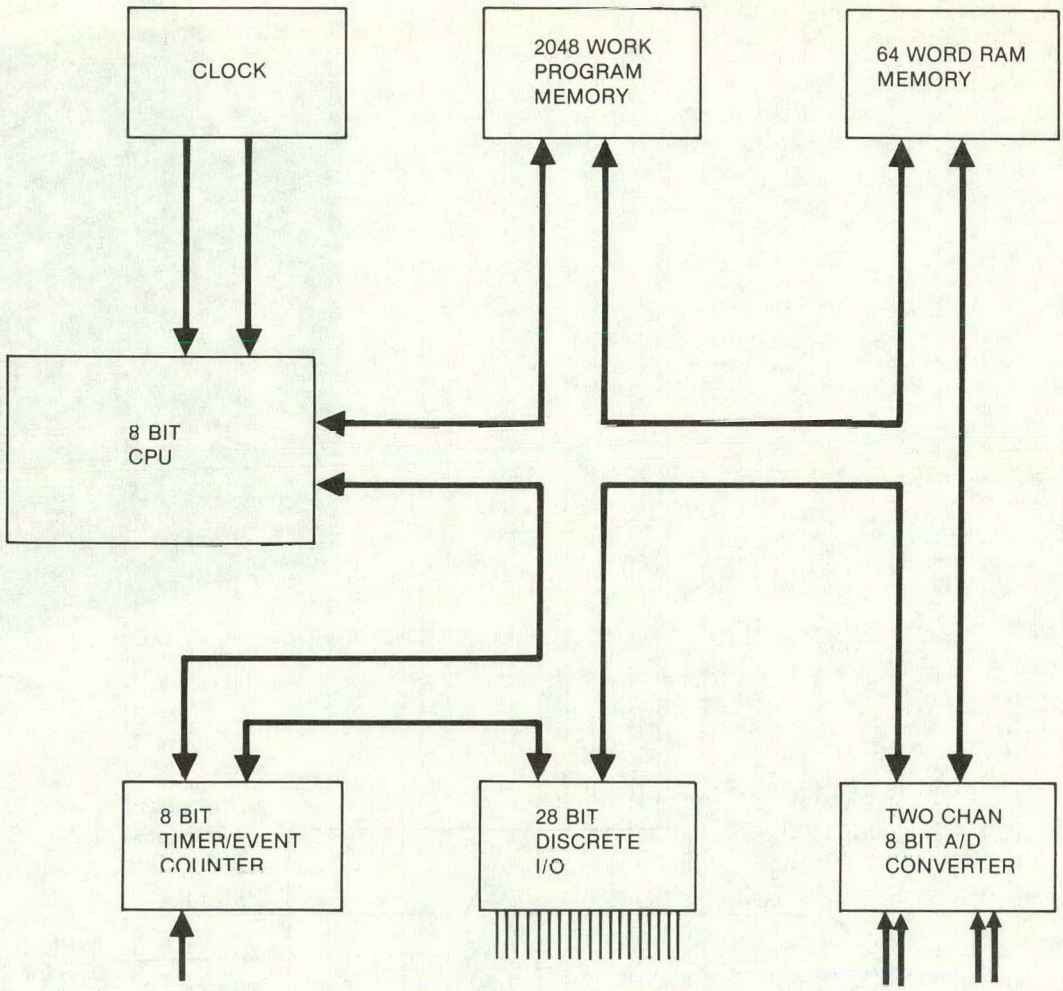

Figure 86. Block Diagram Single Chip Microcomputer

The microcomputer, 2.0 inches long, 0.6 inches wide and 0.2 inches deep, needs to be mounted on a printed circuit board, which will also include some buffering, a crystal oscillator, and a power supply. The minimum size case to enclose this configuration is approximately 4.5 inches high, 2-1/4 inches deep and 2-1/4 inches wide (standard size for the housing of a 110 volt duplex outlet box) (see Fig. 87). The remaining functional features are listed on the comaprison table (Table 11).

5.6 ECONOMIC ANALYSIS

An economic evaluation was determined for the MHHP. The primary cost item in the heat pump is the metal hydride powder. Industry spokesmen have stated that the cost should decrease significantly with increased demand for these alloys. Estimates for the cost of the candidate AB_5 hydrides -- $LaNi_5$ and $LaNi_{4.5}Al_{0.5}$ -- are $10.00 per pound (1981$) in large quantities.

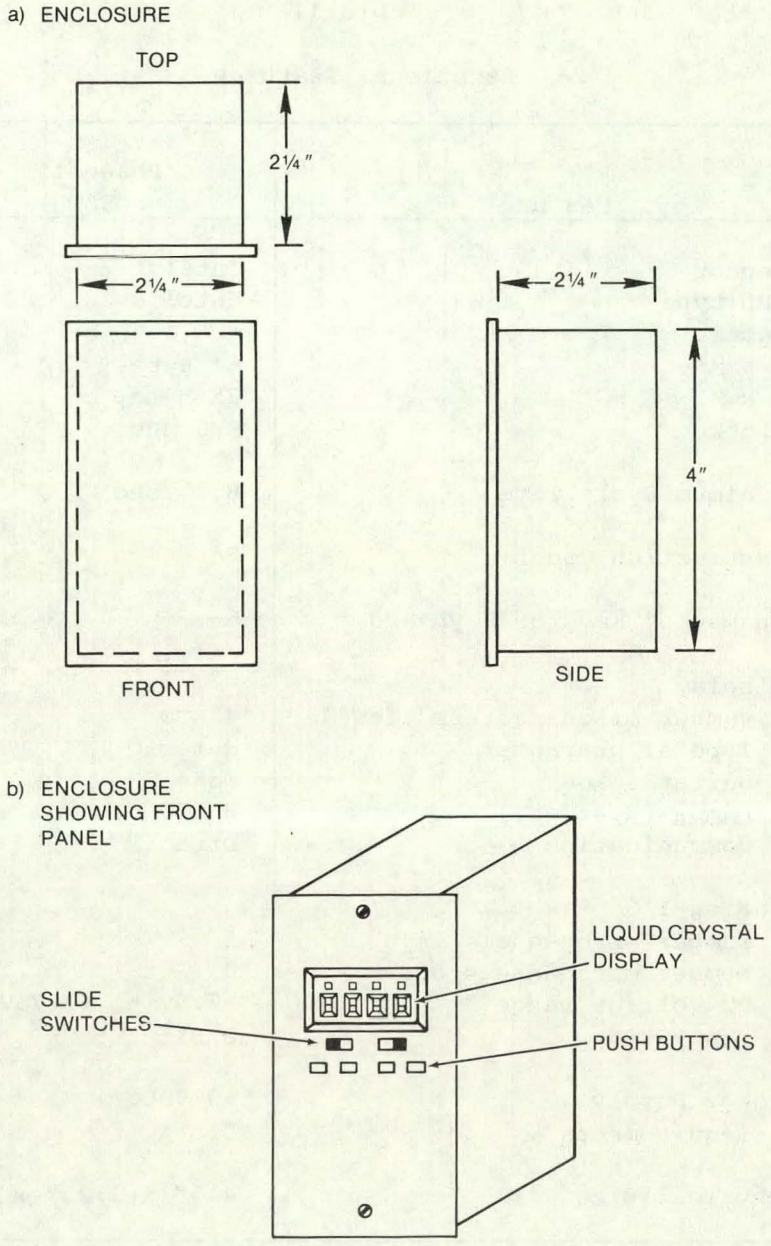

Figure 87. Phase III Control Chasis

Cost comparisons for each MHHP optimum heat exchanger configuration were determined. These costs were evaluated based on material costs only. Assumptions based on manufacturer's estimates are as follows:

copper	\$1.00 per lbm
filter	\$0.81 per in^2

Costs for controls, packaging and labor were not included because these costs ›uld only occur once for a unit of any size.

Table 11

Functional Features

Feature	Phase III EETU
Vendor	Intel
CPU type	Intel 8022
Memory	
RAM	64 Bytes
ROM	2K Bytes
Clock	3.0 MHs
Minimum Cycle Time	8.4 sec
Instruction Count	74
Number of Keys on Keyboard	6
Display	
Number of characters viewed	4 LCD
Type of character	Numeric
Buffer space	None
Lamps (discrete)	8 LCD
Communication	Direct
Analog I/O	
Number of channels in	2
Number of channels out	0
DC voltage range	+5.5V to +2.75V
Resolution	8 Bit
Power Supply	+5 VDC
Requirements	0.5 A
Physical Size	4.5" x 2.25" x 2.25"

Table 12 summarizes the material costs, energy costs and cost per ton for the optimum MHHP configurations. The energy costs is on a footage basis. The energy cost is a ratio of the material cost to the net energy rate. A sample calculation for the net energy rate was shown in Figure 40.

Results showed that, although the net energy rate for the internally finned copper tube was higher than the compact finned tube heat exchanger configuration, design considerations in the direction of the internally finned copper tube were discouraged due to the higher material and energy cost.

Cost targets, as outlined in Section 4, for the MHHP range from $400-00 pe ton for a residential space heating unit to $800-1000 per ton for the indus

Table 12

Economic Evaluation of MHHP Heat Exchanger Configurations*

Configuration	Material Cost ($/ft)	Net Energy Rate (Btu/hr)	Energy Cost (10^{-3} $/ Btu/hr)	Cost Per Ton ($/ton)
Compact finned tube heat exchanger - 0.020 inch fin thickness, 0.150 inch hydride thickness, 0.250 inch fin length, 0.250 inch tube diameter	6.39	1504	4.25	51
1 inch OD copper tube with 6 internal fins (optimum design as shown in Figure 40)	15.22	2174	7.00	84

*Cost includes hydride and heat exchanger materials only.

trial temperature upgrade unit. These costs served as a guideline during design engineering stage of MHHP development.

5.7 OPTIMUM DESIGN FEATURES

As a result of the two parallel hydride heat exchanger configuration studies, the features for two optimum designs were assembled. The design of the tubular configuration is shown again in Figure 88. It is a copper tube with six internal longitudinal copper fins. The copper fins would be brazed to the tube wall with a high temperature braze alloy. A single tube was constructed (Fig. 89) to judge the ease of fabrication. One limitation was the length of tube which could be brazed at once, approximately three feet. This must be an important consideration for this design path.

The design shown in Figure 88 involves a central cylindrical filter inserted in the tube. An alternate design is based on a single end cap (radial) filter at one end of the tube. This tubular design was based on an internal hydride pressure of approximately 2.4 MPa (350 psi) and an external water temperature and pressure of 177°C (350°F) and 1.0 MPa (150 psi) respectively.

Packaging concepts for the finned tube heat exchanger were also investigated. An initial approach to this design is shown in Figure 90. This particular concept consists of six finned tubes surrounding a central filter tube and enclosed in a pressure vessel. This unit has overall dimensions of approxi-

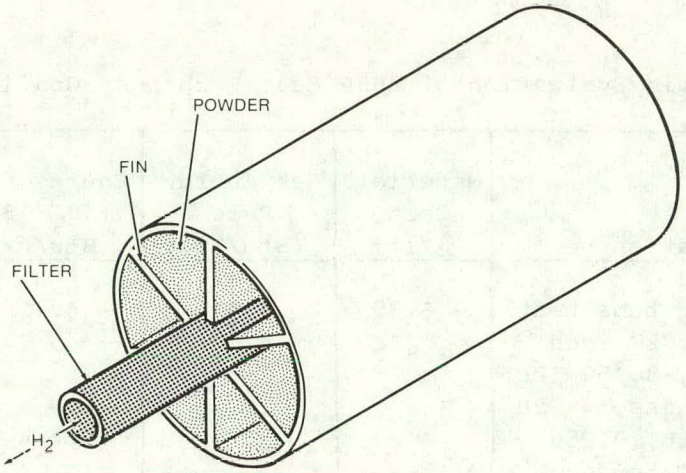

Figure 88. Optimum Tubular Configuration Design

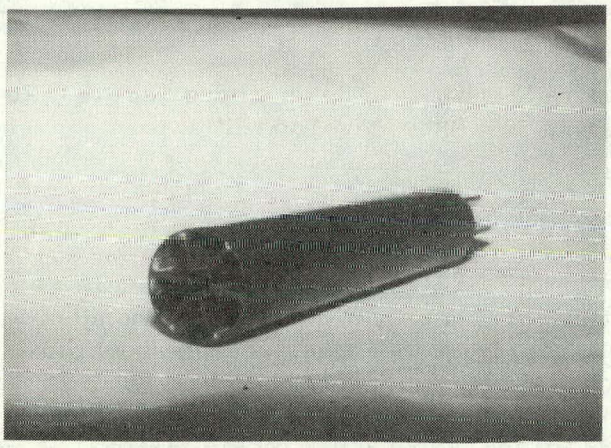

Figure 89. Tube Constructed With Six Copper Fins

mately 15 inches in length and 3 inches in diameter. It is estimated to weigh about 10 lbm, contain 3.7 lbm of hydride and supply 9,000 Btu/hr. The design shown incorporated one of the three methods for installing the filter. An alternate route would be to surround the entire finned tube structure in a wrap-around type annual filter. The third filtering design is to use an end-plate filter at the top of the pressure vessel.

Table 13 is a comparison table between the two optimum designs. Based the more favorable numbers for the compact externally finned hydride he

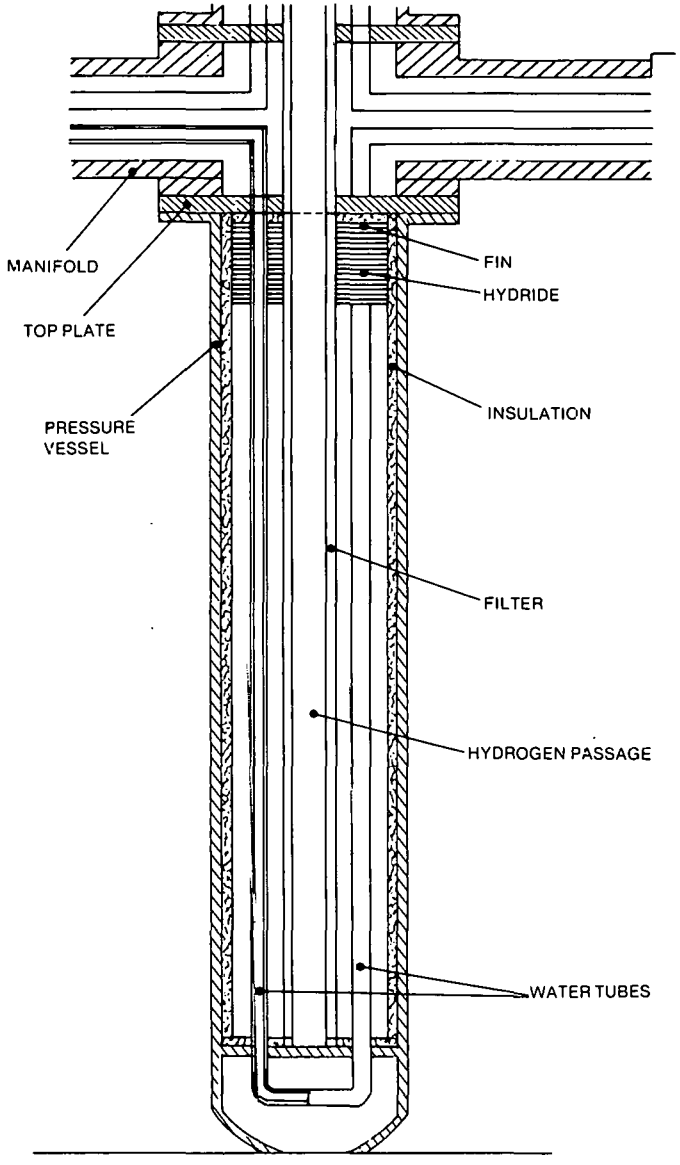

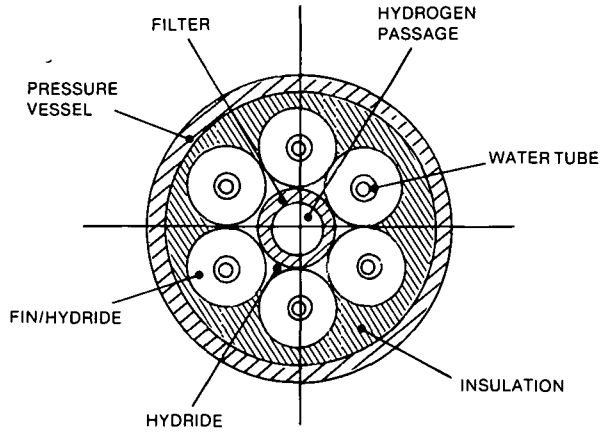

Figure 90. Finned Tube Heat Exchanger

Table 13

Hydride Heat Exchanger Comparisons

Heat Exchanger Configuration	Thermal Mass Ratio	Calculated Cycle Time (minutes)	Specific Heat Rate (Btu/hr·lb Hyd)	Cost ($/Btu/hr)	Filter Area Required (in^2/btu/hr)	COP* Temperature Up Grade	Comments	
							Advantages	Disadvantages
Externally Finned Tube	0.75	1.13	2,443	4.25×10^{-3}		0.42	. pressure vessel containment	. difficult to assure hydride powder filling
a. central tube filter					0.006		. minimizes water inventory	. no definite room for expansion
b. annual filter					0.060		. modular construction	
c. end plate filter					0.003		. standard finned tube technology	
Internally Finned Tube	0.57	1.67	1,554	7.0×10^{-3}		0.38	. proven tubular construction	. difficult to braze fins in long lengths
a. end cap filter					3.5×10^{-4}		. isolation of individual tubes	. little control over water inventory
b. central tube filter					0.004		. easily scaled to larger capacity	. sealing problems

*maximum possible = 0.55 (actual calculations shown for COP in Appendix B)

changer, the decision was made to utilize this design for the MHHP. Major design modifications were evaluated to facilitate manufacture and assembly of the finned tube unit. Problem areas considered were:

1. ease of loading the hydride powder,

2. minimizing seal areas and

3. pressure vessel strength.

Chapter 6 further outlines this final design.

6

FINAL DESIGN OF THE EDTU

The Final Design of the EDTU is outlined in this section. The design is supported by calculations and layout drawings.

6.1 GENERAL DESCRIPTION OF THE EDTU HEAT EXCHANGER MODULE

A detailed design of a proof-of-concept metal hydride heat pump was developed. This unit, the Engineering Development Test Unit (EDTU), was designed for maximum data accessibility and configuration flexibilty. It will operate strictly in a laboratory environment and will be subjected to a broad range of conditions.

The main component of the EDTU is the hydride heat exchanger module. As a result of the extensive computer modelling and laboratory testing, the compact externally finned hydride heat exchanger was selected for the EDTU design. Major design modifications occurred, however, since the initial design approach was shown in Figure 90. That initial approach went through many design iterations to solve the problems of loading the hydride powder, minimizing the seal areas and strengthening the pressure vessel. Also, the design incorporated a cylindrical filter which was found through the filter design studies to produce high pressure drops when immersed in powder.

The EDTU heat exchanger module (Fig. 91) was designed for maximum heat transfer with a low thermal mass. It consists of 14 finned copper tubes in a staggered tube bundle arrangement. The hydride powder is stored in the annular spacing between the fins, and the heat transfer media, pressurized water, flows through the finned tubes. Pressurized water was chosen as the heat transfer media over other substances such as ethylene glycol because it has known properties, it's non-toxic and readily available.

The copper tubes have a 0.250 inch outside diameter and a 0.030 inch wall thickness. The copper fins are brazed externally to the tube and are spaced 0.150 inch apart. The fins are 0.020 inch thick and 0.250 inch wide. The finned length of the tube is one foot.

The 14 finned copper tubes are divided evenly so that seven tubes function as water inlets and seven tubes are water outlets. The flow path through the inlet and outlet tubes are connected by brazing an unfinned copper U-tube to each inlet and outlet tube for a total of seven connections. At the other end, two manifold configurations connect each set of seven tubes to the appropriate flow path. The manifold and flange configuration is machined to form the head assembly. This makes the flanged head and the tube bundle arrange-

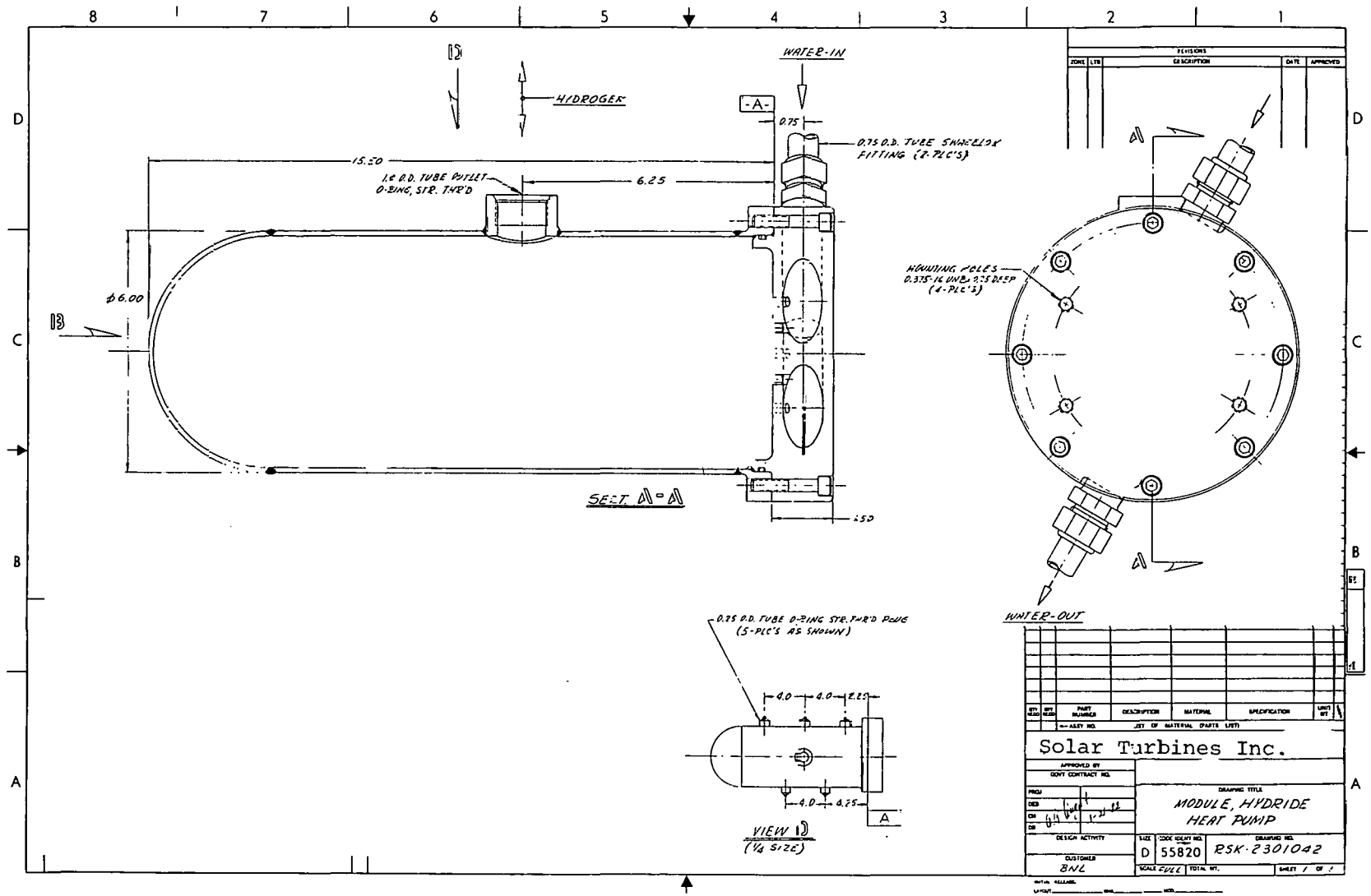

Figure 91. Hydride Heat Pump Module

it integral components. This entire configuration is then loaded into a cylindrical pressure vessel.

The stainless steel vessel has a 6.0 inch outside diameter and 0.125 inch wall thickness (see Appendix 10 for pressure vessel stress calculations). It was designed with a hemispherical cap welded on at one end and with a flanged head assembly connected by eight bolts at the other.

A prime consideration in the EDTU design is the capability to open up the pressure vessel for inspection or component replacement. The flange on the pressure vessel satisfies this consideration. Alternate heat exchanger modules could also be inserted into the pressure vessel, if necessary, during Phase II rebuilding.

Solid insulation thermally isolates the tubes and the hydride particles from the high mass pressure vessel. The insulation to be used is a castable type which is molded externally to the pressure vessel and inserted with the tube bundle. A metal foil separator between the porous insulation and the hydride powder protects against powder migration into the insulation.

A radial separator is located at the hemispherical end of the vessel. Its purpose is to prevent the hydride powder from migrating from the finned tube section into the U-tube connections area. However, to prevent pressure buildup on one side of the separator, four "breathers" are machined into the 0.375 inch thick separator. These "breathers" are essentially filters that allow the hydrogen gas to circulate freely without pressure buildup and prevent hydride particle migration. The filter material is sintered stainless steel.

As well as functioning as "breathers", the filter material is also utilized in the hydrogen gas stream as the gas flows in and out of the pressure vessel. A filter is necessary so that the fine particles of the two hydrides do not intermix by traveling with the hydrogen gas. The filter in the EDTU heat exchanger module was designed with approximately 30 square inches of filter area which is sufficient area to allow the hydrogen gas to rapidly escape with a low pressure drop. The filter is ten inches long, 3 inches wide and 0.035 inch thick. It runs parallel to the tube bundle and is held in place by a stainless steel frame which is tack-welded to the pressure vessel wall.

The heat exchanger module is designed to hold approximately eight and a half pounds of hydride powder. After the pressure vessel is fabricated and pressure checked, the powder is loaded into the vessel through fill ports with pressure plugs located on each side of the vessel (Figs. 91, View D). The ports are staggered along the vessel wall, three on one side and two on the other. This allows for equal and uniform filling of the hydride powder into the voids between the fins. No welding or processing other than replacing the pressure plugs is required. One plug is utilized as a rupture disc as a safety precaution against over-pressure.

The EDTU consists of four of these pressure vessel units connected as two out-of-phase pairs. In each pair, one vessel will contain $LaNi_5$ packed around the 14 finned copper tubes, while the second vessel will contain $LaNi_{4.5}Al_{0.5}$ in a similar configuration. The hydrogen path is located at

the top of the horizontal vessel. The 1.0 inch OD tube hydrogen path short and free of valves and allows uninterrupted hydrogen flow.

Specifications are shown in Table 14.

Table 14

EDTU SPECIFICATIONS
(Based on Two Pressure Vessel Pairs)

17 lbs $LaNi_5$ (8.5 lbs/vessel)
17 lbs $LaNi_{4.5}Al_{0.5}$ (8.5 lbs/vessel)
40,000 Btu/hr upgraded heat @ 176°C (350°F)
Calculated COP = 0.42
Predicted Cycle Time = 68 seconds
Weight 200 lbs (≈50 lbs/vessel)

6.2 EDTU SYSTEM OPERATION

The EDTU is designed for continuous output. Continuous output requires dual pressure vessel pairs and appropriate controls to establish 180 degrees out of phase operation. This allows that at all times one pair is charging while the other is rejecting heat. This type of operation is controlled by a series of valving operations and three water flow paths (Fig. 92).

The EDTU temperature upgrade system operates as follows. (Hydride A1 and A2 in Figure 92 is $LaNi_5$ and Hydride B1 and B2 is $LaNi_{4.5}Al_{0.5}$.) Warm water at T_M is circulated through hydride B1 which allows B1 to desorb hydrogen at P_1 while absorbing heat from the water. Hydride A1, the hydrogen-depleted cold side alloy, is exposed to the heat sink T_L which allows it to absorb the hydrogen at P_4 ($P_1 > P_4$). This is the charge half of the cycle.

At the same time, hydride A2 is exposed to T_M which allows A2 to desorb hydrogen at P_3 while absorbing thermal energy from the medium temperature source. Because hydride A2 is at a higher pressure, the hydrogen flows to the vessel containing hydride B2 which absorbs the hydrogen giving off a high temperature heat.

After a certain amount of time (half of the cycle time) the water paths switch and hydrides A2 and B2 become the charging pair and hydrides A1 and B1 produce the upgraded heat (T_H).

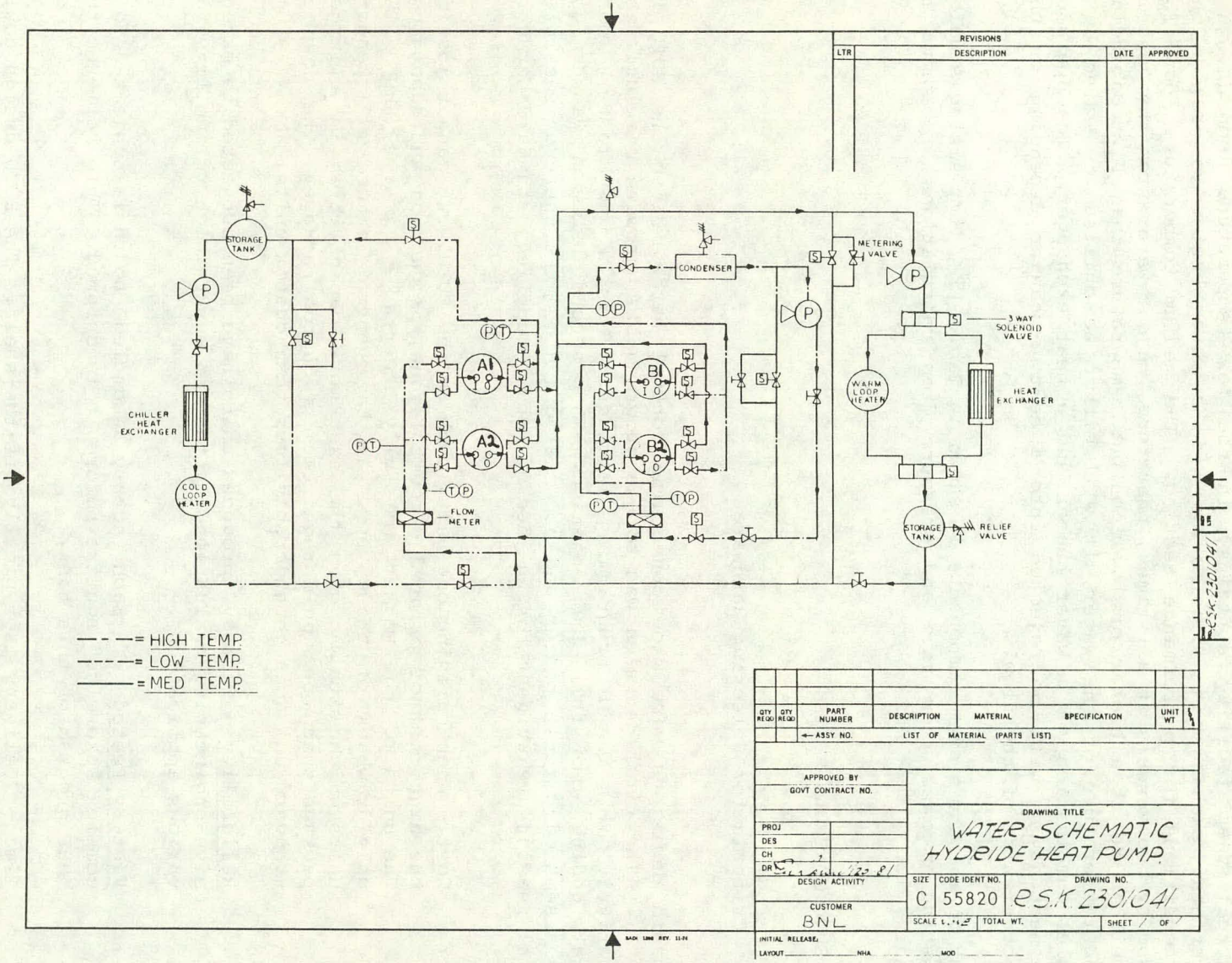

Figure 92. Water Schematic, Hydride Heat Pump

The actual test facility contains, in the low temperature loop (T_L), chiller heat exchanger in combination with a water heater to provide the sink conditions for performance testing. The medium temperature loop (T_M) is used by two vessels at all times, therefore, reject water from the vessels will either be at a higher or lower output temperature than T_M. Depending on the temperature of the water, it will either be chilled or heated by a parallel combination of a water heater and a heat exchanger. The upgraded waste heat (T_H) will be rejected into a heat exchanger depending on the characteristics of the flow.

A list of all the system components is shown in Table 15. Pump sizing studies consisting of mass flow rate and pressure drop calculations are shown in Appendix 11.

6.3 EDTU CONTROLS SYSTEM

6.3.1 Criteria for Selecting Hardware

Two basic decisions were made concerning control hardware for the EDTU in Phase II. The first decision was to use programmable hardware that utilizes a relatively high level programming language. This allows faster, more accurate coding with full documentation. The second decision was to use fully assembled circuit boards and other electronic units wherever possible. Several reasons are evident for the use of vendor supplied, standard hardware sets:

- Cost - When building one unit, such as the EDTU, one cannot justify the high cost of printed circuit layout, production and debugging. The units on the market are fully acceptable for the MHHP. The only drawback of those units is the general nature of standard units which usually give the user more capabilities in a larger package than one would require in a custom package. The cost of standard units is considerably less than custom units.

- Reliability - Factory produced units have been subjected to extensive engineering evaluation and test to ensure high reliability for various applications.

- Factory Tested - Each factory assembled board is subjected to a complex "exercise" routine before it is shipped. This relieves the MHHP program of this task.

- Time - Delivery is typically off-the-shelf. The EDTU design could take 6 months to fully implement. The unique software required for the MHHP will be developed in the interim.

Table 15

EDTU System Components

Number	Item	Quantity
1	Pumps (capacity: 10 gpm, see Appendix 11)	3
2	Flowmeters	4
3	Check valves	16
4	3-way solenoid valves	2
5	2-way solenoid valves	23
6	Metering valves	8
7	Relief valves	4
8	Condenser/heat exchanger	1
9	Water heater for medium temperature loop	1
10	Heat exchanger for medium temperature loop	1
11	Storage tanks (10 gallon capacity	2
12	Chiller heat exchanger	1
13	Water heater for low temperature loop	1
14	Thermocouples	6
15	Pressure transducers	6
16	Water filters	3
17	3/4 inch OD copper tubing	100 ft
18	1/4 inch OD copper tubing	60 ft
19	Filter material (1 sheet)	150 in^2
20	Pressure vessels (includes cylinder body, hemispherical end, flange, connections)	4
21	$LaNi_5$ hydride powder	20 lbs
22	$LaNi_{4.5}Al_{0.5}$ hydride powder	20 lbs
23	Insulation	--
24	Hydrogen gas	5 bottles
25	Controls	--
26	Miscellaneous hardware	--

6.3.2 Comparison of Two Candidate Hardware Sets

The two prime candidates were the "Multi Bus™" microprocessor from Intel Corp. and the "Standard Bus" microprocessor from Prolog Corp. The major distinctions between these two candidates exist at the hardware level. They are generally equivalent at the software level. Both systems are supported by more than one vendor.

Alternate 1: Prolog "Standard Bus"

The Prolog card set is implemented on a 4.5 by 6.5 inch printed circuit board. he card format subdivides the hardware in the following manner:

(a) Microprocessor (8085), 4K RAM and 8K ROM card

(b) DAC 16 line output card

(c) Keyboard and display card

(d) Analog I/O card

(e) Discrete input/output card

The above group of cards are mounted in a card cage. The card cage has edge board connectors and a prewired bus structure (STD BUS). The card cage needed for this application has nominal dimension of 6 inches high, 6 inches deep and 8 inches wide. There is a power supply of similar dimensions required to complete electronic hardware. The minimum size case to enclose this configuration is approximately 9 inches high, 9 inches deep and 18 inches wide.

The keyboard and display card provides a light emitting diode alpha/numeric display section. It can display 64 different ASCII encoded characters in each of the eight display positions. Directly below the 8 window alpha/numeric display are eight status lamps available for additional information display. The keyboard section of this card is made up of a 5 by 5 pushbutton matrix. This matrix includes a standard hexidecimal keyboard and nine additional user defined keys. This card would not be mounted in the card cage. It would be mounted directly to the back side of the front panel with access holes for the display and keyboard.

The remaining functional features of Alternate 1 are listed on the comparison table (Table 16).

Alternate 2: Intel "Multi Bus™"

The Intel "Multi Bus™" card set is implemented on 6.75 by 8.0 inch printed circuit card. The card format subdivides the hardware in the following manner.

(a) Microprocessor (8080) 4 K RAM, and 8K ROM card with 48 I/O lines and serial I/O (Fig. 93).

(b) Keyboard and display panel (not a card) (Fig. 94).

(c) Analog I/O card (Fig. 95)

The above group of cards (except b) are mounted in a card cage. The card cage has edge board connectors and a prewired bus structure ("Multi Bus™"). The card cage needed for this application has nominal dimensions of 8.5 inches high, 3.5 inches deep and 14.25 inches wide. This group of cards needs in addition a power supply with nominal dimensions of 5-1/4 inches high, 2-1/4 inches deep, and 9 inches wide. The minimum size case to enclose this configuration is approximately 11 inches high, 9 inches deep and 16 inches wide (Fig. 96 for chassis design).

Table 16

Functional Features Comparison

Feature	Requirement	Phase II EDTU	
		Alternate 1	Alternate 2
Vendor		Prolog	Intel
CPU type	Programmable using PLM compiler	Intel 8085	Intel 8080
Memory			
RAM	200-400 Bytes	4K Bytes	4K Bytes
ROM	2-4K Byte	8K Bytes	8K Bytes
Clock	1 MHz or greater	6.1 MHz	2.04 MHz
Minimum Cycle Time	5 sec	1.3 sec	1.95 sec
Instruction Count	70-80	111	111
Number of Keys on Keyboard	19 or more	25	42
Display			
Number of characters viewed	10-12	8 (LED)	16 (LED)
Type of character	40 ASCII Codes	64 ASCII Codes	64 ASCII Codes
Buffer space	48 characters	8 characters	80 characters
Lamps (discrete)	4 LEDS	8 LED	6 LED
Communication	Convient.	BUS	RS232
Analog I/O			
Number of channels in	12	16	16
Number of channels out	2	2	2
DC voltage range	5 volts	±10 V or ±5 V	±10 V or ±5 V
Resolution	8 bits	10 bits	12 bits
Power Supply		+5 VDC	+5 VDC -5VDC +12 +12
Requirements	Single preferred	4.25 A	5.8A .1A .2A .2A
Physical Size			
Card cage	Less than 3 cubic	6" x 6" x 8"	3.5" x 8.5" x 14.25"
Power supply	feet	6" x 6" x 8"	2.25" x 5.25" x 9"
Display		4.5" x 6.5" x 0.75"	0.6" x 4.5" x 8.5"

The keyboard and display for this alternative is a micro-terminal that interfaces to the CPU via a serial I/O port (see Fig. 97). It has a 16 position alpha/numeric display. It has four 80 character buffers. Two of these buffers hold messages entered via the 42 key keyboard and two hold messages received from the CPU. The unit has a resident programmable memory section that translates any of the 14 function keys into 80 character messages. A message received from the CPU can be more than 16 characters (up to 80) and still be human readable by using the "Banner Display" mode. This will circulate the longer message into the right side of the display and push it out the left side at a rate readable by humans. The keyboard has 42 pushbuttons in a 6 by 7 matrix. It includes a full alpha character set, a numeric zone and 16 special function keys. It has six status lamps, four of the lamps are dedicated to keyboard definition and two are user defined. This unit is designed to mount on the surface of the front panel. It communicates through a two wire pair to the serial I/O port of the microprocessor card.

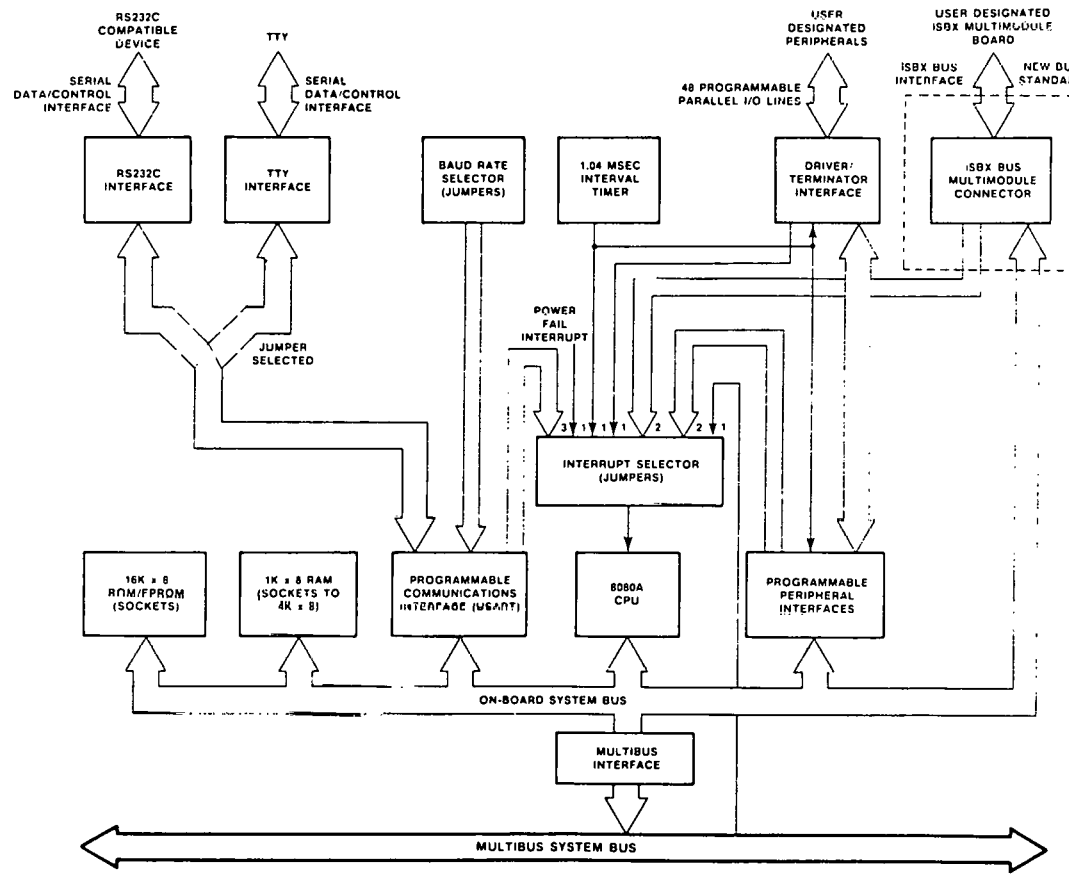

Figure 93. MULTIBUS Single Board Computer

The remaining functional features for Alternate 2 are listed on the comparison table (Table 16).

6.3.3 Results of Comparison

The EDTU prototype control unit will be built utilizing the Intel "Multi Bus™" and catalog circuits compatible to that bus system. The decision was primarily based on the evaluation that a better (more suitable) man/machine communication would result when a micro-terminal is used for the display panel and operator control panel. The alternate approach burdens the operator with considerable computer coded type messages. Both alternatives provide equivalent computing capabilities, analog input-output, size and weight.

6.4 LABORATORY LAYOUT

Figure 98 shows where each major component of the EDTU will be located in the Heat Recovery Laboratory at Solar's Research Facilities in San Dieg-

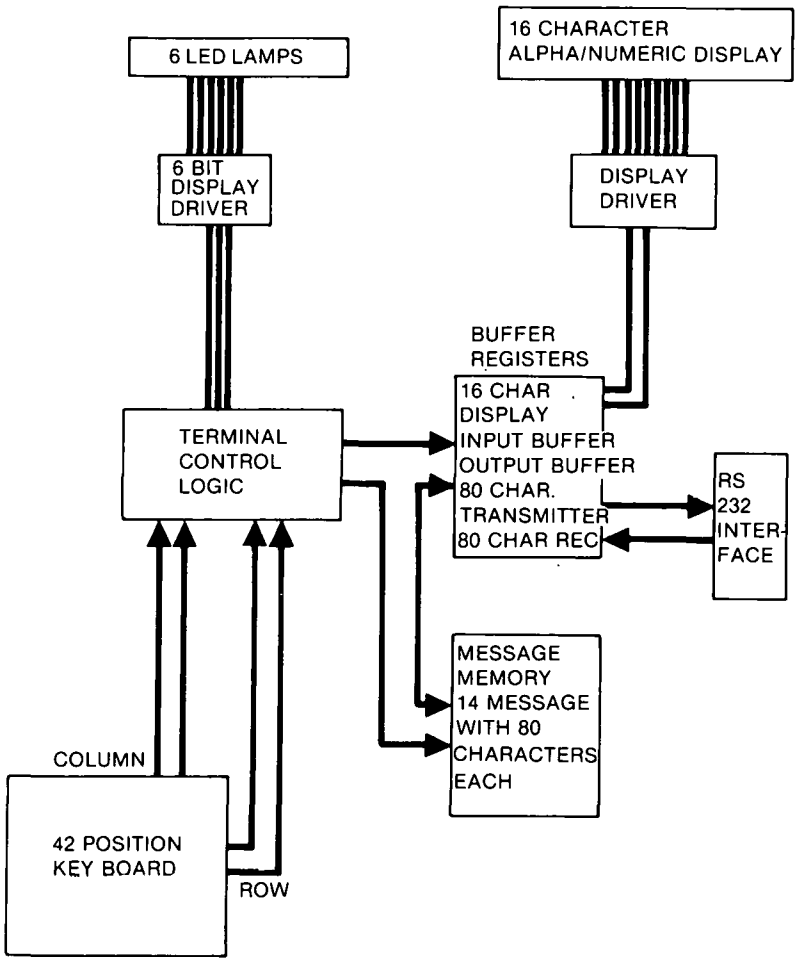

Figure 94. Microterminal Block Diagram

California. A free-standing table centrally located in the Lab will have a plywood board mounted vertically on one long side of the table. Since the hydride heat exchanger vessels are so compact all four will be mounted with the flanged end of the vessel connected to the front of the board (Fig. 99). This allows for easy fabrication, monitoring, demonstration and component replacement.

The pumps and plumbing connections will be located behind the table. The water storage tanks and the water heaters will be situated beneath the table to minimize the plumbing connections and the water inventory. The chiller heat exchanger and condenser/heat exchanger will be installed outside the rooom. All water tubing was designed to be as short as possible to minimize the water inventory and the possible heat losses. A control unit which is used to monitor and control peripheral component operation is placed on the table. A data logger will enable continuous performance data acquisition.

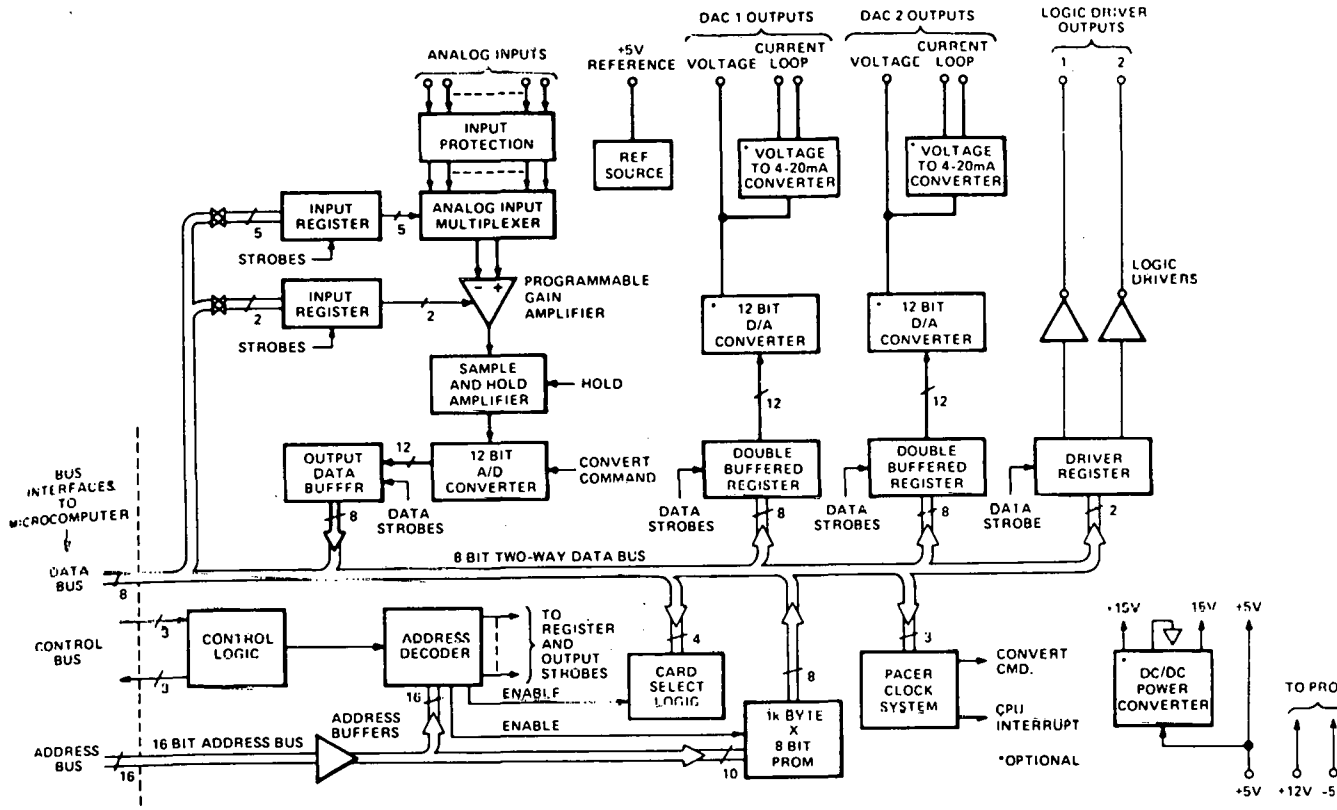

Figure 95. MULTIBUS Analog I/O Card

6.5 DESIGN ISSUES

The EDTU design addresses many of the issues that affect the success of the MHHP. These issues are heat transfer, particle containment, particle expansion and safety.

- Heat Transfer

  The design of the EDTU contains the most advanced hydride heat exchanger technology. Extensive computer modelling and laboratory testing have shown that the externally finned copper tube bundle arrangement provides the maximum heat transfer and the low thermal mass necessary for superior performance.

- Particle Containment

  The EDTU design incorporates the stainless steel filter to contain the hydride particles in the pressure vessel. This filter was found through testing to be adequate in not only rejecting hydride particles form the hydrogen gas stream, but, it also allows the gas to transfer between vessels with a low pressure drop. Thus, the

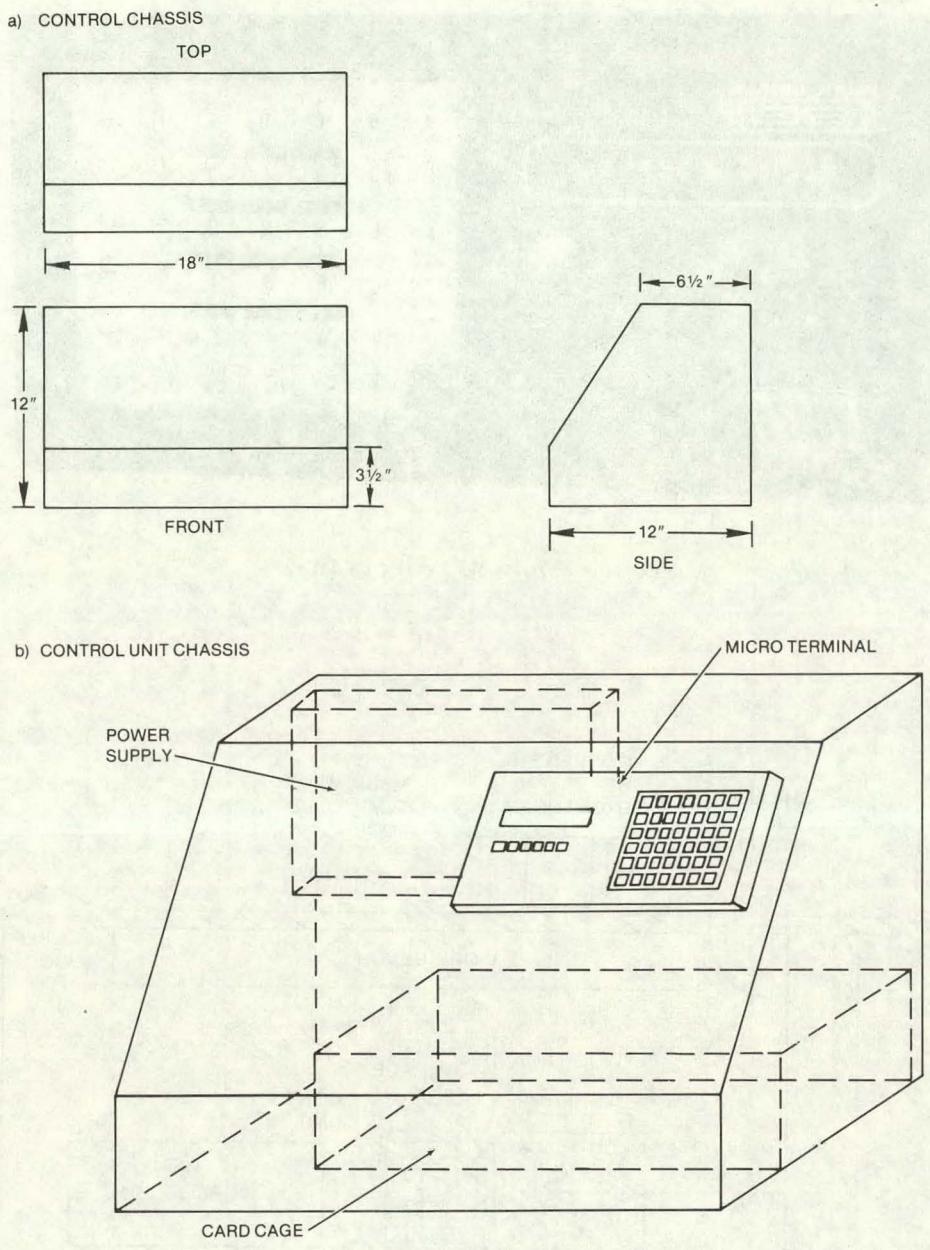

Figure 96. Phase II EDTU Control Chassis

amount of hydride powder necessary to release the required amount of hydrogen gas is minimized, thereby minimizing the cost.

The design also allows for a large filter surface area. The hydrogen gas can then transfer rapidly from one vessel to another. This aids in the reduction of the cycle time.

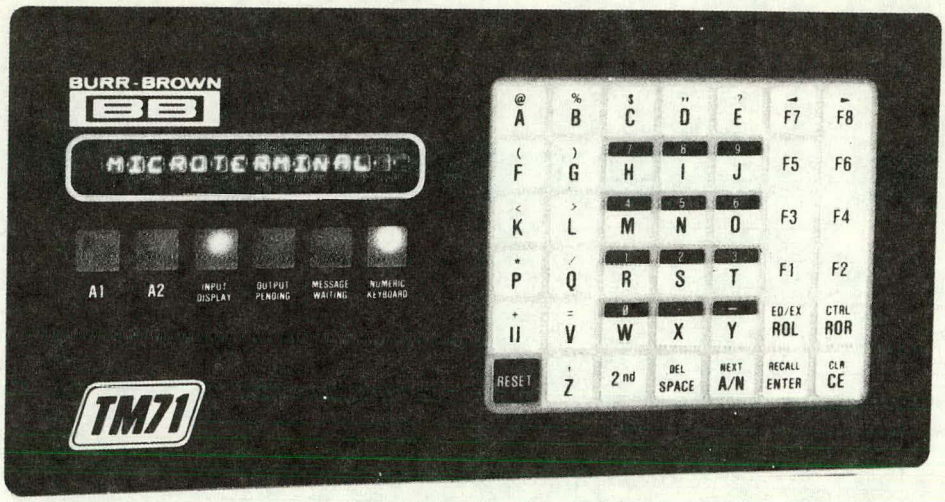

Figure 97. Microterminal

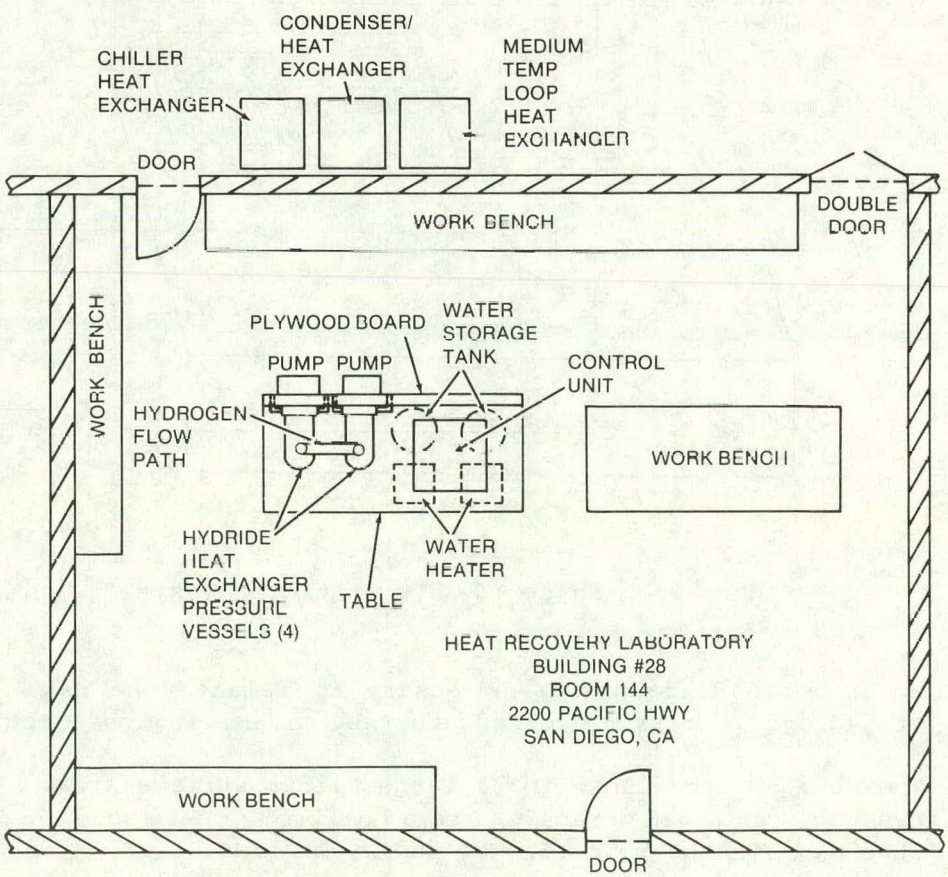

Figure 98. EDTU Laboratory Layout

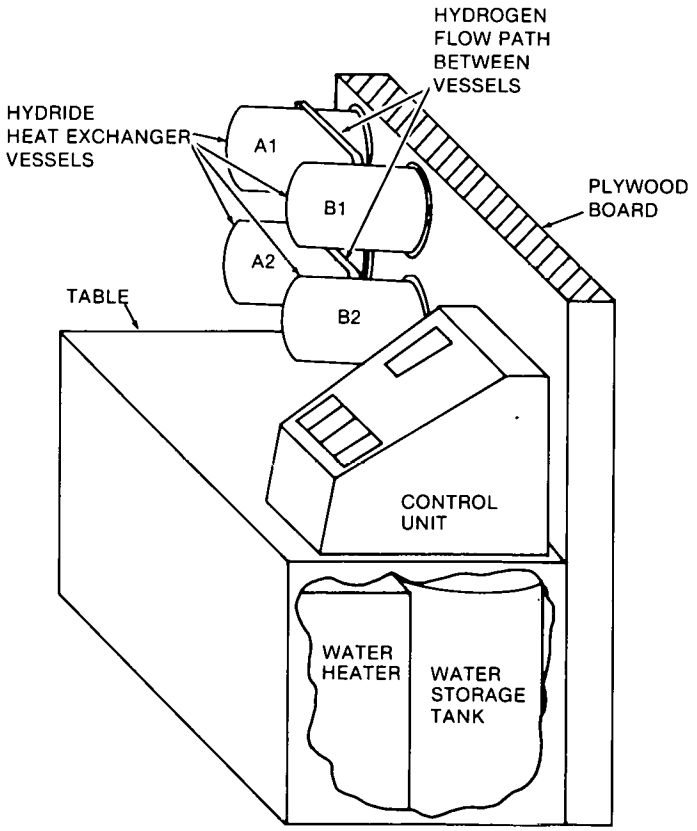

Figure 99. Isometric View of EDTU

Particle Expansion

Particle expansion is a critical parameter because it can cause a large internal pressure which in turn may lead to rupture of the container. The EDTU design resolves this problem by providing for expansion by allowing the fins to be thin enough (0.015 in.) that when expansion occurs, it will be absorbed by the flexible fins.

Safety

Included in the EDTU design are many precautions necessary to provide safety. The major concern is with the leakage of hydrogen gas. In the pressure vessel design, all seal areas are reinforced with welded or brazed joints. X-ray analysis of all welds and brazed connections will be performed to find any cracks or fissures which might allow hydrogen leakage or cause a stress situation through which rupture may occur. Rupture discs and relief valves are incorporated in the pressure vessels and the laboratory facility. A hydrogen detection/alarm device is also installed in the laboratory to warn of any existence of a dangerous situation, thus allowing action to be taken to avoid harm.

7

CONCLUSIONS AND RECOMMENDATIONS

Phase one of a three phase development project to advance the state-of-the-art of metal hydride/chemical heat pumps has been successfully completed. After extensive computer modelling and laboratory testing, program engineers have produced a design for a laboratory verification model of an industrial temperature upgradery. The selection of the temperature upgrader was based on an extensive market study conducted during this Phase.

The project team, consisting of Southern California Gas Company, Solar Turbines, Inc., and Booz Allen & Hamilton, Inc., had individual responsibilities during the execution of this work. SoCal, the prime contractor, managed the program and supplied valuable utility/user information. Booz Allen, having extensive experience in the heat recovery market, conducted the national market study. Solar advanced the technology of the MHHP in its Research Laboratories.

The primary results of Phase I are:

- A conceptual design was delineated.
- Several markets with substantial volume exist for the MHHP. The prime areas are in residential space conditioning, industrial heat recovery and upgrading, and in transportation space conditioning.
- One target application, industrial temperature upgrading, was selected from 14 candidates by a forced ranking procedure.
- Cost targets have been established and initial indications show a good possibility of meeting them with a reasonable amount of R&D.
- Heat transfer has been markedly improved for the MHHP through computer modelling and laboratory testing.
- A unique design for the MHHP with low thermal mass and high heat transfer has been completed.
- No previously unknown problem areas have arisen.
- All reporting requirements have been met.
- The program has been completed within the original budget.

The primary conclusions are (1) there is a market need for an MHHP especially as a temperature upgrader, (2) the MHHP technology, while still not completely resolved, has been advanced greatly, and (3) there is no reason, technical

or market related, to be less enthusiastic about the MHHP now than at tl beginning of Phase I.

These conclusions lead to the primary recommendation to continue the project into Phase II as originally planned (Fig. 100). In that schedule, the team would gain the greatest operating experience by building a 40,000 Btu/hour temperature upgrader that operates in a continuous mode.

The mid-phase rebuild of Phase II would allow the problems encountered in the early tests to be resolved before the second set of tests proceeded. At the conclusion of Phase II the team would prepare an EETU design for Phase III.

During the course of any effort, alternate means develop to accomplish the same objective. Because of those alternates and the constraints of limited budgets, an alternate recommended plan is presented, Phase II - Alternate Plan. In this optional plan, greater emphasis is placed on technology development and the concomitant reduction of risk in the MHHP components. Phase II - Alternate Plan (Fig. 101) begins with subscale testing of the components of the original EDTU design. In that task engineers will experimentally evaluate the 14 tube heat exchanger, operate small amounts of the two hydrides in an actual upgrade cycle and optimize the water inventory system before a large commitment is made to hardware and test loops. These three endeavors should expose any weakness in the EDTU design that might exist.

In the second task of the alternate plan, the final design EDTU of Phase I would be updated using the data and experience of Task 1. That revised design, an alternate EDTU, would be fabricated. To gain flexibility and reduce expenditures, a 20,000 Btu/hour, noncontinuous unit would be built. This change is easily achieved by fabricating two heat exchanger modules instead of the four needed for the larger unit. Facility and data acquisition costs are also reduced. The fabricated unit once installed in a test facility would be subjected to a series of tests similar to those envisioned in the original Phase II plan.

In the Phase II - Alternate Plan, the reporting will be minimized by eliminating one major report and combining others. The Phase III design task will be reduced to a design recommendation task. A savings will accrue by reducing the program management and support functions of SoCal. Program support for site selection and other pre-commercialization test functions will be eliminated.

The team members feel that both program plans will have positive results and will advance the MHHP technology. The original plan emphasizes the system while the alternate plan emphasizes the high technology risk areas. The alternate plan, while less costly would require a total replanning of Phase III.

In summary, Phase I has resulted in the advancement of MHHP market and technology knowledge. No problems are evident that would prohibit the progress of this concept.

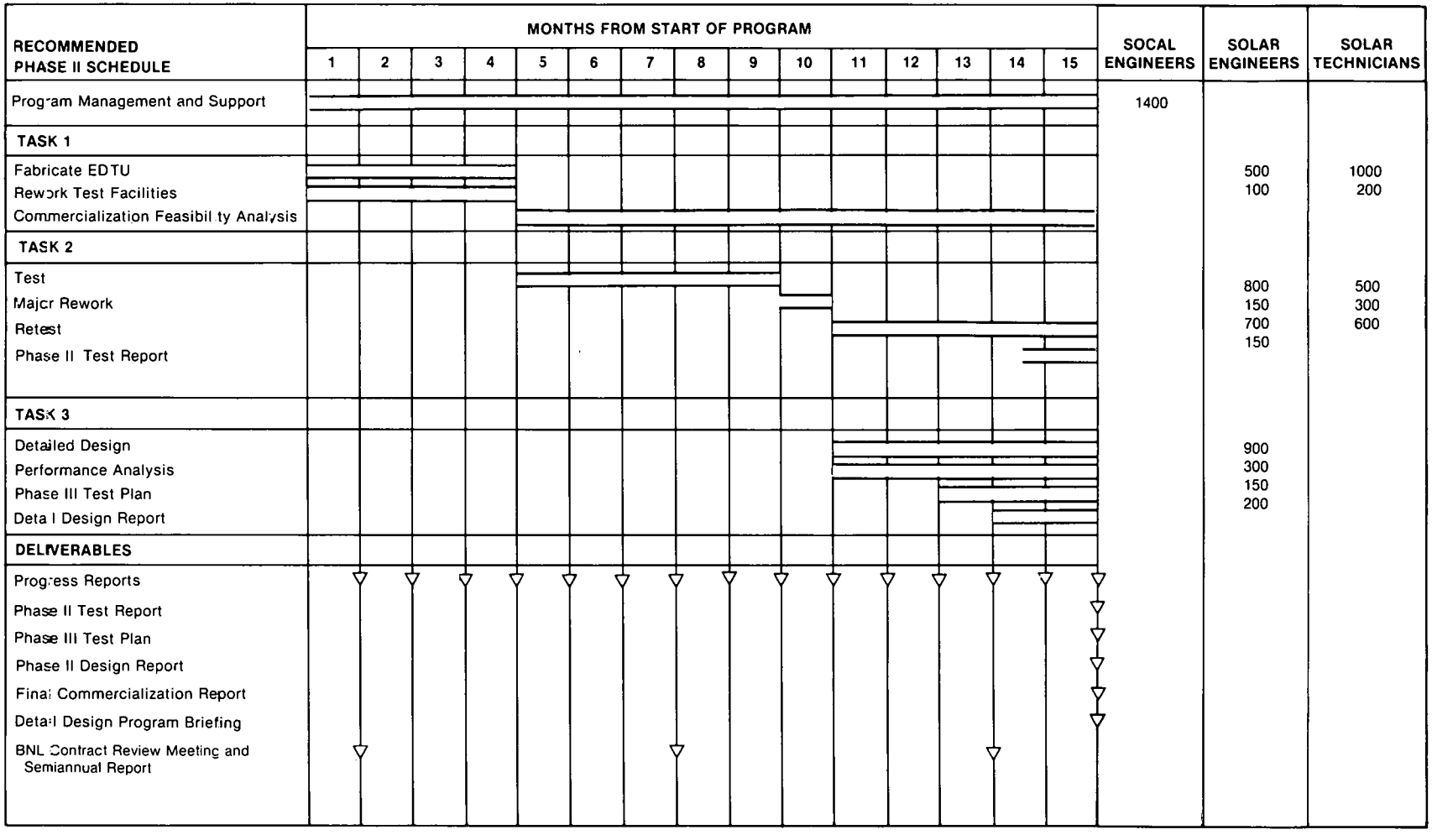

Figure 100. Phase II Milestone Chart

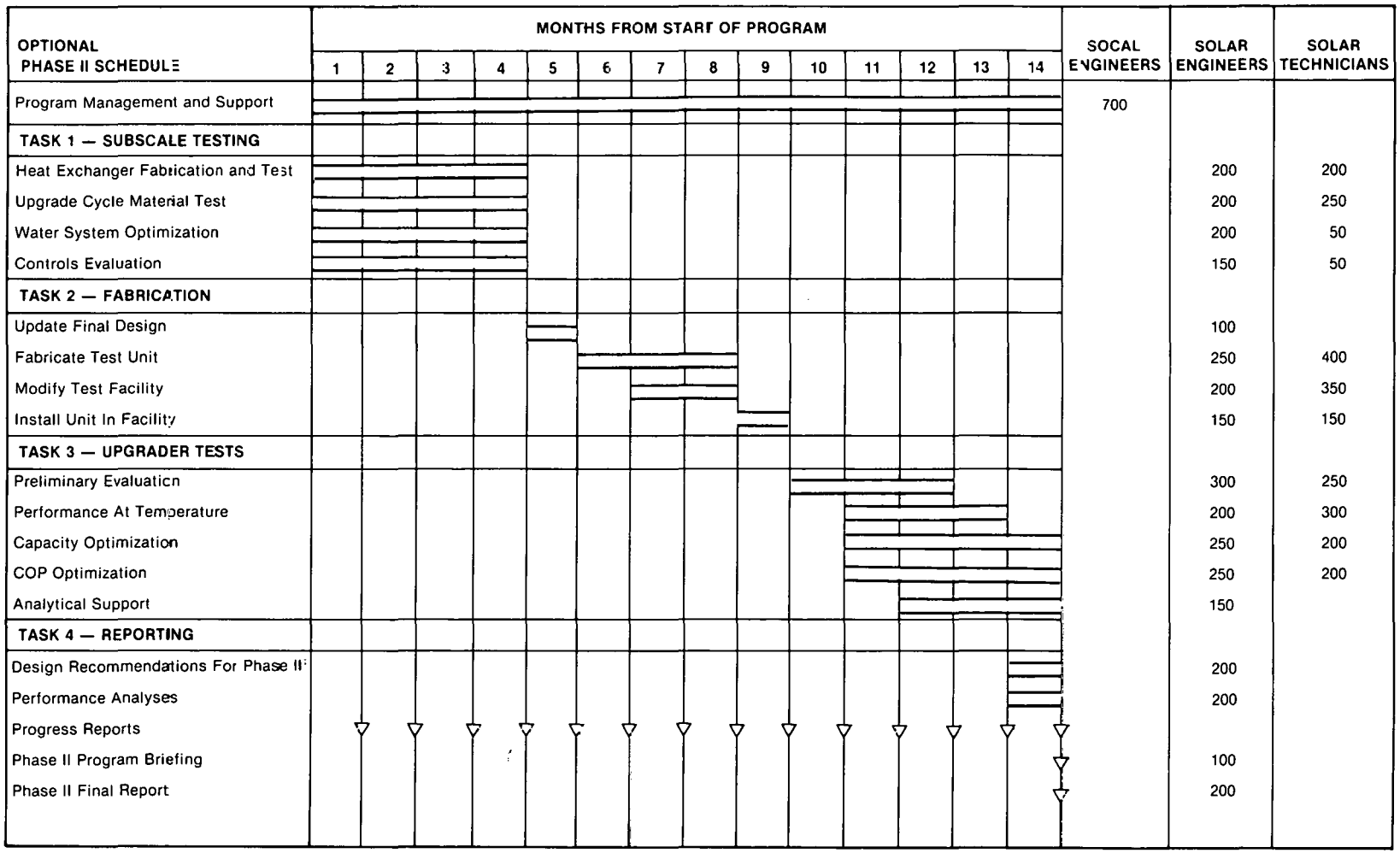

Figure 101. Optional Phase II Schedule

e MHHP offers a unique opportunity to advance a truly new heat pump concept. This concept is one of few that operates at temperatures below 100°C where significant waste (unused) heat is available and provides outputs near 180°C where heat is needed. The MHHP team recommends that BNL accept one of the two plans suggested to continue this work into Phase II.

REFERENCES

1. Reilly, J. J. and Wiswall, R. H., "Iron-Titanium Hydrides: Its Formation, Properties and Applications", BNL 17984, (1973).

2. Lundin, C.E. and Lynch, F.E., "A New Rational for the Hysteresis Effects Observed in Metal-Hydrogen Systems", Proceeding of the International Symosium 'Hydrides for Energy Storage'", Geilo, Norway, 14-19 August 1977, A. F. Andersen and A. T. Makland (Editors), International Association for Hydride Energy, Pergamon Press, New York (1978).

3. Huston, E. L. and Sandrock, G. D., "Engineering Properties of Metal Hydrides", J. Less Common Metals, 74 (1980) pp. 435-443.

4. Mendelsohn, M. H., Gruen, D. M. and Dwight, A. E., "The Effects of Aluminum Additions on the Structural and Hydrogen Absorption Properties of AB_5 Alloys With Particular Reference to the $LaNi_{5-x}Al_x$ Ternary Alloy Systems", J. Less Commmon Metals, 63 (1979), pp. 193-207.

5. Diaz, H. Percheron-Gnegan, A., Achard, J. C., Chatilon, C. and Mathieu, J. C., "Thermodynamic and Structural Properties of $LaNi_{5-y}Al_y$ Compounds and Their Related Hydrides", Int. J. Hydrogen Energy, 4, pp. 445-454 (1979). [Also 2nd World Hydrogen Energy Conference, 1978, p. 2653.]

APPENDIX 1

HYDRIDE ALLOY LITERATURE REVIEW AND REFERENCES

ALLOY	Van't Hoff Relationship	Specific Heat	Thermal Conductivity	Plateau Shape	Hysteresis	H/M	Comminution	Long Term Degradation	ΔH_F	Poisoning	Safety	Chemical Stability
1. $LaNi_5$	1,3,4,5,7, 10,14,15,21, 27,31,32	1,3,24	3	3,4,5,6,7, 12,21,27, 31,32	1,3,4,21, 28,31,32	1,3,4,5,6 7,12,21, 27,31,32	4	26,30	1,4,5,7, 14,15,24,27, 28	25,32		
2. $LaNi_{5.67}$				31	31	31						
3. $LaNi_{11.5}$				31	31	31						
4. $LaCu_5$	8			8		8			8			
5. $LaCo_5$	7,20			6.7,20		6,7,20			7			
6. $La_{0.91}Mg_{0.19}Ni_5$				31	31	31						
7. $La_{0.8}Ca_{0.2}Ni_5$				31	31	31						
8. $La_{0.6}Ca_{0.4}Ni_5$	3			8		8			8			
9. $La_{0.8}Sr_{0.2}Ni_5$				31	31	31						
10. $La_{0.8}Y_{0.2}Ni_5$				7		7						
11. $La_{0.8}Zr_{0.2}Ni_5$				7		7						
12. $La_{0.8}Ba_{0.2}Ni_5$				31	31	31						

ALLOY	Van't Hoff Relationship	Specific Heat	Thermal Conductivity	Plateau Shape	Hysteresis	H/M	Comminution	Long Term Degradation	ΔH_F	Poisoning	Safety	Chemical Stability
13. $La_{0.9}Ce_{0.1}Ni_5$				28	28	28			28			
14. $La_{0.8}Ce_{0.2}Ni_5$				28	28	28			28			
15. $La_{0.7}Ce_{0.3}Ni_5$				28	28	28			28			
16. $La_{0.6}Ce_{0.4}Ni_5$				28	28	28			28			
17. $La_{0.5}Ce_{0.5}Ni_5$				28	28	28			28			
18. $La_{0.4}Ce_{0.6}Ni_5$				28	28	28			28			
19. $La_{0.8}Nd_{0.2}Ni_5$				7		7						
20. $La_{0.8}Gd_{0.2}Ni_5$				7		7						
21. $La_{0.8}Er_{0.2}Ni_5$				7		7						
22. $La_{0.8}Th_{0.2}Ni_5$				7		7						
23. $LaNi_{4.9}Al_{0.1}$	21,31			21,31	21,31	21,31			21			
24. $LaNi_{4.8}Al_{0.2}$	10								10			

ALLOY	Van't Hoff Relationship	Specific Heat	Thermal Conductivity	Plateau Shape	Hysteresis	H/M	Comminution	Long Term Degradation	ΔH_F	Poisoning	Safety	Chemical Stability
25. $LaNi_{4.75}Al_{0.25}$	21			21,30	21,30	21,30			21	30		
26. $LaNi_{4.7}Al_{0.3}$	1			1	1	1			1			
27. $LaNi_{4.6}Al_{0.4}$	9, 10			9	9	9			9,10			
28. $LaNi_{4.5}Al_{0.5}$	9,21			9,21	9,21	9,21			9,21			
29. $LaNi_{4.3}Al_{0.7}$				31	31	31						
30. $LaNi_{4.25}Al_{0.75}$	21			21	21	21			21			
31. $LaNi_{4.0}Al_{1.0}$	10,21			21	21	21			10,21			
32. $LaNi_{3.5}Al_{1.5}$	10								10			
33. $LaNi_{4.0}Cr_{1.0}$				7		7						
34 $La_{0.95}Ni_5Mn_{0.05}$				12		12						
35 $LaNi_{4.95}Mn_{0.05}$				12		12						
36 $LaNi_{4.90}Mn_{0.12}$				12		12						

ALLOY	Van't Hoff Relationship	Specific Heat	Thermal Conductivity	Plateau Shape	Hysteresis	H/M	Comminution	Long Term Degradation	ΔH_F	Poisoning	Safety	Chemical Stability
37. $LaNi_{4.7}Mn_{0.3}$				12		12						
38. $LaNi_{4.6}Mn_{0.4}$	12			12		12			12			
39. $LaNi_{4.5}Mn_{0.63}$				12		12						
40. $LaNi_{4.0}Fe_{1.0}$				7		7						
41. $LaNi_{3.8}Fe_{1.2}$				31	31	31						
42. $LaNi_{4.8}Co_{0.2}$				31	31	31						
43. $LaNi_{4.5}Co_{0.5}$				6		6						
44. $LaNi_{4.0}Co_{1.0}$				7		7						
45. $LaNi_{3.75}Co_{1.25}$				6		6						
46. $LaNi_{3.0}Co_{2.0}$	31			6, 31	31	6, 31						
47. $LaNi_{2.5}Co_{2.5}$				6		6						
48. $LaNi_{2.0}Co_{3.0}$				6		6						

ALLOY	Van't Hoff Relationship	Specific Heat	Thermal Conductivity	Plateau Shape	Hysteresis	H/M	Comminution	Long Term Degradation	ΔH_F	Poisoning	Safety	Chemical Stability
49. $LaNi_{1.5}Co_{3.5}$				6		6						
50. $LaNi_{1.0}Co_{4.0}$				6		6						
51. $LaNi_{4.9}Cu_{0.1}$				30	30	30		30		30		
52. $LaNi_{4.0}Cu_{1.0}$				7		7						
53. $LaNi_{4.5}Pd_{0.5}$				31	31	31						
54. $LaNi_{4.0}Pd_{1.0}$				7		7						
55. $LaNi_{4.0}Ag_{1.0}$				7		7						
56. $LaNi_{4.7}Sn_{0.3}$				31	31	31						
57. $La_{0.5}Ce_{0.5}Ni_{4.8}Co_{0.2}$				23	23	23						
58. $La_{0.5}Ce_{0.5}Ni_{4.5}Co_{0.5}$				23	23	23						
59. $La_{0.5}Ce_{0.5}Ni_{4.0}Co_{1.0}$				23	23	23						
60. $La_{0.5}Ce_{0.5}Ni_{3.0}Co_{2.0}$				23	23	23						

ALLOY	Van't Hoff Relationship	Specific Heat	Thermal Conductivity	Plateau Shape	Hysteresis	H/M	Comminution	Long Term Degradation	ΔH_f	Poisoning	Safety	Chemical Stability
61. $CaNi_5$	8, 14, 17			2, 3	2	2, 8			8			
62. $SmCo_5$	5			5, 31	31	5, 31			5			
63. $CeCo_5$				20		20						
64. $MmNi_{4.06}$	18								18			
65. $MmNi_{4.73}$	18			18	18	18			18			
66. $MmNi_{4.95}$	18			18	18	18			18			
67. $MmNi_{5.0}$	13,14,15 16,17,27			2,12,14 15,16,17 22,27	12,22	2,12,14, 15,16,17 22,27			14,15,16, 17,27			
68. $MmNi_{5.06}$	18								18			
69. $MmNi_{5.17}$				18	18	18						
70. $MmCo_5$	15,16			17		17			15,16,17	11		
71. $Mm_{0.9}Ca_{0.1}Ni_5$	14,17			(14)		14			14			
72. $Mm_{0.8}Ca_{0.2}Ni_5$	1	1		1,2	1	1			1			

ALLOY	Van't Hoff Relationship	Specific Heat	Thermal Conductivity	Plateau Shape	Hysteresis	H/M	Comminution	Long Term Degradation	ΔH_F	Poisoning	Safety	Chemical Stability
73. $Mm_{0.75}Ca_{0.25}Ni_5$	14, 17			(14)		14			14			
74. $Mm_{0.50}Ca_{0.50}Ni_5$	14, 17			2, 17, 18		2, 14, 17, 27			14, 15, 18, 27			
75. $Mm_{0.30}Ca_{0.70}Ni_5$	2			2	2	2			2			
76. $Mm_{0.25}Ca_{0.75}Ni_5$	14, 17			(14)		14			14			
77. $Mm_{0.20}Ca_{0.80}Ni_5$				2		2						
78. $Mm_{0.15}Ca_{0.85}Ni_5$				2		2						
79. $Mm_{0.10}Ca_{0.90}Ni_5$				2		2						
80. $Mm_{0.90}Ti_{0.10}Ni_5$	14, 17			(14), 17		14, 17			14			
81. $Mm_{0.75}Ti_{0.25}Ni_5$	14, 17			(14)		14			14			
82. $Mm_{0.50}Ti_{0.50}Ni_5$	14, 17					27			27			
83. $MmNi_{4.9}Al_{0.1}$				22	22	22						
84. $MmNi_{4.8}Al_{0.2}$				22	22	22						

ALLOY	Van't Hoff Relationship	Specific Heat	Thermal Conductivity	Plateau Shape	Hysteresis	H/M	Comminution	Long Term Degradation	ΔH_F	Poisoning	Safety	Chemical Stability
85. $MmNi_{4.75}Al_{0.25}$				13		13						
86. $MmNi_{4.7}Al_{0.3}$				22	22	22						
87. $MmNi_{4.65}Al_{0.35}$				13		13						
88. $MmNi_{4.6}Al_{0.4}$				22	22	22						
89. $MmNi_{4.5}Al_{0.5}$	1, 2, 13, 14, 27	1		2, 13,14, 22, 27	1, 2, 22	1, 2, 13, 14, 22,27			1,2,14,27			
90. $MmNi_{4.3}Al_{0.7}$				2		2						
91. $MmNi_{4.1}Al_{0.9}$				2		2						
92. $MmNi_{4.5}Si_{0.5}$				14		14						
93. $MmNi_{4.5}Cr_{0.5}$	14, 27			14 27		14, 27			14, 27			
94. $MmNi_{4.7}Mn_{0.3}$	12			12	12	12			12			
95. $MmNi_{3.78}Mn_{0.42}$				12		12						
96. $MmNi_{4.52}Mn_{0.48}$				12		12						

ALLOY	Van't Hoff Relationship	Specific Heat	Thermal Conductivity	Plateau Shape	Hysteresis	H/M	Comminution	Long Term Degradation	ΔH_F	Poisoning	Safety	Chemical Stability
97. $MmNi_{4.5}Mn_{0.5}$	14, 15, 27			2, 12,14, 15, 27	(2), 12	2, 12, 14, 15, 27			14, 15, 27			
98. $MmNi_{5.22}Mn_{0.5}$				12		12						
99. $MmNi_{4.3}Mn_{0.7}$				2, 12,31	12,31	2, 12,31						
100. $MmNi_{4.7}Fe_{0.3}$					22							
101. $MmNi_{4.5}Fe_{0.5}$				2	22	2						
102. $MmNi_{4.15}Fe_{0.85}$	1	1		1	1	1			1			
103 $MmNi_{4.0}Fe_{1.0}$	2			2	2	2			2			
104. $MmNi_{3.5}Fe_{1.5}$				2		2						
105. $MmNi_{4.0}Co_{1.0}$	15			15, 23	23	15, 23			15			
106. $MmNi_{3.0}Co_{2.0}$	15			15, 23	23	15, 23			15			
107. $MmNi_{2.5}Co_{2.5}$	14, 15, 27			14, 15, 27		14,15,27			14,15,27			
108. $MmNi_{2.0}Co_{3.0}$	15								15			

ALLOY	Van't Hoff Relationship	Specific Heat	Thermal Conductivity	Plateau Shape	Hysteresis	H/M	Comminution	Long Term Degradation	ΔH_F	Poisoning	Safety	Chemical Stability
109. $MmNi_{1.0}Co_{4.0}$	15								15			
110. $MmNi_{4.0}Cu_{1.0}$				2		2						
111. $MmNi_{3.5}Cu_{1.5}$	2			2	2	2			2			
112. $MmNi_{2.5}Cu_{2.5}$				2		2						
113. $CFMmNi_{4.8}Al_{0.2}$	9			9	9	9			9			
114. $CFMmNi_{4.6}Al_{0.4}$	10				9	9						
115. $Mm_{0.5}Ca_{0.5}Ni_{4.5}Al_{0.5}$	14								14			
116. $Mm_{0.5}Ca_{0.5}Ni_{4.5}Cr_{0.5}$	14											
117. $Mm_{0.5}Ca_{0.5}Ni_{4.5}Mn_{0.5}$	14											
118. $Mm_{0.5}Ca_{0.5}Ni_{2.5}Co_{2.5}$	14, 15					27			14,15,27			
119. $MmNi_{4.5}Cr_{0.25}Mn_{0.25}$	14			14		14			14			
120. $MmNi_{4.5}Cr_{0.45}Mn_{0.05}$				14		14						

ALLOY	Van't Hoff Relationship	Specific Heat	Thermal Conductivity	Plateau Shape	Hysteresis	H/M	Comminution	Long Term Degradation	ΔH_F	Poisoning	Safety	Chemical Stability
121. $MmNi_{4.5}Cr_{0.46}Mn_{0.04}$				14		14			14			
122. YNi_4Al					9	9						

REFERENCES

1. Huston, E.L. and Sandrock, G.D., "Engineering Properties of Metal Hydrides," J. Less Common Metals, 74 (1980) pp 435-443.

2. Sandrock, G.D., "Development of Low Cost Nickel-Rare Earth Hydrides for Hydrogen Storage," 2nd World Hydrogen Energy Conf., Zurich, Switzerland, Aug 21-24 (1978), Vol. 3, Pergamon, Oxford, 1978, p 1625.

3. NBS - $LaNi_5$

4. Lundin, C.E. and Lynch, F.E, "A Detailed Analysis of the Hydriding Characteristics of $LaNi_5$," IECEC '75 Record, p 1380.

5. van Vucht, J.H.N., Kuijpers, F.A. and Bruning, H.C.A.M., "Reversible Room-Temperature Absorption of Large Quantities of Hydrogen by Intermetallic Compounds," Philips Res. Reports, Vol. 25 (1970) pp 133-140.

6. Van Mal, H.H., Buschow, H.J., and Kuijpers, F.A., "Hydrogen Absorption and Magnetic Properties of $LaCo_{5x}$ Ni_{5-5x} Compounds," J. Less-Common Metals, Vol. 32, (1973), pp 289-296.

7. Van Mal, H.H., Buschow, K.H.J. and Miedema, A.R., "Hydrogen Absorption in $LaNi_5$ and Related Compounds: Experimental Observations and Their Explanation," J. Less-Common Metals, Vol. 35, (1974), pp 76-76.

8. Shinar, J., Shaltiel, D., Davidov, D and Grayevsky, A., "Hydrogen Sorption Properties of the La_{1-x} Cu_xNi_5 and $La(Ni_{1-x}Cu_x)_5$ Systems," J. Less-Common Metals, Vol. 60, (1978), pp. 209-219.

9. Mendelsohn, M.H., Gruen, D.M. and Dwight, A.E., "The Effects of Aluminum Additions on the Structural and Hydrogen Absorption Properties of AB_5 Alloys With Particular Reference to the $LaNi_{5-x}Al_x$ Ternary Alloy Systems," J. Less-Common Metals, Vol. 63, (1979), pp 193-207.

10. Mendelsohn, M.H. and Gruen, D.M., "$LaNi_{5-x}Al_x$ is a Versatile Alloy System for Metal Hydride Applications," Nature, Vol. 269, (1977), p 45.

11. Guildotti, R.A., Atkinson, G.B. and Wong, M.M., "Hydrogen Absorption by Rare Earth - Transition Metal Alloys," J. Less-Common Metals, Vol. 52, (1977), pp 13-28.

12. Lundin, C.E. and Lynch, F.E., "Modification of Hydriding Properties of AB_5 Type Hexagonal Alloys Through Manganese Substitution," Int. Conf. Alternate Energy Source, Miami, Florida, 1977. University of Miami, Florida, 1978, pp. 3803-3820.

13. Osumi, Y., Kato, A., Suzuki, H. and Nakane, M., "Hydrogen Absorption - Desorption Characteristics of Mischmetal-Nickel-Aluminum Alloys," J. Less-Common Metals, Vol. 66, (1979), pp 67-75.

14. Osumi, Y., Suzuki, H., Kato, A., Oguro, K and Nakane, M., "Hydrogen - Absorption-Desorption Characteristics of Misch-metal-Nickel Alloys," Int. J. of Hydrogen Energy (in press).

15. Osumi, Y., Suzuki, H., Kato, A., Nakane, M and Miyake, Y., "Absorption-Desorption Characteristics of Hydrogen for Mischmetal-Nickel-Manganese Alloys," Nippon Kagaku Kaishi, 1, (1979), pp. 45-48.

16. Osumi, Y., Suzuki, H., Kato, A., Nakane, M. and Miyake, Y., "Absorption-Desorption Characteristics of Hydrogen for Mischmetal-Nickel-Cobalt Alloys," Nippon Kagahi, 6, (1979), pp. 722-726.

17. Osumi, Y., Suzuki, H., Kato, A., Nakane, M. and Miyake, Y., "Absorption-Desorption Characteristics of Hydrogen for Mischmetal Based Alloys," Nippon Kagaku Kaishi, 11, (1979), pp. 1472-1477.

18. Kitada, M., "Hydrogen Absorption and Desorption Characteristics in Mischmetal-Nickel Alloys," Nippon Kinzoku Gakkaishi, 41, (1977), pp. 420-425.

19. Bruning, H.A.C.M., van Vucht, J.H.N., Westendorp, F.F. and Zijlstra, H., U.S. Patent #4,242,315 - AB_nH_m Hydrides.

20. Kuijpers, F.A., "Investigations on the $LaCo_5$-H and $CeCo_5$-H Systems," J. Less-Common Metals, 27, (1972), p 27.

21. Diaz, H., Percheron-Gnégan, A., Achard, J.C., Chatillon, C. and Mathieu, J.C., "Thermodynamic and Structural Properties of $LaNi_{5-y}$ Al_y Compounds and Their Related Hydrides," Int. J. Hydrogen Energy, Vol. 4, pp 445-454, (1979). [Also 2nd World Hydrogen Energy Conference, (1978), p 2653.]

22. Suda, S., Komazaki, Y., Miyamoto, M. and Yoshida, K., "Hydriding Properties of Al-Substituted Mischmetal Nickels," Extended Abstract - Miami International Symposium on Metal-Hydrogen Systems," (1981), p 16.

23. Dayan, D., Mintz, M.H., and Daniel, M.P., "Hysteresis Effects in Cerium-containing $LaNi_5$-Type Compounds," J. Less-Common Metals, 73, (1980), pp 15-24.

24. Ohlendorf, D. and Flotow, H.E., "Heat Capacities and Thermodynamic Functions of $LaNi_5$, $LaNi_5H_{0.36}$ and $LaNi_5H_{6.39}$ From 5 to 300 K", J. Less-Common Metals, 73, (1980), pp 25-32.

25. Sandrock, G.D. and Goodell, P.D., Surface Poisoning of $LaNi_5$, FeTi and (Fe, Mn) Ti by O_2, CO and H_2O," J. Less-Common Metals, 73. (1980), pp 161-168.

26. Cohen, R.L., West, K.W. and Wernick, J.H., "Degradation of $LaNi_5$ by Temperature-Induced Cycling," J. Less-Common Metals," 73 (1980), pp 273-279.

27. Osumi, Y., Suzuki, H., Kato, A., Oguro, K. and Nakane, M., "Developme of Mischmetal-Nickel and Titanium-Cobalt Hydrides for Hydrogen Storage," J. Less-Common Metals, 73, (1980), pp 271-277.

28. Huang, Y.C., Tada, M., Watanabe, T. and Fujita, K., "Effect of Ni, Ce and Co on Hydrogen Absorption by La-Ni Alloy, "Proceedings of the 2nd World Energy Conference, Zurich, Switzerland, Aug 1978, Vezirogh, T.N. and Seifritz, W., ed., Pergamon, Oxford, p 1613.

29. Swartzendruder, L.J., Carter, G.C., Kahan, D.J., Read, M.E. and Manning, J.R., "Numerical Physical Property Data for Metal Hydrides Utilized for Hydrogen Storage, " Proceedings of the 2nd World Energy Conference, Zurich, Switzerland, Aug 1978, Vezirogh, T.N. and Seifritz, W., ed., Pergamon, Oxford, p 1973.

30. Belkbir, L., Gérard, N., Percheron-Guégan, A. and Achard, J.C., "Kinetics of Hydrogen Absorption and Desorption by Ternary $LaNi_5$ Type Intermetallic Compounds, "Proceedings of the 2nd World Energy Conference, Zurich, Switzerland, Aug 1978, Vezirogh, T.N. and Seifritz, W., ed., Pergamon, Oxford, pp 2589-2612.

31. Goodell, P.D., Sandrock, G.D., and Huston, E.G., "Microstructure and Hydriding Studies of AB_5 Hydrogen Storage Compounds," SAND79-7095, Contract #13-0524, Jan 1980.

32. Goodell, P.D. and Sandrock, G.D., "Metallurgical Studies of Hydrogen Storage Alloys-Surface Poisoning of $LaNi_5$, FeTi and $Fe_{0.85}Mn_{0.15}Ti$ by CO, CO_2 and H_2O," Report BNL 51174, Contract #BNL45117-5.

APPENDIX 2

MHHP LITERATURE

- BIBLIOGRAPHY -

Sheft, Irving, et al., "HYCSOS: A Chemical Heat Pump and Energy Conversion System Based on Metal Hydrides - 1979 Status Report", Argonne National Laboratory (ANL-79-8), 1979.

2. Sheft, Irving, et al., "Evaluation of the Argonne Multi-Tube Hydride Heat Exchanger", Argonne National Laboraotry, 1980.

3. Aelson, H., et al., "A Thermodynamic Analysis of a Metal Hydride Heat Pump", Argonne National Laboratory Report, 1980 and 1981.

4. Napier, J. C., "Design of the One-Ton Metal Hydride Demonstration Unit", Southern California Gas Co., S.O. 6-4775-7, Solar Research Memo, August 6, 1980.

5. Lynch, F. E., "Operating Characteristics of High Performance Commercial Metal Hydride Heat Exchangers", J. of Less Common Metals, 1980, pp. 411-418.

6. Sheft, Irving, "Current Status and Performance of the Argonne HYCSOS Chemical Heat Pump System", Argonne National Laboratory, 1980, pp. 401-409.

7. Huston, E. L., et al., "Engineering Properties of Metal Hydrides", ibid. pp. 435-443.

8. Goodell, P. D., "Thermal Conductivity of Hydriding Alloy Powders and Comparisons of Reactor Systems", ibid, pp. 175-184.

9. Mackay, Dr. D. B., "Automotive Hydride Tank Design", Proc. of the World Hydrogen Energy Conf., 1976, V.3, Session 7-C, pp. 13-23.

10. Fisher, P. W., et al., "Modeling Solid Hydrogen Storage Beds", Oak Ridge National Laboratory-Chemical Technology Division, 1979.

11. Rosso, M. J, et al., "Hydride Beds: Engineering Tests", Brookhaven National Laboratory, 1979.

12. Letter from George P. Wachtell of Franklin Research Institute to Hector A. Madariaga of SoCal, "Metal Hydride Heat Pump", March 17, 1981.

13. Moshe, Ron, "Metal Hydrides of Improved Heat Transfer Characteristics", 11th IECEC, 1979, pp. 954-960.

14. Steyert, W. A., "New Heat Transfer Geometry for Hydride Heat Engines and Heat Pumps", Los Alamos Scientific Laboratory, 1978.

15. Stickland, G., et al., "The Behavior of Iron Titanium Hydride Test Beds: Long-Term Effects, Heat Transfer and Modeling", Proc. of the World Hydrogen Energy Conf., 1976, V.2, Session 8-B,pp. 41-71.

16. U. S. Patent #4,134,490. Turillon, P. P. and Sandrock, G.D., Gas Storage Containment, Jan. 16,1979.

17. U. S. Patent #4,134,491. Turillon, P. P. and Sandrock, G. D. Hydride Storage Containment, Jan. 16, 1979.

18. U. S. Patent #4,165,569. Mackay, D. B. Hydride Storage and Heat Exchanger System and Method. Aug. 28, 1979.

19. U. S. Patent #4,135,621. Turillon, P. P. and Sandrock, G. D. Hydrogen Storage Module. Jan. 23, 1979.

20. Eaton, E. E., et al., "Mechanically Stable Hydride Composites Designed for Rapid Cycling", Los Alamos Scientific Laboratory (LA-UR-89-2448), 1978.

21. Horowitz, J. S., "Analytical Modeling of a Hydride Heat Exchaner," Argonne National Laboratory (ANL/EES TM-61), Sept. 1979.

22. Mcgerlin, F. E., "Augmentation of Heat Transfer in Tubes by Use of Mesh and Brush Inerts," Journal of Heat Transfer, Mary 1974, pp. 145-151.

23. Clinch, J. M., et. al., "Development of a Metal Hydride Heat Pump", presented at Chemical/Hydrogen Energy Storage Systems Program - Semi-annual Contracts Review, May 1981.

24. Yu, W. S., et al., "Modeling Studies of Fixed Bed Metal Hydride Storage Systems", Proc. of the Hydrogen Energy Conference, 1974, Part A, pp. 621-643.

25. Kuzay, T. M.,"Effective Thermal Conductivity of Porous Solid-Gas Mixtures", ASME Paper 80-WA-HT-63.

APPENDIX 3

GENERAL THEORY OF COMPUTER PROGRAM P315A

...TRODUCTION

The solution of transient and steady state heat transfer problems presents an overwhelming task when attempted by manual methods. Computer program P315A was prepared by Solar Turbine Incorporated to aid the engineer in this time consuming problem.

It considers the fundamental modes of heat transfer: conduction, convection, and radiation. Heat transfer between moving fluids and solid surface (follower nodes technique), heat sources and internal heat generation as well as natural convection can be easily accounted for with P315A. Problems involving change of phase are not considered.

General Theory

The structure under investigation is split into N finite volume elements with the thermal balance being written down for very one of them. Let V_i be the volume of element i with a temperature T_i, A_{ij} its interface with the next element j at temperatures T_j. In case of no heat generation or no heat source, the thermal balance of element i is written:

$$\Sigma_n \, k_{ij} \, \frac{(T_j - T_i)}{\Delta x_{ij}} \, A_{ij} = \rho_i c_i \, V_i \, \frac{\Delta T_i}{\Delta t} \qquad (1)$$

where Δx_{ij} (ft) = the distance between the centers of elements i and j

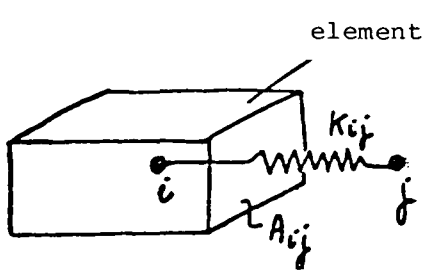

k_{ij} $\frac{\text{btu}}{\text{hr ft-F}}$ is the material thermal conductivity

ρ_i $\frac{\text{lb}}{\text{ft}^3}$ is the material density

C_i $\frac{\text{btu}}{\text{lb °F}}$ is the material specific heat

n is the number of nodes such as j connected to i

t (hr) is the time

In this way, a system of N difference equations is delivered, the unknowns being the temperatures of the N individual elements.

The P315A program solves these N transient heat transfer nodal equations.

Let $K_{ij} = k_{ij} \frac{A_{ij}}{\Delta x_{ij}}$ (btu/hr °F) be called the thermal conductance between nodes i and j and

$\Gamma_i = \rho_i C_i V_i$ (btu/°F) be called the thermal capacitance of node i

Equation (1) becomes

$$\Sigma_n K_{ij} (T_j - T_i) = \Gamma_i \frac{\Delta T_i}{\Delta t} \tag{2}$$

Solving (2):

$$T_i (t + \Delta t) = \frac{\Sigma_n K_{ij} T_j (t)}{\Sigma_n K_{ij}} \left[1 - e^{-\frac{\Delta t}{\Gamma_i} \Sigma_n K_{ij}} \right] + T_i (t) \, e^{-\frac{\Delta t}{\Gamma_i} \Sigma_n K_{ij}} \tag{3}$$

where Δt is the time increment at which the nodal temperatures are re-evaluated. The stability criterion for convergence is governed by the equation:

$$\Delta t \leq \frac{C_i}{\Sigma_n K_{ij}} \tag{4}$$

For example, $\frac{\frac{\Delta t}{\Gamma_i}}{\Sigma_n K_{ij}}$ = 1/4 yields

$$T_i (t + \Delta t) = 0.2212 \frac{\Sigma_n K_{ij} T_j (t)}{\Sigma_n K_{ij}} + 0.7788 \, T_i (t)$$

In fact, all the nodal temperatures are calculated at multiples of a common specific time step, $(RC)_{min}$ where

$$(RC)_{min} = \left[\frac{\Gamma_i}{\Sigma_n K_{ij}} \right]_{min} \text{ (hr)} \tag{5}$$

APPENDIX 4

ACTUAL DATA RUN OF P315A FOR A TUBULAR CONFIGURATION

P-315 THERMAL TRANSIENT ANALYSER REVISION NO. 2.0 08/20/81 12.08.24 PAGE 1
SOLID CYLINDER----QUARTER NODE-----NO Q ADDED-----CHY.DATA 00000010

DUMP CODE	MAX. COUNT	PRINT INTER.	STAB. CRIT.	VAR. TIME	EVALUATION CRIT. TEMP.	PROBLEM START	PRINT START	DUMMY INCREMENTS -1	DUMMY INCREMENTS 0	TIME LIMIT	PUNCH CODE	READ CODE
1	30000	2.7780E-03	1.0000E+00	0.0	0.0	0.0	2.7780E-03	0.0	0.0	10	0	0

GEOMETRIC UNITS FOR RADIATION AND NATURAL CONVECTION CONDUCTANCES INPUT IN INCHES

TEMPERATURE NODES AND CAPACITANCES

NODE	INC	CAP	CURV	RCX	EVX	NO.	TEMP.	CAP. VAL.
1	0	0	0	0	0	0	1.0000E+02	0.0
2	0	1	0	0	0	0	0.0	0.0
3	0	1	0	0	0	0	0.0	1.1980E-02
4	0	1	0	0	0	0	0.0	1.1000E-02
5	0	1	0	0	0	0	0.0	7.3600E-03
6	0	1	0	0	0	0	0.0	3.6800E-03
7	0	1	0	0	0	0	0.0	4.6000E-04

CONDUCTANCES

COND	INC	NODE	INC	NODE	INC	CURV	EVX	NO.	COND. VAL.
1	0	1	0	2	0	0	0	0	2.0830E+01
2	0	2	0	3	0	0	0	0	3.2333E+03
3	0	3	0	4	0	0	0	0	5.1000E+00
4	0	4	0	5	0	0	0	0	3.7000E+00
5	0	5	0	5	0	0	0	0	2.2000E+00
6	0	6	0	7	0	0	0	0	7.0000E-01

OTHER VALUES

LOC. INC NO. VALUE

VARIABLE LINES

ANS	INC	PRMA	INC	PRMB	INC	PRMC	INC	CODE	CURV	EVX	NO.	PARAM. A	PARAM. B	PARAM. C
40C10	0	40010	0	0	0	0	0	6	0	1	0	0.0	0.0	0.0
40C03	1	10003	1	20003	1	0	0	6	0	1	5	0.0	0.0	0.0
40C10	0	40003	1	40010	0	0	0	4	0	1	5	0.0	0.0	0.0
40C11	0	40010	0	0	0	0	0	6	0	1	0	0.0	6.2800E+00	0.0

OUTPUT CODES

I.D.	INC	NO.
10C01	1	7
40C03	1	5
40C10	1	2
0	0	0

PSEUDO SEQUENCE

CAP.	COND.	NODE	RCX	STU	DCND
2			0	0	0
	1	1			
	2	3			
3			0	0	0
	2	2			
	3	4			
4			0	0	0
	3	3			
	4	5			
5			0	0	0
	4	4			
	5	6			
6			0	0	0
	5	5			
	6	7			
7			0	0	0
	6	6			

--------	TIME HR	MINUTES	COUNT	PREV INC	NEXT INC	MIN RC
	0.0	0.0	1	0.0	9.2484E-07	3.6994E-06

PREVIOUS TEMPERATURES

1	2	3	4	5	6	7
1.0000E+02	0.0	0.0	0.0	0.0	0.0	0.0

CURRENT TEMPERATURES

1	2	3	4	5	6	7
1.0000E+02	6.4011E-01	0.0	0.0	0.0	0.0	0.0

CAPACITANCES

2	3	4	5	6	7
0.0	1.1980E-02	1.1000E-02	7.3600E-03	3.6800E-03	4.6000E-04

CONDUCTANCES

1	2	3	4	5	6
2.0830E+01	3.2333E+03	5.1000E+00	3.7000E+00	2.2000E+00	7.0000E-01

MISCELLANEOUS VALUES

3	4	5	6	7	10	11
0.0	0.0	0.0	0.0	0.0	0.0	0.0

TIME CONSTANTS

3	4	5	6	7
3.6994E-06	1.2500E-03	1.2475E-03	1.2690E-03	6.5714E-04

HEAT BALANCE

2	3	4	5	6	7
-2.4414E-04	2.0697E+03	0.0	0.0	0.0	0.0

RELATIVE HEAT BALANCE

2	3	4	5	6	7
5.8981E-08	1.0000E+00	0.0	0.0	0.0	0.0

--------	TIME HR	MINUTES	COUNT	PREV INC	NEXT INC	MIN RC
	2.7780E-03	1.6668E-01	3005	8.6636E-07	9.2484E-07	3.6994E-06

CURRENT TEMPERATURES

1	2	3	4	5	6	7
1.0000E+02	8.5862E+01	8.5774E+01	4.2336E+01	1.7142E+01	6.6355E+00	3.8642E+00

MISCELLANEOUS VALUES

3	4	5	6	7	10	11
1.0276E+00	4.6570E-01	1.2616E-01	2.4419E-02	1.7775E-03	1.6456E+00	1.0335E+01

```
------- TIME HR      MINUTES     COUNT  PREV INC     NEXT INC     MIN RC
        5.5560E-03  3.3336E-01   6011  7.7859E-07  9.2484E-07  3.6994E-06

                    CURRENT TEMPERATURES

   1           2           3           4           5           6           7
1.0000E+02  9.2108E+01  9.2058E+01  6.3973E+01  4.0925E+01  2.6597E+01  2.1649E+01

                    MISCELLANEOUS VALUES

   3           4           5           6           7          10          11
1.1029E+00  7.0370E-01  3.0121E-01  9.7876E-02  9.9584E-03  2.2156E+00  1.3914E+01

-------- TIME HR      MINUTES     COUNT  PREV INC     NEXT INC     MIN RC
         8.3340E-03  5.0004E-01   9018  8.8289E-07  9.2484E-07  3.6994E-06

                    CURRENT TEMPERATURES

   1           2           3           4           5           6           7
1.0000E+02  9.4679E+01  9.4646E+01  7.5251E+01  5.7979E+01  4.6104E+01  4.1738E+01

                    MISCELLANEOUS VALUES

   3           4           5           6           7          10          11
1.1339E+00  8.2776E-01  4.2673E-01  1.6966E-01  1.9200E-02  2.5772E+00  1.6185E+01

-------- TIME HR      MINUTES     COUNT  PREV INC     NEXT INC     MIN RC
         1.1112E-02  6.6672E-01  12025  8.8289E-07  9.2484E-07  3.6994E-06

                    CURRENT TEMPERATURES

   1           2           3           4           5           6           7
1.0000E+02  9.6255E+01  9.6231E+01  8.2503E+01  7.0007E+01  6.1181E+01  5.7884E+01

                    MISCELLANEOUS VALUES

   3           4           5           6           7          10          11
1.1528E+00  9.0754E-01  5.1525E-01  2.2515E-01  2.6627E-02  2.8274E+00  1.7756E+01

-------- TIME HR      MINUTES     COUNT  PREV INC     NEXT INC     MIN RC
         1.3890E-02  8.3340E-01  15032  8.8289E-07  9.2484E-07  3.6994E-06

                    CURRENT TEMPERATURES

   1           2           3           4           5           6           7
1.0000E+02  9.7330E+01  9.7313E+01  8.7521E+01  7.8557E+01  7.2179E+01  6.9786E+01

                    MISCELLANEOUS VALUES

   3           4           5           6           7          10          11
1.1658E+00  9.6273E-01  5.7818E-01  2.6562E-01  3.2102E-02  3.0044E+00  1.8868E+01

-------- TIME HR      MINUTES     COUNT  PREV INC     NEXT INC     MIN RC
         1.6668E-02  1.0001E+00  18039  8.8289E-07  9.2484E-07  3.6994E-06

                    CURRENT TEMPERATURES

   1           2           3           4           5           6           7
1.0000E+02  9.8086E+01  9.8074E+01  9.1071E+01  8.4652E+01  8.0077E+01  7.8358E+01

                    MISCELLANEOUS VALUES

   3           4           5           6           7          10          11
1.1749E+00  1.0018E+00  6.2304E-01  2.9468E-01  3.6045E-02  3.1305E+00  1.9659E+01

-------- TIME HR      MINUTES     COUNT  PREV INC     NEXT INC     MIN RC
         1.9446E-02  1.1668E+00  21046  8.8289E-07  9.2484E-07  3.6994E-06

                    CURRENT TEMPERATURES

   1           2           3           4           5           6           7
1.0000E+02  9.8625E+01  9.8617E+01  9.3598E+01  8.9000E+01  8.5723E+01  8.4492E+01

                    MISCELLANEOUS VALUES

   3           4           5           6           7          10          11
1.1814E+00  1.0290E+00  6.5504E-01  3.1546E-01  3.8866E-02  3.2204E+00  2.0224E+01

-------- TIME HR      MINUTES     COUNT  PREV INC     NEXT INC     MIN RC
         2.2224E-02  1.3334E+00  24053  8.8289E-07  9.2484E-07  3.6994E-06

                    CURRENT TEMPERATURES

   1           2           3           4           5           6           7
1.0000E+02  9.9009E+01  9.9003E+01  9.5400E+01  9.2104E+01  8.9755E+01  8.8873E+01

                    MISCELLANEOUS VALUES

   3           4           5           6           7          10          11
1.1861E+00  1.0494E+00  6.7788E-01  3.3030E-01  4.0882E-02  3.2845E+00  2.0627E+01
```

-------- TIME HR MINUTES COUNT PREV INC NEXT INC MIN RC
2.5002E-02 1.5001E+00 27060 8.8289E-07 9.2484E-07 3.6994E-06

CURRENT TEMPERATURES

1	2	3	4	5	6	7
1.0000E+02	9.9283E+01	9.9278E+01	9.6686E+01	9.4319E+01	9.2633E+01	9.2001E+01

MISCELLANEOUS VALUES

3	4	5	6	7	10	11
1.1894E+00	1.0635E+00	6.9418E-01	3.4089E-01	4.2320E-02	3.3303E+00	2.0914E+01

-------- TIME HR MINUTES COUNT PREV INC NEXT INC MIN RC
2.7718E-02 1.6631E+00 30000 9.2484E-07 9.2484E-07 3.6994E-06

PREVIOUS TEMPERATURES

1	2	3	4	5	6	7
1.0000E+02	9.9475E+01	9.9472E+01	9.7586E+01	9.5869E+01	9.4648E+01	9.4190E+01

CURRENT TEMPERATURES

1	2	3	4	5	6	7
1.0000E+02	9.9475E+01	9.9472E+01	9.7587E+01	9.5870E+01	9.4649E+01	9.4191E+01

CAPACITANCES

2	3	4	5	6	7
0.0	1.1980E-02	1.1000E-02	7.3600E-03	3.6800E-03	4.6000E-04

CONDUCTANCES

1	2	3	4	5	6
2.0830E+01	3.2333E+02	6.1000E+00	3.7000E+00	2.2000E+00	7.0000E-01

MISCELLANEOUS VALUES

3	4	5	6	7	10	11
1.1917E+00	1.0735E+00	7.0560E-01	3.4831E-01	4.3328E-02	3.3624E+00	2.1116E+01

TIME CONSTANTS

3	4	5	6	7
3.6994E-06	1.2500E-03	1.2475E-03	1.2690E-03	6.5714E-04

HEAT BALANCE

2	3	4	5	6	7
2.2839E-01	1.0920E+00	3.2609E+00	3.6676E+00	2.3648E+00	3.2064E-01

RELATIVE HEAT BALANCE

2	3	4	5	6	7
1.0554E-02	5.3742E-02	2.0423E-01	4.0577E-01	7.8668E-01	1.0000E+00

APPENDIX 5

COMPUTER PROGRAM TF1

```
      1
00010       DIMENSION Q(100), AK(100),AC(100)
00020 C      FINITE   ELEMENT   HEAT   TRANSFER   INFORMATION
00030       CP1=.092
00040       CP2=.107
00050       CK=0
00060       N=4
00070       TW1=0.0280
00080       H=100.
00090       ANG=3.1416/2
00100       RHO1=558
00110       RHO2=259
00120       COND1=200
00130       COND2=0.30
00140       IA=1
00150       IC=30000
00160       PI=.003333
00170       ST=0.10
00180       TAMB=70
00185       THG=69.0
00190       WRITE(6,1)
00200     1 FORMAT    (' INPUT   FIN   THICKNESS   (INCHES)')
00210       READ (5,*) D1
00220       WRITE (6,2)
00230     2 FORMAT    (' INPUT   HYDRIDE   THICKNESS   (INCHES)')
00240       READ (5,*) Y1
00250       WRITE (6,3)
00260     3 FORMAT    (' INPUT   FIN   LENGTH   (INCHES)')
00270       READ (5,*) FL1
00280       WRITE (6,4)
00290     4 FORMAT    (' INPUT   BOUNDARY   TEMPERATURE   (F)')
00300       READ (5,*) T1
00310       WRITE (6,300)
00320   300 FORMAT (' INPUT CONV HEAT TRANS COEFF (BTU/HR FT**2 F)')
00330       READ (5,*) H
00340       TW=TW1/12
00350       WRITE (6,40)
00360    40 FORMAT (' INPUT TUBE DIAMETER (INCHES)')
00370       READ (5,*) TD1
00380       WRITE (6,106)
00390   106 FORMAT (' HEAT GENERATION? 1=YES 2=NO')
00400       READ (5,*) HG
00410       TD=TD1/12
00420       D=D1/12
00430       Y=Y1/12
00440       FL=FL1/12
00450       DL=FL/(N-1)
00460       V1A=(D+Y)*TW
00470       C1A=RHO1*CP1*V1A
00480       AK1=COND1*D/(TW+DL)
```

```
00490         AK2=COND1*D/2/DL
00500         AK3=2*Y/(TW/COND1+DL/COND2)
00510         AK4=COND2*Y/DL
00520         AK6=(D+Y)/(1/H+TW/2/COND1)
00530         AK5=1/(D/COND1/DL/4+Y/COND2/DL/2)
00540         C1=RHO1*CP1*DL*D/2
00550         C2=RHO2*CP2*DL*Y
00560         AC(1)=ANG*(TD-TW)/2
00570         DO 41 I=2,N
00580         AC(I)=ANG*(TD+(2*I-3)*DL)/2
00590    41   CONTINUE
00600         AK(1)=ANG*(TD/2-TW)
00610         DO 42 I=2,N
00620         AK(I)=ANG*(TD/2+(I-2)*DL)
00630    42   CONTINUE
00640         QC=90*RHO2*DL*Y
00650         DO 10 I=2,N
00660         Q(I)=QC*AC(I)
00670    10   CONTINUE
00680         VOLH=FL*Y*AC(N/2+1)
00690         VOLF=FL*D*AC(N/2+1)
00700         VOLTB=V1A*AC(1)
00710         SHTB=VOLTB*RHO1*CP1
00720         SHH=VOLH*RHO2*CP2
00730         SHF=VOLF*RHO1*CP1
00740         VOLFT=VOLTB+VOLF
00750         VOLT=VOLFT+VOLH
00760         SHFT=SHF+SHTB
00770         SHT=SHH+SHF+SHTB
00780         SHR=SHH/SHT
00790         SHR1=SHFT/SHT
00800         IF (CK .EQ. 0) GO TO 500
00810         WRITE(6,*) AK1,AK2,AK3,AK4,AK5,C1,C2,VOLH,VOLF,SHH,SHF
00820         WRITE (6,*) V1A,V2A,C1A,C2A,AK100,AK300
00830    500  CONTINUE
00840         WRITE (8,5)    D1,FL1,Y1,H,TD1,HG
00850     5   FORMAT    (' FIN THCK=',F6.3,1X,'FIN LNGTH=',F5.2,1X,
00860        X'HYD THCK=',F6.3,1X,'H=',F5.0,1X,'TD=',F4.2,1X,'HG=',F8.
00870         WRITE (8,6)    IA,IC,PI,ST
00880     6   FORMAT '(I2,I6,F8.5,4X,F4.2)
00890         C1AA=C1A*AC(1)
00900         WRITE (8,7)    TAMB,C1AA
00910     7   FORMAT    (3X'10001',7X,'1',2X,F6.1,F8.7)
00920         DO 43 I=2,N
00930         C1Z=C1*AC(I)
00940         WRITE (8,8) I,TAMB,C1Z
00950     8   FORMAT (2X,I2,'2001',7X,'2',4X,F4.1,F8.7)
00960     43  CONTINUE
00970         DO 44 I=2,N
00980         C2Z=C2*AC(I)
00990         J=I+10
```

```
01000        WRITE (8,9) J,TAMB,C2Z
01010     9  FORMAT (2X,I2,'0001',7X,'1',4X,F4.1,F8.7)
01020    44  CONTINUE
01030        WRITE (8,19) T1
01040    19  FORMAT (2X,'3101',9X,'1',2X,F6.1)
01041        IF (HG .GT. 1) GO TO 107
01050        WRITE (8,20) THG
01060    20  FORMAT (2X,'320101',7X,'90000',F4.1)
01061   107  CONTINUE
01070        WRITE (8,100)
01080   100  FORMAT ('       ')
01090        AK1A=AK1*AK(2)
01100        WRITE (8,11)    AK1A
01110     11 FORMAT    (3X,'12000010000022000000',F8.3)
01120        J=N-1
01130        DO 45 I=2,J
01140        AK2A=AK2*AK(I+1)
01150        K=I+1
01160        WRITE (8,12) I,I,K,AK2A
01170     12 FORMAT (2X,I2,'2000',I2,'2000',I2,'20000002',F8.3)
01180     45 CONTINUE
01190        AK3A=AK3*AK(2)
01200     13 FORMAT (2X,'11000001000012000000001',F8.3)
01210        WRITE (8,13)    AK3A
01220        J=N-1
01230        DO 46 I=2,J
01240        AK4A=AK4*AK(I+1)
01250        K1=I+10
01260        K2=I+11
01270        WRITE (8,14) K1,K1,K2,AK4A
01280     14 FORMAT (2X,I2,4X,I2,4X,I2,7X,'1',F8.3)
01290     46 CONTINUE
01300        DO 49 I=2,N
01310        AK5A=AK5*AC(I)
01320        J1=I+28
01330        J2=I+10
01340        WRITE (8,15) J1,I,J2,AK5A
01350     15 FORMAT (2X,I2,'0900',I2,'1000',I2,'10000002',F8.3)
01360     49 CONTINUE
01370        AK6A=AK6*AK(1)
01380        WRITE (8,21) AK6A
01390     21 FORMAT (2X,'50000031000001000000001',F8.3)
01391        IF (HG .GT. 1) GO TO 104
01400        DO 104 I=2,N
01410        0100=0(I)
01420        IK=49+I
01430        IN=10+I
01440        IC=30+I
01450        WRITE (8,103) IK,IN,IC,0100
01460   103  FORMAT (2X,I2,'0100',I2,'0100',I2,'01000001',F8.3)
01470   104  CONTINUE
```

```
01480       WRITE (6,100)
01490       WRITE (8,100)
01500       WRITE (8,101)
01510   101 FORMAT ('040010000040010',19X,'60001',10X,'0.')
01511       IF (HG .GT. 1) GO TO 108
01520       WRITE (8,105)
01530   105 FORMAT ('10032011001201000000000000000500010100l.0')
01531   108 CONTINUE
01540       WRITE (8,100)
01550       WRITE (8,100)
01560       WRITE (8,102)
01570   102 FORMAT ('0001000100010030')
01580       WRITE (8,100)
01590   200 CONTINUE
01600       WRITE (6,23)
01610    23 FORMAT ('1',/,'      FINNED TUBE HYDRIDE HEAT EXCHANGER')
01620       WRITE (6,28)
01630    28 FORMAT ('0**************************************************
01640       WRITE (6,29)
01650    29 FORMAT ('0        INPUT VALUES'/)
01660       WRITE (6,24) D1
01670    24 FORMAT ('  FIN THICKNESS          ',F6.3,'  INCHES')
01680       WRITE (6,25) Y1
01690    25 FORMAT ('  HYDRIDE THICKNESS      ',F6.3,'  INCHES')
01700       WRITE (6,26) FL1
01710    26 FORMAT ('  FIN LENGTH             ',F6.3,'  INCHES')
01720       WRITE (6,27) T1
01730    27 FORMAT ('  WATER TEMPERATURE      ',F6.1,'  F')
01740       WRITE (6,301) H
01750   301 FORMAT ('  CONV HEAT TRANS COEFF',F6.1,'  BTU/HR FT**2 F
01760       WRITE (6,302) TW1
01770   302 FORMAT ('  TUBE WALL THICKNESS    ',F5.4,'  INCHES')
01780       WRITE (6,303)  TD1
01790   303 FORMAT ('  TUBE DIAMETER          ',F5.3,'  INCHES')
01791       IF (HG .GT. 1) GO TO 109
01792       WRITE (6,600)
01793   600 FORMAT('0 HEAT GENERATION              YES')
01794       GO TO 601
01795   109 WRITE (6,602)
01796   602 FORMAT ('0 HEAT GENERATION               NO')
01797   601 CONTINUE
01800       WRITE (6,30)
01810    30 FORMAT ('1',/,'       MATERIAL PROPERTIES'/)
01820       WRITE (6,31)
01830    31 FORMAT (20X'          TUBE/FIN       HYDRIDE'/)
01840       WRITE (6,32) CP1,CP2
01850    32 FORMAT ('  SPECIFIC HEAT (BTU/LBM F)      ',F6.3,6X,F6.3)
01860       WRITE (6,33) RHO1,RHO2
01870    33 FORMAT ('  DENSITY      (LBM/FT**3)      ',F8.2,5X,F8.2)
01880       WRITE (6,34) COND1,COND2
01890    34 FORMAT ('  CONDUCTIVITY (BTU/HR FT F)   ',F8.2,5X,F8.
```

```
01    1       WRITE (6,35)
01910   35    FORMAT (////'          CALCULATED VALUES'/)
01920         WRITE (6,36)
01930   36    FORMAT (20X,'           TUBE/FIN       HYDRIDE         TOTAL'/)
01940         WRITE (6,37) VOLFT,VOLH,VOLT
01950   37    FORMAT ('  VOLUME (FT**3)',13X,F8.7,5X,F8.7,5X,F8.7)
01960         WRITE (6,38) SHFT,SHH,SHT
01970   38    FORMAT ('  HEAT CAPACITY (BTU/F)       ',F8.7,5X,F8.7,5X,F8.7)
01980         WRITE (6,39) SHR1,SHR
01990   39    FORMAT ('  HEAT CAP/TOTAL HEAT CAP     ',F8.5,5X,F8.5,////)
02000         CALL   EXIT
02010         END
```

APPENDIX 6

OUTPUT FROM TF1

FINNED TUBE HYDRIDE HEAT EXCHANGER

◆◆

INPUT VALUES

FIN THICKNESS	0.020	INCHES
HYDRIDE THICKNESS	0.150	INCHES
FIN LENGTH	0.250	INCHES
WATER TEMPERATURE	170.0	F
CONV HEAT TRANS COEFF	1000.0	BTU/HR FT◆◆2 F
TUBE WALL THICKNESS	.0200	INCHES
TUBE DIAMETER	0.250	INCHES
HEAT GENERATION	NO	

MATERIAL PROPERTIES

	TUBE/FIN	HYDRIDE
SPECIFIC HEAT (BTU/LBM F)	0.092	0.107
DENSITY (LBM/FT◆◆3)	558.00	259.00
CONDUCTIVITY (BTU/HR FT F)	200.00	0.30

CALCULATED VALUES

	TUBE/FIN	HYDRIDE	TOTAL
VOLUME (FT◆◆3)	.0000015	.0000085	.0000100
HEAT CAPACITY (BTU/F)	.0000766	.0002362	.0003128
HEAT CAP/TOTAL HEAT CAP	0.24485	0.75515	

APPENDIX 7

ACTUAL DATA RUN OF P315A FOR THE COMPACT FINNED TUBE CONFIGURATION

FIN THCK= 0.020 FIN LNGTH= 0.25 HYD THCK= 0.150 H=1000. TD=0.25 HG=2. 0000000

DUMP CODE	MAX. COUNT	PRINT INTER.	STAB. CRIT.	VAR. TIME	EVALUATION CRIT. TEMP.	PROBLEM START	PRINT START	DUMMY INCREMENTS -1	0	TIME LIMIT	PUNCH CODE	READ CODE
1	30000	3.3300E-03	1.0000E-01	0.0	0.0	0.0	3.3300E-03	0.0	0.0	1.0	0	0

TEMPERATURE NODES AND CAPACITANCES

NODE	INC	CAP	CURV	RCX	EVX	NO.	TEMP.	CAP. VAL.
1	0	1	0	0	0	1	7.0000E+01	1.8200E-05
2	20	1	0	0	0	2	7.0000E+01	6.5000E-06
3	20	1	0	0	0	2	7.0000E+01	9.7000E-06
4	20	1	0	0	0	2	7.0000E+01	1.3000E-05
12	0	1	0	0	0	1	7.0000E+01	5.2500E-05
13	0	1	0	0	0	1	7.0000E+01	7.8700E-05
14	0	1	0	0	0	1	7.0000E+01	1.0500E-04
31	1	0	0	0	0	1	1.7000E+02	0.0

CONDUCTANCES

COND	INC	NODE	INC	NODE	INC	CURV	EVX	NO.	COND. VAL.
1	20	1	0	2	20	0	0	2	6.3300E-01
2	20	2	20	3	20	0	0	2	6.5400E-01
3	20	3	20	4	20	0	0	2	9.1600E-01
11	0	1	0	12	0	0	0	1	1.8000E-02
12	0	12	0	13	0	0	0	1	1.5000E-02
13	0	13	0	14	0	0	0	1	2.1000E-02
30	9	2	10	12	10	0	0	2	7.0000E-03
31	9	3	10	13	10	0	0	2	1.1000E-02
32	9	4	10	14	10	0	0	2	1.5000E-02
50	0	31	0	1	0	0	0	1	1.9400E-01

OTHER VALLES

LOC.	INC	NO.	VALUE

VARIABLE LINES

ANS	INC	PRMA	INC	PRMB	INC	PRMC	INC	CODE	CURV	EVX	NO.	PARAM. A	PARAM. B	PARAM. C
40010	0	40010	0	0	0	0	0	6	0	1	0	0.0	0.0	0.0

OUTPUT CODES

I.D.	INC	NO.
10001	1	30
0	0	0

FIN THCK= 0.020 FIN LNGTH= 0.25 HYD THCK= 0.150 H=1000. TD=0.25 HG=2. 0000000

PSEUDO SEQUENCE

CAP.	COND	NODE	RCX	STU	DCND
1			0	0	0
	1	2			
	11	12			
	21	22			
	50	31			
2			0	0	0
	1	1			
	2	3			
	30	12			
22			0	0	0
	21	1			
	22	23			
	39	12			
3			0	0	0
	2	2			
	3	4			
	31	13			
23			0	0	0
	22	22			
	23	24			
	40	13			
4			0	0	0
	3	3			
	32	14			
24			0	0	0
	23	23			
	41	14			
12			0	0	0
	11	1			
	12	13			
	30	2			
	39	22			
13			0	0	0
	12	12			
	13	14			
	31	3			
	40	23			
14			0	0	0
	13	13			
	32	4			
	41	24			

FIN THCK= 0.020 FIN LNGTH= 0.25 HYD THCK= 0.150 H=1000. TD=0.25 HG=2. 0000000

TIME HR	MINUTES	COUNT	PREV INC	NEXT INC	MIN RC
0.0	0.0	1	0.0	1.2558E-06	5.0232E-06

PREVIOUS TEMPERATURES

1	2	3	4	5	6	7	8	9	10
7.0000E+01	7.0000E+01	7.0000E+01	7.0000E+01	0.0	0.0	0.0	0.0	0.0	0.0
11	12	13	14	15	16	17	18	19	20
0.0	7.0000E+01	7.0000E+01	7.0000E+01	0.0	0.0	0.0	0.0	0.0	0.0
21	22	23	24	25	26	27	28	29	30
0.0	7.0000E+01	7.0000E+01	7.0000E+01	0.0	0.0	0.0	0.0	0.0	0.0
31									
1.7000E+02									

CURRENT TEMPERATURES

1	2	3	4	5	6	7	8	9	10
7.0000E+01	7.0000E+01	7.0000E+01	7.0000E+01	0.0	0.0	0.0	0.0	0.0	0.0
11	12	13	14	15	16	17	18	19	20
0.0	7.0000E+01	7.0000E+01	7.0000E+01	0.0	0.0	0.0	0.0	0.0	0.0
21	22	23	24	25	26	27	28	29	30
0.0	7.0000E+01	7.0000E+01	7.0000E+01	0.0	0.0	0.0	0.0	0.0	0.0
31									
1.7000E+02									

CAPACITANCES

1	2	3	4	12	13	14	22	23	24
1.8200E-05	6.5000E-06	9.7000E-06	1.3000E-05	5.2500E-05	7.8700E-05	1.0500E-04	6.5000E-06	9.7000E-06	1.3000E-05

CONDUCTANCES

1	2	3	11	12	13	21	22	23	30
6.3300E-01	6.5400E-01	9.1600E-01	1.8000E-02	1.5000E-02	2.1000E-02	6.3300E-01	6.5400E-01	9.1600E-01	7.0000E-03
31	32	39	40	41	50				
1.1000E-02	1.5000E-02	7.0000E-03	1.1000E-02	1.5000E-02	1.9400E-01				

MISCELLANEOUS VALUES

10
0.0

TIME CONSTANTS

1	2	22	3	23	4	24	12	13	14
1.2314E-05	5.0232E-06	5.0232E-06	6.1354E-06	6.1354E-06	1.3963E-05	1.3963E-05	1.1170E-03	1.3569E-03	2.0588E-03

HEAT BALANCE

1	2	22	3	23	4	24	12	13	14
1.9400E+01	0.0	0.0	0.0	0.0	0.0	0.0	0.0	0.0	0.0

RELATIVE HEAT BALANCE

1	2	22	3	23	4	24	12	13	14
1.0000E+00	0.0	0.0	0.0	0.0	0.0	0.0	0.0	0.0	0.0

TIME HR	MINUTES	COUNT	PREV INC	NEXT INC	MIN RC
3.3300E-03	1.9980E-01	2653	1.2435E-06	1.2558E-06	5.0232E-06

CURRENT TEMPERATURES

1	2	3	4	5	6	7	8	9	10
1.5475E+02	1.5281E+02	1.5120E+02	1.5052E+02	0.0	0.0	0.0	0.0	0.0	0.0
11	12	13	14	15	16	17	18	19	20
0.0	1.3088E+02	1.1628E+02	1.1298E+02	0.0	0.0	0.0	0.0	0.0	0.0
21	22	23	24	25	26	27	28	29	30
0.0	1.5281E+02	1.5120E+02	1.5052E+02	0.0	0.0	0.0	0.0	0.0	0.0

TIME HR	MINUTES	COUNT	PREV INC	NEXT INC	MIN RC
6.6600E-03	3.9960E-01	5306	8.8662E-07	1.2558E-06	5.0232E-06

CURRENT TEMPERATURES

1	2	3	4	5	6	7	8	9	10
1.6259E+02	1.6163E+02	1.6083E+02	1.6048E+02	0.0	0.0	0.0	0.0	0.0	0.0
11	12	13	14	15	16	17	18	19	20
0.0	1.5185E+02	1.4379E+02	1.4121E+02	0.0	0.0	0.0	0.0	0.0	0.0
21	22	23	24	25	26	27	28	29	30
0.0	1.6163E+02	1.6083E+02	1.6048E+02	0.0	0.0	0.0	0.0	0.0	0.0

TIME HR	MINUTES	COUNT	PREV INC	NEXT INC	MIN RC
9.9900E-03	5.9940E-01	7959	9.3877E-07	1.2558E-06	5.0232E-06

CURRENT TEMPERATURES

1	2	3	4	5	6	7	8	9	10
1.6634E+02	1.6587E+02	1.6547E+02	1.6530E+02	0.0	0.0	0.0	0.0	0.0	0.0
11	12	13	14	15	16	17	18	19	20
0.0	1.6113E+02	1.5708E+02	1.5569E+02	0.0	0.0	0.0	0.0	0.0	0.0
21	22	23	24	25	26	27	28	29	30
0.0	1.6587E+02	1.6547E+02	1.6530E+02	0.0	0.0	0.0	0.0	0.0	0.0

TIME HR	MINUTES	COUNT	PREV INC	NEXT INC	MIN RC
1.3320E-02	7.9920E-01	10612	9.3877E-07	1.2558E-06	5.0232E-06

CURRENT TEMPERATURES

1	2	3	4	5	6	7	8	9	10
1.6819E+02	1.6795E+02	1.6775E+02	1.6767E+02	0.0	0.0	0.0	0.0	0.0	0.0
11	12	13	14	15	16	17	18	19	20
0.0	1.6561E+02	1.6360E+02	1.6290E+02	0.0	0.0	0.0	0.0	0.0	0.0
21	22	23	24	25	26	27	28	29	30
0.0	1.6795E+02	1.6775E+02	1.6767E+02	0.0	0.0	0.0	0.0	0.0	0.0

TIME HR	MINUTES	COUNT	PREV INC	NEXT INC	MIN RC
1.6650E-02	9.9900E-01	13265	9.3877E-07	1.2558E-06	5.0232E-06

CURRENT TEMPERATURES

1	2	3	4	5	6	7	8	9	10
1.6909E+02	1.6898E+02	1.6838E+02	1.6884E+02	0.0	0.0	0.0	0.0	0.0	0.0
11	12	13	14	15	16	17	18	19	20
0.0	1.6781E+02	1.6631E+02	1.6646E+02	0.0	0.0	0.0	0.0	0.0	0.0
21	22	23	24	25	26	27	28	29	30
0.0	1.6898E+02	1.6838E+02	1.6884E+02	0.0	0.0	0.0	0.0	0.0	0

-------- TIME HR MINUTES COUNT PREV INC NEXT INC MIN RC
1.9980E-02 1.1988E+00 15918 9.3877E-07 1.2558E-06 5.0232E-06

CURRENT TEMPERATURES

1	2	3	4	5	6	7	8	9	10
1.6954E+02	1.6948E+02	1.6943E+02	1.6941E+02	0.0	0.0	0.0	0.0	0.0	0.0
11	12	13	14	15	16	17	18	19	20
0.0	1.6889E+02	1.6839E+02	1.6822E+02	0.0	0.0	0.0	0.0	0.0	0.0
21	22	23	24	25	26	27	28	29	30
0.0	1.6948E+02	1.6943E+02	1.6941E+02	0.0	0.0	0.0	0.0	0.0	0.0

-------- TIME HR MINUTES COUNT PREV INC NEXT INC MIN RC
2.3310E-02 1.3986E+00 13571 9.3877E-07 1.2558E-06 5.0232E-06

CURRENT TEMPERATURES

1	2	3	4	5	6	7	8	9	10
1.6976E+02	1.6973E+02	1.6971E+02	1.6970E+02	0.0	0.0	0.0	0.0	0.0	0.0
11	12	13	14	15	16	17	18	19	20
0.0	1.6943E+02	1.6918E+02	1.6909E+02	0.0	0.0	0.0	0.0	0.0	0.0
21	22	23	24	25	26	27	28	29	30
0.0	1.6973E+02	1.6971E+02	1.6970E+02	0.0	0.0	0.0	0.0	0.0	0.0

-------- TIME HR MINUTES COUNT PREV INC NEXT INC MIN RC
2.6640E-02 1.5984E+00 21224 9.3877E-07 1.2558E-06 5.0232E-06

CURRENT TEMPERATURES

1	2	3	4	5	6	7	8	9	10
1.6987E+02	1.6986E+02	1.6984E+02	1.6984E+02	0.0	0.0	0.0	0.0	0.0	0.0
11	12	13	14	15	16	17	18	19	20
0.0	1.6969E+02	1.6956E+02	1.6952E+02	0.0	0.0	0.0	0.0	0.0	0.0
21	22	23	24	25	26	27	28	29	30
0.0	1.6986E+02	1.6984E-02	1.6984E+02	0.0	0.0	0.0	0.0	0.0	0.0

-------- TIME HR MINUTES COUNT PREV INC NEXT INC MIN RC
2.9970E-02 1.7982E+00 23877 9.3877E-07 1.2558E-06 5.0232E-06

CURRENT TEMPERATURES

1	2	3	4	5	6	7	8	9	10
1.6993E+02	1.6992E+02	1.6991E+02	1.6991E+02	0.0	0.0	0.0	0.0	0.0	0.0
11	12	13	14	15	16	17	18	19	20
0.0	1.6982E+02	1.6975E-02	1.6973E+02	0.0	0.0	0.0	0.0	0.0	0.0
21	22	23	24	25	26	27	28	29	30
0.0	1.6992E+02	1.6991E-02	1.6991E+02	0.0	0.0	0.0	0.0	0.0	0.0

-------- TIME HR MINUTES COUNT PREV INC NEXT INC MIN RC
3.3300E-02 1.9980E+00 26530 9.3877E-07 1.2558E-06 5.0232E-06

CURRENT TEMPERATURES

1	2	3	4	5	6	7	8	9	10
1.6995E+02	1.6995E+02	1.6994E+02	1.6994E+02	0.0	0.0	0.0	0.0	0.0	0.0
11	12	13	14	15	16	17	18	19	20
0.0	1.6988E+02	1.6984E+02	1.6983E+02	0.0	0.0	0.0	0.0	0.0	0.0
21	22	23	24	25	26	27	28	29	30
0.0	1.6995E+02	1.6994E+02	1.6994E+02	0.0	0.0	0.0	0.0	0.0	0.0

-------- TIME HR MINUTES COUNT PREV INC NEXT INC MIN RC
3.6630E-02 2.1978E+00 29183 9.3877E-07 1.2558E-06 5.0233E-06

CURRENT TEMPERATURES

1	2	3	4	5	6	7	8	9	10
1.6996E+02	1.6995E+02	1.6996E+02	1.6995E+02	0.0	0.0	0.0	0.0	0.0	0.0
11	12	13	14	15	16	17	18	19	20
0.0	1.6992E+02	1.6989E+02	1.6988E+02	0.0	0.0	0.0	0.0	0.0	0.0
21	22	23	24	25	26	27	28	29	30
0.0	1.6996E+02	1.6996E+02	1.6995E+02	0.0	0.0	0.0	0.0	0.0	0.0

---STABILITY CRITERION SATISFIED---

-------- TIME HR MINUTES COUNT PREV INC NEXT INC MIN RC
3.7582E-02 2.2549E+00 29941 1.2558E-06 1.2558E-06 5.0232E-06

CURRENT TEMPERATURES

1	2	3	4	5	6	7	8	9	10
1.6996E+02	1.6996E+02	1.6996E+02	1.6995E+02	0.0	0.0	0.0	0.0	0.0	0.0
11	12	13	14	15	16	17	18	19	20
0.0	1.6992E+02	1.6990E+02	1.6989E+02	0.0	0.0	0.0	0.0	0.0	0.0
21	22	23	24	25	26	27	28	29	30
0.0	1.6996E+02	1.6996E+02	1.6995E+02	0.0	0.0	0.0	0.0	0.0	0.0

---STABILITY CRITERION SATISFIED---

-------- TIME HR MINUTES COUNT PREV INC NEXT INC MIN RC
3.7583E-02 2.2550E+00 29942 1.2558E-06 1.2558E-06 5.0232E-06

PREVIOUS TEMPERATURES

1	2	3	4	5	6	7	8	9	10
1.6996E+02	1.6996E+02	1.6996E+02	1.6995E+02	0.0	0.0	0.0	0.0	0.0	0.0
11	12	13	14	15	16	17	18	19	20
0.0	1.6992E+02	1.6990E+02	1.6989E+02	0.0	0.0	0.0	0.0	0.0	0.0
21	22	23	24	25	26	27	28	29	30
0.0	1.6996E+02	1.6996E+02	1.6995E+02	0.0	0.0	0.0	0.0	0.0	0.0

31
1.7000E+02

CURRENT TEMPERATURES

1	2	3	4	5	6	7	8	9	10
1.6996E+02	1.6996E+02	1.6996E+02	1.6995E+02	0.0	0.0	0.0	0.0	0.0	0.0
11	12	13	14	15	16	17	18	19	20
0.0	1.6992E+02	1.6990E+02	1.6989E+02	0.0	0.0	0.0	0.0	0.0	0.0
21	22	23	24	25	26	27	28	29	30
0.0	1.6996E+02	1.6996E+02	1.6995E+02	0.0	0.0	0.0	0.0	0.0	0.0

31
1.7000E+02

CAPACITANCES

1	2	3	4	12	13	14	22	23	24
1.8200E-05	6.5000E-06	9.7000E-06	1.3000E-05	5.2500E-05	7.8700E-05	1.0500E-04	6.5000E-06	9.7000E-06	1.3000E-05

CONDUCTANCES

1	2	3	11	12	13	21	22	23	30
6.3300E-01	6.5400E-01	9.1600E-01	1.8000E-02	1.5000E-02	2.1000E-02	6.3300E-01	6.5400E-01	9.1600E-01	7.0000E-03

31	32	39	40	41	50
1.1000E-02	1.5000E-02	7.0000E-03	1.1000E-02	1.5000E-02	1.9400E-01

MISCELLANEOUS VALUES

10
0.0

TIME CONSTANTS

1	2	22	3	23	4	24	12	13	14
1.2314E-05	5.0232E-06	5.0232E-06	6.1354E-06	6.1354E-06	1.3963E-05	1.3963E-05	1.1170E-03	1.3569E-03	2.0588E-03

HEAT BALANCE

1	2	22	3	23	4	24	12	13	14
1.8387E-04	1.2926E-04	1.2926E-04	5.0211E-04	5.0211E-04	3.4085E-04	3.4085E-04	1.2406E-03	1.4548E-03	2.0440E-03

RELATIVE HEAT BALANCE

1	2	22	3	23	4	24	12	13	14
1.3568E-02	2.2813E-02	2.2813E-02	8.1392E-01	1.1392E-01	1.5089E-01	1.5089E-01	6.9293E-01	8.5242E-01	1.0000E+00

APPENDIX 8

TEMPERATURE UPGRADE COP CALCULATIONS FOR OPTIMUM DESIGN

Hot side alloy = $LaNi_{4.5}Al_{0.5}$

Cold side alloy = $LaNi_5$

Hydrogen/metal ratio:

H/M = 3.18 gmole H_2/lbm $LaNi_{4.5}Al_{0.5}$ (Ref. 1)
H/M = 3.14 gmole H_2/lbm $LaNi_5$ (Ref. 2)

For equal amounts of H_2 absorbed/desorbed:

$$\frac{\text{3.14 gmole } H_2\text{/lbm } LaNi_5}{\text{3.18 gmole } H_2\text{/lbm } LaNi_{4.5}Al_{0.5}} = 0.987$$

Use:

1.0 lbm $LaNi_5$
0.987 lbm $LaNi_{4.5}Al_{0.5}$

This yields:

3.14 gmole H_2 (absorbed/desorbed)

and

Q_{LaNi_5} = 92.2 Btu (Ref. 3)

$Q_{LaNi_{4.5}Al_{0.5}}$ = 114.6 Btu (Ref. 2)

where Q = heat of absorption/desorption

Hydride utilization factor = 70%

Therefore:

Q_{LaNi_5} = (0.7) (92.2 Btu) = 64.5 Btu

$Q_{LaNi_{4.5}Al_{0.5}}$ = (0.7) (114.6 Btu) = 80.2 Btu

$$COP_{upgrade} = \frac{Q_{abs(LaNi_{4.5}Al_{0.5})} + SH_{(LaNi_{4.5}Al_{0.5})} (T_M - T_H)}{Q_{des(LaNi_{4.5}Al_{0.5})} + SH_{(LaNi_{4.5}Al_{0.5})} (T_H - T_M) + Q_{des(LaNi_5)} + SH_{LaNi_5} (T_L - T_M)}$$

where the heat of desorption has a negative value and the heat of absorption has a positive value.

Thus:

$Q_{abs(LaNi_{4.5}Al_{0.5})}$ = 80.2 Btu $\quad$ $Q_{des(LaNi_{4.5}Al_{0.5})}$ = -80.2 Btu

$$Q_{abs(LaNi_5)} = 64.5 \text{ Btu} \qquad Q_{des(LaNi_5)} = -64.5 \text{ Btu}$$

Let:

$$T_H = 350°F \qquad T_M = 200°F \qquad T_L = 80°F$$

$$COP_{upgrade} = \frac{80.2 \text{ Btu} + SH_{(LaNi_{4.5}Al_{0.4})} (200°F - 350°F)}{-80.2 \text{ Btu} + SH_{(LaNi_{4.5}Al_{0.4})} (350°F - 200°F) + (-64.5 \text{ Btu}) + SH_{(LaNi_5)} (80°F - 200°F)}$$

$$= \frac{80.2 \text{ Btu} + SH_{(LaNi_{4.5}Al_{05})} (-150°F)}{-144.7 \text{ Btu} + SH_{(LaNi_{4.5}Al_{0.5})} (150°F) + SH_{(LaNi_5)} (-120°F)}$$

Internally Finned Tube

Sensible heat (from computer model) = 0.187 Btu/°F·lbm alloy

For 1.0 lbm $LaNi_5$ and 0.987 lbm $LaNi_{4.5}Al_{0.5}$:

$$SH_{LaNi_5} = 0.187 \text{ Btu/°F}$$

$$SH_{LaNi_{4.5}Al_{0.5}} = 0.185 \text{ Btu/°F}$$

Substituting into $COP_{upgrade}$ equation:

$$COP_{upgrade} = \frac{80.2 + (0.185)(-150)}{-144.7 + (0.185)(150) + (0.187)(-120)}$$

$$= \frac{52.45}{-139.39} = -0.38$$

Externally Finned Tube

Sensible heat (from computer model) = 0.142 Btu/°F·lbm alloy

For 1.0 lbm $LaNi_5$ and 0.987 $LaNi_{4.5}Al_{0.5}$:

$$SH_{LaNi_5} = 0.142 \text{ Btu/°F}$$

$$SH_{LaNi_{4.5}Al_{0.5}} = 0.140 \text{ Btu/°F}$$

Substituting into $COP_{upgrade}$ equation:

$$COP_{upgrade} = \frac{80.2 + (0.140)(-150)}{-144.7 + (0.140)(150) + (0.142)(-120)}$$

$$= \frac{59.2}{-140.7} = -0.42$$

Theoretical maximum $COP_{upgrade}$:

(asumes no sensible heat)

$$COP_{upgrade} = \frac{80.2}{-80.2 - 64.5} = -0.55$$

Water System Sensible Heat Burden for Externally Finned Tube Hydride Heat Exchanger

Initial coefficient of performance values for various configurations were calculated with the system boundary located at the inner tube wall/water system interface. To include the water system sensible heat burden in the COP calculations, the sensible heat of the water was calculated assuming 50 percent mixing -- one-half of the water located in the hydride unit would be heated or cooled during the thermal cycling.

Volume of H_2O in one EDTU pressure vessel = 5.1 $in.^3$

Weight of hydride powder in one unit = 8.63 lb

Yielding: 0.02 lb water/lb hydride x (0.5 mixing)

= 0.01 lb water/lb hydride

The sensible heat of water = 1 Btu/16°F

Thus

SH_{H_2O} = 0.01 Btu/°F lb alloy

The sensible heat for the externally finned tube = 0.142 Btu/lb alloy

The total sensible heat including water = 0.152 Btu/lb alloy

For 1.0 lb $LaNi_5$ and 0.987 $LaNi_{4.5}Al_{0.5}$

SH_{LaNi_5} = 0.152 Btu?°F

$SH_{LaNi_{4.5}Al_{0.5}}$ = 0.150 Btu/°F

Substituting into $COP_{upgrade}$ equation:

$$COP_{upgrade} = \frac{80.2 + (0.150)(-150)}{-144.7 + 0.150)(150) + (0.152)(-120)}$$

$$= \frac{57.7}{-140.44} = -0.41$$

References

1. van Vucht, J. H. N., Kuijpers, F. A. and Bruning, H. C. A. M., "Reversible Room-Temperature Absorption of Large Quantities of Hydrogen by Intermetallic Compounds," Philips Res. Reports, Vol. 25 (1970) pp. 133-140.

2. Mendelsohn, M. H., Gruen, D. M. and Dwight, A. E., "The Effects of Aluminum Additions on the Structural and Hydrogen Absorption Properties of AB_5 Alloys With Particular Reference to the $LaNi_{5-x}Al_x$ Ternary Alloy Systems," J. Less Commmon Metals, Vol. 63 (1979), pp. 193-207.

3. van Mal, H. H., Buschow, K. H. J. and Miedema, A. R., "Hydrogen Absorption in $LaNi_5$ and Related Compounds: Experimental Observations and Their Explanation," J. Less Common Metals, Vol. 35 (1974), pp. 65-76.

APPENDIX 9

METHOD FOR SOLVING FOR REQUIRED FILTER AREA PER POUND OF HYDRIDE POWDER

Assume:

ΔH_{LaNi_5} = 60 Btu/lb_{LaNi_5} = 19 Btu/mole H_2

Capacity = 12000 Btu/hr (1 ton) = 200 Btu/min.

Temperature = 80°F (540°R)

Pressure = 1 atm (14.7 psi)

Amount of hydride powder = 5 lbs

$$\text{Hydrogen Flow Rate} = \frac{200 \text{ Btu/min.}}{19 \text{ Btu/mole } H_2} = \frac{10.5 \text{ mole } H_2}{\text{min.}}$$

$$\text{Volumetric Flow Rate} = \dot{V} = \frac{\dot{m} R T}{P}$$

where $\dot{m}$ = hydrogen flow rate
R = gas constant, 766.5 ft·lb_f/lb_m°R
T = temperature
P = pressure

$$\dot{V} = \frac{(10.5 \text{ mole } H_2/\text{min})(2 \text{ grams/mole } H_2)(766.5 \text{ ft } lb_f/lb_m°R)(540°R)}{(14.7 \text{ } lb_f/in^2)(144 \text{ } in^2/ft^2)(454 \text{ grams}/lb_m)}$$

= 9 ft^3/min. (cfm)

As an example, from Figure 79 which has been duplicated in this Appendix, the maximum allowed pressure drop of 5 psi and a vertical downward hydrogen flow through 1/2 inch hydride powder corresponds to a flow density of 70 acfm/ft^2.

Theretore:

$$\text{Required filter surface area} = \frac{9 \text{ cfm}}{70 \text{ acfm/ft}^2} = 0.13 \text{ ft}^2 = 18.5 \text{ in}^2$$

Filter area per pound of powder = (18.5 in^2/ton)(1 ton/5 lbs powder)

= 3.7 in^2/lb powder

APPENDIX 10

PRESSURE VESSEL STRESS CALCULATIONS

Objective: to find the optimum pressure vessel wall thickness

Assume: internal pressure = 1050 psi[1]
(actual design pressure = 350 psi, safety factor = 3)
allowable stress for stainless steel = 30,000 psi
pressure vessel radius = 3.0 inches

Reference: Popov, E. P., Mechanics of Materials, Prentice Hall, Inc. 1976.

Stress formulas:

1. Circumferential stress (hoop stress) $\longrightarrow \sigma_c = Pr/t$

2. Longitudinal stress $\longrightarrow \sigma_L = Pr/2t$

where P = internal pressure (psi)
r = radius (in.)
t = wall thickness (in.)

Solving equations 1 and 2 for t, wall thickness, yields

$t_c = Pr/\sigma_c$ and $t_L = Pr/2\sigma_L$

$$t_c = \frac{(1050 \text{ psi})(3 \text{ inches})}{30{,}000 \text{ psi}} = 0.105 \text{ inches}$$

$$t_L = \frac{(1050 \text{ psi})(3 \text{ inches})}{(2)(30{,}000 \text{ psi})} = 0.053 \text{ inches}$$

Therefore, design for circumferential stress condition; next standard wall thickness greater than 0.105 inch is 0.125 inch thick.

[1]At the design temperature of 177°C (350°F), the internal hydrogen pressure is 2.4 MPa (350 psi). In the case of a sudden internal temperature rise above 177°C, the corresponding hydrogen pressure increases logarithmically. A factor of safety equal to 3 adequately safeguards this event.

APPENDIX 11

HEAT TRANSFER/PRESSURE DROP ANALYSIS

Objective: to calculate the mass flow rates and pressure drops through water tubes

Nomenclature:

h	=	external heat transfer coefficient			
Nu	=	Nusselt number			
Re	=	Reynolds number	ΔP	=	pressure drop
Pr	=	Prandtl number	f	=	friction factor
D	=	tube inside diameter	ρ	=	density
K	=	thermal conductivity	L	=	tube length
U_m	=	mean velocity	g_c	=	gravitational constant ($32.2\ ft/s^2$)
ν	=	kinematic viscosity			

Assume:

L = 24 in. (approximate length of water flow path in one EDTU pressure vessel)

D = 0.19 in. (wall thickness = 0.03 in.)

h = 1000 Btu/hr ft^2 °F

temperatures - T_L = 80°F, T_M = 200°F, T_H = 350°F

cold side alloy (CSA) = $LaNi_5$, T_{mean} = (80°F + 200°F)/2 = 140°F

warm side alloy (WSA) = $LaNi_{4.5}Al_{0.5}$, T_{mean} = (200°F + 350°F)/2 = 275°F

Reference: Özisik, M. N., Basic Heat Transfer, McGraw-Hill Inc., 1977.

Governing Equations:

1. $Nu = 0.23\ Re^{0.8} Pr^{0.3}$

2. $Nu = h \cdot D/K$

3. $Re = U_m \cdot D/\nu$

4. $\Delta P = \dfrac{f \cdot L \cdot \rho \cdot U_m^2}{2 \cdot D \cdot g_c}$

Mass Flow Rates

CSA Analysis:

properties of water at 140°F -

ν = 0.018 ft^2/hr
K = 0.38 Btu/hr ft °F
Pr = 3.01
ρ = 61.4 lb/ft^3

Using Equation 2:

$$Nu = \frac{(1000 \text{ Btu/hr ft}^2 \text{ °F})\ (0.19 \text{ in.})\ (1 \text{ ft}/12 \text{ in.})}{(0.3 \text{ Btu/hr ft °F})} = 41.67$$

Substituting Nu value into Equation 1:

$$41.67 = 0.023\ Re^{0.8}\ (3.01)^{0.3}$$

$$Re = 7818$$

Substituting Re value into Equation 3:

$$7818 = \frac{(U_m)\ (0.19 \text{ in.})\ (1 \text{ ft}/12 \text{ in.})}{(0.018 \text{ ft}^2/\text{hr})}$$

$$U_m = 8888 \text{ ft/hr}$$

Coversion to gallon per minute:

$$U_m = 0.87 \text{ qpm} \approx 1 \text{ gpm} \cdot 7 \text{ tubes/pressure vessel} = 7 \text{ gpm}$$

WSA Analysis:

properties of water at 275°F = ν

ν = 0.009 ft^2/hr
K = 0.39 Btu/hr ft °F
Pr = 1.3
ρ = 56.0 lb/ft^3

Using Equation 2:

$$Nu = \frac{(1000 \text{ Btu/hr ft}^2 \text{ °F})\ (0.19 \text{ in.})\ (1 \text{ ft}/12 \text{ in.})}{(0.39 \text{ Btu/hr ft f})} = 40.60$$

Substituting Nu value into Equation 1:

$$40.67 = 0.023\ Re^{0.8}\ (1.3)^{0.3}$$

$$Re = 10392$$

Substituting Re value into Equation 3:

$$10392 = \frac{(U_m)\ (0.19 \text{ in.})\ (1 \text{ ft}/12 \text{ in.})}{(0.009 \text{ ft}^2/\text{hr})}$$

$$U_m = 5907 \text{ ft/hr}$$

Covert to gallon per minute:

$$U_m = 0.58 \text{ gpm} \approx 1 \text{ gpm} \cdot 7 \text{ tubes/pressure vessel} = 7 \text{ gpm}$$

Pressure Drop

CSA Analysis: (assume smooth pipe)

CSA friction factor = 0.0305 (p. 256, Ozisik)

$$\Delta P = \frac{(0.0305)(24\text{ in.})(61.4\text{ lb/ft}^3)(8888\text{ ft/hr})^2(1\text{ ft}^2/144\text{ in.}^2)}{(2)(0.19\text{ in.})(32.2\text{ ft/s}^2)(1.296 \times 10^7\text{s}^2/1\text{ hr}^2)} = 0.16\text{ psi}$$

WSA Analysis: (assume smooth pipe)

WSA friction factor = 0.027 (p. 256, Ozisik)

$$\Delta P = \frac{(0.027)(24\text{ in.})(56.0\text{ lb/ft}^3)(5907\text{ ft/hr})^2(1\text{ ft}^2/144\text{in.}^2)}{(2)(0.19\text{ in.})(32.2\text{ ft/s}^2)(1.296 \times 10^7\text{s}^2/1\text{ hr}^2)} = 0.06\text{ psi}$$